Surface-selective and Controllable Photo-grafting for Synthesis of Tailored Macroporous Membrane Adsorbers

(Oberflächenselektive und kontrollierbare Photopfropfung für die Synthese von maßgeschneiderten makroporösen Membranadsorbern)

by

Dongming He
Jiangxi, China

Thesis submitted to the Department of Chemistry of
Universität Duisburg-Essen, in partial fulfillment of
the requirements of the degree of
Dr. rer. nat.

Approved by the examining committee on *July 3, 2008*:

Chair : Prof. Dr. Heinz Wilhelm Siesler

Advisor : Prof. Dr. Mathias Ulbricht

Reviewer : Prof. Dr. Thomas Schrader

Essen, 2008

Abstract

Photo-grafting is a straightforward and promising technique for surface modification of polymeric membranes. This work emphasized on the development and investigation of surface-selective photo-grafting method from polar organic solution; on the other hand, on the preparation of membrane adsorbers via the proposed grafting methods and evaluation of the resulting membrane adsorbers.

Two novel surface-selective photo-grafting methods have been developed: synergist immobilization and iniferter immobilization methods. Hydrophilized polypropylene (PP) microfiltration (MF) membrane, whose surface polymer layer contains polyacrylate, was used as base membrane for both methods; track-etched polyethylene terephthalate (PET) MF membranes (PET200 and PET400) were used for extension of synergist immobilization method and further investigation; methanol or acetonitrile solution of acrylamide (AAm) with/without cross-linker (EDMA) was applied for investigation of grafting mechanism.

For synergist immobilization method, the synergist (tertiary amino groups) for photo-initiator benzophenone (BP) was introduced onto the membrane surface via an aminolysis reaction with diethyl ethylenediamine (DEEDA). The reaction conditions have been optimized. The proposed grafting mechanism was verified by the significant difference in degree of grafting (DG) between original and aminolysed membranes. In order to better understand and improve this novel method, detailed investigation of functionalization parameters and affecting factors has been carried out. The grafted membranes were characterized by ATR-IR, contact angle, SEM, permporometry, liquid permeability and zeta potential. The obtained results demonstrated that the highest surface-selectivity of photo-grafting could be achieved only under the optimum grafting conditions, i.e., inert solvent to excited BP should be used to reduce/avoid homopolymerization in bulk solution; appropriately low UV intensity should be applied to exclude the uncontrolled side grafting reaction (another functionalization mechanism was discovered at high UV intensity based on direct generation of starter radical); appropriately low BP concentration was used to reduce the non-selective photo-grafting. Thus, the grafted layer could be well controlled by immobilized synergist concentration, UV irradiation time, monomer concentration and initiator concentration. In addition, this method has been successfully applied to track-etched PET membrane, and it is also expected to functionalize other polymeric membranes with similar chemical structure.

For iniferter immobilization method, the reaction conditions for immobilization of photo-iniferter (dithiocarbamate group) have been optimized. The grafting mechanism has been verified by the relationship between DG and photo-iniferter concentration. Detailed investigation with respect to grafting efficiency, uniformity on the whole membrane surface and controlled grafted layer structure has been carried out. This grafting method exhibited high grafting efficiency, uniform modification and high controllability. However, the re-initiation efficiency was low for the selected grafting system based on the significant difference in DG value obtained by continuous and intermittent UV irradiation.

Via developed synergist immobilization method and conventional photo-initiator adsorption method, three types of anion-exchange membranes (low and high grafting density and slightly cross-linked grafted layer) have been prepared in aqueous solution of (2-(methacryloyloxy)ethyl) trimethylammonium chloride (MAETMAC) with/without EDMA, using hydrophilized PP MF membrane as support. The effect of grafted layer architecture on protein binding capacity and liquid permeability has been investigated. Buffer/elution solution permeability, static and dynamic protein binding behaviors have been determined for selected resulting anion-exchange membranes. Analyses demonstrated that cross-linking of grafted layer and high grafting density can improve the liquid permeability of membrane adsorbers. But the protein binding capacity was relatively low for high grafting density membrane. In comparison, the membranes with slightly cross-linked grafted layer exhibited improved overall performance. In addition, compared to conventional adsorption method, synergist immobilization method is a more efficient and suitable grafting technique for the preparation of anion-exchange membranes with three-dimensional grafted layer based on the higher grafting efficiency and better dynamic performance for membrane adsorbers prepared via this method.

For the preparation of affinity membrane, track-etched PET400 membrane was grafted with a special functional copolymer with bisphosphonate ester groups via synergist immobilization method from acetonitrile solution. The resulting affinity membrane showed high binding capacity for selected proteins. Especially, it was found that markedly higher binding capacity and affinity have been achieved for lysozyme than for cytochrome C, both proteins with similar pI value and protein size. With this affinity membrane, the protein separation has been realized in the 1:1 mixture solution of lysozyme and cytochrome C with a very high selectivity.

Using hydrophilized PP MF membrane, MIP thin-layer composite membranes have been prepared via synergist immobilization. However, the imprinting effect was not observed

probably due to the influence of synergist on the stability of formed complex between functional monomer and template and template concentration in bulk solution. The optimization of composition for MIP has been performed.

Iniferter immobilization method would be a promising alternative. MIP thin-layer composite membranes have been synthesized via this method, but the evaluation and further investigation is still in progress.

This thesis is dedicated

to my wife (Liu Na)

for her love, endless support and encouragement.

This work was performed during the period from July 2005 to May 2008 at the Institute of Technical Chemistry (Lehrstuhl für Technische Chemie II), Department of Chemistry, Universität Duisburg-Essen, under the supervision of Prof. Dr. Mathias Ulbricht.

I declare that this dissertation represents my own work, except where due acknowledgement is made.

Dongming He

Acknowledgement

This thesis could not be finished without the help and support of many people who are gratefully acknowledged here.

At the very first, I'm honored to express my deepest gratitude to my dedicated supervisor, Prof. Dr. Mathias Ulbricht, with whose able guidance I could have worked out this dissertation. He has offered me valuable ideas and suggestions with his profound knowledge and rich research experiences. His patience and kindness are greatly appreciated. Besides, because of the financial support provided by him, I could continue and complete my PhD study.

I'm also extremely grateful to my reviewer Prof. Dr. Thomas Schrader (Organische Chemie, UDuE) for his advice and discussion as well as giving a good opportunity for cooperation.

I am greatly indebted to the Hanns-Seidel foundation (in Germany) for providing two-year scholarship and giving an opportunity to start my PhD study in Germany. I would like to give special thanks to the leaders for their understanding about my special situation during the time.

I would like to thank Sun Wei (Organische Chemie, UDuE) for the very pleasant cooperation and discussion, and to all members of our research group at Lehrstuhl für Technische Chemie II, Universität Duisburg-Essen, namely, Inge, Claudia, Jun, Haofei, Heru, Mehmet, Qian, Yu, Abdus, Marcel, Halim, Nico, Christian, Danuta, Alex, Falk, Rafael, Monica, Nadia, Eva, Su-Hyoun, Dr. Illing, Polina, Frau Steffens and Frau Nordmann for providing nice company, help and excellent working environment.

I am pleased to thank the group of Prof. Dr. H.W. Siesler (Physikalische Chemie, UDuE) for help with the FTIR measurements, S. Boukercha (Anorganische Chemie, UDuE) for the SEM analyses, and Dr. T. Schaller (Organische Chemie, UDuE) for Solid state NMR measurement.

Last but no least, I would love to pay my special gratitude to my wife, my parents and parents-in-law for their endless love, understanding and support all the way from the very beginning of my PhD study in Germany.

Contents

List of tables

List of Figures

Chapter 1 Introduction

1.1 Background and existing problems

Chromatography is widely used for the separation, isolation, purification and analytical characterization of biomolecules. Due to some limitations associated with the conventional packed bed column chromatography, such as high pressure drop, internal diffusion limitation or compaction of the soft particles, many efforts have been made to improve the performance of the processes by alternative stationary phase materials. Afeyan et al. [1] prepared a functionalized bead having pores through which a protein can be transported by convection and showed that diffusive resistance in the bead-packed bed could be neglected. Brandt et al. [2] designed a porous affinity chromatography membrane which allows the mass transfer of protein molecules to the ligands mainly by convection, and the aforementioned limitations of traditional particles could also be eliminated. Ease of scale-up makes the membrane format very attractive. Furthermore, Muller [3] first proposed the idea of "multilayer binding" of protein on the extending polymer chains attached on the surface of adsorber particles. This idea has also been successfully applied for obtaining higher binding capacity of porous membrane adsorbers [4, 5].

So far, membrane chromatography has been intensively investigated and industrially applied as a promising alternative to the conventional technology [6-8]. However, it has been realized that membrane chromatography has its limitations such as unclear mass transport phenomena and relatively lower binding capacity compared to adsorber particles. Therefore, recent research work mainly focuses on the clarification of transport phenomena in membrane chromatographic processes and the enhancement of binding capacity. For the latter, the effective solution would be emphasized on membrane chemistry (i.e., synthesis of membrane adsorbers with high binding capacity), although the more effective ligand utilization by the optimized chromatographic processes could also improve the binding capacity.

Due to the limited surface area of porous membrane, enhancing the binding capacity by "multilayer binding" becomes a main research direction. This certainly will lead to the reduction of liquid permeability due to the extension of longer grafted chains into the pore interior. However, from the viewpoint of practicability, the tradeoff between high binding capacity and low liquid permeability needs to be overcome. This requires a new design for grafted functional active layers. For example, grafted chains containing ion-exchange groups expand or shrink depending on the ionic strength, pH and kind of solvent used. The

swelling of grafted polymer is helpful for protein binding but reduces the liquid permeability, affecting the mass transfer of proteins. Cross-linking of the grafted chains has been shown to be effective in reducing the swelling and improving the stability [9], but in this case, the cross-linked grafted layer led to a low protein binding capacity and nearly no protein could be eluted. In addition, with the same ligand amount, the increase of grafting density can also increase the liquid permeability of membrane adsorbers. Therefore, this may be another approach to overcome the trade-off on condition that the ligand utilization yield can be guaranteed. However, rare reports regarding improving membrane adsorbers performance by adjustment of grafted layer structure have been found [10].

For the preparation of membrane adsorbers with high binding capacity, surface graft modification on commercial membranes has shown itself a good solution. Commercially available Sartobind membrane adsorbers have been prepared by grafting cross-linked functional polymer chains onto the base cellulose membrane and used for the same purpose later as well (cf. ref. [8]). However, those adsorbers showed a limited dynamic binding capacity. Investigators have developed several alternative techniques to attach the functional ligands in an appropriate form onto the surface of commercial macroporous membranes. Saito et al. [4] have employed radiation-induced graft polymerization to prepare various ion-exchange membranes. Husson et al. have developed a method for surface-initiated atom transfer radial polymerization (ATRP) for the preparation of cation-exchange membrane adsorbers [11]. However, to achieve a fully controlled grafting via ATRP requires significant efforts which may be hard to implement in large technical scale. Photo-initiated graft copolymerization had been proposed and successfully applied as an easy and robust approach for the preparation of bio-affinity [12] or of high-capacity cation-exchange membranes [10, 13].

More photo-grafting techniques have also been proposed for other membrane functionalities [14, 15]. To some extent, the developed photo-grafting methods exhibit high surface-selectivity and controllability when they are applied to modify membranes from aqueous solution. However, to my best knowledge, there is still a technique gap that no efficient photo-grafting method, via which polymeric membranes can be surface-selectively grafted from polar organic solution of monomer, had been developed. This greatly limits the use of a variety of functional monomers. In addition, precise design of grafted layer is still a challenging issue.

1.2 Objectives of the research

The overall objectives of this research are

(i) to find efficient surface-selective photo-grafting methods for polymeric membranes according to the main criteria: graft polymerization is initiated from the whole membrane surface; effective grafting can be manipulated in polar organic solution of monomer; grafted polymer layer can be well controlled.

(ii) to prepare membrane adsorbers with well-defined grafted layer architectures via the proposed grafting techniques and evaluate the performance of such membrane adsorbers.

To be more specific, the research tasks involve

i. Study on the already developed photo-grafting methods according to the criteria proposed above.

ii. Proposal of novel photo-grafting strategies and study on the grafting mechanisms.

iii. Investigation of various factors affecting grafting efficiency and surface-selectivity.

iv. Proof / extension of the proposed technique by applying to another membrane made of similar polymer structure.

v. Preparation of anion-exchange membrane adsorbers with designed grafted layer from aqueous solution via the proposed grafting method.

vi. Preparation of affinity membrane adsorbers from polar organic solution.

vii. Preparation of molecularly imprinted polymer (MIP) composite membranes from polar organic solution.

viii. Evaluation of the performance of the novel membrane adsorbers.

1.3 Scope of this dissertation

Already known photo-initiator entrapping method and sequential photo-induced method were used for graft functionalization of unmodified polypropylene (PP) microfiltration (MF) membrane. Membrane functionalizations were performed from acrylamide (AAm) aqueous solution and in AAm acetonitrile solution via respective grafting approaches. The difference in grafting efficiency was analysed by more detailed experiments and determinations.

A novel photo-grafting strategy—synergist immobilization—was proposed toward the functionalization of hydrophilized PP MF membrane from polar organic solutions. Tertiary amino groups as synergist (co-initiator) of benzophenone (BP) were immobilized on the whole membrane surface via aminolysis reaction. The proposed grafting mechanism was evaluated by comparing grafting efficiency of aminolysed and original membranes using simultaneous method (BP dissolved in monomer solution). In order to better control the

grafting behavior, the factors that affect the surface-selectivity of photo-grafting such as solvent, UV irradiation time and intensity, monomer and photo-initiator concentration have been investigated in detail. To extend the application of this grafting technique, the functionalization of track-etched polyethylene terephthalate (PET) membranes (PET200 and PET400) have been performed and the controllability of grafted polymer layer was further verified, and characterization of prepared layer was completed.

Another photo-grafting method—iniferter immobilization method—has also been developed based on the introduction of dithiocarbamate groups as photo-iniferter onto the hydrophilized PP membrane surface. The grafting mechanism was studied and the investigation of grafting controllability was carried out by modifying membrane at varied functionalization parameters and by various characterizations of grafted membranes. The "livingness" of graft polymerization via this method was also investigated.

Anion exchange membrane adsorbers with various grafted layer architectures (low and high grafting density, with and without slight cross-linking) have been prepared from (2-(methacryloyloxy)ethyl) trimethylammonium chloride aqueous solution via synergist immobilization method and conventional photo-initiator adsorption method. The performances of various membrane adsorbers have been evaluated by buffer (with and without extra salt) permeability, static and dynamic binding capacity as well as breakthrough and elution curves. The grafting efficiency and controllability during surface functionalization as well as the performances of the resulting membrane adsorbers (with similar degree of grafting (DG) and grafted layer structure) were compared between two photo-grafting methods.

Affinity membranes have been prepared from acetonitrile solution of functional monomers via synergist immobilization method. Track-etched PET400 membrane was used as support. A series of proteins with different size and isoelectric point have been used to detect the binding capacity on the resulting affinity membranes. Based on the significant difference in binding capacity between lysozyme and cytochrome C, the separation of protein mixture (lysozyme:cytochrome C = 1:1) was performed using poly(M1-co-M2)-grafted membrane adsorber (M1 and M2 stand for methacryloylamino-2-hydroxy-propane and 5-(methacryloylamino-m-xylylene bisphosphonic acid tetramethylester, respectively), and the separation effect has been qualitatively evaluated using UV-Vis spectrophotometer.

In order to realize the separation of anantiomers Boc-D/L-phenylalanine (Boc-D/L-PhA), Boc-L-PhA imprinted composite membranes have been synthesized via synergist immobilization and also via iniferter immobilization method. Non-imprinted polymer (NIP)

composite membranes as blank samples have been prepared in the absence of template (Boc-L-PhA) under the identical other conditions. MIP/NIP polymers with various composites were prepared by UV-induced radical polymerization to optimize the recipe (ratio among templat, functional monomer and cross-linker) for better imprinting effect. UV spectrophotometer and high performance liquid chromatography (HPLC) were used to determine the binding capacity of amino acid and the separation factor of enantiomers for both MIP and NIP composites membranes and polymers.

Chapter 2 Theory

2.1 Surface grafting techniques for polymeric membranes

With the extending applications of membrane technology in many fields such as water purification, food and pharmaceutical industry and life sciences, the increasing demands on the quantity and the function of polymeric membranes need to be met. Since demanded interfacial characteristics can rarely be achieved by bulk modifications of the membrane forming polymer without complications in membrane fabrication or with respect to membrane stability, membrane surface modification becomes a unique alternative approach to confer new and improved properties and hence fulfill the higher requirements. Of the modification techniques, surface grafting turned out to be a promising technique to design appropriate membranes for target applications. Overall, the ultimate aim of membrane surface modification is either to minimize undesired interactions (adsorption or adhesion) which reduce the performance (membrane fouling), or to introduce additional interactions (charge, affinity, responsiveness or catalytic properties) for improving the selectivity or creating an entirely novel separation function. Basically, the grafting techniques, which have been developed for polymer surface modification [16], are applicable to polymeric membranes. Therefore, a fast development with respect to membrane modification has been seen in recent years. However, it must be noted that the controllability of membrane modifications is still a challenging issue due to the significantly different reactions in membrane pores from that on the nonporous polymer surface and the limited characterization techniques, especially for the small and irregular pores, as well as the less stability of polymer pore structure under modification conditions. So far, the exploited grafting techniques for polymeric membranes mainly include chemical grafting, radiation-induced, plasma-induced and photo-chemical grafting techniques.

2.1.1 Chemical grafting

Chemical grafting can proceed along two major routes: direct chemical reactions and graft polymerization from membrane surface. Surface modification by direct chemical reactions is usually applied for the membranes with reactive surface groups. Otherwise, a strong chemical environment (e.g., strongly basic or acidic or oxidizable) has to be provided to change the surface properties of membranes.

It was reported [17] that the surface of the cross-linked poly(vinyl alcohol) (PVA) membrane was hydrophilically modified by reacting with monochloroacetic acid, and the resulting membrane exhibited a significantly improved permselectivity for water while the flux was unchanged, compared to the unmodified membrane. Lee et al. [18] prepared novel phosphorylated chitosan membranes by the reaction of orthophosphoric acid and urea on the surface and used them to separate 90 wt% ethanol/water mixtures. The surface carboxylation had been proved to be a very effective method to improve pervaparation (PV) performance of chitosan membrane for the separation of aqueous organic mixtures [19]. In addition, a moisture content-responsive polyurethane (PU) membrane has been obtained via the reaction with hexamethylene diisocyanate followed by poly(ethylene glycol) (PEG) grafting [20]. Synthesis of polypeptides onto the whole surface of track-etched PET membrane has been realized via pre-functionalization (oxidation and amination) of PET membrane [21].

However, it has been realized that limited number of membranes can be modified via direct chemical reaction; on the other hand, the harsh reaction conditions may destruct the base membrane structure. In addition, usually it is hard to deal with the uniform modification with macromolecules, which would limit the exploitation of novel membrane functions. This, however, can be realized by graft polymerization. Free radicals are produced from the added initiators and transferred to the substrate, leading to graft polymerization in the presence of monomers. Redox initiator system is found to be often used for membrane surface modification. For instance, Fe^{2+}/H_2O_2 were applied for graft functionalization of polyacrylonitrile (PAN) membrane in AAm solution to improve the water wettability [22]. Commercial polyamide composite membrane was successfully grafted with polymethacrylate (PMA) and poly(ethylene glycol methacrylate) (PEGMA), which was initiated by $K_2S_2O_8/Na_2S_2O_5$ system [23]. Ce^{4+} as an oxidizer also can induce the graft modification of some polymeric membranes with oxidizable groups, e.g., PAN [24] and hydroxylated PP membranes [25]. In addition, surface modification of a hydrophobic poly(vinylidine fluoride) (PVDF) membrane using a polar monomer had been performed via chemical grafting using benzoyl peroxide to impart permanent hydrophilicity [26]. Using the same initiator and supercritical CO_2 as a solvent, pH sensitive membrane was prepared by grafting poly(acrylic acid) (PAA) on the porous PP membrane [27]; the modification of PVDF membrane with maleic anhydride/styrene improved the biocompatibility [28]. Relative to direct chemical reaction, free radical polymerization, in most cases, is undertaken in mild conditions. However, the grafting efficiency may be low

because of the occurrence of homopolymerization in bulk solutions. Apart from the general free-radical mechanism, atom transfer radical polymerization (ATRP) is also an interesting technique to carry out grafting. Prior to graft polymerization, halogen should be introduced on the membrane surface generally by chemical reactions. Husson et al. modified the microprous PVDF membrane using ATRP [29]. It was claimed that it is possible to tune the ion-exchange capacity and the average pore size of the resulting grafted membrane in rational ways. Later, a cation-exchange membrane with high binding capacity has been prepared via the same method on the basis of cellulose membrane [11]. This technique had been also used for the graft modification of PP microporous membrane [30] and track-etched PET membrane [31, 32].

2.1.2 Radiation-induced grafting

In a review paper by Nasef and Hegazy [33], it was reported in detail about the radiation-induced graft copolymerization for the preparation of ion-exchange membranes. Because the excitation with high energy irradiation has a low selectivity, bond scissions in the volume of a membrane material cannot be avoided. This grafting method is relatively rarely used for polymeric membrane modification except for some membranes with inert surfaces, e.g., polyethylene (PE) and PVDF. For the formation of radicals, electron beam and Co-60 (γ-radiation) are usually applied. Saito and his co-workers have developed a grafting method based on the radical initiation by electron beam [34]. Using this method a variety of functional groups had been introduced on the porous PE hollow fiber as well as HDPE membranes for different applications, e.g., various membrane adsorbers [35-37]. Graft modification of PVDF porous membrane with AA and sodium 4-styrenesulfonate (SSS) was also initiated by electron beam [38]. In addition, the graft functionalization of PE sheet membrane was induced by γ-irradiation for the preparation of ion-exchange membrane [39]; Temperature-responsive [40] PVDF membrane as well as a dialysis chloroprene rubber membrane [41] had also been realized by grafting PolyNIPAAm and PolyHEMA, respectively, on the membrane surface under γ -irradiation.

2.1.3 Plasma-induced grafting

Plasma-induced grafting is a useful technique in the modification of surface properties. The excitation with plasma is very surface selective [42]. Currently, more attention is being given to its applications in membrane separation science. Low temperature plasma technique has extensively been used to modify membrane surface. Overall, three effective

routes could be involved: plasma treatment, plasma treatment followed by graft polymerization and plasma polymerization.

Via direct plasma treatment membrane surface property can be readily modified (e.g., usually the hydrophilicity) by the introduction of various polar functional groups due to the optional process gases. For example, He [43], CO_2 [44], N_2 [45], O_2 [46], H_2O [47], NH_3 [48, 49] and He/H_2O [50] have been used to improve the hydrophilicity of membranes. One of the major drawbacks of plasma treatment is, however, that the physicochemical characteristics of the modified surfaces, including surface composition, can be time dependent. Polar and chain group reorientation in the surface region can result in gradual deterioration of the surface functionality. This process, called aging or "hydrophobic recovery", partially restores the original hydrophobic surface to the extent that it adapts composition to the interfacial force. This hydrophobic recovery should be reduced or eliminated to obtain long-term hydrophilicity for practical applications of the membrane.

This can be avoided by further graft functionalization, i.e., two steps are involved: Polymeric membrane is first plasma-treated in the presence of inert gas (e.g., Ar or He); subsequently, monomer in solution or in vapor phase is initiated to polymerize from membrane surface. In many cases, a layer of peroxide groups are formed upon the plasma-treated membrane was taken out of the plasma reactor. Subsequent graft polymerization proceeds in monomer solution via thermal decomposition of peroxide groups. Graft polymerization of PAN and polysulfone (PSf) UF membrane surfaces, which were treated by pure helium plasma, was performed in hydrophilic monomer solutions [51]. By this means, stimuli-responsive composite membranes have been prepared by grafting environmental sensitive monomer (AA or NIPAAm) onto membrane surface [52, 53]. In another route, membrane modification is achieved by Ar- or He-plasma treatment followed by graft copolymerization with monomer in the vapor phase. PAAm and PSt have been grafted on the microporous PES and PAN UF membrane surfaces, reapectively, via this modification route [54, 55].

Plasma polymerization is a procedure, in which gaseous monomers (saturated or unsaturated), stimulated through a plasma, condense on freely selectable substrates. In this case, cross-linking structure is generally formed; grafted layer with functional groups has high stability but very low controllability due to the complicated reactions. Generally, this route is applied for simple modifications (e.g., improvement of hydrophilicity) [56, 57]. In some cases, the "hydrophobic recovery" was also observed [58].

However, the ablation tendency of the base polymer may be significant [50], although the

plasma treatment conditions could be adjusted and optimized. In addition, modifications in small pores (diameter <100 nm) are complicated because this dimension is smaller than the average free path length of the active species in the plasma [59].

2.1.4 Photo-chemical grafting

The excitation with UV irradiation has the great advantage that the wavelength can be adjusted selectively to the reaction to be initiated, and, hence, undesired side reactions can be avoided or at least reduced very much. Photo-initiation can be used without problems also in small pores. The UV technology can be integrated into continuous manufacturing processes simply and cost-efficiently. Photo-initiated processes have their largest potential when complex polymer morphologies need to be surface-selectively functionalized with minimal degradation of the base membrane, and when they are used to create macromolecular layers via 'grafting-to' or 'grafting-from' [59]. So far, many photo-grafting routes have been developed and used for various modifications of polymeric membranes; and various membrane functionalies has been realized via photo-grafting methods (detailed see section 2.2).

A key feature of a successful surface modification is to realize a synergy between the useful properties of the base membrane and the changed chemical structure within the barrier or the novel functional polymer (layer) added to the barrier. This synergy can only be achieved by a mild and controllable modification technique, and photo-chemical processes have a large potential in that regard.

2.2 Photo-graft functionalization on polymeric membranes

For surface selective photo-chemical processes, two alternative approaches are distinguished: (i) coupling small molecular entities or larger macromolecules to the surface ("grafting-to") or (ii) heterogeneous graft copolymerization where monomers are polymerized using starter groups on the surface ("grafting-from").

2.2.1 "Photo-grafting-to" functionalization

"Photo-grafting-to" functionalization of a polymeric membrane is based on the photo-reaction between membrane polymers and functionalization agents. Therefore, at least one type of photo-reactive group which has a distinct, selective and efficient reactivity is required. Aromatic azides or diazo compounds including their carbonyl "cousins" (azidocarbonyl or diazocarbonyl) are important examples. Under the photo-

irradiation the decomposition of these compounds takes place along with the release of nitrogen, which can subsequently lead to addition (via nitren / isocyanate or carben / ketene) or to cross-linking reactions (via nitren dimerization) (Fig. 2.1). Such reactions are also being used for "photo-affinity labeling" of bio-molecules, e.g., proteins [45]. Another important principle is the photo-induced dimerization via [2+2] cycloaddition, e.g., of cinnamate, coumarin or styrylpyridine groups (this reaction is only possible via the excited state). Depending on the chemistry of the photo-reactive groups, controlled elimination or addition reactions are possible, also including dimerization reactions leading to cross-linking of macromolecule chains.

Therefore, according to the location of these photo-reactive moieties, two routes can be classified: via photo-reactive membrane polymer and via photo-reactive functionalization agents (Fig. 2.2). Since this approach is relatively independent on the chemical composition of materials (cf. above), various functionalization agents can be attached onto a membrane surface with photo-reactive moieties, or a variety of membranes (non-porous and porous, different membrane polymers) can be modified without any pre-treatment by using photo-reactive functional molecules.

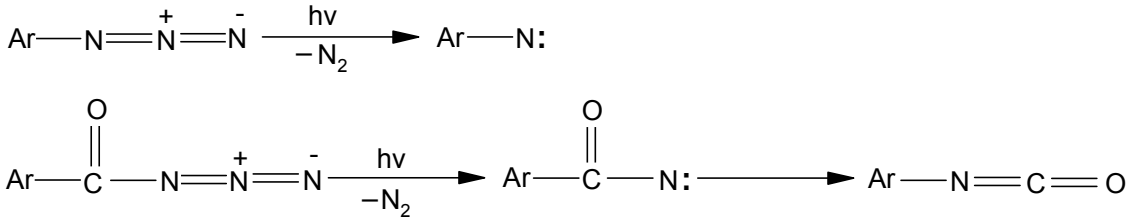

Aromatic azides

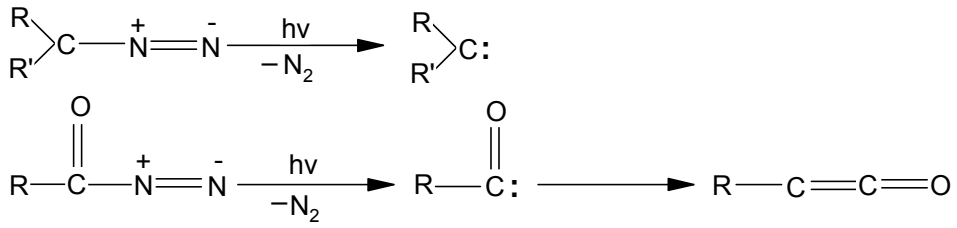

Diazo compounds

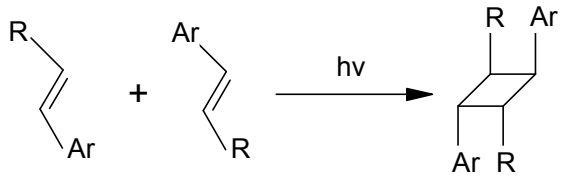

Aromatic vinyl compounds ([2+2] cycloaddition)

Figure 2.1: Three groups of photo-reactive moieties and their main photo-initiated reaction pathways.

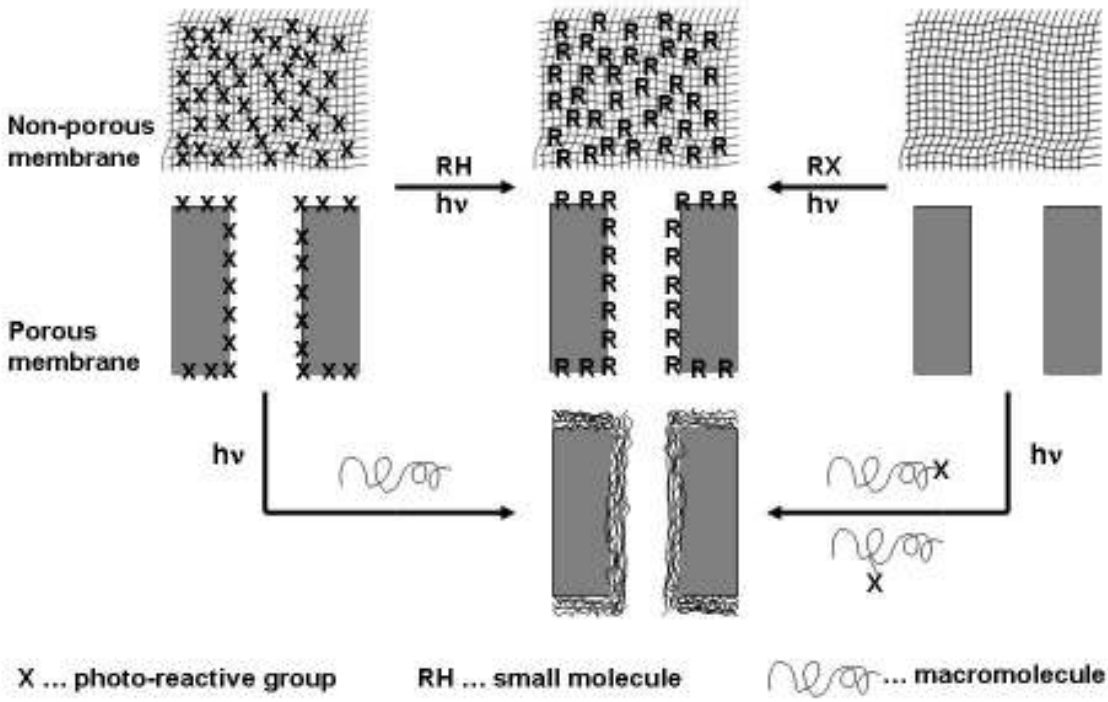

Figure 2.2: Depiction of principal mechanisms for photo-functionalization of polymeric membranes: via photo-reactive membrane polymer (from left) and via photo-reactive functionalization agents (from right).

Photo-reactive membrane polymer. Taking advantage of the photo-reactivity of such typical moieties, membrane surface modification had been extensively investigated. One of the approaches is by direct synthesis of membrane forming polymer with photo-reactive groups. For example, Darkow et al. [61] synthesized a new type of membrane polymer, poly(acrylonitrile-co-butadiene-co-styrene-co-2-(4-ethenyl)phenyl-5-phenyl-2H-tetrazole), containing a photo-sensitive moiety, yielding a reactive nitrilimine (1,3-dipole) after photolysis. Non-porous membranes with a thickness around 15 μm have been prepared and then functionalized using a variety of dipolarophiles and phenolic compounds to alter the polarity of the membrane surface. The photo-functionalization with more polar groups led to an increase in permselectivity towards benzene in a cyclohexane / benzene mixture in PV. A photo-chemically reactive thin-film composite membrane was produced by the interfacial copolymerization of 3-diazo-4-oxo-3,4-dihydro-1,6-naphthalene disulfonylchloride and naphthalene-1,3,6-trisulfonylchloride with 1,6-hexanediamine on a PSf UF membrane [62, 63]. The post-functionalization of the resulting polysulfonamide membrane surface was carried out via a photolysis of the polymer-bound diazo-carbonyl groups in the presence of various nucleophiles, yielding membranes containing various functionalities such as acid, ester, bromoethyl ester, dioxolan and hydroxyethyl ester (cf. Fig. 2.1). These changes of membrane polarity resulted in significant and predictable

changes of the reverse osmosis separation performance.

Owing to the often complicated synthesis of special polymers and good membranes from such novel polymers, an alternative is that reactive groups are immobilized onto an already prepared (and optimized) membrane by either chemical reaction or polymer coating. Nahar et al. [64, 65] prepared a photo-reactive cellulose membrane by the coupling of 1-fluoro-2-nitro-4-azidobenzene to the hydroxyl groups of cellulose. The reactive membrane was used for UV- or sunlight-induced covalent immobilization of proteins, which is similar to a well-known technique for photo-affinity labeling of biomolecules [60]. It should also be possible to further functionalize these photo-reactive membranes for other applications.

A new "photo-grafting-to" surface modification technique has been developed as well, based on the coating of the membrane (here a 0.22 μm MF membrane from a cellulose ester) with a monolayer of allyldimethylchlorosilane [66]. A triblock copolymer of polyethylene oxide and polypropylene oxide (PEO-PPO-PEO) was covalently linked to this reactive surface membrane by UV irradiation at wavelength >215 nm. Reduced fouling and better cleaning during microfiltration of protein solutions were observed. However, this approach has an obvious disadvantage, i.e., the short wavelength UV irradiation also degraded the base membrane; it had been reported that the resulting membranes became too fragile after 1.5 hr UV irradiation.

Photo-reactive functionalization agent. In comparison with the routes above, the use of "tailored" photo-reactive agents for surface functionalization can have significant advantages with respect to process simplicity and controllability. For example, using well-defined aryl azide (cf. Fig. 2.1), a single and generic procedure ("photo-grafting-to") should permit covalent attachment of a wide variety of chemical moieties, making it a very versatile process also from the practical point of view.

PAN UF membranes were photo-chemically functionalized with low molar mass aromatic azide derivatives comprising different hydrophilic and hydrophobic substituents [67, 68]. These functionalization agents were coated to the membrane surface and the degree of functionalization could also be controlled by UV irradiation time. The separation characteristics and protein fouling tendency were markedly changed depending on the type of functional groups introduced. In an extension of that work, well-defined photo-reactive α-4-azidobenzoyl-ω-methoxy-PEG (ABMPEG) was synthesized and photo-grafted onto the PSf ultrafiltration membranes by exposing the pre-adsorbed ABMPEG to UV irradiation [69]. An optimum membrane performance had been achieved using

monofunctional ABMPEG at relatively high concentrations during the photo-grafting procedure, yielding predominately end-on attached PEG chains on the membrane active layer surface. The hydrophilicity of modified membranes increased and the irreversible character of the grafting procedure was proved, indicating the covalent attachment of ABMPEG upon photo-initiation. The significant reduction of protein adsorption by photo-grafted PEGs contributes to both fundamental and practical solutions of the protein fouling problem [70]. Two different "photo-grafting-to" routes for the PEGylation of the important membrane polymer PSf by using arylazides have been compared recently [71]. Due to steric hindrance between grafted PEG chains, the complete surface coverage of the base polymer was hard to achieve; however, such PEGylated surfaces with incomplete surface coverage showed a significantly improved biocompatibility [72, 73], presumably due to the stabilization of the native conformation of adsorbed proteins [74]. Therefore, those PEG functionalizations may find application in membrane-based tissue-culture systems for sensitive adhesion-dependent cells.

Temperature-responsive polymer conjugates, two types of azidophenyl-derivatized poly(NIPAAm)s [poly(NIPAAm)-Az—aryl azide group only on chain end, and poly(NIPAAm-co-AA/Az)—aryl azide groups as side groups on the chain], were photo-chemically grafted in track-etched polycarbonate (PC) membranes (pore diameter 200 nm) [75]. Different thermo-sensitive composite membranes were obtained depending on the type and amount of modifier; "thin-layer" or "pore-filling" functionalized membranes showed opposite temperature responsiveness of barrier properties as judged from filtration and diffusion experiments with tryptophan as solute. A model has been presented for the interpretation of the observed phenomena (Fig. 2.3). Another thermo-responsive membrane was prepared by photo-grafting poly(N-vinylcaprolactam) (P(VCL-co-AA/Az)) chains via their aryl azide conjugates to the surface of PET track-etched membranes (pore diameter 400 nm) [76]. However, the authors claimed that photo-grafting occurred only on the outer PET membrane surface instead of in the pores. This is consistent with the observations when the same membrane was modified using simultaneous "grafting-from" method [77] (see below).

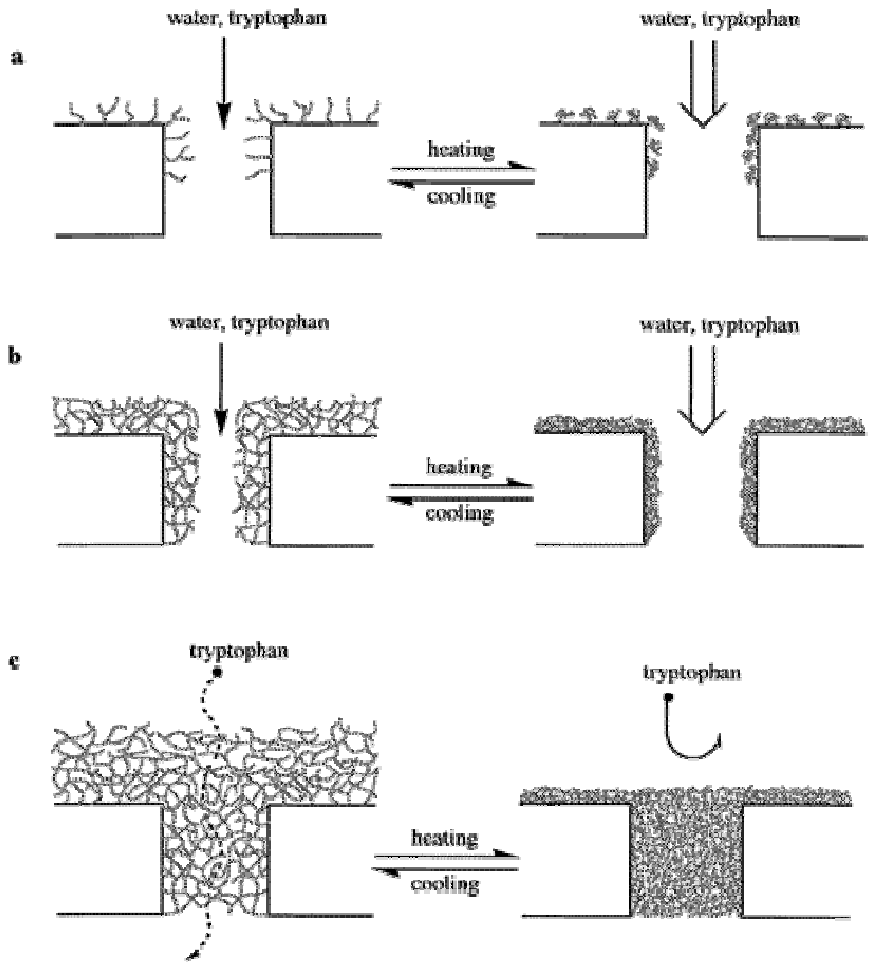

Figure 2.3: Thermo-responsive permeation of water or trytophan through polymer-immobilized membranes. (a) poly(NIPAAm) grafted membrane; (b) poly(NIPAAm-co-AA)-grafted membrane (low grafted mass); (c) poly(NIPAAm-co-AA)-grafted membrane (large grafted mass) ([75]).

PEG "brushes" (thickness ~20 nm) were photo-grafted via their azide conjugates onto the PSf UF membrane surface, by that means obtaining a membrane with PEG-immobilized silver salt as fixed carrier which showed facilitated transport for olefins. High propylene permeance and selectivity (12 for propylene over propane) were observed [78]. This is the only example, that a porous barrier had been changed into a non-porous one by a "grafting-to" method.

In conclusion, "photo-grafting-to" method has the potential advantage that the structure of the functionalization agent (e.g., a photo-reactive polymer conjugate) to be used for surface modification can be well controlled by synthesis and characterized in detail. However, the grafting densities and homogeneity on the surface and hence the modification efficiency are limited due to the steric hindrance effect which is increasing with the size of the functionalization agent. Moreover, photo-reactive polymer conjugates may react not only with the membrane surface but also with adjacent other molecules. This is even more

pronounced if conjugates with more than one photo-reactive group are used (see [69, 75]). In addition, accessibility to membrane pores for macromolecular functionalization agents may be limited.

2.2.2 Heterogeneous graft copolymerization ("Photo-grafting-from")

The stability and controllability of grafted polymer layers on the surface of a base polymer membrane are two crucial evaluation parameters for functionalization techniques. Especially the controllability has received increasing attention in terms of architecture and property of grafted polymers. Due to disadvantages of "photo-grafting-to", especially with respect to grafting density, "photo-grafting-from" technique has been increasingly used and developed.

In order to really tailor and optimize the membrane performance, various routes have been developed depending on initial membrane materials and structures, architectures of grafted polymer, and used modification system including properties of monomer and solvent. It should be mentioned that radical polymerization has almost exclusively been used until now. Photo-grafting can proceed in two ways: without or with an added photo-initiator. The approach "without added photo-initiator" involves the direct generation of free radicals from the base membrane polymers under UV irradiation. Therefore, such methods require either a photo-sensitive base polymer (photo-reactive side group or part of polymer backbone) (cf. Fig. 2.4a) or the introduction of photo-sensitive groups onto the membrane surfaces prior to graft copolymerization (Fig. 2.4b). For approach "with added photo-initiator", initiating radical sites should be generated on the membrane surface by the reaction of photo-initiator with the base membrane polymer under UV irradiation. One possibility is that the formed radicals by homolysis of initiator transfer to the base polymer, which initiates graft copolymerization (cf. Fig. 2.4c). But the homopolymerization may simultaneously take place in bulk solution, affecting surface grafting. Another more surface-selective grafting approach is to use Norrish type II initiator (e.g., benzophenone (BP) or xanthone, and their derivatives). The excited initiator by UV irradiation abstracts hydrogen from the membrane polymer. The resulting radicals on membrane surface are reactive to initiate polymerization, whereas the radicals formed in initiator side are relatively inert (Fig. 2.4d). Therefore, the surface-selective photo-grafting can be reached. In addition, the addition of the additives or co-initiators may enhance the surface-selectivity of photo-grafting.

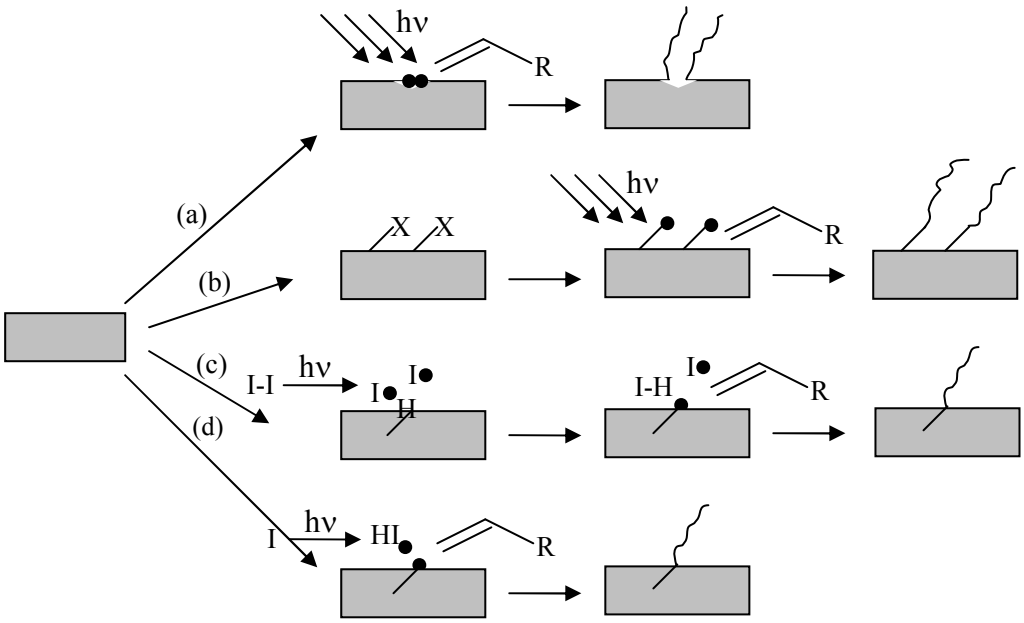

Figure 2.4: Heterogeneous radical graft copolymerization ("photo-grafting-from") of functional monomer on membrane surfaces initiated by (a) degradation of the membrane polymer (main chain scission or cleavage of side groups), (b) cleavage of photo-reactive groups immobilized on membrane surfaces, (c) decomposition of an initiator in solution and radical transfer (here hydrogen abstraction) to membrane surfaces, (d) hydrogen abstraction of the excited Norrish type II initiator under photo-irradiation. ● stands for radicals formed under photo-irradiation; X represents photo-reactive groups.

Without added photo-initiator. PSf and PES, due to their mechanical, thermal and chemical stability as well as excellent film forming properties, are frequently used as materials for high performance UF or MF membranes. However, the hydrophobicity of the materials can cause problems, e.g., in applications with proteins where adsorption and deposition yield membrane fouling. Therefore, attachment of hydrophilic polymer chains to the membrane surface to significantly increase the wettability of membrane surfaces and hence reduce fouling is a promising strategy to extend their applications. It had been discovered that all poly(arylsulfone)s are intrinsically photo-sensitive and generate free radicals upon UV irradiation (cf. Fig. 2.4a). Taking advantage of this knowledge, Crivello, Belfort and coworkers [79, 80] have developed a novel method for surface modification of poly(arylsulfone) membranes. And different hydrophilic polymers have been successfully photo-grafted from vinyl monomers in water or methanol onto poly(arylsulfone) membranes with a high surface-selectivity. The investigation of the reaction mechanism had verified that the phenoxyphenyl sulfone groups as chief chromophores are responsible for the photo-reactivity of poly(arylsulfone)s. As shown in Fig. 2.5 [81], the first step involves the absorption of light by the phenoxyphenyl sulfone chromophores in the

backbone of the polymer chain. The homolytic cleavage of a carbon-sulfur bond at the sulfone linkage takes place due to the photo-excitation. Generated aryl radical and sulfonyl radicals are reactive enough to act as starter for a radical polymerization. Alternatively, the sulfonyl radical may lose sulfur dioxide to generate an additional aryl radical which may also initiate polymerization. Ulbricht et al. had also investigated the mechanism for photo-grafting of PES and PSf, including a comparison without vs. added photo-initiator [82].

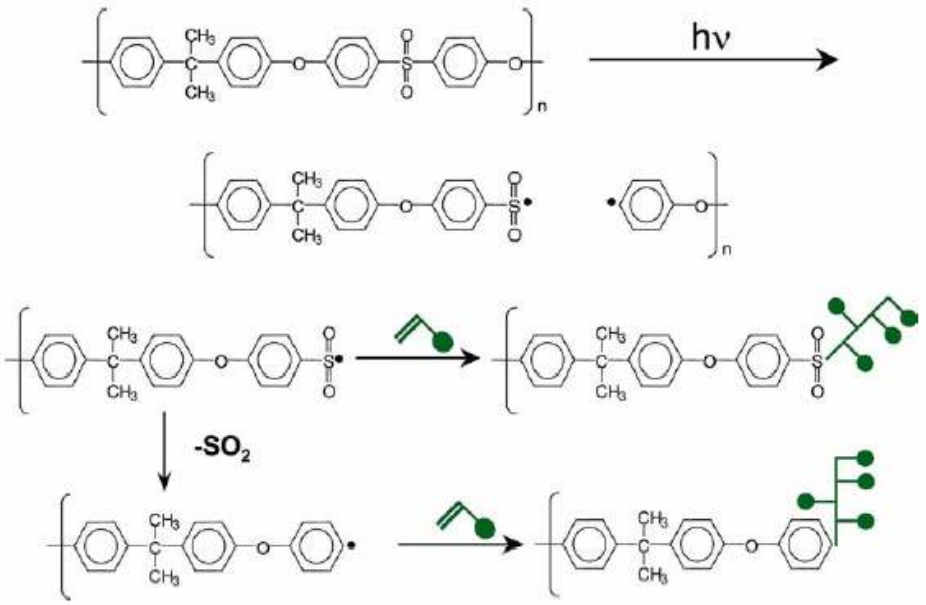

Figure 2.5: Proposed mechanism for the photo-chemical modification of poly(arylsulfone)s with vinyl monomers.

However, it was found that the membrane pores become larger under UV-irradiation due to the polymer degradation [80, 83]. To improve the application properties of poly(arylsulfone)-based composite membranes prepared via this technique, intensive investigations have been carried out in the group of Belfort, involving the dependence of grafting efficiency and properties of modified membranes on base membrane [84], monomer type [85], UV wavelength and intensity [86, 87], employed polymerization methods [88] as well as chain transfer agent [89].

Recently, low-fouling PES-based ultrafiltration membranes have been successfully established via simultaneous photo-graft polymerization of the hydrophilic monomer PEGMA onto the membrane surface [90, 91]. The grafted new thin-layer polymer hydrogel had significant influences on the flux and selectivity depending on its surface coverage, layer chain conformation, layer swelling and thickness. In addition, the addition of the cross-linker during modification may improve both permeate flux and solute rejection

during ultrafiltration [90].

The first example of a combination of two different photo-irradiation techniques is an optically reversible switching PES membrane surface, obtained by photo-grating a monomer with photo-chromic side groups [92].

Due to its potential, this technique is also being seriously evaluated by membrane manufacturers. An interesting example with respect to both, photo-irradiation and membrane technologies, had been made via the continuous photo-functionalization of the outer skin of PSf hollow-fiber membranes with an anionic grafted polymer layer to obtain nanofiltration (NF) membranes [93].

With other photo-sensitive polymers, where UV irradiation leads to formation of polymer-bound radical, addition of photo-initiator is also not required for "photo-grafting-from". A typical example is that the BP structure is present along the membrane polymer chain. The photo-reduction of BP structure under UV irradiation can generate radicals by abstracting hydrogen from monomer and/or bulk polymer itself (similar to Fig. 2.4d, but without addition of initiator). In this case, cross-linking may occur in the absence of monomer upon UV irradiation. Yanagishita et al. [94] functionalized an UF membrane made of a polyimide (PI) with benzophenone structure (BTDA-p-PDA) via UV irradiation in presence of monomer in gas phase or liquid phase. The obtained pore-filled composite membrane showed benzene permselectivity for benzene/cyclohexane mixture in PV. Successful graft modifications have also been observed for other membranes with BP structures [95, 96].

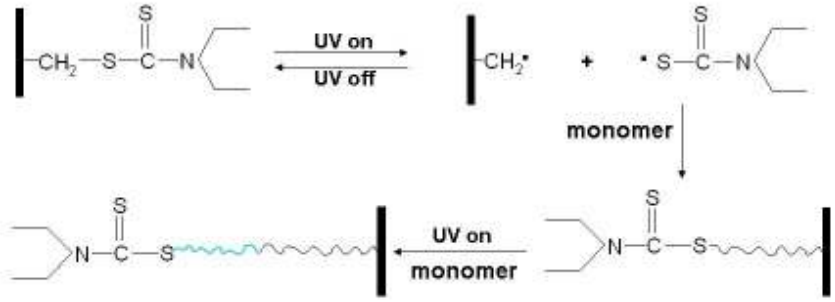

Figure 2.6: Mechanism of "living" polymerization for modification of membrane with iniferter.

Another often used photo-sensitive moiety for polymer surface modification is the benzyl N,N-diethyldithiocarbamate group (cf. Fig. 2.4 b). The possibility to use it for initiation of a controlled ("living") radical polymerization has attracted much attention, and this property had also been termed "iniferter" (initiator, transfer agent and terminator). The mechanism of surface modification is illustrated by Fig. 2.6. Kobayashi et al. [97] have

successfully grafted a thin-layer of a theophylline (THO) imprinted polymer onto the UF membrane, which had been prepared from synthesized poly(acrylonitrile-co -diethylaminodithiocarbamoylmethylstyrene). The resulting MIP composite membrane has been evaluated as a membrane adsorber, and it had been found that it could recognize the THO vs. the similar substance caffeine (CAF) with a high selectivity.

However, the synthesis of these special polymers containing photo-sensitive groups and the following formation of membrane might be a problem in many cases. Therefore, alternatively, a benzyl N,N-diethyldithiocarbamate group had been chemically immobilized on the surface of an established membrane via simple coupling reactions. Using immobilized photo-active iniferter, a molecule-responsive "gate" membrane was prepared via surface functionalization of the skin layer in the pores of a commercial cellulosic dialysis membrane with a hydrophilic MIP [98]. The increase in DG value for re-initiation via multiple sequential UV irradiation periods indicated that graft copolymerization may proceed via a controlled ("living") mechanism. Such an approach should be helpful for the preparation of more sophisticated architectures, e.g., block structures, of the grafted layer.

Guan et al. have developed another photo-grafting route, based on the combined use of photo-oxidization and UV irradiation grafting [99]. Hydroperoxide groups were created on the membrane surface by photo-oxidation in hydrogen peroxide in the first step. Grafted copolymer layer on the membrane has then been obtained in the presence of monomer under UV irradiation in the second step. To minimize the homopolymerization, an appropriate amount of iron (II) was added in the monomer solution as a reductant. The grafted membranes have been applied for promotion of human endothelial cell adhesion and growth [100-102].

With added photo-initiator. Many surface modifications of porous membranes in laboratory and technical scale are performed using cross-linking polymerization to form thin layers covering the entire pore surface. For such modification, conventional ("type I") photo-initiators (for example, benzoin derivatives, or organic peroxides or azo compounds, i.e., starter radials are directly formed by cleavage of a weak bond in the initiator; cf. Fig. 2.4c) can be very efficient because very fast processes can be realized under ambient conditions. During the reaction, radical transfer to base polymer is possible (except for chemically very stable materials such as Teflon). Therefore, chemical grafting of the newly formed polymer layer to the support membrane may take place to some extent. The most important example for a commercial application is the hydrophilization of MF membranes

made, for instance, from PVDF [103] or PP [104], using hydrophilic polyacrylates; this modification improves the wetting of the porous membranes by water and reduces the non-specific binding of (bio)macromolecules (i.e., membrane fouling). Another very special example is the synthesis of thin-layer MIP composite membranes based on MF membranes via a cross-linking polymerization initiated with help of the photo-initiator benzoin ethyl ether [105, 106].

In order to achieve better control over the heterogeneous "photo-grafting-from" of polymer surfaces, the "type II" photo-initiators, mostly BP or its derivatives, were frequently used. This type of photo-initiator undergoes photo-reduction by hydrogen atom abstraction from surrounding chemical species, which leads to the generation of initiating radicals (cf. Fig. 2.4d). Therefore, a preferential hydrogen abstraction from the substrate polymer is an essential prerequisite for high surface selectivity of graft copolymerization; the homopolymerization in solution should be minimized. For this purpose, several strategies have been proposed (Fig. 2.7).

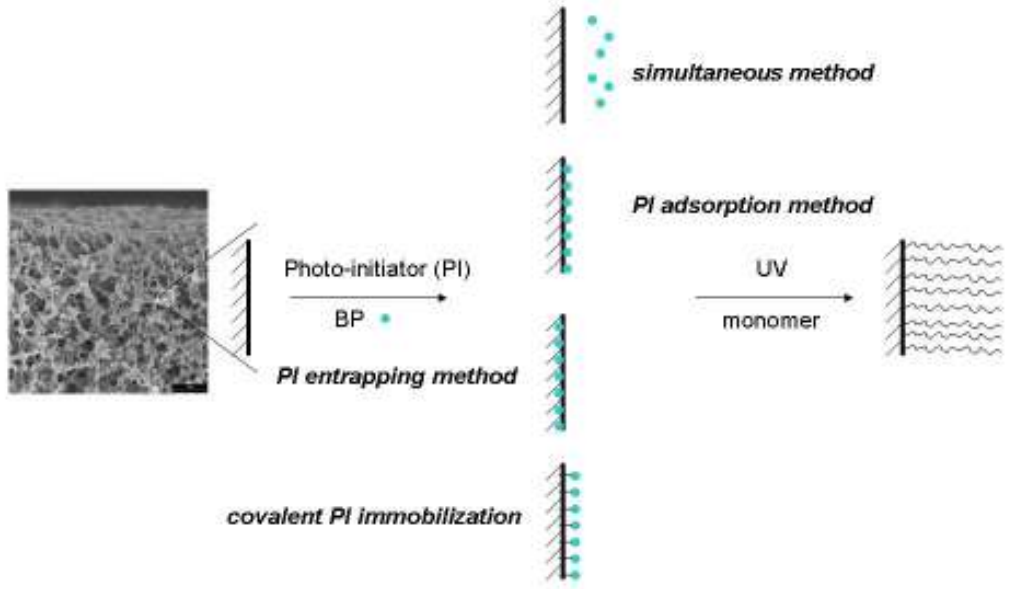

Figure 2.7: Schematic depiction of methods for the immobilization of a "type II" photo-initiator (here benzophenone) for photo-grafting functionalization of membranes.

As known for rather long time for the modification of polymer surfaces (not in the context of membranes), BP and its derivatives can be used to graft various functional polymers by just dissolving the initiator in the monomer solution [107-109]. Recently, Yang et al. [77, 110, 111] modified PET Nucleopore membranes using the same approach, i.e., the simultaneous method. They observed that the photo-grafting occurred only on the top surface rather than in the membrane pores. Membranes with thermo- or pH-sensitive

permeability have been obtained by photo-grafting NIPAAm or 4-vinylpyridine (4VP), respectively. Via a similar method, Liu et al. [112] prepared a thermo-sensitive nylon MF membrane, by a rapid bulk photo-grafting polymerization of N,N-diethylacrylamide (the photo-initiator BP was dissolved in the liquid monomer, used without any solvent). The grafted polymer was observed on the top surface and in the pores, but not on the backside (remote from UV). Photo-grafting / pore-filling with poly(PEG acrylate) has also been realized on/in PAN UF membranes via simultaneous method [113]. The obtained thin and defect-free barrier layer contributes to the high membrane performance for CO_2/N_2 separation.

Though this simultaneous approach is a quite facile technique, there are significant disadvantages. First, usually, the hydrogen atoms in many commercial membrane polymers are not very reactive to the excited BP. In that case, the selection of solvent should be considered very carefully, in particular only solvents without labile hydrogen (e.g., water or acetonitrile) should be used to minimize homopolymerization and enhance the surface-selectivity. Second, the local concentration of BP on the membrane surface is quite low because BP moves to the membrane surface only by diffusion, whereas high bulk BP concentration may give rise to side reaction such as homopolymerization. These two factors lead to a low grafting efficiency and/or not well defined polymer architecture (in the examples mentioned above, the contribution of branched grafted copolymer, cross-linked polymer or entangled homopolymer to the final membrane properties can be significant). Moreover, the use of monomers which do not have common solvent with BP (for instance, BP is almost insoluble in water) is limited.

In order to improve the grafting efficiency, the photo-initiator adsorption method has been proposed [114,115] (cf. Fig. 2.7). The local BP concentration was increased via pre-coating of BP on the membrane surface, and the BP concentration in the bulk of monomer solution was kept very low or close to zero, which minimized the homopolymerization. Those conditions can be realized very well by using aqueous monomer solutions because the solubility of BP is low. This method has been extensively applied to various types of membrane polymers, PAN [116], PP [117,118], Nylon [115], PSf [82, 119], PET [120], PVDF [121] and the novel photo-functionalized (composite) membranes have found applications as membrane adsorber [117] or as enzyme-membrane [120]. Main reasons are the flexibility with respect to selection of support membranes (only hydrogen donor properties are required) and grafted polymer functionality and structure. However, the conditions need to be optimized for each membrane material, pore structure, graft

functionality and layer design to meet the needs of different applications; this will be discussed with the help of examples below.

Pore-filled PAN UF membrane has been successfully established by grafted functional polymer chains attached to surface when two necessary conditions have been met: DG ≥ $DG_{critical}$ and small pores in the skin layer of the support membrane (≤ 12 nm in diameter) [122]. An extension of that work for the separation of aromatic/aliphatic mixture has also been reported [123-126].

PAN UF membranes was also grafted with monomethoxy poly(ethylene glycol) methacrylates (MePEG200MA) [127]. A hydrophilic and low-protein-adsorbing UF membrane with relatively high permeability has been established by adjusting the degree of grafting via UV irradiation time and monomer concentration.

By applying longer UV wavelength and the photo-initiator BP, PSf UF membranes also have been modified in a controlled way with PAA layer for covalent immobilization of biomolecules [82]. This technique avoids the negative effect of using direct UV irradiation above that desired functionalization was usually accompanied by strong pore etching in the UF membrane active layer (see above). Borcherding et al. [117] reported that a PP MF membranes functionalized with the reactive poly(glycidyl methacrylate) (polyGMA) preserved its high permeability and exhibited high receptor coupling capacity for recombinant protein A, due to the thin grafted layer and a great deal of epoxy groups introduced on membrane surface. Based on the very promising results, it is possible to tailor both membrane structure and application protocols towards other attractive affinity separations of biomolecules.

Due to the high surface-selectivity of this method, a thin and compact cross-linked layer can also be synthesized onto the whole surface of a porous membrane, which maintains a high permeability and relatively large specific surface area, e.g., for affinity binding. Thin-layer MIP composite membranes, covered with an imprinted polymer layer selective to small molecules (shown for herbicides) in a mixture with similar compounds, have been prepared by Piletsky et al. [118] and Sergeyeva et al. [121]. The high affinity of these synthetic affinity membranes to templates together with their straightforward and inexpensive preparation provides a good basis for the development of applications of imprinted polymers in fast separation processes such as solid-phase extraction [128, 129]. This photo-grafting method was successfully adopted also by other groups [130, 131].

The even, tight and defect-free filling of large membrane pores (from PP or PET) with porous polyacrylate-based monoliths was based on a pre-functionalization of the pore wall

with a compatible photo-grafted copolymer [132]. MIP-pore-filled membranes of such type are currently evaluated for continuous enantio-selective separations [128].

Enzyme membrane reactors also have been prepared based on modified PP MF membranes with polyGMA [133]. An enzymatic chain elongation of maltooligosaccharide molecules was achieved during passage through a membrane activated with immobilized amylosucrase. Commercially available capillary pore membranes (PET) have also been modified for covalent enzyme immobilization within the pores using this approach [120].

It should be kept in mind that the aforementioned extensive applications of photo-initiator adsorption method were based on the graft modification in aqueous solutions, where solvent water does not strongly influence the local BP concentration on the surface. However, to preserve the tenet of this photo-initiator adsorption technique and to achieve the high surface-selectivity, the parameters which could reduce the local BP concentration should be taken into account. For example, a good solvent for BP should not be chosen for high grafting efficiency, though in one special example, a MIP composite PVDF membrane has been successfully prepared from the methanol solution, in which a small amount of BP was added to prevent the rapid reduction of high BP concentration on the surface [118].

To further improve the grafting efficiency and controllability and to extend the application of "photo-grafting from" technique, more efforts have been made in our group, mainly focusing on the immobilization of BP. One improvement is that the weak physical adsorption of BP onto the membrane surface was replaced by ionic interaction between respective functional groups on the surface and the photo-initiator [14], which can be realized by the introduction of charged groups onto the base membrane and the application of counter charged BP derivatives. This stronger immobilization of photo-initiator enabled an efficient and surface selective functionalization because a better control of grafting density and a reduction of photo-initiated side reactions along with a more efficient use of the photo-initiator were possible. Thermo- and pH-responsive PET membranes have been prepared via this method [14, 134]. Various measurements (for example, the trans-membrane zeta potential) indicated the even surface coverage of the pore walls with the grafted polymer. This was the basis for a quantitative analysis of effective layer thickness as function of synthesis conditions and solution conditions.

Another improved strategy –"photo-initiator entrapping"– also has been proposed to strengthen the immobilization of BP in the membrane surface [13]. In this process, BP entrapping was realized by the procedures as follows: membrane was soaked in the BP solution whose solvent can swell base membrane polymer. After drying, slight washing

with non-swelling solvent of membrane polymer followed for removing the adsorbed BP on the surface. The entrapped BP density in the membrane surface could be tuned by the initial BP concentration. Controllable three-dimensional grafted layer structure has been achieved via BP entrapping method to lead to an improved protein binding capacity. Xu et al. modified PP MF membranes via this technique to improve the biocompatibility [135-137]. For example, a novel sugar-containing monomer (D-gluconamidoethyl methacrylate) was grafted on PP via UV-induced graft copolymerization [135]. Results with respect to BSA adsorption and platelet adhesion imply strongly that a considerable enhancement of biocompatibility had been achieved. Using the same conditions, PP hollow fiber MF membranes have been grafted with a hydrophilic layer to improve the anti-fouling characteristics in a submerged membrane-bioreactor [138]. This method had also been used to prepare cross-linked grafted layers, and it had been demonstrated that the dynamic performance of porous membrane adsorbers could be improved [10]; a very high surface selectivity is mandatory for such reaction conditions, because otherwise cross-linked insoluble polymer would be immobilized in an uncontrolled way in the pore space.

In addition, the membrane grafting efficiency has been improved by addition of ferric chloride with optimum concentration, when simultaneous method or adsorption method was adopted [139]. This is ascribed to the "synergistic effect" between Fe^{3+} and BP.

Ma et al. [15, 140] proposed and investigated another photo-induced variant of this graft copolymerization method —"covalent photo-initiator immobilization"— consisting of two steps. This method is based on the discovery of Yang and Ranby that also with BP, a more controlled ("living") grafting mechanism can be realized [108]. In the first step, in the absence of monomer, BP abstracts hydrogen from the substrate to generate surface radicals and semipinacol radicals, which combine to form surface-bound photo-initiators. In the second step, the monomer solutions are added onto the active substrate and a living graft copolymerization is initiated under UV irradiation. In this method, graft density and graft polymer chain length can be controlled by choosing the reaction conditions in the first step and in the subsequent step independently. Moreover, the formation of undesired homopolymer and cross-linked or branched polymer can be substantially eliminated. This approach has been employed to modify membranes for fouling reduction [141, 142]. However, in this process, the cleavage of covalent bond requires high energy, which leads to a low grafting efficiency and might also cause photo-degradation of many graft copolymers.

Combining adsorption and covalent photo-initiator immobilization methods, poly(N,N-dimethylaminoethyl methacrylate) had been photo-grafted onto the PP MF membrane [143]. Based on this reactive polymer layer, phospholipids-analogous polymers have been tethered on the membrane to improve surface biocompatibility in the next reaction.

In brief, many routes for "photo-grafting-from" technique have been developed for polymeric membrane modification via heterogeneous graft copolymerization. In contrast, the synthesis of surface anchored polymers via "photo-grafting-from" is often less controlled with respect to polymer structure, but a very wide variation of grafting densities and chain lengths can be obtained under relatively convenient reaction conditions. Various applications of obtained composite membrane have been found in many fields depending on its membrane material and structure, properties and architecture of grafted layer.

2.3 Membrane functionalities achieved by "photo-grafting-from"

Generally, there are three main composite membrane types, which could meet various demands in different fields: thin-film-, pore surface-functionalized and pore-filled membranes (Fig. 2.8 [59]).

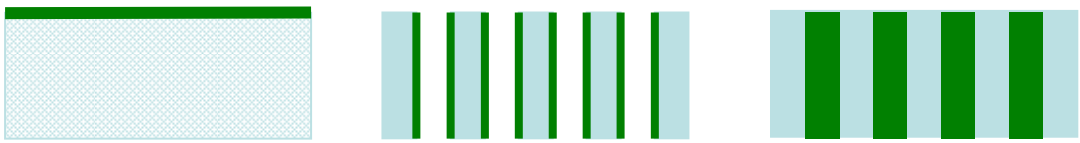

Figure 2.8: Depiction of three main composite membrane types: (a) thin-film, (b) pore surface-functionalized, (c) pore-filled.

In principle, all three types of composite membranes introduced could be prepared via "photo-grafting-from" techniques. However, thin-film composite membranes with non-porous barriers for gas separation or reverse osmosis have been only rarely prepared by grafting (and no report on photo-grafting), because the very high grafting density required for using the intrinsic properties of the new polymer in a non-swollen state as selective barrier are hard to achieve (see recent work with controlled surface-initiated polymerization, e.g., [144]). Many examples can be found for more "loose" grafted layers which should still be permeable, typical examples are anti-fouling modifications, e.g., for UF membranes. Consequently, most composite membranes prepared via "photo-grafting-from" are pore surface-functionalized. Depending on initial pore size (micro/meso pores vs. macropores), grafted layer thickness (ultrathin or extending over 10s

or 100s of nanometers) and its distribution over the membrane cross-section (outer surface vs. entire internal surface) largely different membrane functionalities can be achieved. Representative membrane functionalities achieved via "photo-grafting from" functionalization are illustrated (cf. Fig. 2.9).

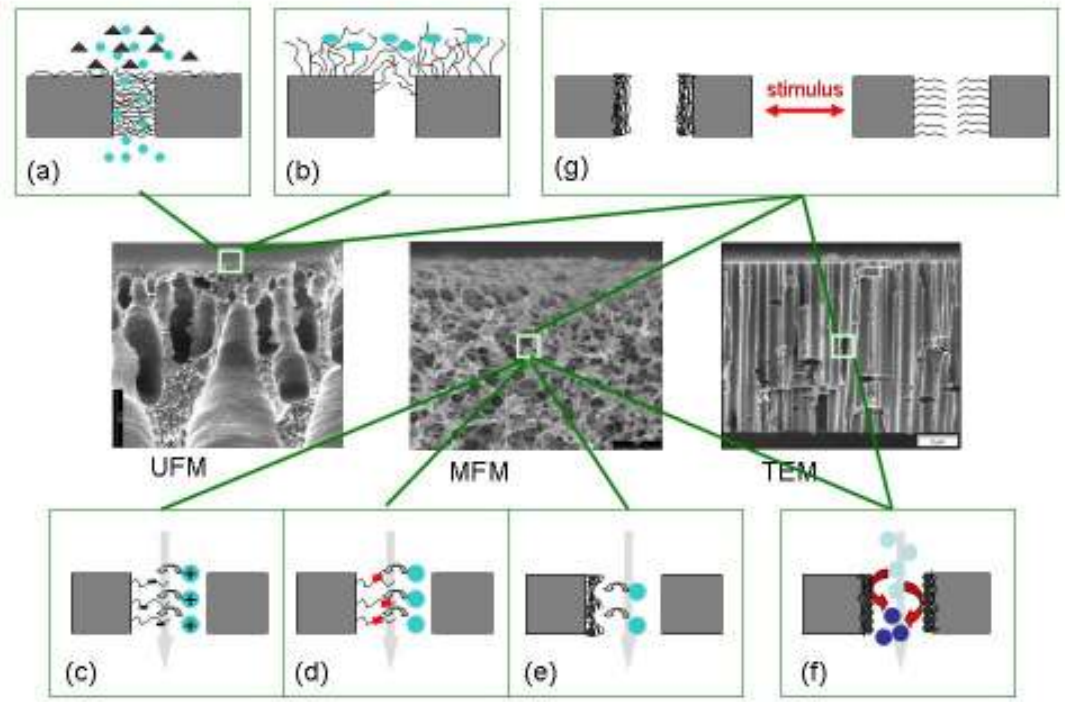

Figure 2.9: Depiction of representative membrane functionalities achieved by "photo-grafting-from" with various base membranes (UF, MF or track-etched membrane): (a) pore-filling selective polymer, (b) grafted anti-fouling layer, (c) ion-exchange membrane adsorber, (d) affinity membrane adsorber, (e) thin-layer MIP membrane adsorber, (f) (bio)catalytic membrane, (g) stimuli-responsive membrane (valve).

Grafted polymer as selective barrier. Via "photo-grafting from", selective polymers, which swell significantly in water or organic solvents, can be mechanically stabilized by the fixation in the membrane pores (Fig. 2.9a). Especially for the function in organic solvents and/or in order to achieve a high selectivity for small molecules, excessive swelling can be prevented by small pores. For example, pore-filled PAN UF membranes (active layer pore diameter between 5 and 15 nm) have been established for the separation of organic mixtures in PV [122]. High selectivity and extraordinarily high permeate fluxes in PV of organic liquid mixtures had been achieved due to the prevention of excessive swelling of the selective polymer (by complete filling of the small pores) and the low effective PV barrier thickness (<1 µm, i.e., the skin layer of the base UF membrane). The performance can be adjusted by controlling the hydrophilicity/hydrophobicity balance of grafted copolymer and pore size of the base membrane.

Grafted polymer as anti-fouling layer. Low-fouling UF membranes (Fig. 2.9b) can be prepared under photo-grafting conditions where the degradation of the base membrane pore structure is minimized. The composition, surface coverage and thickness of the grafted layer are crucial for final membrane performance, i.e., low fouling at preserved size exclusion property and competitive flux [90, 114].

Grafted polymer layer comprising functional groups for reversible binding. Surface functionalized MF membrane adsorbers for fast protein purification (Fig. 2.9c,d) have been prepared via photo-grafting of two- or three-dimensional layers with suited functional groups [13, 117]. A novel type of MIP composite membranes (Fig. 2.9e), with high binding specificity at high throughput, has been obtained by surface initiated photo-grafting of a very thin cross-linked functional layer [118, 121]. All these cases require a sufficient permeability, in order to use the main advantage of porous membrane adsorbers, i.e., the reduction of mass transfer limitations by convective flow though the membrane pores.

Grafted polymer layer for immobilization of (bio)catalyst. Iso-porous track-etched membranes with a larger pore diameter (between 100 nm and 3 μm) as well as PP MF membrane had been functionalized via "grafting-from" reactions in order to prepare enzyme-membranes as convective flow microreactors (Fig. 2.9f) [120, 133]. Enzyme-membranes with high permeability and essentially unchanged FTF activities have been yielded with grafted poly-(2-aminoethyl methacrylate) layer followed by glutardialdehyde activation and coupling of fructosyltransferase (FTF, inulinsucrase from Streptococcus mutans). A continuous enzymatic reaction driven by trans-membrane substrate flow has been realized by using membranes with rather spacious cylindrical pores (3 μm) to avoid their blocking by the product polyfructan (inulin) with a molecular weight between 30-50 Mio g/mol. The covalent immobilization of epoxy-reactive nanoparticles on the pore walls of PET membrane, subsequently photo-grafted with poly(amino-ethyl acrylate), also increased the productivity and lowered pore-blocking tendency [145].

Grafted stimuli-responsive polymer layer. Using tailored grafted functional polymer layers on the pore walls of membranes, it is possible to reversibly change the permeability and/or selectivity. The most straightforward mechanism is the alteration of the effective pore diameter by changing the conformation of a grafted polymer via solution conditions as 'stimulus' (Fig. 2.9g). For example, reversible switching of permeability had been achieved using photo-grafted pH-responsive (PAA or PMA) [13, 14, 115] or temperature-responsive chains (polyNIPAAm) [134].

2.4 Membrane adsorbers

As mentioned in section 1.1, membrane adsorber can overcome the limitations associated with packed bed. In membrane chromatography processes, the transport of solutes to their binding sites takes place predominantly by convection, reducing both process time and recovery liquid volume. The pressure drop is significantly lower compared to packed beds as the flow path, even for a stack of multiple membranes, is much shorter. Another major advantage of membrane adsorbers is the relative ease of scale-up. In addition, for large proteins, the surface area available for binding is significantly greater with membranes [146]. However, membrane chromatography has its limitations towards pore size distribution and uneven thickness of membrane, inlet flow distribution and lower binding capacity, which indirectly or directly influences the performance of membrane chromatography such as the efficiency of protein separation and ligands utilization. Therefore, intensive investigations on membrane adsorbers have been carried out (detailed see below).

2.4.1 Classification of membrane adsorbers

Membrane adsorbers are chromatographic membranes carrying functional groups (ligands) for the binding of biomolecules. They are not filters, although the structure looks similar. Separation is achieved by reversibly binding the interests to the ligands. Generally, macroporous membranes are used.

According to the module geometry, membrane adsorbers can be classified into flat sheet (including single and stacked-membrane), hollow fiber and spiral wound membranes (Fig. 2.10) [6, 8]. Previously, membrane adsorbers were sold in the form of single thin sheet having pore size of the order of 1 μm. However, the capacity of these membranes was low, and small thickness and porosity variations severely degraded membrane performance. The next generation is stacks of several flat sheets, which are housed within membrane modules. In addition to providing more adsorbent volume, the use of membrane stacks can average out the side effect of variation of pore size distribution and membrane thickness for single flat sheet, leading to sharper breakthrough curves and higher binding capacities (cf. below). Based on the statistics of the literatures [8, 147], flat sheet membranes are by far most widely used.

A single thin sheet wound around a permeable cylindrical core can be similarly packaged (spiral wound membrane). It is claimed to be suitable for large-scale applications and for use in the bind and elute mode. However, the biggest challenge would be the poor flow

distribution because the membrane area increases in a radially outward direction, causing a drop in superficial velocity of the liquid stream during its flow through the membrane. In addition, the binding and elution processes might be difficult to be modeled and predicted. Nevertheless, this type of membrane adsorbers has been used by companies such as Sartorius and Pall (provided in ref. [8]).

A hollow fiber membrane adsorber usually has a tubular geometry, consisting of a bundle of several hundred fibers potted together within a module in a shell and tube heat-exchanger-type configuration. It provides a high membrane surface area to volume ratio. The reduction in accumulation of particles near the pore entrance is another advantage using hollow fibers due to the cross-flow. However, this type of adsorber can not be used for pulse chromatography because the duration is insignificant when compared with the overall processing time. Even in the bind and elute mode, the breakthrough is expected to be broadened, leading to poor adsorber utilization.

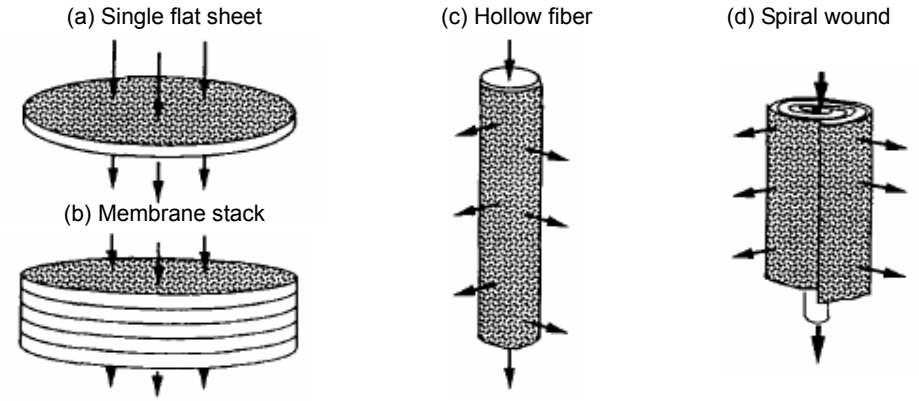

Figure 2.10: Schematic description for membrane adsorber geometries. Arrows illustrate the direction of bulk flow; pattern indicates the membrane cross-sectional area [6].

According to the interaction mode (the active ligands), membrane adsorbers involve affinity membrane, ion-exchange membrane, hydrophobic interaction based membrane and reversed-phase based membrane. Based on the collected literatures [8, 147], affinity separation seems to be the largest segment. The ligands used for affinity membrane chromatography mainly include immunoaffinity ligands e.g., [148, 149], protein A or G e.g., [150, 151], dyes e.g., [152, 153] and immobilized metal ions e.g., [154, 155] as well as peptides e.g., [156]. In terms of chromatographic membranes commercially available, ion-exchange membranes constitute the largest segment. To achieve a corresponding interest binding, membranes have been modified with different charged groups such as sulfonic acid [157], acrylic acid [10] and di/ethylamino group [37]. Along with affinity and ion-exchange chromatographies, chromatography based on hydrophobic interaction has

wide applications for protein purifications. Alkyl, e.g., butyl and octyl, and aryl, e.g., phenyl, groups are representative ligands for this type of adsorber. For the reversed-phase based membrane, few reports had been found. The different types of membrane adsorbers used for chromatographic separation have been reviewed in the review papers (e.g., refs. [8,147]).

In addition, a novel type of membrane adsorber has been received a great interest, which is based on a novel molecular imprinting technology. The MIP composite membrane (see Fig. 2.9e) can be obtained by in situ preparation [158] or grafting MIP thin-layer on the membrane surface [118]. The interaction mode can be covalent bonding, hydrogen bonding, ionic interaction or hydrophobic interaction; more importantly, the shapes of the synthesized fixed recognition cavities take more responsible for the selective affinity of interest. The resulting membrane adsorbers can be used for separation of the compounds with similar chemical and physical properties such as enantio-separation.

2.4.2 Investigation on membrane adsorbers

In order to clearly understand adsorption behavior of membrane adsorbers and improve the overall performance of membrane chromatography, both chromatographic processes and membrane chemistries have been being simultaneously investigated.

Chromatographic processes. To properly design, operate and apply the membrane-based separation processes, hence maximize the throughput and the degree of separation, many efforts have been directed towards the process engineering aspects, especially to the mass transport phenomena of membrane chromatography, usually using flat sheet membranes as the model system. The earliest work regarding transport phenomena was reported by Briefs and Kula [159]. A mathematical formulation for an idealized membrane adsorber based on 100 stacks of flat sheets was presented and solved to predict breakthrough and elution profiles. The mathematical analysis was experimentally verified by dynamic adsorption and elution studies using the enzyme formate dehydrogenase and pyruvate decarboxylase. Suen and Etzel [160] formulated a mathematical model including convection, diffusion and Langmuir-type adsorption to analyze the design and operation of affinity membrane bioseparations. From the analysis it was predicted that for thin membranes, the flow-rate is limited by the ligand-protein association kinetics and even small variations of thickness and porosity severely degrade membrane performance, which would be overcome by the use of stacks of several thin membranes. The mass transport implications of this mathematical model were also explored using experimental studies [161]. Later, using

ion-exchange membranes with larger pore size (150 μm), Etzel and his co-workers found based on new mathematical models that the breakthrough curve and elution peak strongly depend on flow-rate, and the maximum allowable pore size which eliminates this limitation was calculated for different molecular weight solutes [162]. Also, the performance of ion-exchange membrane was analyzed using different models, which incorporated nonlinear sorption isotherm and mass transfer coefficient. The models allow the determination of the rate-controlling mass-transfer phenomena and solid-phase concentration, and prediction of the operating and membrane-design parameters needed to obtain sharp breakthrough curves [163]. Tennikova and Svec [164] investigated the mass transport phenomena of membrane chromatography primarily based on operating parameters. They claimed that the process efficiency of the systems was not limited by flow-rate. It was explained that the increase in flow rate led to the enhancement of diffusive protein transport (i.e., increase in mass transfer coefficient). From the calculations, the diffusivity of the proteins within the pores is about four orders of magnitude higher than their respective free solution diffusivities. Tejeda et al. [165] have also discussed the implications of mass transfer in the design of membrane adsorbers.

Recently, the mathematical models have been developed using different adsorption mechanisms rather than Langmuir adsorption, such as bi-Langmuir [166] or Freundlich adsorption [167, 168]. In addition, Ghosh et al. [169] designed a new membrane module with enhanced both feed flow distribution and effluent collection. The membrane modules showed significant higher lysozyme binding capacities than the corresponding conventional modules, measured both in the breakthrough mode and in the pulse chromatography mode.

In addition to the analyses of breakthrough and elute curves, the visual confocal laser scanning microscopy (CLSM) images for protein adsorption may provide a helpful guidance for grafted layer design [170, 171].

Membrane chemistry (Immobilization of ligands). The immobilization of ligands, on one hand, reduces the non-specific binding; on the other hand, provides specific binding sites for interests. The motivations for membrane chemistry investigation are 2-fold: one is to immobilize ligands as many as possible on the membrane surface for high binding capacity (or the prerequisite of high binding capacity); another is to ensure the availability of ligands (i.e., the structure of modified layer should be considered) and the operable chromatographic processes (e.g., membrane permeability related to flow rate). In the review papers, Klein [7] and Zeng and Ruckenstein [172] summarized the modifications of

existing membranes for membrane adsorbers, concentrating on the chemical modifications as well as radiation-induced grafting method. Chemical modifications mainly are applicable to the membranes with reactive groups on the surfaces (e.g., polysulfone and nylon-6 hollow fibers). Two important issues should be considered: one is the effect of reaction conditions on the stability of base membranes. Another is that either small functional molecules are immobilized (it is hard to improve the binding capacity) or macromolecules are bound to the membrane surface via "grafting-to". For the latter, the structure of grafted polymer and uniformity of functionalization would be complicated to control. As for radiation-induced grafting method, the major body of work has been conducted by Saito and his co-workers. Graft of commercially available PE MF with PolyGMA had been perfomed through initiating by electron beam and then exposed to air-free vapors of glycidylmethacrylate. The introduced epoxide groups offer many possibilities for the immobilization of various ligands. The resulting membranes can be applied as affinity membranes [35], cation/anion-exchange membranes [157, 36] and hydrophobic interaction-based membranes [173]. To improve the performance of membrane adsorbers, the grafting layer property was adjusted by varied ligand density [4] and cross-linking [9]. In addition, photo-induced grafting method has been used for synthesis of membrane adsorbers. As discussed above, this method including several grafting routes is more flexible to synthesize desired grafted layer architectures. Main work came from Ulbricht and his co-workers. For example, affinity membranes [82, 117, 119], cation-exchange membrane [10, 13] and MIP composite membranes [105, 121, 129, 130] have been prepared via photo-initiator adsorption and entrapping method. Xu et al also prepared affinity membrane induced by UV irradiation [136]. Recently, ATRP has been extensively used for membrane surface modification. Ion-exchange cellulose membrane has been established [11]. Based on inorganic alumina membranes, high-capacity affinity membrane adsorbers were prepared via ATRP as well [5]. For the preparation of membrane adsorbers via graft polymerization, a tradeoff between binding capacity and flow rate needs to be overcome. Therefore, the emphasis of membrane chemistry is put on the structure design of grafted functional layer. Slightly cross-linking structure would be promising according to the report in the literature [10].

In addition, Wessling [174, 175] described a concept for a single-step process preparation of ion-exchange adsorber membranes having particulate material entrapped in the porous matrix as potential chromatographic systems (mixed matrix adsorber membrane), which possesses a good accessibility for protein to the adsorptive sites.

Chapter 3 Experiments

3.1 Materials

Hydrophobic (unmodified) PP membrane (2E HF) with a nominal cut-off pore diameter of 0.2 μm and a thickness of 150 μm from Membrana GmbH was used for the investigations of photo-initiator entrapping method and sequential photo-induced method as well as as the reference for hydrophilized PP membrane.

Hydrophilized PP MF membrane (GHP) with a nominal cut-off pore diameter of 0.2 μm and with a thickness of 101 μm were purchased from Pall Corporation. This membrane was used for the investigations of synergist immobilization method and iniferter immobilization method. Anion-exchange membrane adsorbers and MIP composite membranes were also prepared on such membranes as base supports.

Track-etched PET membranes with a nominal pore diameter of 200 nm (PET200) and 400 nm (PET400) and both with a thickness of 23 μm were products of Oxyphen GmbH (Dresden, Germany). Both membranes were applied for further investigations of synergist immobilization method, and PET400 membrane were used for the preparation of affinity membrane adsorbers.

Benzophenone (BP; GC), citric acid anhydrous (p.a. ≥ 99.5%), acetic anhydride (p.a.), 4-(dimethylamino)pyridine (DMAP, ≥ 98.0%) and benzene (HPLC grade) were from Fluka. Ethylene glycol dimethacrylate (EDMA), 2,2-dimethoxy-2-phenylacetophenone (DMPAP), pure enantiomers Boc-D-PhA and Boc-L-PhA, N,N-diethylethylenediamine (DEEDA; 98+%), N,N'-methylene-bis-acrylamide (MBAA), acid orange II (AO), tetraethylenepentamine (TEPA), 2-bromoisobutyryl bromide (98%) and triethylamine were obtained from Acros. Methacrylic acid (MAA), acrylamide (AAm; 99+%) and (2-(methacryloyloxy)ethyl) trimethylammonium chloride (MAETMAC; 75 wt.% aqueous solution) were from Aldrich.

Ethyl acetate (p.a.), heptane (p.a.), chloroform (p.a.) and acetone (p.a.) were from AppliChem. Bovine serum albumin (BSA, 67 kDa, pI 4.9; used for binding capacity measurement of anion-exchange membrane), lysozyme (14 kDa, pI 9.1) was purchased from ICN. Soybean trypsin inhibitor (type I-S, 20 kDa, pI 4.5), cytochtome C (12 kDa, pI 9.2), myoglobin (17 kDa, pI 7.0) and trypsin (22 kDa, pI 8.3) , HEPES (≥ 99.5%) and sodium N,N-diethyldithiocarbamate trihydrate were obtained from Sigma; proteinase K (29 kDa, pI 7.7) from Boehringer Mannheim GmbH; BSA (66 kDa, pI 5.8; used for binding capacity measurement of affinity membrane) and N,N-dimethylformamide (DMF)

from Merck. Tris-(hydroxymethyl)-aminomethane (Tris) was from Riedel-deHaen. Methanol, ethanol (HPLC grade), sodium hydroxide and hydrochloric acid were from VWR. Methacryloylamino-2-hydroxy-propane (M1) and 5-(methacryloylamino)-m-xylylene bisphosphonic acid tetramethylester (M2) were synthesized by organic chemistry (prof. Schrader's group), Universitaet Duisburg-Essen, Germany. All chemicals were used as received except that sodium N,N-diethyldithiocarbamate trihydrate was recrystallised in ethanol. Water purified with a Milli-Q system (Millipore) was used for all experiments.

For anion-exchange membrane adsorbers, 50 mM Tris-HCl buffer (pH=7.0) and the same buffer containing 1 M NaCl were used for protein binding and elution, respectively. 25 mM HEPES buffer (pH=7.1) and the same buffer containing 1 M NaCl were applied for evaluation of affinity membrane adsorbers.

3.2 Photo-grafting of membranes

3.2.1 Photo-initiator entrapping method

Photo-initiator immobilization. Pre-weighed circular unmodified PP membrane sample with a diameter of 25 mm was presoaked in 3 mL 10 mM BP solution in heptane (or in pure heptane as reference) for 15 min in a Petri dish (60 mm in diameter), then taken out and dried in the air for 10 min. To remove the BP on the membrane surface, the sample was washed twice (2 min and 1 min, respectively) in 5 mL methanol. However, longer soaking time and washing time were performed for more detailed investigation (e.g., effect of washing on BP uptake). After being dried in the air, the sample was weighed using electric analytical balance (Sartorius; accuracy is 10 μg). For further determination of entrapped initiator, membrane was immersed in pure heptane for initiator elution. The washed and the eluted solutions were detected at 256 nm using Cary 50 UV-Vis spectrophotometer (VARIAN Inc.).

Photo-graft functionalization. An UV illumination system (UV A Print, Hoenle AG, Gräfelfing, Germany) equipped with a high-pressure mercury lamp and a glass filter ($\lambda >$ 300 nm) was used, and the UV intensity was about 40 mW/cm^2 (measured with the UVA meter, Hoenle AG). The same UV system was used for the whole work unless otherwise mentioned.

After washing (mentioned above), the membrane was taken out and quickly wiped with filter paper in order to remove the adhering solvent, then directly immersed in 3 mL AAm aqueous (or acetonitrile) solution in a Petri dish (60 mm in diameter) and fixed between

two sheets of filter paper. After 15 min equilibration, UV irradiation followed for 15 min (effective intensity: 7.5 mW/cm^2). Afterwards, the sample was thoroughly washed with water and methanol (last time washing) to remove residual initiator, unreacted monomer and homopolymer. Finally, the modified membrane was dried in oven under 45^{0}C overnight and weighed. The experimental setup for membrane photo-grafting is given in Fig. 3.1, and all the photo-grafting was carried out using the same setup unless otherwise mentioned.

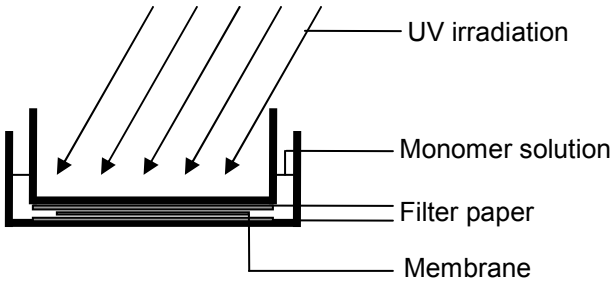

Figure 3.1: Experimental setup for membrane photo-grafting.

3.2.2 Sequential photo-induced method

Surface-initiator immobilization. Before use, the commercial unmodified PP membrane was soaked in benzene overnight and dried to constant weight. The pre-weighed membrane sample with a diameter of 44 mm was saturated with 250 mM BP solution in benzene (deaerated by bubbling nitrogen for 10 min; and pure benzene was used for reference sample) for 5 min, then taken out and fixed between two Petri dishes. Immediately, UV irradiation followed for a selected time. Afterwards, the sample was taken out and the residual, unreacted solutions were extracted by acetone. Finally, the sample was dried at room temperature in the air and weighed for determination of the amount of surface-initiator. Another control sample was treated by same procedures but without UV-irradiation.

Photo-graft functionalization. Membrane functionalization was performed similar to that of photo-initiator entrapping method (see Fig. 3.1). Briefly, the surface-initiator-immobilized membrane was immersed in 3 mL AAm solution and fixed between two sheets of filter paper. 15 min UV irradiation followed. Then the sample was washed, dried and finally weighed.

3.2.3 Synergist immobilization method

Synergist immobilization by aminolysis. A circular membrane sample with a diameter of 47 mm (for hydrophilized PP membrane; 26 mm in diameter for track-etched PET membranes) was put into a sealed vessel and 3 mL DEEDA were added. After equilibrating for 10 min at room temperature, the system reacted at constant temperature in a thermostat for a given time. Then, membranes were taken out from the vessel, rinsed with methanol, washed four times with methanol on a shaker (each for 30 min) and finally dried at 45°C overnight. For PET membranes, the sample was weighed before and after aminolysis reaction for the determination of mass loss.

Photo-initiated graft copolymerization. Pre-weighed original or aminolysed membranes were immersed into 3 mL AAm solution in methanol or acetonitrile, containing the photo-initiator BP of a give concentration, in a Petri dish (diameter 60 mm) and fixed between two sheets of filter paper (diameter 50 mm; Whatman). After 10 min equilibration, UV irradiation followed (effective UV intensity due to the UV filter action of the paper was about 7.5 mW/cm^2). Thereafter, the samples were taken out immediately and washed with water three times (each 30 min, the second time at 60°C, the other two times at room temperature) and once with methanol to remove unreacted monomer, residual initiator and homopolymer. Then, the membranes were dried in vacuum at 45°C overnight. For the preparation of the membranes with cross-linked grafted layers, a certain amount of cross-linker was added into the monomer solution.

3.2.4 Iniferter immobilization method

Iniferter immobilization. For the investigation of this method, hydrophilized PP membrane was used. In this case, the immobilization of photo-iniferter (dithiocarbamate) involves three reactions (see Fig. 4.36). First, aminolysis reaction was undertaken for the introduction of amino groups. A circular membrane sample with a diameter of 47 mm was put in 4 mL 25 vol.% TEPA solution of DMF in a sealed vessel. After equilibrating for few minutes at room temperature, the system reacted at constant temperature in a thermostat for a selected time. Then, membranes were taken out from the vessel, washed three times with DMF and once with methanol on a shaker (each for 30 min) and finally dried at 45 ^{0}C for 4 hr. Thereafter, the sample was put in 8 mL of a solution of 50 mM 2-bromoisobutyryl bromide (from 10 mM to 150 mM for optimization), 55 mM trimethylamine (adjusted corresponding to the concentration of 2-bromoisobutyryl bromide) and 5 mM DMAP in dry acetonitrile for 4 hr at room temperature. The reaction was performed in a 50 mL sealed glass vessel. After reaction, the sample was washed three times with acetonitrile and rinsed with methanol and

dried at 45^0C overnight. For the immobilization of photo-iniferter (dithiocarbamate group), the sample reacted in ethanol solution of 0.3 mol/L sodium N,N-diethyldithiocarbamate trihydrate at 30^0C overnight. Afterwards, the sample was rinsed with methanol then thoroughly washed with water. Finally, it was dried at 45^0C overnight.

Photo-graft polymerization. The pre-weighed iniferter-immobilized membrane was immersed in 2.5 mL monomer solution (deaerated by bubbling nitrogen for 10 min) and fixed between two sheets of filter paper. UV irradiation followed for a given time. Cooling water was used to prevent the temperature in grafting system rising. After being grafted, the membrane was washed, dried and finally weighed.

3.3 Preparation of membrane adsorbers

3.3.1 Anion-exchange membrane

Quaternary ammonium groups as strongly basic anion-exchange moieties were introduced to the entire surface of a porous membrane via two different photo-grafting routes. For photo-initiator adsorption method, varied BP concentrations were used for the pre-coating to prepare anion-exchange membranes with different grafting densities. A pre-weighed hydrophilized PP membrane was soaked in a solution of BP in methanol for 30 min, then taken out and dried. For synergist immobilization method, partial aminolysis of the thin hydrophilic polyarylate layer as a pre-treatment of the membrane was carried out according to the section 3.2.3. Briefly, membranes reacted with DEEDA for 2 h at 60°C, washed with methanol and dried. Afterwards, the BP-coated membrane (for adsorption method) or the pre-weighed aminolysed hydrophilized PP membrane (for synergist immobilization method) was immersed in 3 mL MAETMAC aqueous solution saturated with BP (≈ 0.5 mM) in Petri dishes and fixed between two sheets of filter paper. 15 min UV irradiation followed (effective UV intensity was around 6.5 mW/cm^2) (cf. Fig. 3.1) Thereafter, the sample was taken out and washed thoroughly with pure water and methanol to remove unreacted monomer, residual initiator and homopolymer. At the end, the grafted membrane was dried at 45°C overnight. A certain amount of cross-linker (MBAA) (5 or 10% of total monomer) was added in some cases to obtain cross-linked grafted layer when synergist immobilization method was adopted. The anion-exchange membranes prepared via synergist immobilization and photo-initiator adsorption method are denoted “S x% CL” and “A y mM”, respectively. Here, x and y are the weight percentage of cross-linker in functional monomer and the BP concentration employed for the photo-initiator pre-coating,

respectively.

3.3.2 Affinity membrane

Affinity membranes were prepared via synergist immobilization method as well. Track-etched PET400 was used as base membrane. An aminolysis reaction proceeded with DEEDA at 70^0C for 2 hr for the introduction of tertiary amino groups, by which nearly full coverage of the PET surface with a monolayer of tertiary amino groups had been achieved (see Chapter 4). Subsequently, the photo-graft polymerization of aminolysed membranes was carried out in acetonitrile solutions of functional monomers with an appropriate concentration (cf. Table 4.10) and containing 1.5 mM BP. In brief, an aminolysed PET membrane sample with a diameter of 26 mm was immersed in 2.5 mL of monomer solution and fixed between two sheets of filter paper in Petri dishes (60 mm in diameter). 12 min UV irradiation followed after few minutes equilibration (the effective UV intensity was about 7.0 mW/cm^2). Afterwards, the grafted membranes were taken out immediately and washed 3 times with acetonitrile to remove the unreacted monomer, residual initiator and homopolymer. Then, the membranes were dried overnight in vacuo at 45°C. A constant molar ratio of 4:1 between monomers M1 and M2 was employed for the preparation in the copolymer-grafted membranes. For the conversion of the phosphonate methyl ester groups of grafted copolymer to their respective Li salt, a polymer-analogous cleavage reaction was performed in 2 mL dry acetonitrile solution containing 0.5 mM LiBr (the double molar amount of comonomer M2 in the grafted copolymer) at 75^0 for 24 hr. As control samples, grafted membranes with M1 (polyM1-grafted membranes) have been also prepared under the same conditions.

3.3.3 MIP composite membrane

MIP composite membranes have been prepared by surface functionalization of hydrophilized PP membrane with a thin-layer MIP via synergist immobilization and iniferter immobilization methods. The aminolysed membranes pre-functionalized at 60^0C for 2 hr and the iniferter-immobilized membranes synthesized under optimized conditions were used for graft functionalization via synergist immobilization method and iniferter immobilization method, respectively. To obtain the imprinted polymer layer on the membrane surface, the pre-functionalized membrane was immersed in a solution containing 10 mM Boc-L-phenylalanine as template, 40 mM AAm (or MAA) as functional monomer and 200 mM EDMA as cross-linker, and UV-grafted as mentioned above for both grafting methods. MIP membranes with different DG were obtained by varying the UV exposure time. The

composition of MIP layer was adjusted by varied the molar ratio among the template, functional monomer and cross-linker. As blank samples, the non-imprinted polymer (NIP) composite membranes were also synthesized under the same conditions but without template. In addition, to obtain the optimum structure with respect to recognition sites, the MIP and NIP polymers with various compositions were prepared as well using different recipes (varied functional monomer concentration; Table 4.12) via photo-induced radical polymerization. The total monomer concentration in acetonitrile was about 50 wt%.

3.4 Characterizations of membranes

3.4.1 Membrane surface

Chemical structure of membrane surface. FTIR spectra of the surfaces of original, aminolysed and photo-grafted membrane samples were recorded with a spectrometer IFS 55 EQUINOX (Bruker) equipped with a horizontal ATR unit. A nominal resolution of 4 cm^{-1} and 64 scans were used. In addition, the ^{31}P solid state NMR experiments were performed using a Brucker Avance 400 instrument to confirm the polyM2 chain segment on the poly(M1-co-M2)-grafted affinity membrane and the conversion of phosphonate methyl ester into phosphonate salt.

Contact angles of membranes. Contact angle of the membrane was measured via the static sessile drop method using an optical contact angle measurement system (OCA 15 plus; Dataphysics, Germany). A drop of water (5 μL) was injected with a syringe onto the sample surface, and the data for 5 drops on different locations were averaged to obtain the contact angle of one membrane sample.

Zeta potential from streaming potential. The cell and experimental setup for the measurement of the trans-membrane streaming potential is shown in Fig. 3.2. Orignal, aminolysed and various grafted PET400 membranes were selected to detect the surface charge. Experiments were always started from pH 7 with a 10^{-3} M KCl aqueous solution; the other pH values were adjusted by the addition of dilute HCl solutions until pH 3. For each pH value, at least five hydrodynamic pressure differences were adjusted in the range of 0-2 bar (PET membrane is too flimsy to stand high pressure). The zeta potential ζ was calculated with the Helmholtz-Smoluchowski equation

$$\zeta = \frac{\kappa_L \cdot \eta}{\varepsilon_r \cdot \varepsilon_0} \cdot \frac{\Delta E}{\Delta P} \quad \text{.....(3.1)}$$

where k_L is the liquid conductivity, η is the liquid viscosity, ε_r is the liquid permittivity, ε_0 is the permittivity of free space, ΔE is the streaming potential, and ΔP is the hydrodynamic pressure difference.

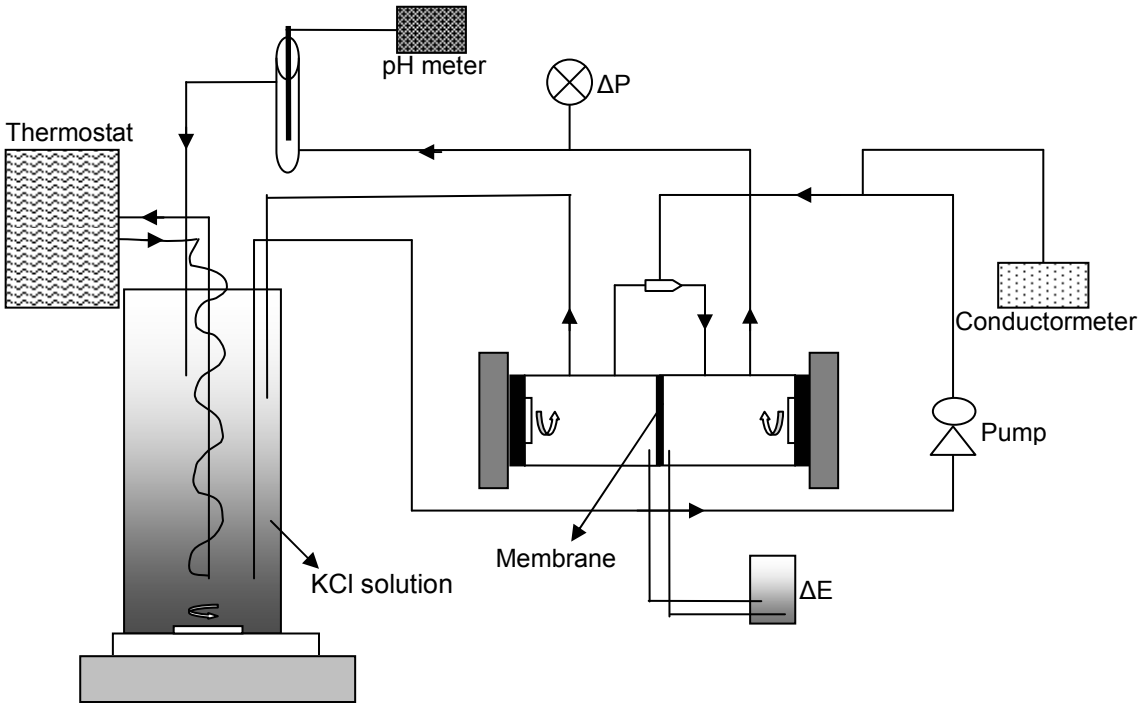

Figure 3.2: Schematic description of experimental setup for trans-streaming potential measurement (Zeta potential measurement).

3.4.2 Membrane pore structure

Morphology of membranes. The images of the top surface and cross-section of membranes were taken by environmental scanning electron microscopy (ESEM Quanta 400 FEG, FEI, USA) after sputter coating with gold/palladium.

Specific surface area of membranes. BET specific surface area of the membrane was determined by using the surface area analyzer SA 3100 (Beckmann-Coulter GmbH, Krefeld, Germany) for measuring the nitrogen adsorption isotherm. For relatively large pore size, the accuracy is low. Therefore, the specific surface area of PET400 was calculated according to the measured pore diameter and porosity, assuming that the pores are cylindrical and "isolated" (not overlapped). The value ($S_{spec.}$) can be obtained from the formula:

$$S_{spec.} = \frac{4\varepsilon}{\rho_{membr.} \cdot d} \quad \text{.....(3.2)}$$

Where ε is porosity of membrane; $\rho_{membr.}$ is density of membrane (membrane mass/total

volume); d is the pore diameter of membrane.

Permeability measurement. Liquid permeability of membrane can be used to estimate pore diameter and it also reflects the structure and swelling property of grafted polymer. The water (or ethanol or buffer) flux of membranes with a diameter of 25 mm was measured using stirred cells with 10 mL volume and 3.14 cm^2 effective membrane area (Amicon Model 8010, Millipore). 0.2-1.5 bar transmembrane pressure was used by adjusting nitrogen pressure. The pore size and its change can be analysed using Hagen-Poiseuille equation:

$$\frac{J}{A} = \frac{\varepsilon \cdot r^2}{8\eta\tau} \cdot \frac{\Delta P}{\Delta x} \quad \text{.....(3.3)}$$

where J is liquid flux; A stands for outer membrane surface area; ε is the porosity of membrane; r is membrane pore radius; η represents viscosity of liquid; ΔP is transmembrane pressure; Δx is the thickness of membrane and τ is the pore tortuosity.
The pore radius ratio before and after photo-grafting was calculated by the following formula deduced from the Hagen-Poiseuille equation:

$$\frac{r_{gr.}}{r_{am.}} = \sqrt{\frac{J_{gr.}}{J_{am.}}} \quad \text{.....(3.4)}$$

where $r_{am.}$ and $r_{gr.}$ represent the hydrodynamic radius of membranes before and after grafting, respectively, and $J_{am.}$ and $J_{gr.}$ stand for the water fluxes of membranes before and after functionalization, respectively. Because these ratios were determined for each individual membrane sample, influences of pore density of the base membrane samples were minimized.

Pore size distribution of the membrane. Transmembrane pore size distribution was determined by liquid dewetting of membrane pores using the Capillary Flow Porometer CFP-34RTG8A-X-6-L4 (PMI Inc., Ithaca, NY, USA). Membrane samples with a diameter of 30 mm were characterized via the "Dry up / Wet up" method. For the "Wet up" part, the membranes were wetted with 1,1,2,3,3,3-hexafluoropropene ("Galwick", PMI, having a surface tension of 16 $dyn \cdot cm^{-1}$). The maximum transmembrane pressure for the air flow measurements was 5 bar. The pore size distribution was estimated using the PMI software.

Swelling property and porosity of membranes. Membrane samples were soaked in the selected solvents for 24 hr. the pre-weighed membrane sample (W_0) was taken out and immediately and carefully wiped with filter paper to remove the solvent on the outer surface and weighed using an electric analytical balance (W_1). The occupied volume of

solvent in the membrane ($V_{occupied}$), which was obtained by the equation below, reflects the swelling property of membrane in the solvent. Afterwards, the samples were dried in the oven at 45^0C overnight and weighed again (W_0'). The obtained mass loss of membrane (W_0-W_0') reflects membrane dissolution in the solvent.

$$V_{occupied} = \frac{W_1 - W_0}{\rho_{solvent}} \quad \text{.....(3.5)}$$

Where $\rho_{solvent}$ represents density of solvent.

Ethanol and acetonitrile were used for the porosity determination of hydrophobic and hydrophilized PP membranes due to the negligible swelling/dissolution of membrane but good wettability in both solvents. After few hours' immersion in pure solvent, Porosity (ε) of the membrane sample was obtained by calculating through the following equation and averaging the data from five samples.

$$\varepsilon = \frac{W_1 - W_0}{\rho_{solvent} \cdot V_{membr.}} \quad \text{.....(3.6)}$$

Where $V_{membr.}$ is the volume of wet membrane.

In addition, according to Hagen-Poiseuille equation, the membrane porosity can also be calculated from the measured pore diameter by permporometry and liquid permeability.

3.4.3 Determination of (tertiary) amino groups

Determination solution ("D-solution") [176] was made up with 150 mM citric acid in acetic anhydride and ethyl acetate (v/v = 1/1). Original or aminolysed membranes were added into the D-solution, reacted at about 50°C, and the color change of the membrane was observed visually: Qualitative estimations about synergist immobilization efficiency could be made.

A quantitative staining method with the anionic dye AO [21] was employed to analyze the amount of (tertiary) amino groups on the aminolysed membrane samples. Membrane samples were shaken overnight in a solution of 0.5 mM AO in water (pH 3, HCl) at room temperature. The samples were washed three times with water (pH 3) and then immersed in 10 mL of water (pH 12, NaOH) to elute the ionically bound dye. After shaking for 15 min, the UV-Vis absorption of the solution was recorded at 485 nm. A calibration curve was obtained with AO in an aqueous solution of pH 12.

3.4.4 Degree of grafting (DG)

DG was determined gravimetrically to characterize the amount of grafted copolymer on the membrane surface. It can be described by the following equations:

$$DG(\%) = \frac{W_1 - W_0}{W_0} \times 100\% \quad \text{.....(3.7)}$$

$$\text{or} \quad DG(\mu g / cm^2) = \frac{W_1 - W_0}{A_{top}} \quad \text{(relative to top surface area) .....(3.8)}$$

$$\text{or } DG(\mu g / cm^2) = \frac{W_1 - W_0}{W_0 \cdot S_{spec.}} \quad \text{(relative to specific surface area) .....(3.9)}$$

where W_0 and W_1 stand for membrane weight before and after photo-grafting, respectively; A_{top} and $S_{spec.}$ represent top surface area and specific surface area of the membrane, respectively.

3.4.5 Static protein binding capacity

For anion-exchange membrane adsorbers. Protein solution was prepared by dissolving the protein in 50 mM Tris-HCl buffer (pH=7.0). The static protein adsorption capacity was measured using batch experiments. Various membranes were cut into 13-mm-diameter circular pieces and three pieces were incubated in 5 mL protein solutions of different initial concentrations, with shaking on the Heidolph® Promax 2020 shaker with the speed of 90 rpm at room temperature overnight. The equilibrated membrane samples were taken out from the solution and washed twice using buffer (each time 20 min). Thereafter, the protein-adsorbed membranes were soaked in 5 mL elution buffer for release of the bound protein, with shaking at room temperature for 2 hr. The concentrations of the equilibrated and eluted solutions were determined spectrophotometrically at 280 nm. Adsorption capacity was calculated from the mass balances between initial and equilibrated solutions. The recovery was estimated by the ratio of the amount of eluted protein and the adsorbed amount for the experiments where 3 mg/mL initial protein concentration was employed.

For affinity membrane adsorbers. 25 mM HEPES buffer (pH=7.1) was used. Various membranes with a diameter of 26 mm were incubated in 1 mL protein solutions of 40 mg/L initial concentrations at room temperature overnight. The equilibrated membrane samples were taken out from the solution and washed 3 times using buffer (each time 20 min). Thereafter, the protein-adsorbed membranes were soaked in 1 mL elution buffer for release of the bound protein, with shaking at room temperature for 2 hr. The concentrations of the equilibrated and eluted solutions were determined spectrophotometrically at 562 nm (protein assay using bicinchoninic acid (BCA) kit; from Thermo Scientific Pierce). Briefly, BCA working reagent (WR) was prepared by mixing 50 parts of reagent A with 1 part of reagent B. 100 μg sample solution and 800 μg WR were added into each well on

24-microwell plate. After being shaken at room temperature for 2 hr, the absorbance at 562 nm was measured on a plate reader (μQuant Bio-TEK Instrument INC.). The standard curve was made for respective measurement. Binding capacity was calculated from eluted solutions via standard curve.

3.4.6 Dynamic adsorption of proteins

The dynamic adsorption behavior of anion-exchange membranes was monitored using an Äkta Purifier-900 (GE Life Science). Membranes were cut into 13-mm-diameter circular pieces. A stack of 3 membrane sheets was loaded in the sample holder (CIM, BIA Inc.). 50 mM Tris-HCl (pH=7.0) was employed as loading and washing buffer. The elution buffer consisted of 1 M NaCl in the loading buffer. Prior to breakthrough curve (BTC) experiments, the membranes were equilibrated with the loading buffer. Then 10 ml protein solution of 3 mg/ml was injected using a 50 ml super-loop at a flow rate of 1 ml/min or 5 ml/min. Calibration were done without loading membranes in the CIM module. The dynamic binding capacity was calculated from the peak area of eluted protein according to the obtained calibration.

3.4.7 Separation of proteins

The same procedures with that for static binding capacity measurement (for affinity membrane) were followed to determine the separation property of poly(M1-co-M2)-grafted membrane in 1:1 mixture of lysozyme and cytochrome C with a 35 mg/L initial concentration, respectively. An adsorption spectrum of the eluted solution was recorded using a UV-Vis spectrophotometer (Jasco V550). For comparison, spectra of the lysozyme and cytochrome C solutions with the same concentration as eluted from the membranes (18 mg/L) were measured as well.

3.4.8 Determination of imprinting effect

The pre-weighed resulting MIP and NIP composite membranes, respectively, were incubated in 2 mL template (Boc-L-PhA) solution in acetonitrile for 24 hr at ambient temperature on a shaker. Then membranes were taken out and washed twice (each time for 10 min) with acetronitrile. Afterwards, the samples were put in 2 mL methanol to elute the bound Boc-L-PhA. The initial, equilibrium and eluted Boc-L-PhA solutions were detected spectrophotometrically at 217 nm. The sorption and binding capacities were obtained by calculating the difference in Boc-L-PhA concentration between initial and equilibrium solutions and eluted Boc-L-PhA concentration, respectively.

Another method was used to detect the imprinting effect of MIP composite membranes or polymers. The pre-weighed membranes or polymers were incubated in the racemic solutions (mixing the equal amounts of Boc-L- and Boc-D-PhA) for 24 hr at ambient temperature. The concentrations of L-isomer and D-isomer in initial and equilibrium solutions were determined using a HPLC system (Dionex, Germany) equipped with a chiral column Nucleocel Alpha-RP-S (Macherey-Nagel GmbH & Co., Germany). The chromatographic separations were performed at 0.5 mL/min using 0.12% trifluoro acetic acid (TFA) in water/acetonitrile (60/40) as an eluent. Injection volume was 20 μL and effluent was monitored by the UV detector at 217 nm.

The total binding capacity of Boc-PhA and the enantioselectivity can be obtained. The selective factor (α) was calculated according to the equation:

$$\alpha = \frac{E_D / E_L}{I_D / I_L} \quad \text{.....(3.10)}$$

where E_D and E_L stand for the concentration of D-isomer and L-isomer in equilibrium solution, respectively. I_D and I_L represent the concentration of D- and L-isomer in initial solution, respectively.

Chapter 4 Results

The experimental results, which are classified into three main sections, are presented in this chapter: i) Characterizations of initial membranes; ii) Investigation of surface-selective photo-grafting methods including photo-initiator entrapping method (section 4.2), sequential photo-induced method (section 4.3), synergist immobilization method (section 4.4) and iniferter immobilization method (section 4.5); iii) Preparation and characterization of various macroporous membrane adsorbers, such as anion-exchange membrane (section 4.6), affinity membrane (section 4.7) and MIP composite membrane (section 4.8).

4.1 Characterizations of initial membranes

In order to better understand the functionalization mechanism and efficiently improve the performance of resulting membrane adsorbers, it is essential to know the properties of initial membranes before modifying or applying them. In all experiments, four kinds of membranes (see Table 4.1) have been used for the investigation of photo-grafting methods and preparation of membrane adsorbers. The basic data from manufacturers have been shown in Table 4.1. However, on one hand, these data are insufficient for our studies. On the other hand, the actual properties for received membranes might have deviations from the supplied data.

Therefore, more detailed characterizations have been carried out for all the membranes as received (see Fig. 4.1 and Table 4.2). The SEM images of top surface and cross-section of various membranes demonstrate that all the selected membranes possessed isotropic structures as it was claimed by manufacturers. The pore morphologies of hydrophilized PP membrane were very similar to that for unmodified PP membrane which was manufactured via the thermally induced phase separation process (TIPS). Track-etched PET membranes, overall, had regular (isocylindrical) pores. However, for PET200 membrane, many overlapped pores were observed. Relatively, the pores of PET400 membrane were much more “isolated”. The other properties have been summarized and shown in Table 4.2. In comparison with the nominal pore diameter values manufacturers supplied, the average pore sizes measured by liquid dewetting of membrane pores were obviously greater for all the used membranes (the deviations were approximately 25% for unmodified PP membrane and 75% for the other three membranes), which also can be observed from the SEM images. In addition, the BET specific surface area and porosity have been either

directly measured as described in Chapter 3 or calculated from water permeability and average pore size by the Hagen-Poiseuille equation. Both unmodified and hydrophilized PP membranes had high porosity and BET specific surface area (about 78% and 28 m^2/g and 75% and 15 m^2/g for unmodified and hydrophilized PP membrane, respectively), while both track-etched PET membranes possessed low porosity and low specific surface area (see Table 4.2), but regular capillary pores and narrow pore size distribution. It must be noted that different batches may have some deviations in some properties for the same type of membrane, e.g., the different data for two batches of PET200 membranes used in this work are shown in Table 4.2.

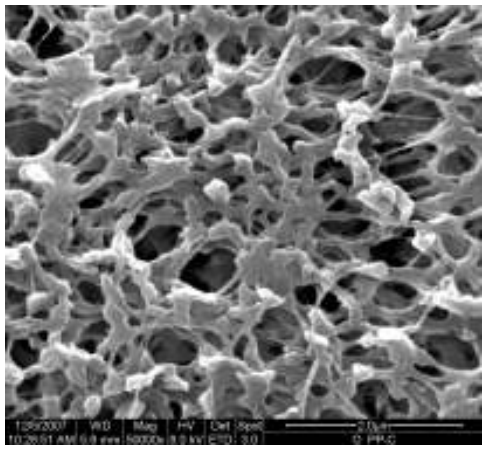
(a)

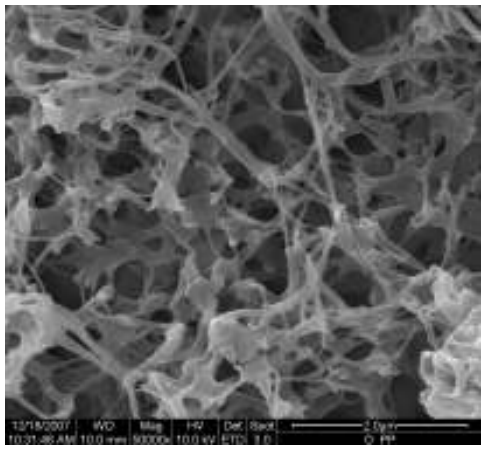
(b)

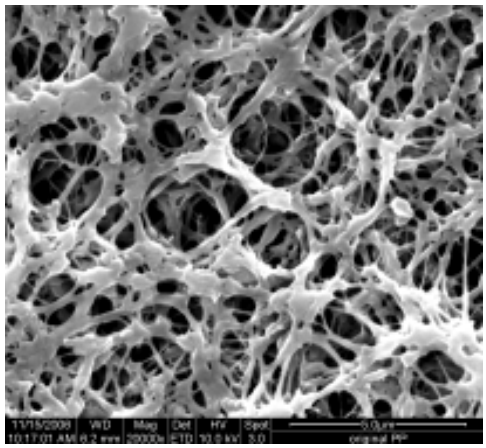
(c)

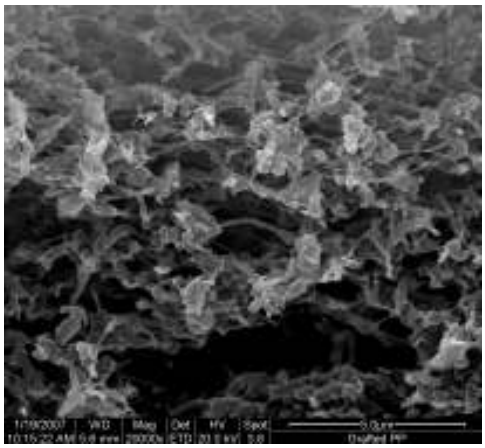
(d)

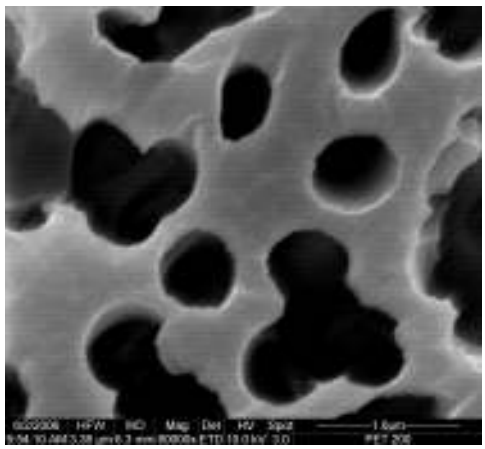
(e)

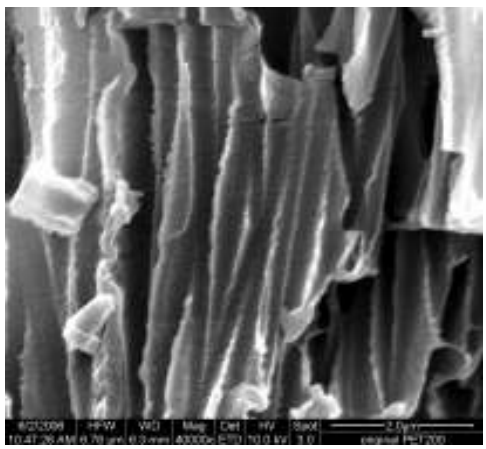
(f)

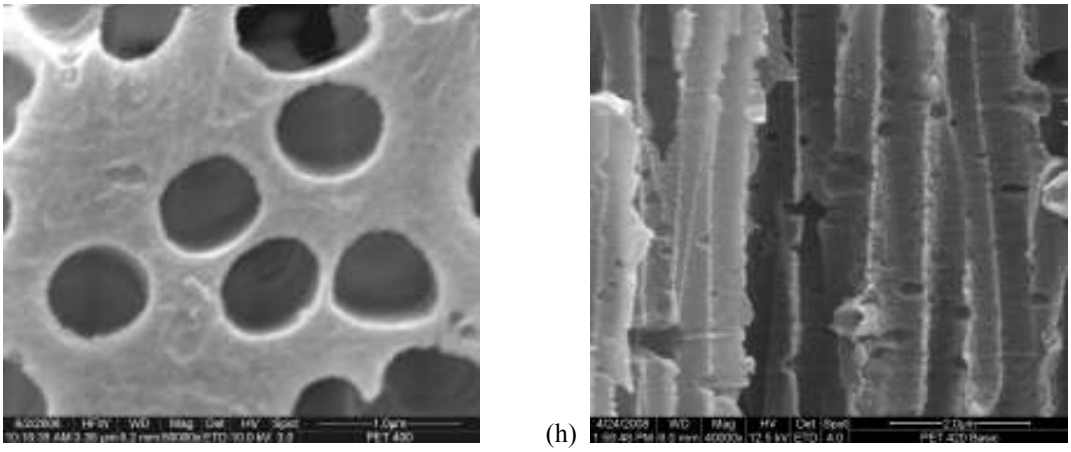

Figure 4.1: SEM images of top surface (a, c, e, g) and cross-section (b, d, f, h) for various initial membranes. (a, b) unmodified PP membrane; (c, d) hydrophilized PP membrane; (e, f) track-etched PET200 membrane; (g, h) track-etched PET400 membrane.

In addition, for hydrophilized PP membrane, the structure of hydrophilic polymer layer has been analyzed by ATR-IR spectroscopy and contact angle measurement, along with those for unmodified PP membrane as references. The contact angle of the modified PP membrane was too small to be measured, while for the unmodified membrane with the same nominal pore diameter a value of 145^0 was observed. As shown in Fig. 4.2, besides the typical PP bands seen for the unmodified PP membrane, the IR spectrum of the hydrophilized PP membrane contained additional absorption peaks at 1728, 1111 and 1246 cm^{-1} (Fig. 4.2), which corresponds to C=O, C-O-C (ether group) and C-O (ester group) bands, respectively.

It should be noted that all the calculations and analyses in subsequent chapters were based on the measured data in Table 4.2.

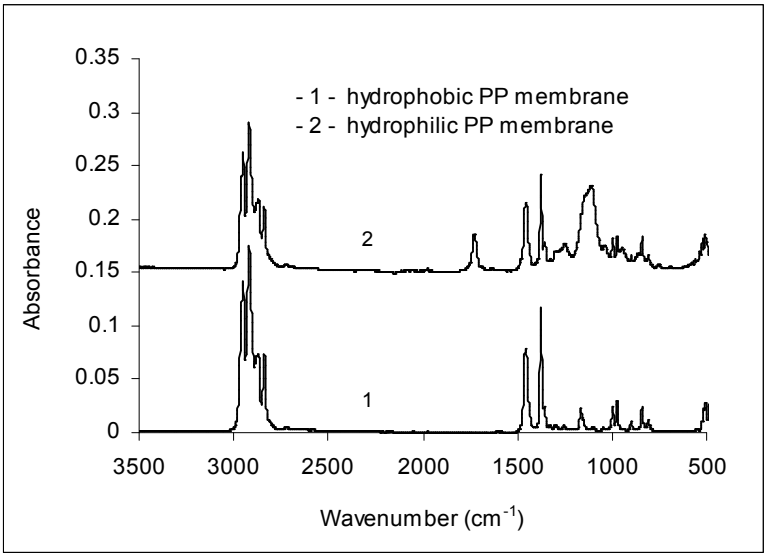

Figure 4.2: ATR-FTIR spectra of unmodified and hydrophilized PP membranes.

Table 4.1 Initial membrane data supplied by manufacturers.

Membrane	Unmodified PP	Hydrophilized PP	Track-etched PET200	Track-etched PET400
Pore diameter (μm)	0.2	0.2	0.2	0.4
Thickness (μm)	150	101	23	23
Pore density (*10^8/cm^2)	-	-	3.2	1.0
Calculated porosity (%)	-	-	10.0	12.6

Table 4.2 Measured data for various initial membranes.

Membrane	Average pore size [(a)] nm	Thickness μm	BET specific surface area m^2g^{-1}	Porosity %	Pore type	Chemical structure on the surface
Unmodified PP	~250	186	28	78	irregular	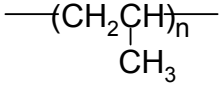
Hydrophilized PP	~350	90	15	75	irregular	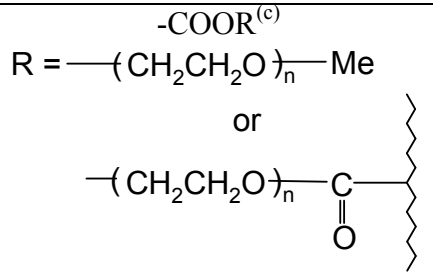
PET200	~350[1], 370[2]	23	2.8 (3.9[1], 2.7[2])[(b)]	34[1], 24[2(b)]	cylindrical	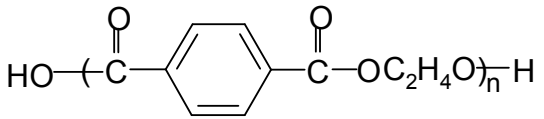
PET400	~700	23	1.7 [(b)]	28[(b)]	cylindrical	

Note: [1] and [2] (for PET200 membrane) represent different batches. (a) Measured via liquid dewetting technique using Capillary Flow Porometer; (b) calculated from water permeability and average pore size; (c) deduced from IR spectrum and contact angle, referring to the patent [104].

4.2 Photo-initiator entrapping method

This photo-grafting method had been developed previously in our group [13] and cation-exchange functional layers had been prepared on the unmodified PP membrane from aqueous solution of acrylic acid [10, 13]. Based on the more stable immobilization of photo-initiator in the membrane surface (by BP entrapping; compared with the simple physical adsorption for conventional adsorption method [114]), in this study, an attempt was made to extend the application to the photo-graft functionalization of membranes from polar organic solution system.

4.2.1 Photo-initiator immobilization

According to the proposed mechanism (see Fig. 5.10), moderate swelling of base membrane is the pre-requisite for the effective immobilization of photo-initiator. In this work, therefore, five kinds of good solvents of BP have been chosen to investigate the swelling property of unmodified PP membrane. As shown in Table 4.3, two groups can be classified according to the obtained results. The group including chloroform, benzene and heptane occupied significantly larger volume in the membrane and also caused a much greater mass loss of bulk polymer after 24-hr immersion than another group consisting of ethanol and acetonitrile, indicating that a better swelling of PP membrane has been achieved with the former. Here, therefore, heptane was chosen as the solvent of initiator. Nevertheless, the porosity of PP membrane has been estimated from the occupied volume of methanol and acetonitrile (see Table 4.3), which was similar to the porosity value determined with water (after pre-wetting).

Table 4.3 Swelling property of unmodified PP membrane in various solvents.

Solvent	Occupied volume by solvent* (10^{-3}mL/mg)	Mass loss (‰)	Estimated porosity** (%)
Ethanol	5.37	1.39	77.8
Acetonitrile	5.39	1.62	78.4
Chloroform	5.91	7.64	-
Benzene	5.96	6.19	-
Heptane	6.01	6.55	-

Unmodified PP membrane was immersed in solvent for 24 hr. *: calculated from the equation 3.5. **: obtained through the equation 3.6.

The amount of immobilized photo-initiator is a crucial factor which determines the subsequent photo-grafting efficiency and grafting density. Therefore, the BP uptake has

been determined gravimetrically (accuracy of the balance was 10 µg) after twice quick washing (2 min and 1 min, respectively) with non-swelling solvent, methanol, by which the adsorbed BP on the membrane surface had been verified to be completely removed [13]. Note that control samples have been analyzed with pure solvent (heptane) under the same conditions for correction for mass loss by extraction. Fig. 4.3 shows BP uptake of membrane as function of soaking time or BP concentration. It seems that no more BP was effectively entrapped in the membrane surface for the further immersion after about 2.5 µg/cm^2 (relative to top surface) was achieved in 15 min. In addition, the amount of immobilized BP only had a slow increase with the BP concentration used, and did not show a pronounced difference when the BP concentration was varied from 10 mmol/L to 100 mmol/L.

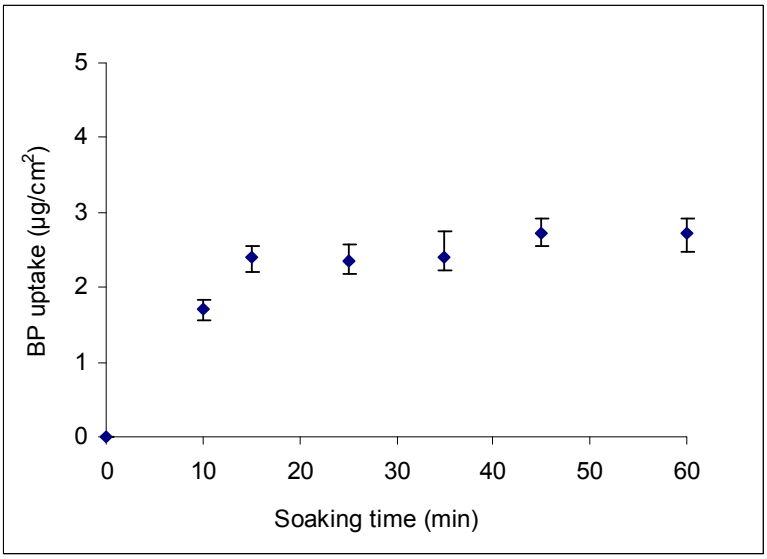

(a)

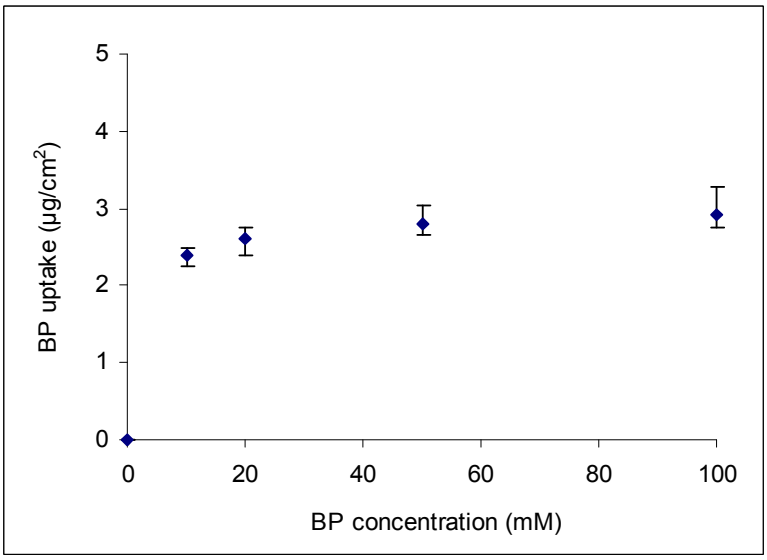

(b)

Figure 4.3: Effect of soaking time and initiator concentration on BP uptake. a) Effect of soaking time (10 mmol/L BP in heptane); b) Effect of BP concentration (15 min soaking).

4.2.2 Effect of washing on initiator immobilization

In the original literature for this method [13], water, as the medium of polymerization system, had little influence on the entrapped BP during photo-graft polymerization because of the negligible solubility of BP and no swelling of PP in water in limited time.

However, this work aimed at the membrane functionalization from polar organic solution. Therefore, it is important and necessary to know the immobilization stability of entrapped initiator during graft polymerization because the initiator BP is soluble in most of organic solvents. For this purpose, pure polar solvent, methanol, has been used to simulate the environment of graft polymerization system instead of the monomer solution. Moreover, this part of study was merged into the washing procedure prior to photo-grafting. Therefore, the washing procedure was different from that previously adopted, but similar to the procedures for membrane functionalization in monomer solution, i.e., including 10-15 min equilibrium and 10-15 min photo-irradiation time. In this case, multi-time-washing was set up (Table 4.4). The washed solutions were detected spectrophotometrically at 256 nm. As it is shown in Table 4.4, washing of the dried BP-adsorbed membrane was carried out with methanol for three or four times depending on the BP concentration used. After soaking in BP solution of 10 mM and 100 mM, respectively, BP still could be detected in the solutions after the second and third time-washing, respectively. After that, the extraction of BP has been performed with heptane. However, very low absorbance (in the error range) was observed for the extraction solution, i.e., residual amount of BP in membrane was negligible (not shown).

Table 4.4 UV absorbance of washed solutions at 256 nm.

Washing conditions	BP concentration (mmol/L)	
	100	10
1st (10 mL, 10 min)	3.855	1.123
2nd (5 mL, 5 min)	1.110	0.334
3rd (5 mL, 5 min)	0.197	-0.002
4th (5 mL, 5 min)	0.001	-

Note: The membrane with a diameter of 44 mm was used for this experiment.

4.2.3 Effect of washing on membrane photo-grafting

Photo-graft polymerization of the membranes with different washing times has been performed in AAm aqueous solution. As comparisons, same membranes have also been grafted via conventional photo-initiator adsorption method (i.e., heptane was replaced with

methanol). Fig. 4.4 shows that for adsorption method, the DG decreased rapidly with the washing time and a low constant value was achieved at only 1.5 time-washing, whereas, a gradual reduction in DG value can be observed in the case of entrapping method. However, a tendency towards the constant low value seems to be unavoidable.

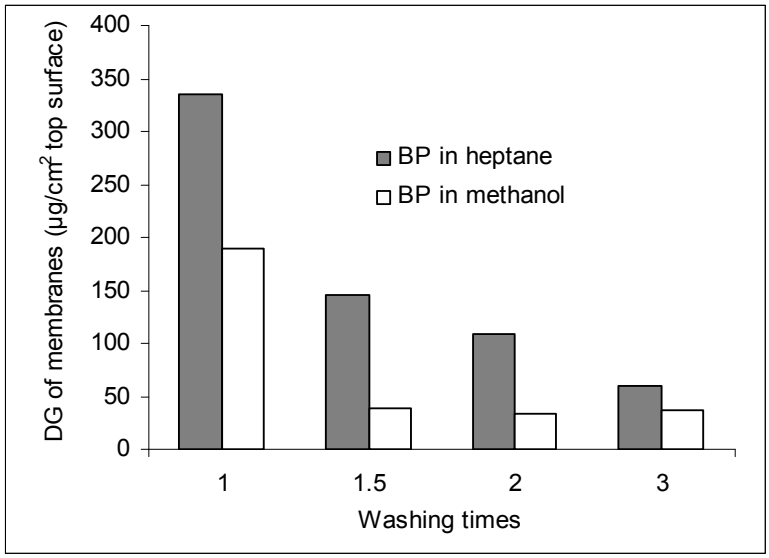

Figure 4.4: Effect of washing times on unmodified PP membrane photo-grafting via entrapping and conventional adsorption methods. Each time: one sample was washed in 5 mL methanol for 5 min. half time: 3 samples were washed in 5 mL methanol for 2 min. 10 mM BP was used for the pre-treatment of PP membrane; Photo-grafting conditions: 36 g/L AAm aqueous solution, 15 min UV irradiation.

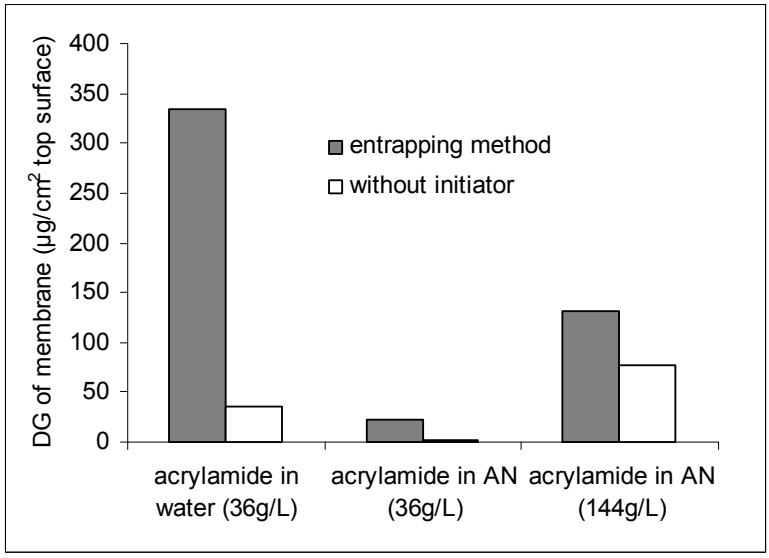

Figure 4.5: Effect of solvent on DG of membrane. Membranes were washed once prior to graft polymerization. 10 mmol/L BP was used for the pre-treatment of PP membrane; Polymerization conditions: 15 min UV irradiation.

4.2.4 Effect of solvent on membrane photo-grafting

As shown in Fig. 4.5, photo-graft polymerization of BP-entrapped and without initiator-treated (as blank sample; treated by same procedures but no initiator in heptane) PP membranes have also been conducted from acetonitrile solution of AAm. Compared to that from aqueous solution, the obtained DG value was significantly lower under the same grafting conditions. A DG value of approximately 135 $\mu g/cm^2$ has been obtained even though the high monomer concentration of 144 g/L was applied. Moreover, in this case, the DG value of the blank membrane also clearly increased.

4.3 Sequential photo-induced method

Earlier, photo-grafting of polymer films had been investigated using BP as initiator and it was discovered that the termination reaction of this graft system was mainly by combination of growing chain radicals and semipinacol radicals [104, 177]. Taking advantage of this characteristic, Bowman and co-workers had developed a novel two-step method for unmodified PP membrane photo-grafting (see Fig. 5.10) [15]. The current work focuses on the investigation of photo-graft functionalization in polar organic solution using the same method and base membrane.

The PP membrane saturated with benzene solution of 250 mmol/L BP was fixed between two pieces of glass and exposed under UV irradiation. At a given time, initiator has been covalently bond to the PP membrane surface (see reaction mechanism in Fig. 5.1). The amount and surface coverage of surface-initiator as well as BP conversion are shown in Fig. 4.6. The concentration of immobilized surface-initiator increased nearly linearly as a function of UV irradiation time in the studied range where BP conversion was very low (the maximum conversion was less than 4%). This is in agreement with the results reported by Bowman [15]. Assuming that the occupied area of one BP molecule is 90 $Å^2$ [13], a surface coverage of approximately 95% has been achieved at 15 min UV irradiation, while further irradiation led to the degradation of membrane due to the rising temperature.

Surface-initiator-immobilized PP membranes have been UV-functionalized in aqueous and acetonitrile solution of AAm for 15 min, respectively, along with the control samples (one was original membrane; another was treated with all the procedures except for UV irradiation). Fig. 4.7 shows the relationship between DG value and surface-initiator amount, as membranes were grafted from aqueous solution. The DG values were significantly higher for initiator-immobilized membranes than for original membrane and the membrane without pre-UV-irradiation. Moreover, a good correlation can be seen between obtained

DG values and surface-initiator concentration. It was noticed that an obvious difference in DG value has been observed between the membrane without pre-UV irradiation and original membrane.

In strong contrast, a much lower DG has been obtained from acetonitrile solution of AAm under the same conditions, even for the membranes with high surface-initiator concentration (Fig. 4.8). For the comparable DG, much higher monomer concentration (here 144 g/L in acetonitrile solution vs. 36 g/L in aqueous solution) was required. On the other hand, the DG of the control sample was higher as higher monomer concentration was used.

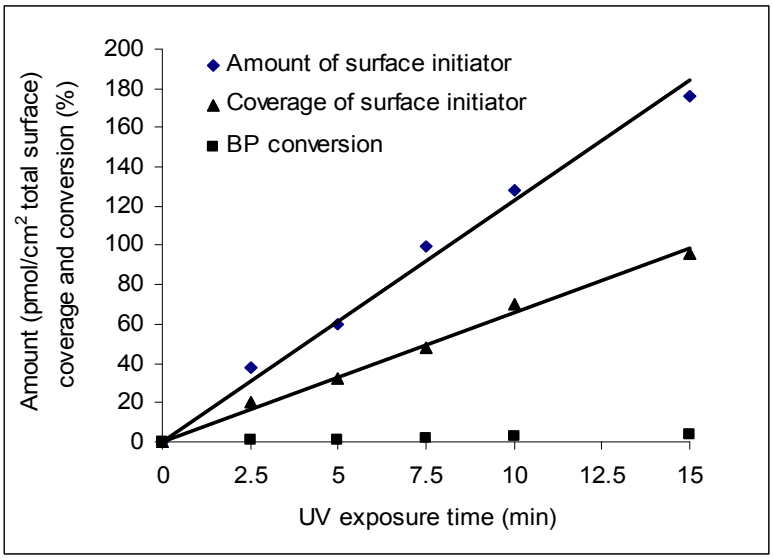

Figure 4.6: Dependence of immobilized surface-initiator on UV irradiation time. 250 mmol/l BP in benzene and 25 mW/cm^2 UV irradiation were used.

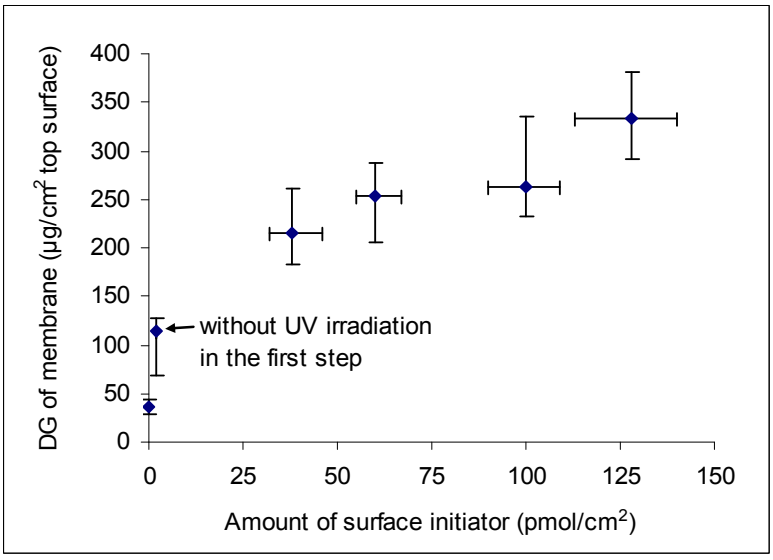

Figure 4.7: Effect of surface-initiator concentration on DG of membrane. The membranes have been grafted in the aqueous solution of 36 g/L AAm for 15 min UV irradiation.

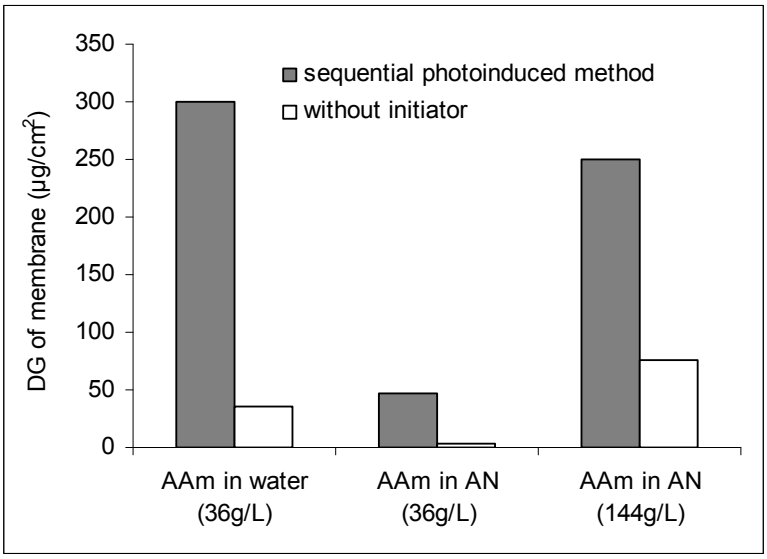

Figure 4.8: Comparison of photo-graft functionalization from water and acetonitrile solutions. Surface-initiator concentration on membrane surface was about 160 pmol/cm^2. Grafting conditions: 15 UV irradiation time.

4.4 Synergist immobilization method

4.4.1 Immobilization of tertiary amino groups

Thermally induced aminolysis, which is based on the nucleophilic reaction of an organic amine agent with the ester group along a polymer chain, had already been used to treat polymer fibers or membrane surfaces [178, 179]. According to the chemical structure of hydrophilic polymer layer (Table 4.2), hydrophilized PP membrane would be possible to be modified using the same reaction. Therefore, in this work, DEEDA (Fig. 4.9) was used to pre-functionalize the hydrophilized PP membrane surface with tertiary amino groups.

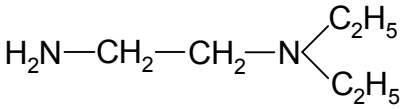

Figure 4.9: Chemical structure of diethyl ethylenediamine (DEEDA).

The immobilized tertiary amino groups have been determined by ATR-IR (Fig. 4.10a). From the spectra of aminolysed membranes, unfortunately, no amide absorption peaks could be detected after the reaction. However, the intensity ratio between the bands at 1728 and at 1375 cm^{-1}, which represents ester and methyl groups (the latter as reference peak for PP), respectively, has been observed as function of reaction conditions, i.e., the intensity ratio decreased with the rising aminolysis temperature and reaction time (Fig. 4.10b and 4.10c). In addition, a characteristic color reaction has been used to qualitatively detect

tertiary amino group as well (using "D-solution"; see Section 3.4.3). A wine-red color was observed on the aminolysed membrane samples, while no color was found for the control samples.

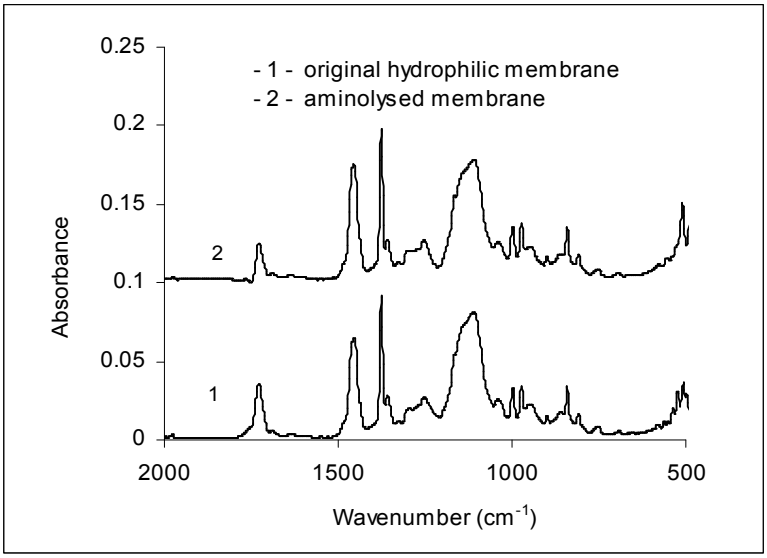

(a)

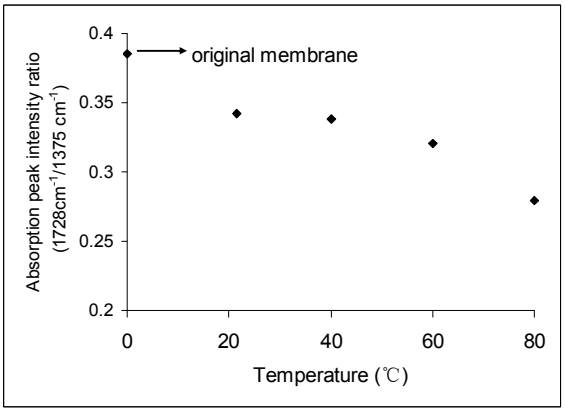

(b)

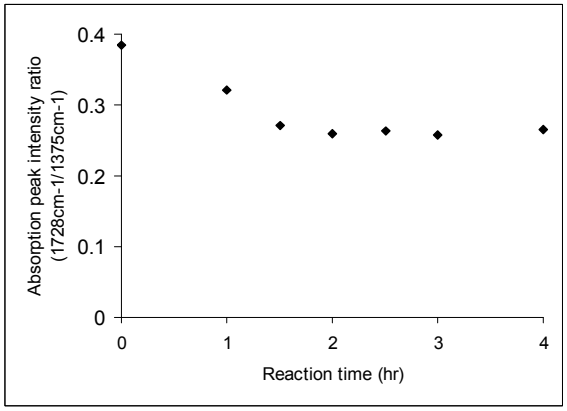

(c)

Figure 4.10: (a) ATR-FTIR spectra for original hydrophilized and aminolysed membranes (2 hr at 60^0C); and the dependence of absorption peak intensity ratio between the bands at 1728 cm^{-1} and at 1375 cm^{-1} on aminolysis temperature (reaction time: 1 hr) (b) and reaction time (aminolysis temperature: 60^0C) (c).

Reversible staining with an anionic dye is a simple, effective and frequently applied approach for qualitative and quantitative determination of amino groups [14. 21, 179]. Here AO (Fig. 4.11) was used to detect the extent of aminolysis quantitatively.

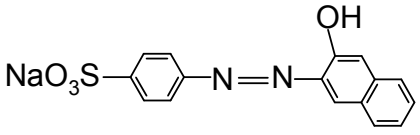

Figure 4.11: Chemical structure of acid orange II (AO).

At a given time (1 hr), the influence of aminolysis temperature on the surface amount of tertiary amino groups was measured (Fig. 4.12a). It can be seen that tertiary amino group concentration increased with the reaction temperature. For convenience, 60^0C was adopted for more detailed studies. As shown in Fig. 4.10b, at 60^0C, the maximum value of surface amount of tertiary amino groups has been achieved at the longest aminolysis time. However, the surface amount of tertiary amino groups as a function of the reaction time seemed to grow in two stages, i.e., in the ranges of 1.5-2.0 hr and 3.0-4.0 hr, respectively.

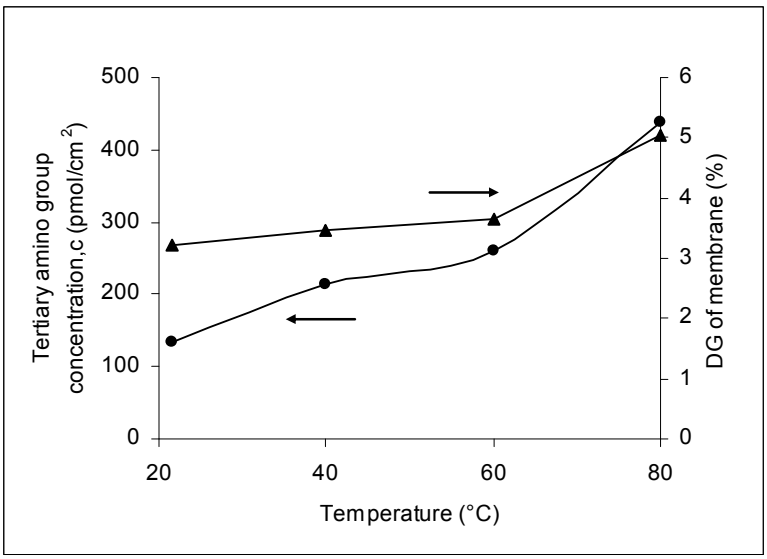

(a)

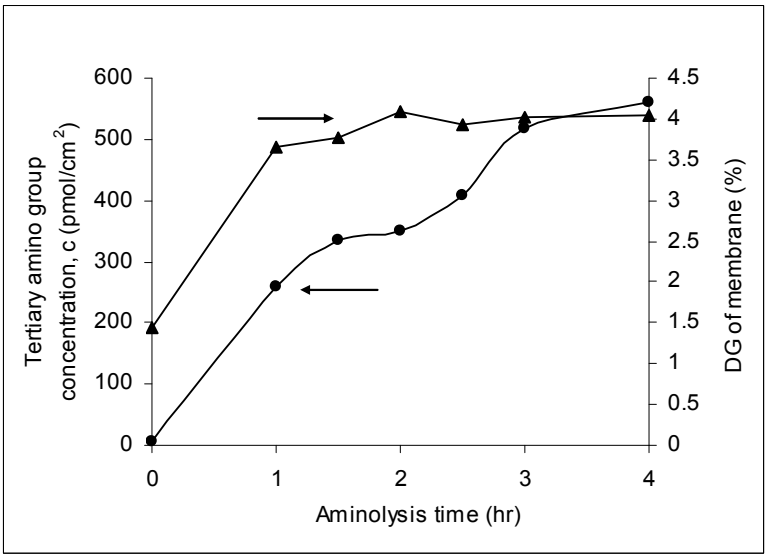

(b)

Figure 4.12: Effect of aminolysis process parameters on the amount of tertiary amino groups formed on the membrane surface (relative to the specific surface area of the membrane) and DG value of the membrane obtained in the subsequent photo-grating step (36 g/L AAm and 5 mM BP in methanol, 10 min UV irradiation). (a) Effect of aminolysis temperature, reaction time 1 hr. (b) Effect of aminolysis time, reaction temperature 60^0C. (Note that a DG = 1% corresponds to 24 μg cm^{-2} relative to the top surface area and to 0.067 μg cm^{-2} relative to the specific surface area.)

4.4.2 Photo-graft polymerization on membranes

To evaluate the proposed method, photo-grafting functionalization of original and aminolysed membranes has been carried out in methanol solution of AAm via simultaneous method (i.e., photo-initiator BP dissolved in monomer solution). The results demonstrate that for the original hydrophilized PP membrane, DG was very low and hardly affected by varying the parameters in the studied range. Even for the highest monomer concentration, the DG value of the membrane reached only about 0.17 μg/cm^2 (Fig. 4.18). In contrast, for the aminolysed membranes, much higher DG values have been achieved. Furthermore, for the membranes after varied aminolysis conditions, there was a good correlation between the surface content of tertiary amino groups and the DG values (Fig. 4.12).

In addition, ATR-IR spectra of functionalized membranes with different DG values have been recorded to characterize the chemical structure of grafted layer (Fig. 4.13). An amide I band at 1665 cm^{-1} appeared which was not present in the case of the original hydrophilized and not detectable for the aminolysed membrane (cf. Fig. 4.10a). Moreover, the intensity of the absorption peak at 1665 cm^{-1} was correlated with the DG values.

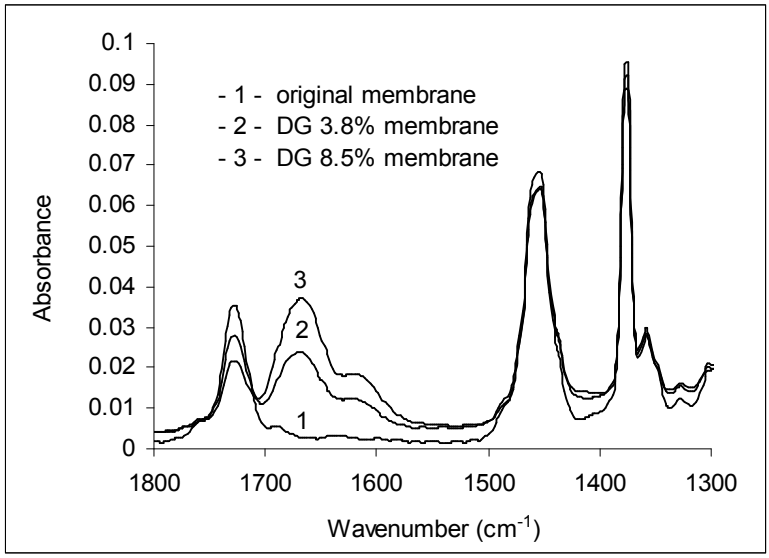

Figure 4.13: ATR-FTIR spectra for original hydrophilized and PAAm-grafted PP membranes with different DG.

For the modification of porous membranes, a key issue is that the original pore structure should not be degraded during the intended functionalization. The morphologies of the top surface of the membranes were observed using SEM (Fig. 4.14). No differences in morphology could be detected between original and aminolysed membranes. However, it should be noted that in the original and aminolysed membranes a large amount of fiber-like

polymer was seen. These features were less pronounced for the membrane with the lower DG, and they had disappeared nearly completely after photo-grafting at a DG of 8.5%. That additional polymer layer has been attached evenly and tightly on the pore surface of the membrane, and no aggregates or polymer globules were observed on the surface and in the pores.

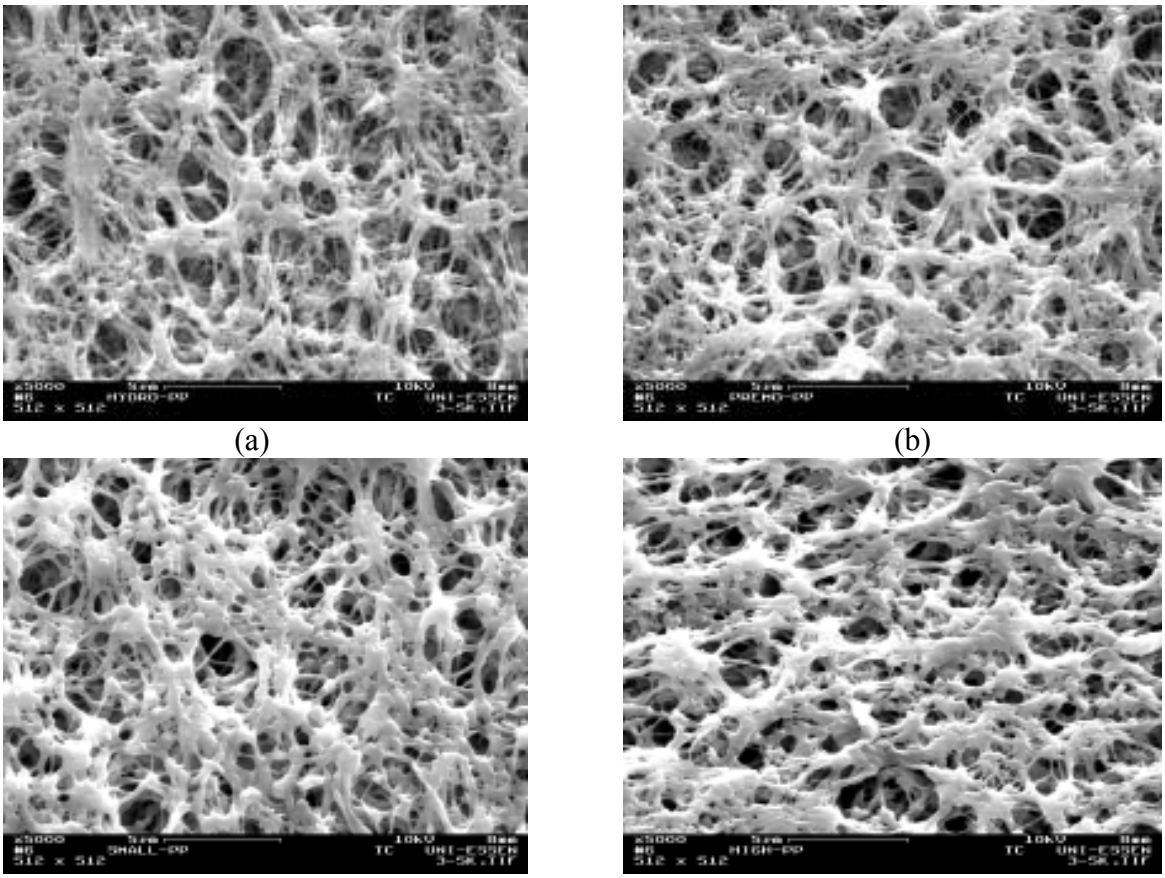

Figure 4.14: SEM top surface images of porous PP membranes: (a) original hydrophilized; (b) aminolysed (2 hr at 70^0C); (c) photo-grafted with PAAm (DG = 3.8%); (d) photo-grafted with PAAm (DG = 8.5%).

4.4.3 Factors affecting photo-graft polymerization

In this system, hydrogen atom abstraction by the excited state of BP took place from the surface layer of the membrane as intended. However, there are many factors which may affect the grafting architecture, efficiency and surface-selectivity of photo-grafting such as concentration of immobilized synergist, solvent, UV irradiation time and intensity, monomer and BP concentration. A clear understanding of these factors has great significance for the applicability of this method. And a more accurate controllability of heterogeneous graft copolymerization could be achieved only based on using optimized settings of such factors. Therefore, the detailed investigations on these factors are necessary and have been carried out as follows.

Effect of immobilized synergist concentration

Fig. 4.12 reflected the dependence of DG on the amount of the immobilized tertiary amino groups. DG value rose with the increase of synergist concentration until a maximum DG value has been achieved for 2 hr, and a longer aminolysis time did not further increase the grafting yield.

Effect of solvent

Graft copolymerization is anticipated to be initiated by starter radicals created on the substrate surface (Fig. 5.2). However, homopolymerization can also occur if starter radicals are generated by the reaction of dissolved photo-initiator with the solvent or monomer. Such competition will definitely decrease the controllability of the graft polymerization, in particular its surface-selectivity. To clarify such an effect, two different solvents (methanol is relatively reactive and acetonitrile is inert to the excited BP) have been used in the current work. The DG of membranes grafted from methanol and acetonitrile solutions at varied UV irradiation time is given in Fig. 4.15.

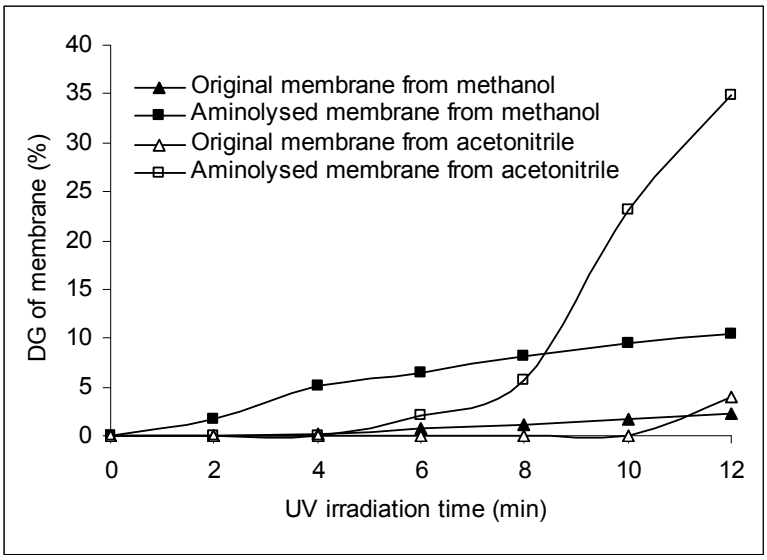

Figure 4.15: Effect of solvent on DG of membranes. 54 g/l AAm, 1.25 mM and 1.0 mM BP in methanol and acetonitrile, respectively.

The graft copolymerization efficiency during the first few minutes of UV irradiation was found to be very low. In comparison, the inhibition period in methanol solution was shorter than that in acetonitrile solution. However, for longer UV irradiation time, the photo-grafting rate of AAm for the aminolysed membranes appeared much higher from acetonitrile solution. As a consequence, the surface selectivity of photo-grafting —expressed as ratio between DG for the aminolysed membrane versus the one for the original membrane—was apparently higher as well. For instance, for 4 and 12 min UV

irradiation, the surface selectivity of grafting was 27 and 4.8, respectively, for functionalizations from methanol solution, whereas for the reactions from acetonitrile solution it was infinite (no modification of original membrane) and 8.9, respectively (Fig. 4.15).

Effect of initiator concentration

In order to elucidate the influence of BP concentration on the surface-selectivity of photo-grafting, the functionalization of the original hydrophilized PP membrane from both methanol and acetonitrile solutions has been performed first (Fig. 4.16). Only very low DG values were obtained from methanol solution and weakly dependent on the BP concentration. Even in the acetonitrile solutions, grafting was gravimetrically detectable only when BP concentration was more than 1 mmol/L. But in this case with the increasing BP concentration, the DG also strongly increased.

As expected, compared to the original membrane, higher DG values have been achieved for the aminolysed membrane from both methanol and acetonitrile solutions (Fig. 4.17 and 4.18a). However, a peak in DG appeared with the increase of initiator concentration, when membrane was grafted in methanol solution, i.e., between concentration of 0.625 and 1.25 mmol/L, while differently, with the increasing BP concentration the DG had a tendency to reach a plateau value in acetonitrile solution (Fig. 4.17a). In addition, it is evident that the surface-selectivity of grafting enhanced with the higher BP concentration at the low concentration range, then started to decrease and tended to be even close to 1 at a high concentration (e.g., for acetonitrile solution containing 5 mmol/L BP) (cf. Fig. 4.17b).

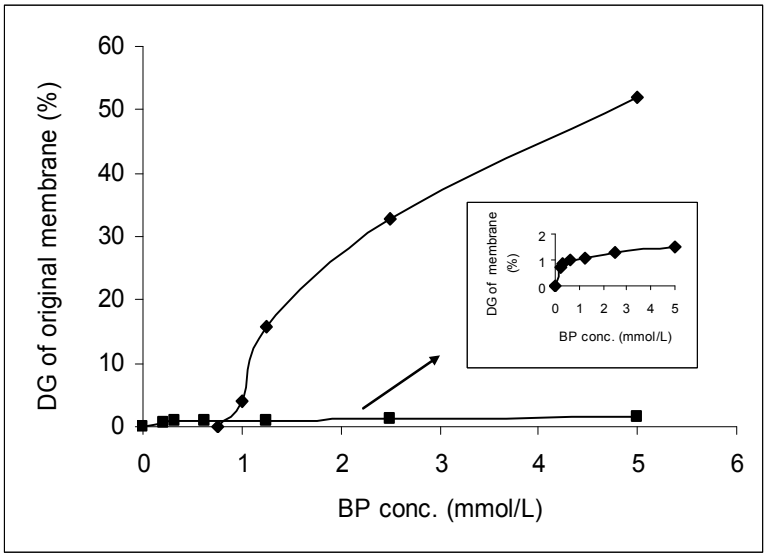

Figure 4.16: Effect of BP concentration on grafting on original hydrophilized PP membrane. (■) 8 min UV irradiation, 54 g/l AAm in methanol, ♦) 12 min UV irradiation, 54 g/l AAm in acetonitrile.

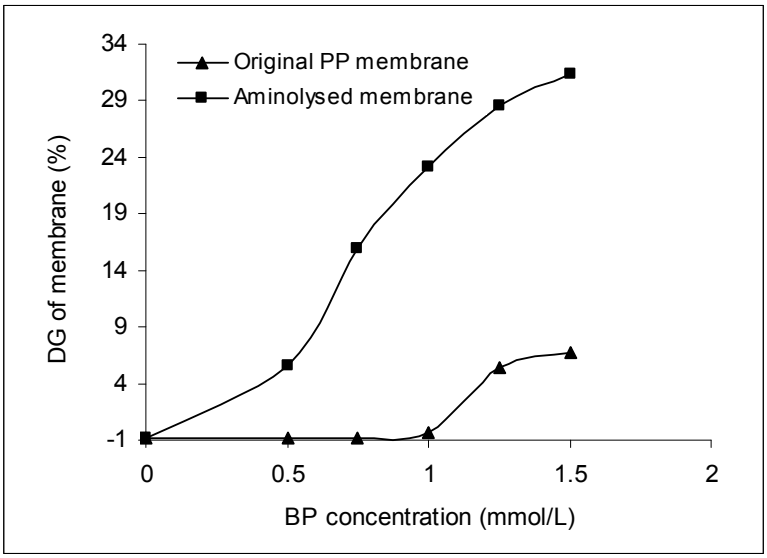

(a)

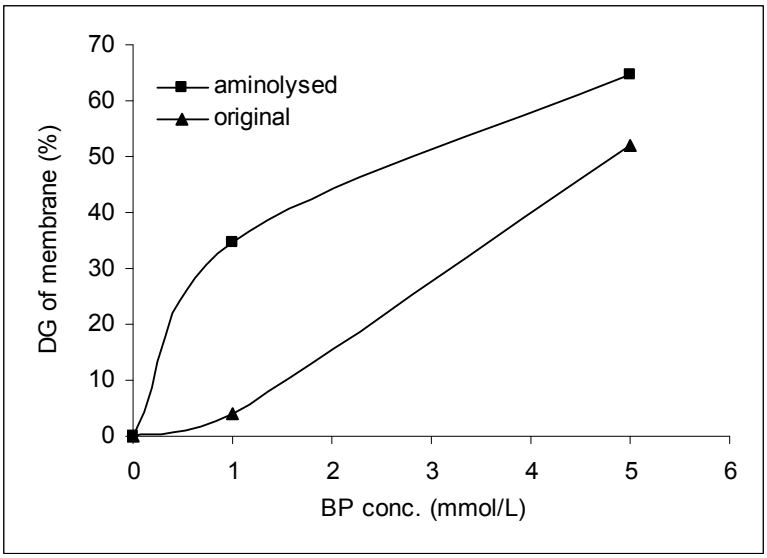

(b)

Figure 4.17: Effect of BP concentration on the surface selectivity of grafting on hydrophilized PP membranes from acetonitrile solution containing 54 g/l AAm. a) 10 min UV irradiation; b) 12 min UV irradiation.

Effect of UV irradiation time

The DG values could also be adjusted by the UV irradiation time (Fig.18b). Low graft copolymerization efficiency below 2 min exposure was observed. Afterwards, a continuously increasing DG was achieved with UV irradiation time. In addition, a much higher DG ratio (aminolysed vs. original), i.e., surface-selectivity of photo-grafting was found for shorter grafting time.

Effect of monomer concentration

As expected, the DG values increased with monomer concentration (Fig.18c). Similar to the maximum for short UV irradiation time, the functionalization process exhibited the

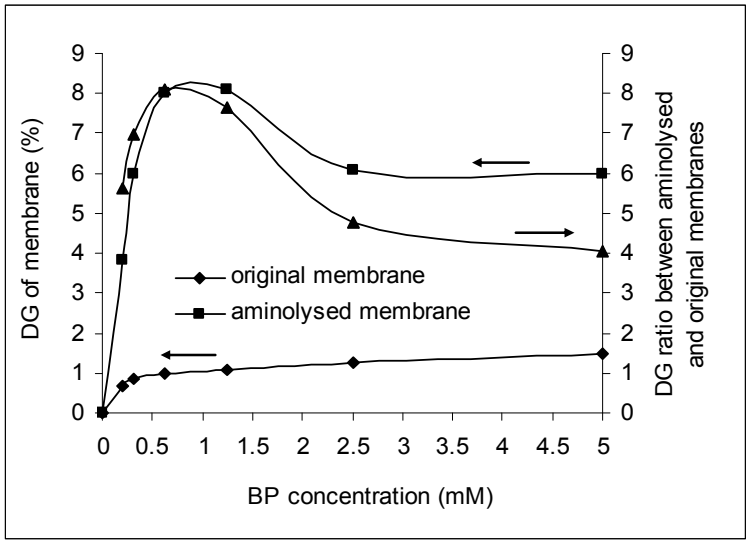

(a)

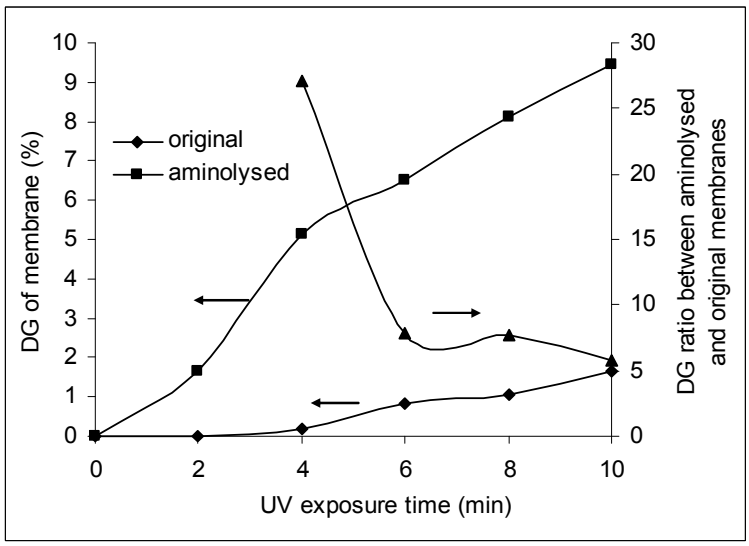

(b)

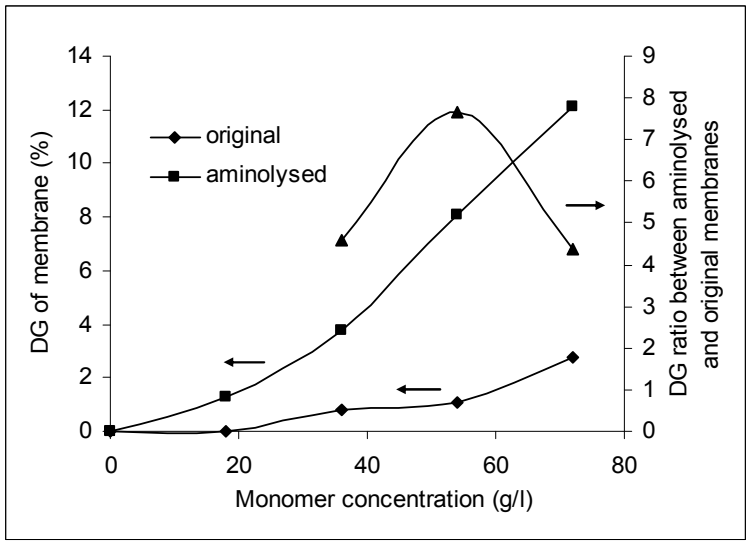

(c)

Figure 4.18: Effect of main functionalization parameters on DG and surface-selectivity of photo-grafting from methanol monomer solution. (a) Effect of BP concentration. 54 g/l AAm in methanol, 8 min UV irradiation time. (b) Effect of UV irradiation time. 1.25 mM BP, 54 g/L AAm, (c) Effect of monomer concentration. 1.25 mM BP, 8 min UV irradiation.

highest grafting surface-selectivity at the lowest monomer concentration; no DG was obtained for the original membrane. However, the large DG differences have been achieved at the high monomer concentration, although the surface-selectivity was relatively lower.

Effect of UV intensity

It is well known that increasing the intensity of UV irradiation can accelerate the photo-reduction of BP. Therefore, UV irradiation at 7.5 mW/cm^2 and 38 mW/cm^2 have been applied to investigate the influence of UV intensity on the DG and the surface-selectivity of photo-grafting, using the two different polymerization systems (Fig. 4.19).

In the case of original membrane, at high UV intensity significant DG values (6.2% and 5.2%; cf. Fig. 4.17b) were obtained from both solutions containing BP, which were higher than those DG data at low UV intensity (1.6% and ~0%; cf. Fig. 4.19a) at same UV irradiation time. As expected, in the absence of BP, no grafting has been observed, even when exposed to high-intensity UV irradiation (~38 mW/cm^2). However, surprisingly, under the identical conditions, relatively high DG values of 4.2% (from methanol) and 15.4% (from acetonitrile) have been achieved for the aminolysed membranes. But the results were still low compared with the data obtained in the presence of BP (10.8% and 46.3% from methanol and acetonitrile solutions, respectively).

In order to clarify the grafting phenomenon under high-intensity UV irradiation in the absence of photo-initiator, aminolysed membranes in 54 g/L AAm solutions without BP were exposed to UV irradiation with systematically varied intensity (Fig. 4.20). It is clear that under the selected conditions, grafting of the aminolysed membranes could be gravimetrically detected only for UV irradiation intensities beyond ~20 mW/cm^2.

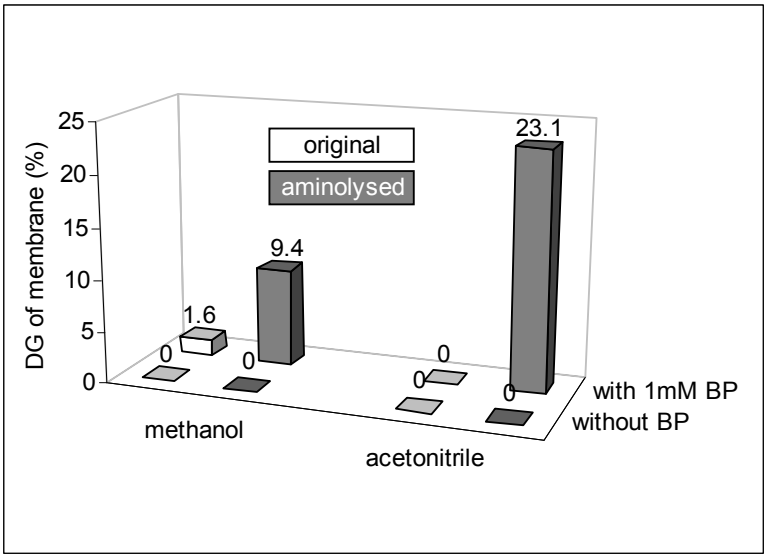

(a)

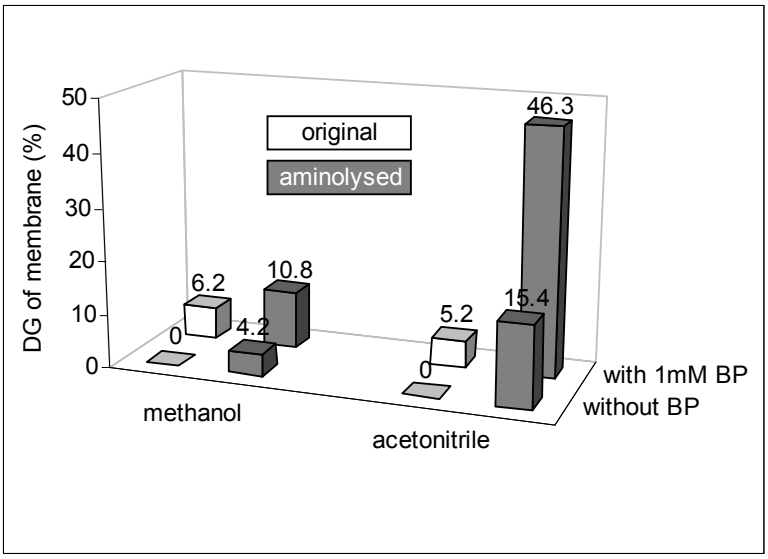

(b)

Figure 4.19: Effect of UV intensity on hydrophilized PP membrane photo-grafting from methanol or acetonitrile solutions containing 54 g/l AAm and using 10 min UV irradiation. UV intensity: a) ≈7.5 mW/cm^2, b) ≈38 mW/cm^2.

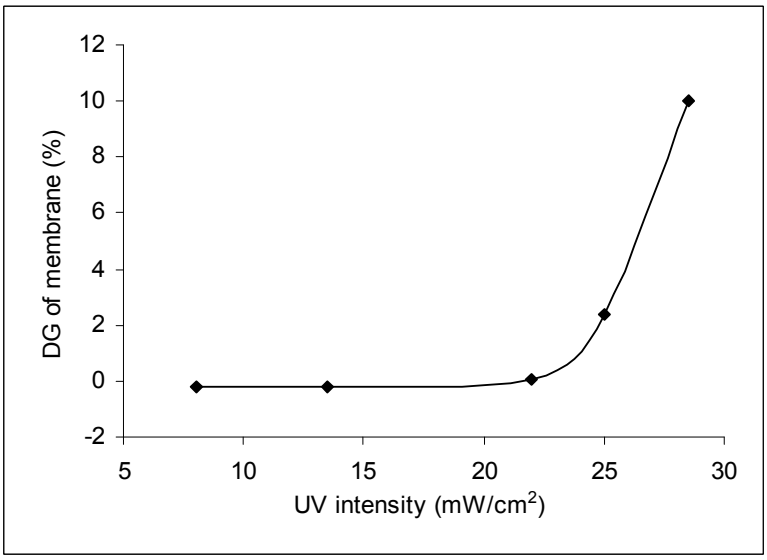

Figure 4.20: Effect of UV intensity on grafting of aminolysed PP membrane. Grafting conditions: 12 min UV irradiation, 54 g/l AAm in acetonitrile without BP.

4.4.4 Characterizations of grafted membranes

Pore size distribution

For MF membranes with a relatively isotropic pore size distribution, the layer with the smallest trans-membrane pores (i.e., the selective "barrier") is typically located inside the membrane. Further information about this barrier pore size can be retrieved from permporometry which is based on a liquid dewetting of the pores as a function of trans-membrane pressure (Fig. 4.21). Obviously, the aminolysis reaction had a small but significant effect on the internal pore structure; the pore size distribution became wider and

the characteristic pore diameter was somewhat larger (about 20 nm) than for the original membrane. As expected, the pore size decreased gradually with the increase of the DG (cf. Fig. 4.21). The reductions in pore radius due to photo-grafting, i.e., the differences compared to the data for the aminolysed membrane, were 8 nm for DG = 3.8% and 20 nm for DG = 8.5%. Assuming that the entire surface area of porous membrane was evenly covered with grafted polymer, the thickness of grafted layers can be calculated from DG and specific surface area of hydrophilized PP membrane (15 m^2/g): 2.5 nm for DG = 3.8% and 6 nm for DG = 8.5%. These data are comparable with the differences in pore radius measured by liquid dewetting method (above). While the relative increase with DG was in good correlation, although a significant discrepancy was observed for the absolute values.

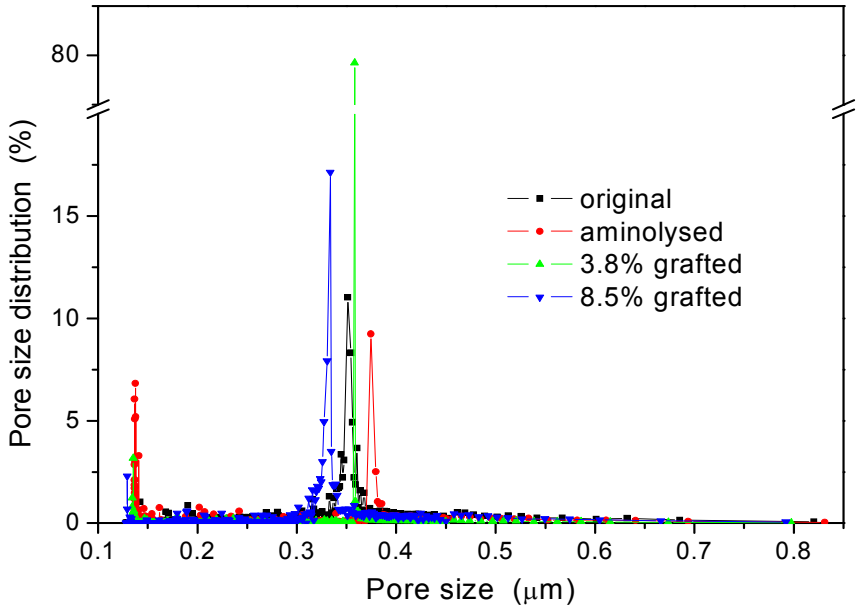

Figure 4.21: Pore size distribution from liquid dewetting permporometry for original hydrophilized, aminolysed and two photo-grafted membranes (the peak values of pore diameter were 351 nm for the original membrane, 374 nm for the aminolysed membrane, as well as 358 nm and 334 nm for the functionalized membranes with DG of 3.8% and 8.5%, respectively).

Water permeability

The water permeability of a MF membrane is an important criterion for its performance, but these data can also be analysed with respect to porosity and average pore diameter (Fig. 4.22). In general, the water permeability reduced with the DG values. For the photo-grafted membranes with a DG of 8.5%, a value of 8000 L/m^2hbar was obtained, while the water permeability of the aminolysed membrane was almost identical to the data for the original hydrophilized membrane (15000 L/m^2hbar). Very similar results had been found for functionalization of the unmodified PP membrane with similar nominal pore size using the

BP entrapping method, i.e., a permeability reduction from 16000 L/m^{2}hbar for the original membrane to 8000 L/m^{2}hbar for photo-grafted membranes with an average dry polymer layer thickness of 5-7 nm [13]. Using Hagen-Poiseuille equation and the known membrane thickness and porosity, this flux reduction corresponded to an average pore radius reduction of about 45 nm for the grafted membrane with DG=8.5%. In addition, the curves of water flux as a function of DG from different polymerization parameters were not identical (cf. Fig. 4.22). At the same DG value, the water permeability of the membranes modified at high BP concentrations (2.5 mM and 5 mM) was much higher than for the membranes modified at lower BP concentrations ($\leq$ 1.25 mM).

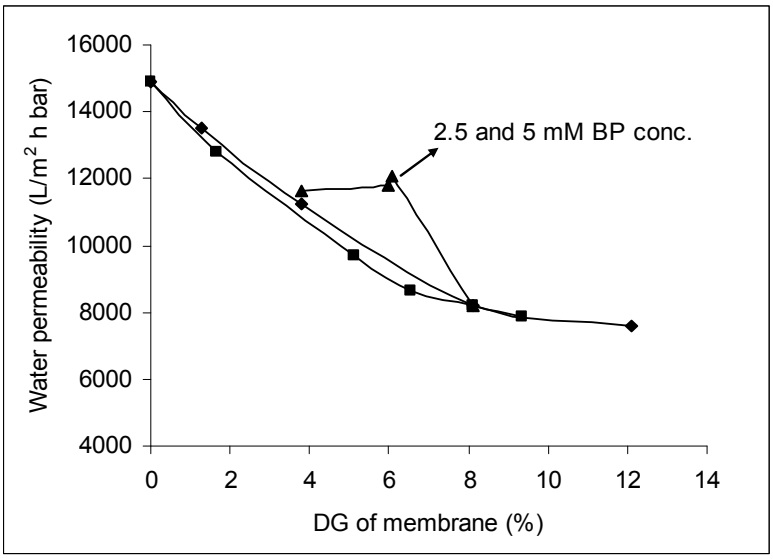

Figure 4.22: Effect of DG for photo-grafted membranes onto water permeability. ▲: varied BP concentration, 54 g/l AAm in methanol, 8 min UV irradiation (cf. Fig. 4.18a); ■: varied UV irradiation time at 54 g/l AAm in methanol, 1.25 mM BP (cf. Fig. 4.18b); ♦: varied AAm concentration, 1.25 mM BP, 8 min UV irradiation (cf. Fig. 4.18c).

Cross-linked grafted layer

In many cases, the grafted layer on membrane surface is required to be cross-linked in order to improve its stability or achieve certain special performance (e.g., MIP structure [118,121]). Therefore, high surface-selectivity of graft functionalization is necessary to avoid the uncontrollability of grafted layer architecture. According to the results obtained above, it seems to be feasible to meet this requirement. Therefore, two monomer solutions were employed for this study. Fig. 4.23 shows the morphologies of grafted polymer layers on original and aminolysed PP membranes functionalized from methanol and acetonitrile solutions containing cross-linker monomer (MBAA and EDMA, respectively) and AAm in molar ratio of 5:1. Totally different structures have been observed for the membranes grafted from methanol and acetonitrile solutions. A very even and compact thin layer could

be seen on the membrane, which has been grafted from acetonitrile solution, while a number of loose aggregates or globules were attached on the surface when methanol was employed as the medium, in particular, the deposition of polymer aggregates/globules was more pronounced for the grafted original membrane (Fig. 4.23a and 4.23b).

Cross-linked structure improves not only the chemical and mechanical properties of grafted layer, but also suppresses the swelling of grafted polymer chains in good solvent, which may be beneficial to some desired performance [9, 10]. As expected, all the membranes grafted from acetonitrile solution maintained high water flux, which was close to that of original membrane. The reduction could be observed only for the membranes with high DG (Fig. 4.24). However, the significantly lower water permeability has been obtained for all the membranes grafted from methanol solution even with low DG. Furthermore, this reduction was more obvious for the grafted original membrane with the same DG.

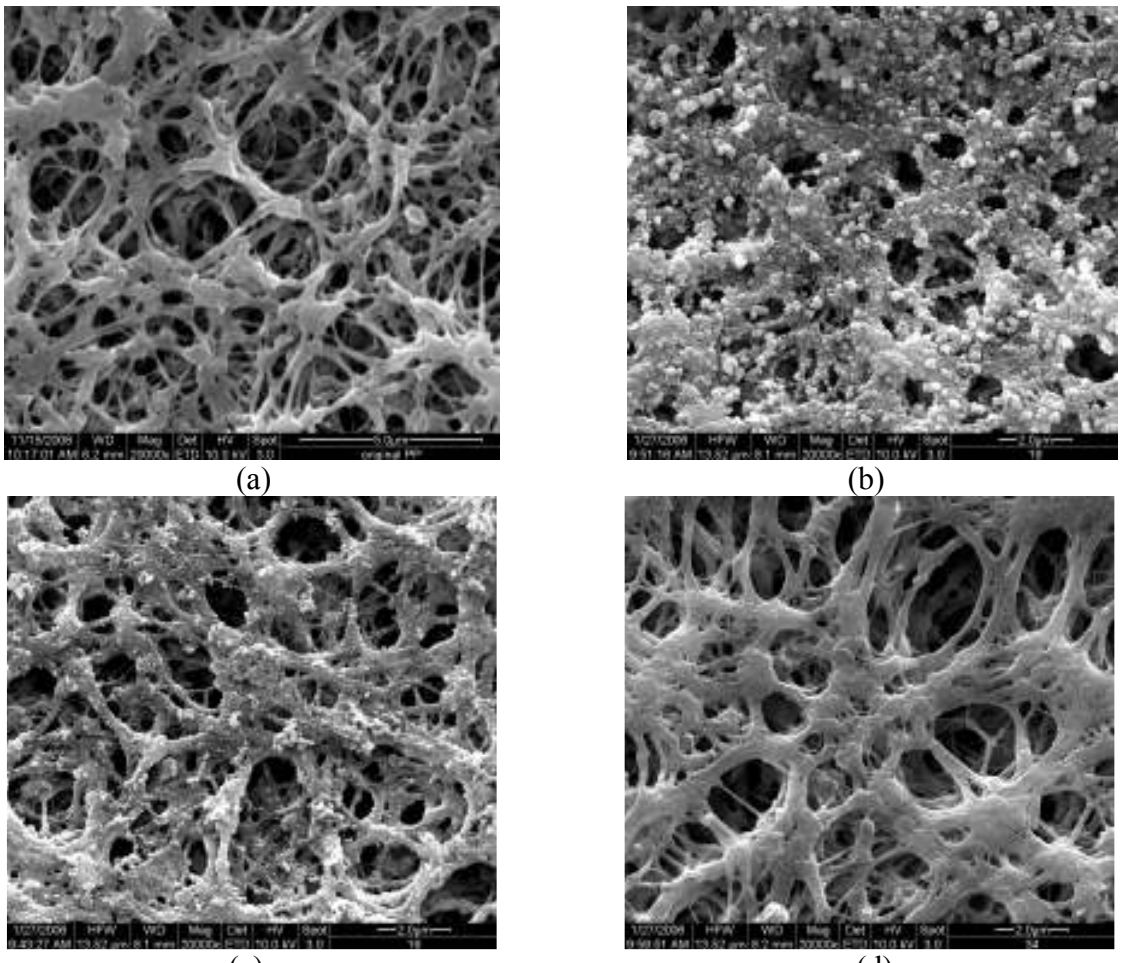

(a) (b) (c) (d)

Figure 4.23: SEM images of original and grafted membranes from different solutions. (a) original membrane, (b) grafted original membrane from methanol solution of MBAA and AAm (5:1) (DG: ~9%), (c) grafted aminolysed membrane from methanol solution (DG: ~8%), (d) grafted aminolysed membrane from acetonitrile solution of EDMA and AAm (5:1) (DG: ~ 20%).

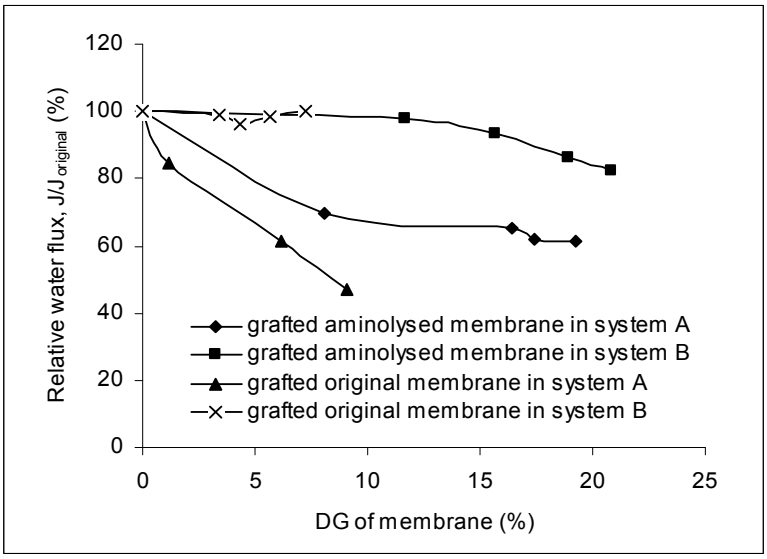

Figure 4.24: Effect of DG and grafting conditions of membranes on relative water flux.

4.4.5 Application of synergist immobilization method to PET membrane

Poly(ethylene terephthalate) (PET), like the hydrophilic polyacrylate layer of the hydrophilized PP membrane, has an ester group in its repeating unit, what is a pre-requisite for synergist immobilization via aminolysis. In addition, track-etched PET membranes have regular capillary pores with a very narrow size distribution (Fig. 4.1). Consequently, they are good candidates as model surface for fundamental research. As an example for extending the application of the novel method, the surface functionalization of track-etched PET via "grafting-from" using the synergist immobilization method has been investigated and characterized.

First of all, some explorative experiments had been done on PET film under similar conditions used above for hydrophilized PP membrane photo-grafting. IR spectra and contact angle of aminolysed and grafted film have been determined (Fig. 4.25 and Table 4.5). An additional absorption peak at 1665 cm^{-1} appeared in the grafted PET film, which corresponds to the amide I band, and the contact angle reduced dramatically from about 73^0C for aminolysed PET film to approximately 20^0C for the grafted membrane with a DG of 6%. All the data indicate that synergist immobilization method could be successfully applied to PET substrate.

Table 4.5 Contact angle of various PET films.

Membrane	Original PET	Aminolysed PET	Grafted PET
Contact angle / ^{0}	86 ± 4	73 ± 4	20 ± 8

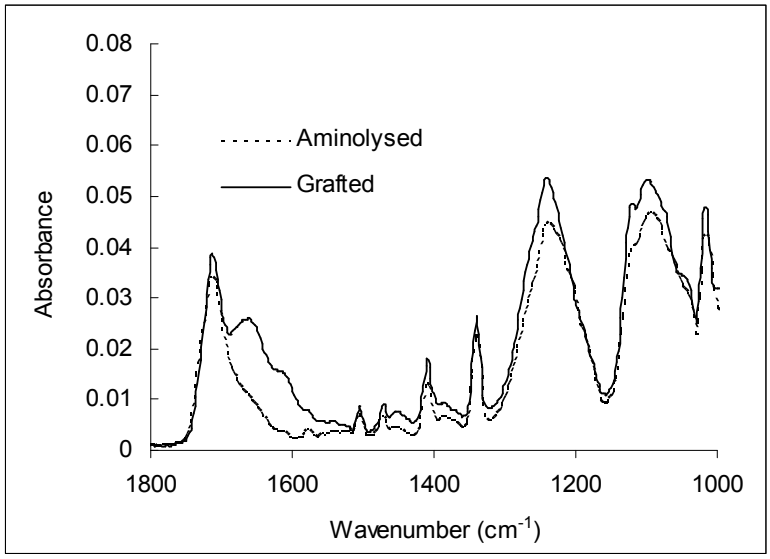

Figure 4.25: ATR-FTIR spectra of aminolysed and grafted PET film. (aminolysis reaction: 70^0C for 2 hr; graft polymerization: 54 g/L AAm in acetonitrile, 10 min UV irradiation, 1.25 mmol/L BP).

Optimization of aminolysis reaction for PET membrane

In order to examine the conditions which are suited for the heterogeneous reaction, the mass loss of membranes was measured after varied time of aminolysis by DEEDA at varied temperatures (Fig. 4.26a). Higher temperature and longer reaction time led to larger mass losses under the selected conditions. For better controllability of the reaction, 70^0C had been used for further studies. The amino group concentration on the membrane surface, which has been determined using reversible staining with an anionic dye (AO), increased as a function of the reaction time at 70^0C. 374 pmol/cm^2 amino groups (relative to the specific surface area) were determined at 2 hr. This was almost identical to the data obtained after 2 hr aminolysis of hydrophilized PP membrane at 60^0C.

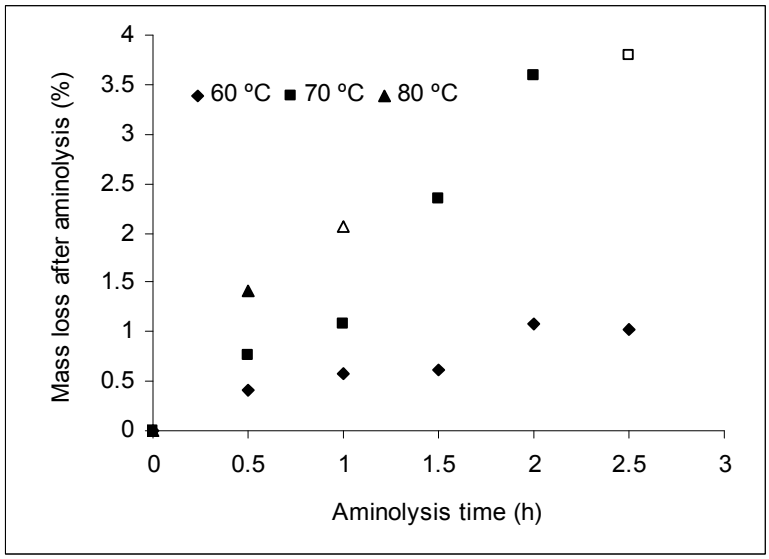

(a)

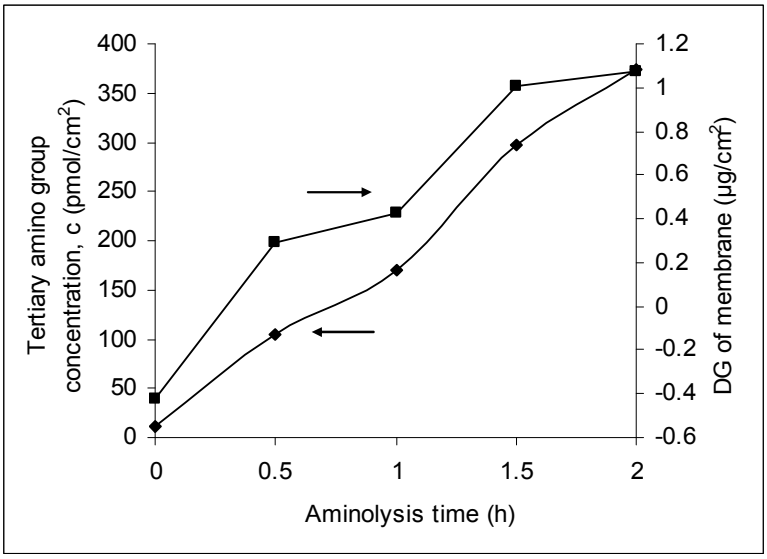

(b)

Figure 4.26: Optimization of aminolysis process parameters for PET200 membranes (batch 1). a) Effect of aminolysis temperature and time on mass of membrane (open symbols represent broken membranes). b) Effect of aminolysis time at 70^0C on tertiary amino group concentration and subsequent DG (grafting conditions: 10 min UV irradiation, 54 g/l AAm in acetonitrile with 1 mmol/l BP).

In addition, the reaction caused also an increase of the specific surface area: from 2.79 m^2/g for the original membrane, to 3.54 m^2/g for the membrane aminolysed for 2 h at 70°C. Moreover, a shift of the peak of the pore size distribution by 10 nm had been detected (Fig. 4.27).

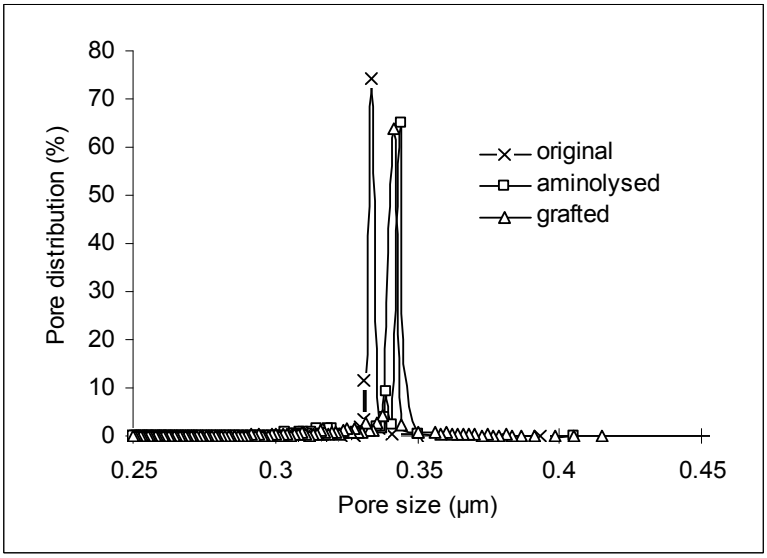

Figure 4.27: Pore size distribution of various PET200 membranes (batch 1). Original (maximum: 334 nm), aminolysed for 2 h at 70 ºC (maximum: 344 nm), and grafted (DG = 1.34 µg/cm^2; maximum: 342 nm).

Photo-grafting on aminolysed PET membrane

The graft copolymerization of aminolysed PET200 membrane has been performed in acetonitrile solution of AAm. As expected, the DG of membrane increased with the

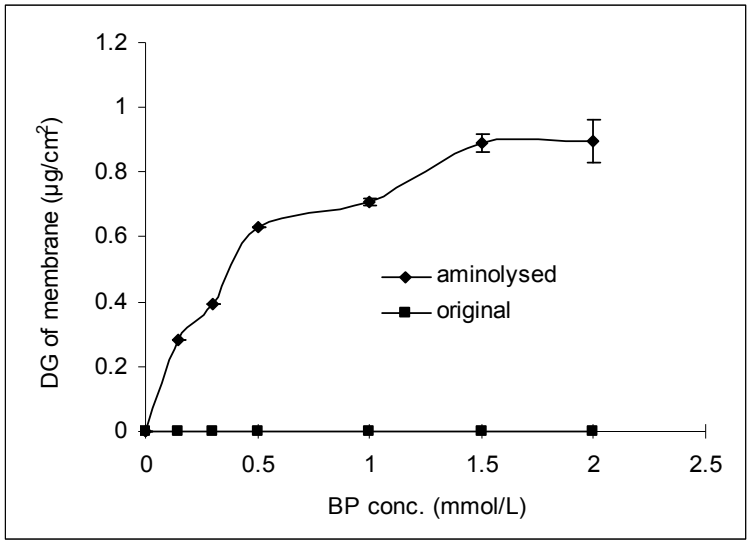

(a)

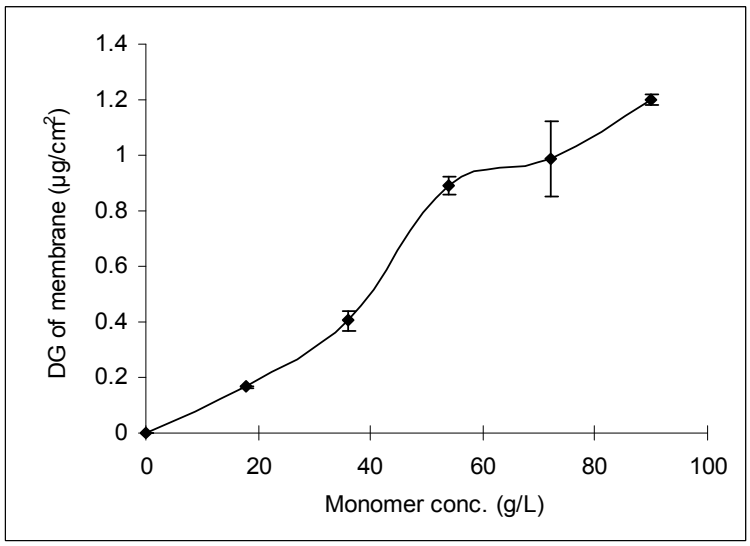

(b)

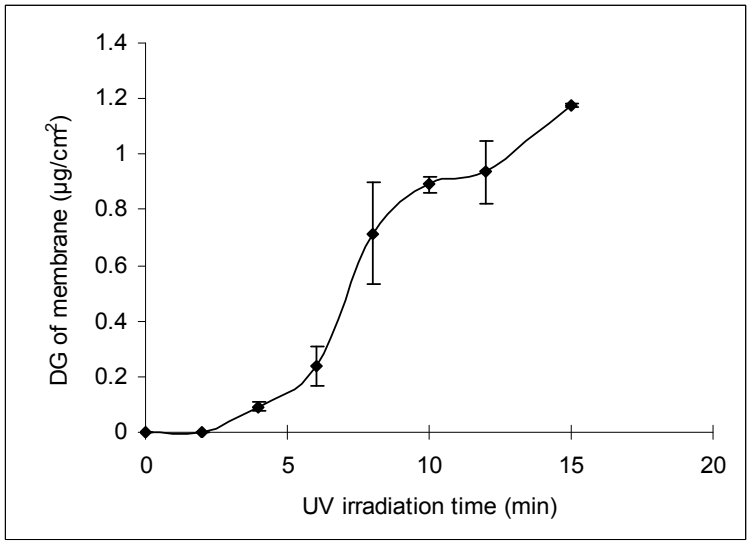

(c)

Figure 4.28: Effect of functionalization parameters on grafting onto PET200 membrane (batch 2) from monomer solution in acetonitrile at low UV intensity (7.0 mW/cm^2). a) 54 g/l AAm, 10 min UV irradiation, b) 10 min UV irradiation, 1.5 mmol/l BP, c) 54 g/l AAm and 1.5 mmol/l BP.

increasing concentration of tertiary amino groups on the membrane surface (Fig. 4.26b). As a consequence, the pore size of grafted PET was observed to shift towards smaller values compared to the aminolysed membrane (cf. Fig. 4.27).

Under low intensity UV irradiation, for the original PET membrane no grafting was detected, but a pronounced dependence of DG of the aminolysed PET membrane on the BP concentration was observed (Fig. 4.28a). Hence, complete surface selectivity of the synergist immobilization method has been achieved. The DG grew up to a saturation value of ~0.9 µg/cm^2 when the BP concentration reached about 1.5 mM under the selected conditions. Like for the hydrophilic PP membrane, the graft polymerization of aminolysed PET membrane can also be well adjusted by the varied UV irradiation time and monomer concentration (see Fig. 4.28).

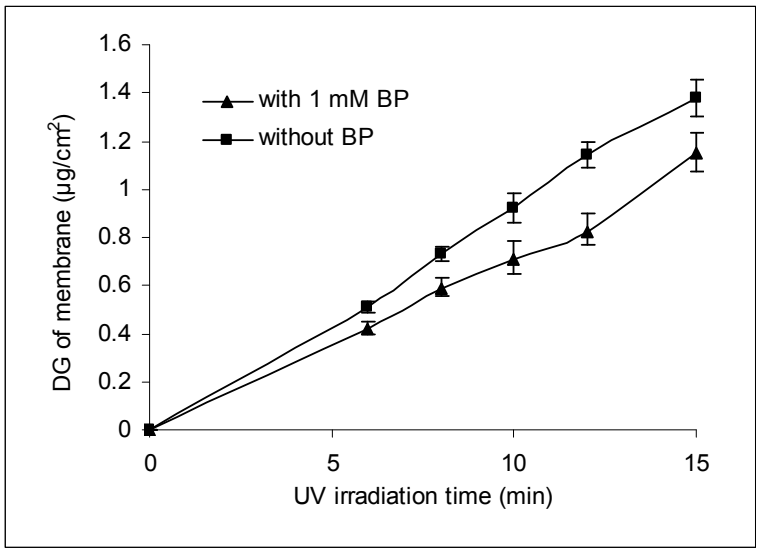

(a)

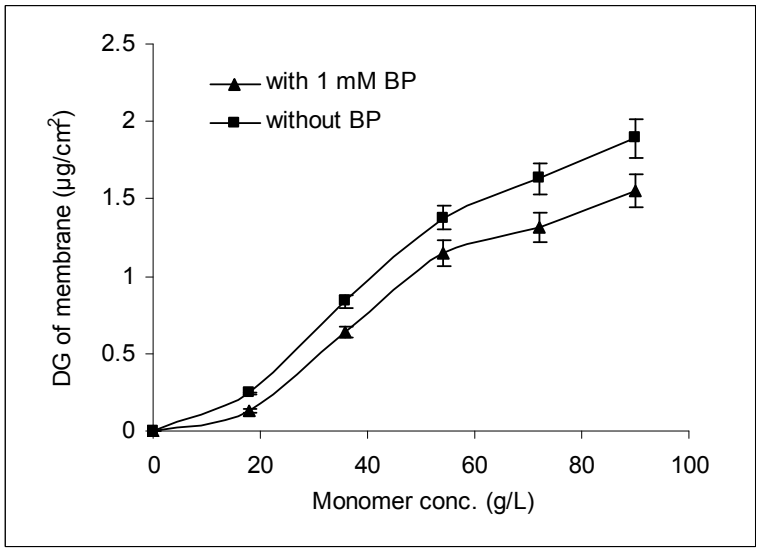

(b)

Figure 4.29: Effect of monomer concentration and UV irradiation time on grafting onto PET200 membrane (batch 1) from monomer solutions in acetonitrile at high UV intensity (32 mW/cm^2). a) 54 g/l AAm, b) 15 min UV irradiation.

When investigating the photo-grafting of PET in more detail, it was found that like aminolysed hydrophilized PP membrane, under high intensity UV irradiation, the photo-graft polymerization of aminolysed PET membrane also occurred in the absence of BP, and surprisingly, the resulting DG values were even higher than those of membranes grafted in monomer solution containing BP (Fig. 4.29). However, under the same conditions, no grafting was observed for the original PET membrane, without or with 1 mmol/L BP in the monomer solution.

Characterization of PET membranes

Surface coverage. To obtain the information about the surface properties, contact angles of aminolysed membrane and PAAm-grafted membranes prepared with varied UV irradiation time have been measured (Fig. 4.30). As the grafting time increased, the contact angle of the resulting membrane decreased until a lowest value has been reached at 12 min UV irradiation, which was similar to that for PAAm-grafted PET film (see Table 4.5). Longer graft copolymerization did not cause the further reduction in contact angle.

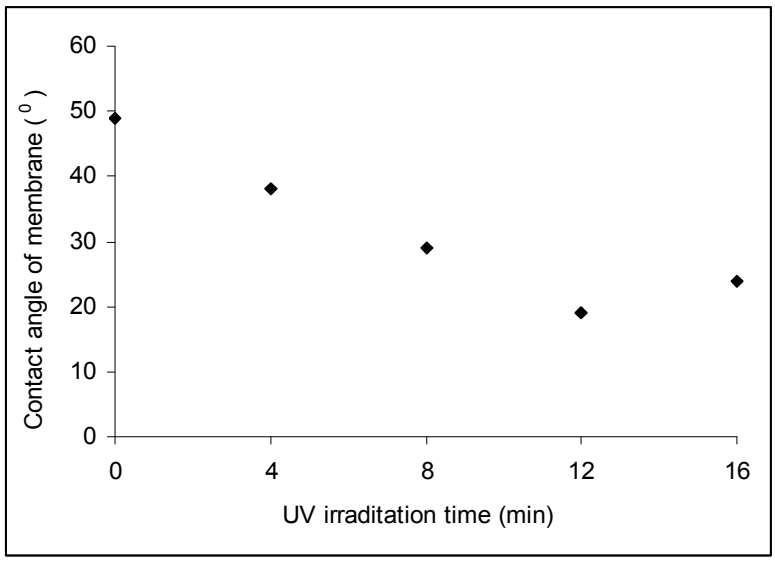

Figure 4.30: Effect of UV-grafting time on contact angle of PET400 membranes. Aminolysis: 2 hr at 70^0C; photo-grafting: 54 g/L AAm in acetronitrile containing 1.5 mM BP.

Zeta potentials were determined as function of pH in 10^{-3} M KCl solution in order to evaluate the surface charge property of initial and functionalized PET400 membrane samples. Fig. 4.31 shows the zeta potential versus pH curves for selected membranes. It can be seen that the surface charge of the unmodified PET400 membrane was clearly negative at pH 4 with a tendency to reach a value of zero (isoelectric point) at lower pH (approximately 1.8). At higher pH, it became increasingly negative, reaching a plateau

value of -25 mV at pH >6. The aminolysed PET membrane had a positive charge with a zeta potential approaching 5 mV at the lowest pH value. An increase in pH caused a decrease in the zeta potential, and a value of -5 mV was reached at pH 7. The isoelectric point of this membrane was determined at pH 6. When the aminolysed membranes have been modified with PAAm, the concentration of positive charge decreased with the UV irradiation time up to no detectable net charge at 12 min UV irradiation.

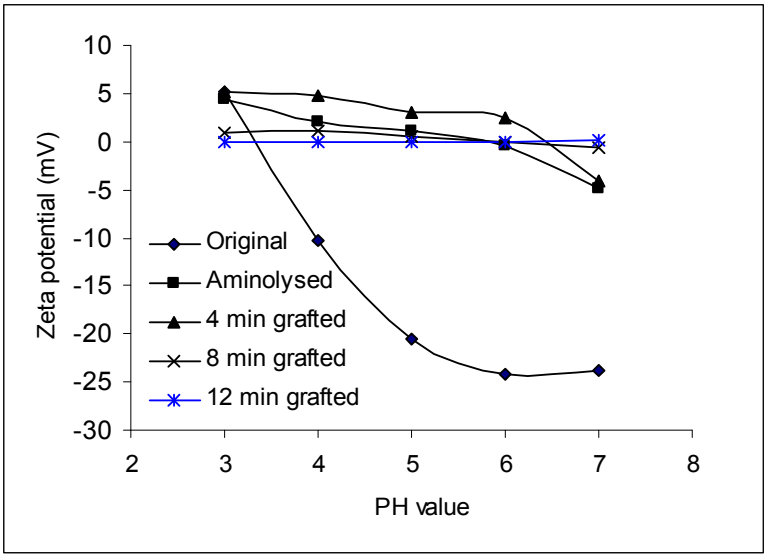

Figure 4.31: Zeta potential vs. pH for original, aminolysed (2 hr at 70^0C) and selected grafted PET400 membranes. Grafting conditions: 54 g/L AAm in acetonitrile containing 1.5 BP.

Liquid permeability. Water and ethanol fluxes were measured for the selected aminolysed and grafted membranes and converted into the pore radius change using the Hagen-Poiseuille equation. Fig. 4.32 shows the relationships between DG of the functionalized membranes and the change of pore size in water and ethanol. For all membranes, the measured pore sizes with ethanol were close to those of the aminolysed membranes. The grafted layer thickness calculated from the ethanol flux was similar to the one for the dry layer, estimated from DG value and assuming an even coverage on the specific surface area of 3.54 m^2/g, determined by nitrogen adsorption/BET analysis (for a DG of 1.35 μg/cm^2, 30 nm was estimated from ethanol flux, and 27 nm from gravimetrical data). However, a strong reduction of permeability (and hence pore radius) was observed for grafted membranes with water as test fluid.

With a certain DG value, the grafted membrane adjusted by UV irradiation time exhibited the similar water permeability. However, a pronounced reduction was found with the increase of DG values adjusted by monomer concentration (cf. Fig. 4.32 and 4.33). Interestingly, under high-intensity UV irradiation, pore radii of the membranes grafted

from the monomer solution containing BP appeared smaller than those of the membranes grafted in the absence of BP (cf. Fig. 4.32).

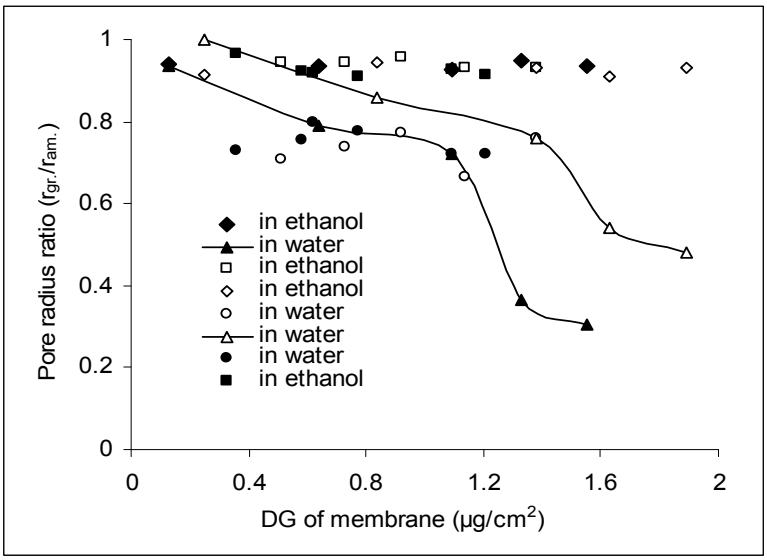

Figure 4.32: Effect of DG for PET200 membranes (batch 1), grafted with PAAm from acetonitrile at high intensity UV (32 mW/cm^2) on reduction of apparent pore radius in ethanol or water. DG had been adjusted by UV irradiation time (circle and square) and monomer concentration (triangle and diamond). Filled and open symbols refer to the grafted membranes from solution with and without BP, respectively.

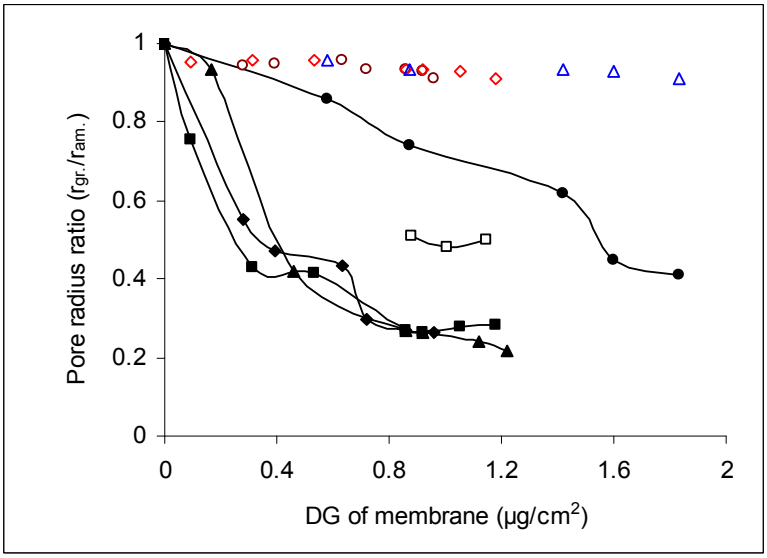

Figure 4.33: Effect of DG for PET200 membranes (batch 2), grafted with PAAm from acetonitrile at low intensity UV (7.0 mW/cm^2) on reduction of apparent pore radius in water or ethanol (colorful symbols). DG had been adjusted by UV irradiation time (filled square, open square – for comparison: membrane grafted at 32 mW/cm^2 UV in the absence of BP), BP concentration (diamond), and monomer concentration (triangle). Chemical cross-linking in the grafted layer had been achieved by addition of 10 wt% EDMA in the monomer solution (circle).

In addition, at the same DG value, the pore radius ratio between grafted and aminolysed membranes was much higher after high intensity than that after low intensity UV irradiation (at ~ 0.8 µg/cm^2: 0.5 (0.7 from batch 1) and 0.25, for high and low intensity UV, respectively; cf. Fig. 4.32 and 4.33). For this phenomenon, a hypothesis has been brought forward that cross-linking has occurred during the graft polymerization under high intensity UV irradiation. Thus, to provide evidence for this hypothesis, aminolysed membranes have been photo-grafted from a monomer solution containing a certain fraction of a cross-linker (EDMA) under low intensity UV irradiation. These membranes showed a significantly lower reduction of pore radius with the same DG, especially when compared with the membranes grafted under controlled conditions, i.e., the combination of BP, synergist and low intensity UV irradiation (cf. Fig. 4.33).

Cross-linked grafted layer

Cross-linked polymer layers have been prepared on the aminolysed PET400 membrane from AAm solution in acetonitrile containing varied EDMA contents (Fig. 4.34). The DG increased with the rising EDMA content until a highest value has been achieved at 10 wt% EDMA in total monomer, and then the DG went down with the higher cross-linker concentration. It seems that DG value started to be constant at the EDMA concentration of 25 wt%.

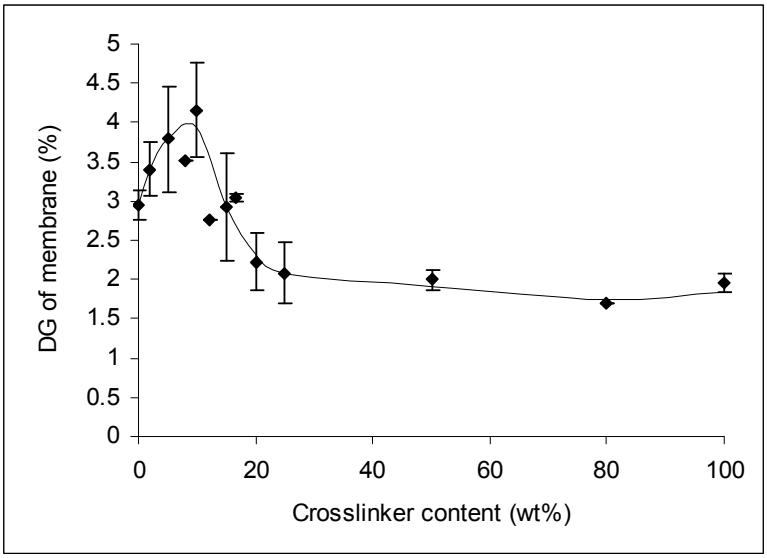

Figure 4.34: Effect of crosslinker content on DG of PET400 membrane (12 min UV irradiation, 54 g/L total monomer concentration, 1.5 mM BP).

Membranes with similar DG value but differing in the composition of grafted layer have been prepared from the acetonitrile solution containing varied molar ratio of AAm and EDMA. Water and ethanol permeability have been measured for those grafted membranes

(Fig. 4.35). As expected, ethanol permeability values for all membranes are similar and close to that of aminolysed membrane. However, depending on the cross-linker content used, the water permeability of grafted membranes differed. When the cross-linker content was in the range of 0-5 wt%, the water permeability was low and almost constant for the grafted membranes, then going up with the further increasing cross-linker concentration until a plateau, which is close to that of aminolysed membrane, was achieved at 15 wt% cross-linker. Only at high cross-linker content, the slightly lower values were observed.

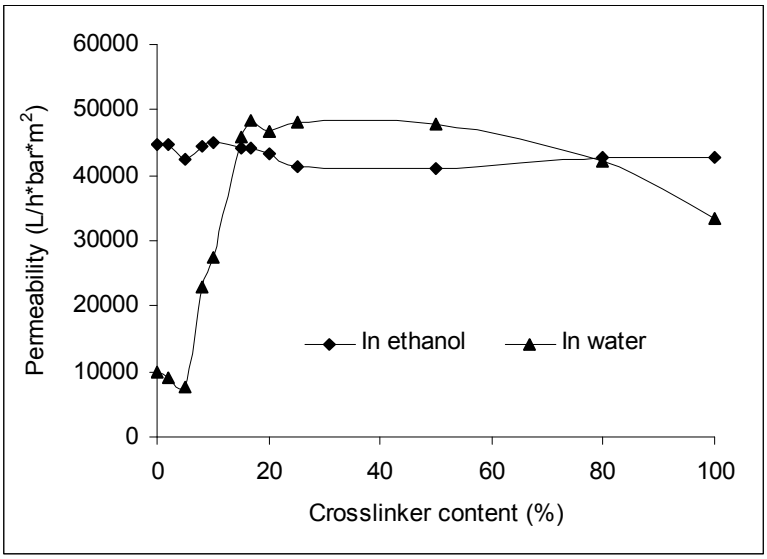

Figure 4.35: Effect of crosslinker content on water or ethanol permeability of grafted PET400 membrane (DG = (2.6 ± 0.3)% for all grafted membranes).

4.5 Iniferter immobilization method

Dithiocarbamate has been investigated as a photo-reactive moiety to initiate graft polymerization on various surfaces, especially for the preparation of well-defined grafted layer due to its characteristic as an iniferter [180-182]. However, the application of this technique to polymeric membranes has been rarely reported [183]. Therefore, we attempted to further exploit the photo-grafting technique for polymeric membranes using the concept of iniferter, mainly aiming at the preparation of controllable grafted functional layer on the membranes from polar organic solution.

4.5.1 Photo-iniferter immobilization

As shown in Fig. 4.36, in this work, the iniferter, dithiocarbamate was immobilized on the hydrophilized PP membrane by 3 steps.

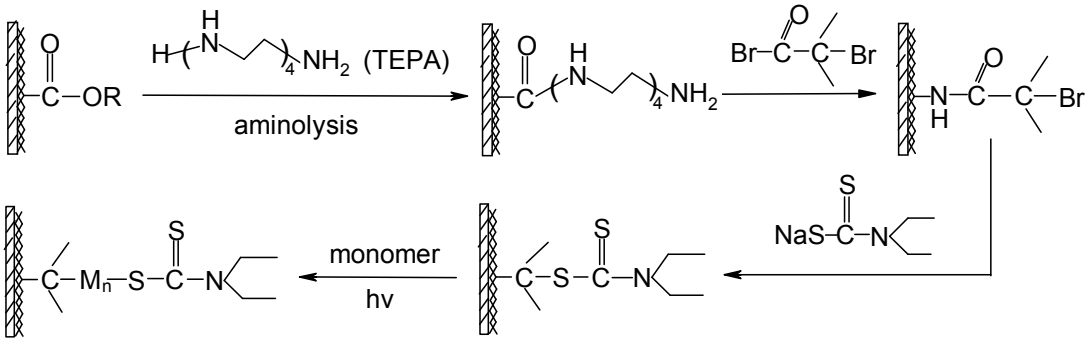

Figure 4.36: description for immobilization of iniferter and subsequent photo-grafting of membrane.

Preliminary experiments have been undertaken to optimize the reaction conditions. In the first step, the amino groups were introduced by aminolysis reaction with 25 wt% TEPA in DMF. The amount of amino groups on the resulting aminated membranes was determined using dye staining method with AO as before. Fig. 4.37 shows the dependence of amino group concentration on reaction temperature and time. At both 60^0C and 70^0C, the amino group concentration increased with the reaction time until a saturated value of around 500 pmol/cm^2 was achieved at 4 hr, which is comparable with the data reported in previous literature (400 and 700 pmol/cm^2 on track-etched PET membrane [14, 21]). Therefore, the aminated membranes with ~500 pmol/cm^2 amino group have been prepared for the following studies.

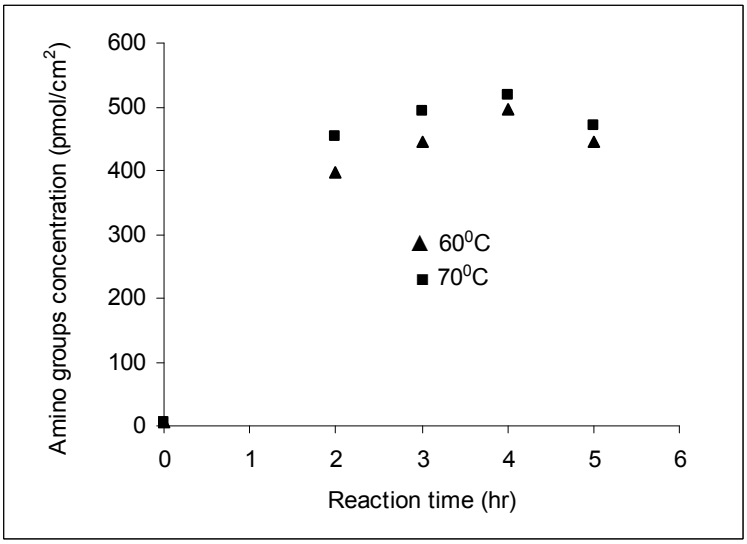

Figure 4.37: Effect of reaction time and temperature on amino group concentration. Reaction proceeded in DMF solution of 25% TEPA.

Different concentrations of 2-bromoisobutyryl bromide in the range of 10 to 150 mM have been adopted in the 2nd step, which proceeded at 30^0C for 4 hr (Table 4.6). The conversion of amino groups increased with the bromide concentration until approximately 70% was

achieved at 50 mM. Therefore, this concentration was chosen for all the following investigations unless otherwise mentioned. Similar to the reaction for the introduction of dithiocarbamate on the planar surface [182], the subsequent immobilization of iniferter (the 3rd step) was carried out in ethanol solution of 0.3 M sodium N,N-diethyldithiocarbamate at room temperature overnight.

Table 4.6: Optimization of 2-bromoisobutyryl bromide concentration in the 2nd step (cf. Fig. 4.36).

	1#	2#	3#	4#
2-bromoisobutyryl bromide (mM)	10	50	100	150
Triethylamine (mM)	13	55	105	155
DMAP (mM)	5	5	5	5
Acetonitrile (ml)	9.96	9.86	9.72	9.6
Amino group (pmol/ cm^2)	230	149	137	141
Conversion (%)	55	71	73	73

Reaction was performed at 30^0C for 4 hr; the used membranes had been treated by the 1st step at 70^0C for 4 hr.

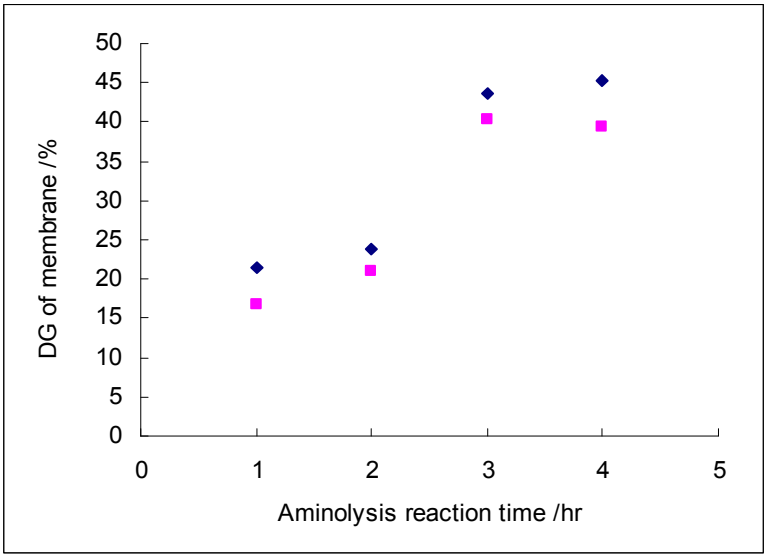

Figure 4.38: Effect of aminolysis reaction time on photo-grafting of iniferter-immobilized membrane. Grafting conditions: 54 g/L AAm in acetonitrile, 10 min UV irradiation. ♦: 7.5 mW/cm^2, without controlling temperature (with UV irradiation, the temperature in UV chamber was rising up to about 60^0C after 10 min); ■: 11.0 mW/cm^2, at ambient temperature (cooling water was used).

4.5.2 Photo-graft polymerization on iniferter-immobilized membrane

Graft polymerization of the iniferter-immobilized membrane and bromoisobutylated membrane (treated by the first two steps) has been performed in acetonitrile solution of AAm under 7.5 mW/cm^2 UV irradiation. No grafted polymer was detectable

gravimetrically for the bromoisobutylated membrane, whereas a quite higher DG value was achieved on the iniferter-immobilized membrane under the same grafting conditions (e.g., the DG values of ≈ 0% and ≈ 38% were obtained from acetonitrile solution of 54 g/L AAm under 8 min UV irradiation, respectively). In addition, the DG rose with the iniferter concentration under two different graft polymerization conditions until a plateau value was reached at 3 hr aminolysis reaction (Fig. 4.38).

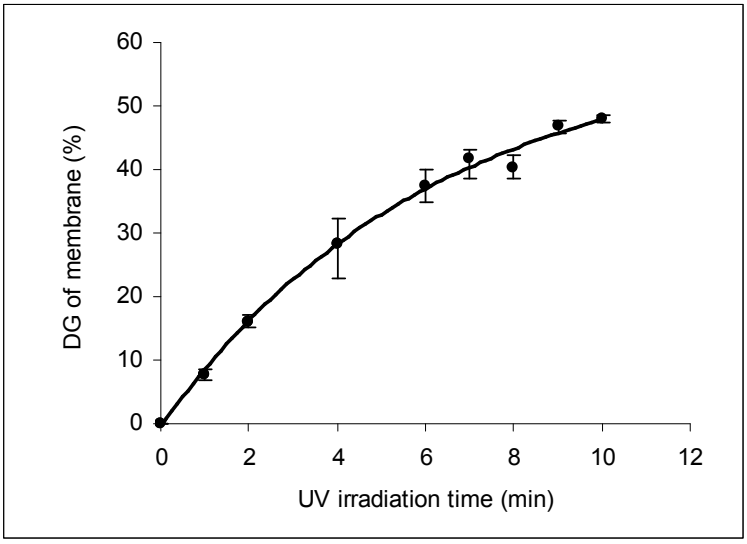

(a)

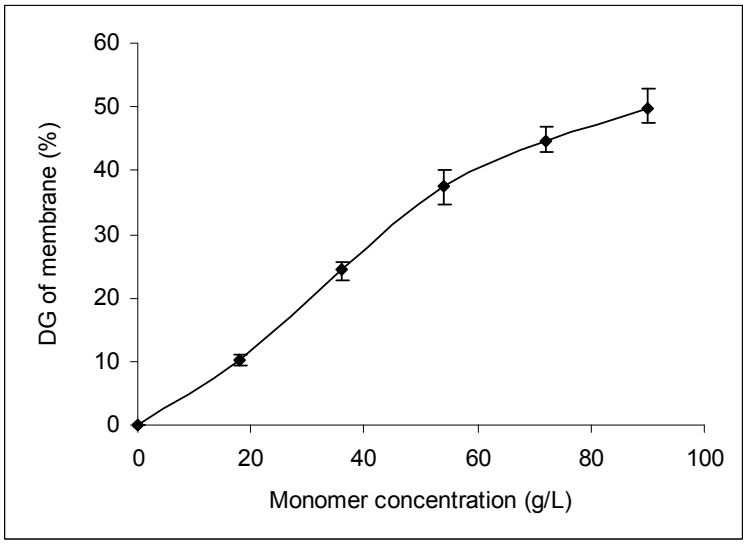

(b)

Figure 4.39: Effect of graft functionalization parameters on DG of membrane. (a) Effect of UV irradiation. 54 g/L AAm in acetonitrile. (b) Effect of monomer concentration. 6 min UV irradiation.

To better understand the proposed mechanism, the factors affecting graft functionalization of iniferter-immobilized membrane have been investigated. Fig. 4.39 shows the DG values of grafted membranes as function of UV irradiation time and monomer concentration. Under the studied conditions, the iniferter-immobilized membranes exhibited a higher

photo-grafting rate at the short irradiation time, and then the propagation rate declined with the longer irradiation time. As expected, the DG of membrane increased with the rising monomer concentration. However, like for the long UV irradiation time, the grafting rate slightly decreased at high monomer concentration. Nevertheless, the DG of grafted membranes can be well adjusted by varied UV irradiation time or monomer concentration. Fig. 4.40 shows the IR spectra of PAAm-grafted membranes with various DG values adjusted by varied AAm concentration. The peak intensity at about 1675 cm^{-1}, corresponding to amide I group, increased and had a good correlation with the DG value.

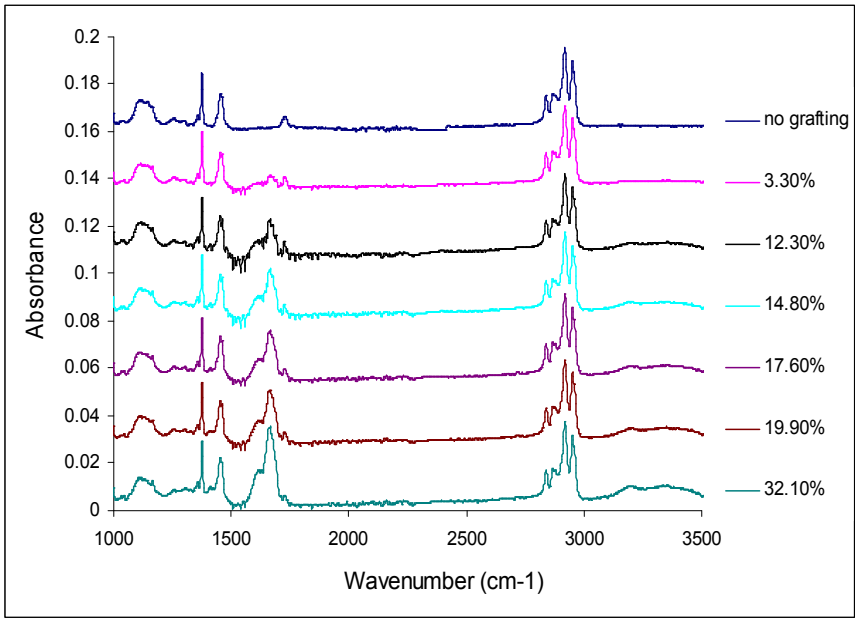

Figure 4.40: IR spectra of iniferter-immobilized and PAAm-grafted membranes with various DG (beside the curves).

The morphologies of the selected membranes have been observed using SEM (Fig. 4.41). Negligible change can be seen between original and iniferter-immobilized membranes. In strong contrast, from the images of functionalized membrane, a compact grafted polymer layer was observed uniformly covering on the top surface and inner wall of membrane pores rather than in the pores (Fig. 4.42c). In order to further verify the uniformity of grafted layer in the axial direction of membrane (through the membrane pores), the structure of cross-section of grafted membrane was also examined. Grafted polymer can be seen and no clear difference has been found among the upper, middle and bottom layers of the same membrane (Fig. 4.42a-c). In addition, another experiment has been done, i.e., two sheets of iniferter-immobilized membranes were used as stack and photo-grafted in acetonitrile solution of 54 g/L AAm for 8 min. The obtained DG values were 40% and 32% for upper membrane and bottom membrane, respectively.

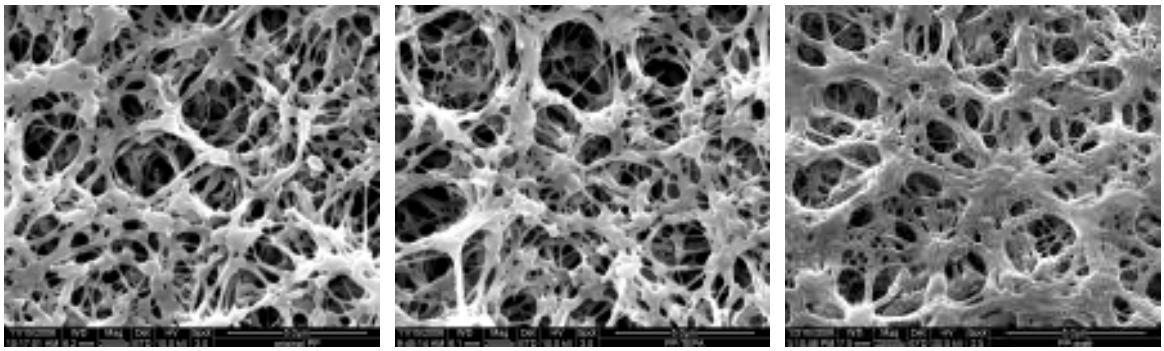

(a) (b) (c)

Figure 4.41: SEM top surface images for various membranes. (a) Original, (b) iniferter-immobilized, (c) PAAm-grafted (DG = 40%).

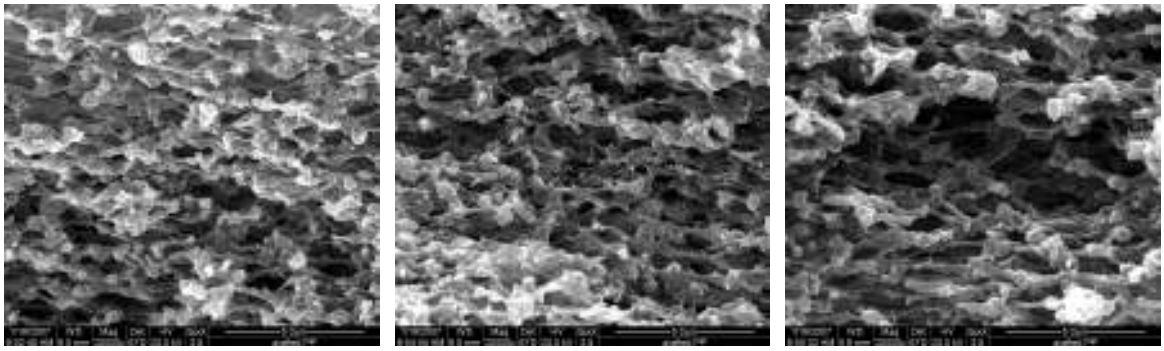

(a) (b) (c)

Figure 4.42: SEM images of cross-section of grafted membrane (DG = 40%). (a) Upper layer, (b) middle layer, (c) bottom layer.

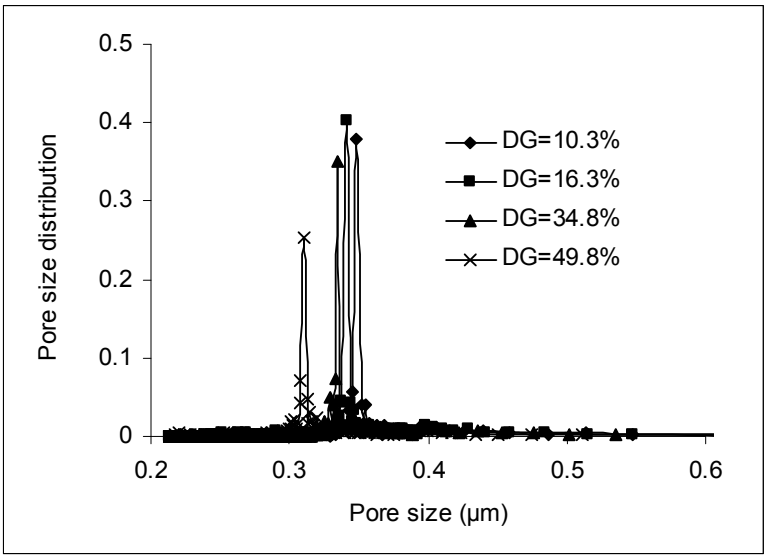

Figure 4.43: Pore size distribution of grafted membranes with different DG values. 10.3% (348.4 nm), 16.3% (340.8 nm), 34.8% (334.5 nm), 49.8% (310.4 nm).

Further information about the barrier pore size can be obtained from permporometry (Fig. 4.43). As expected, the pore size decreased gradually with the increase of the DG value from 348 nm for about 10% to 310 nm for approximately 50%, which is comparable with calculated data (dry grafted polymer thickness is 6.5 nm for 10% and 33 nm for 50%) from

DG and specific surface area (15 m^2/g), assuming uniform grafting on the whole surface. In addition, the water permeability of a MF membrane can also characterize the change of average pore diameter. Fig. 4.44 shows the pore radius ratio between grafted and iniferter-immobilized membranes as a function of DG value achieved by varied UV irradiation time and monomer concentration, respectively. The water permeability reduced almost linearly with the increasing DG value, and the straight lines nearly overlapped independent of the varied functionalization parameters (cf. Fig. 4.44).

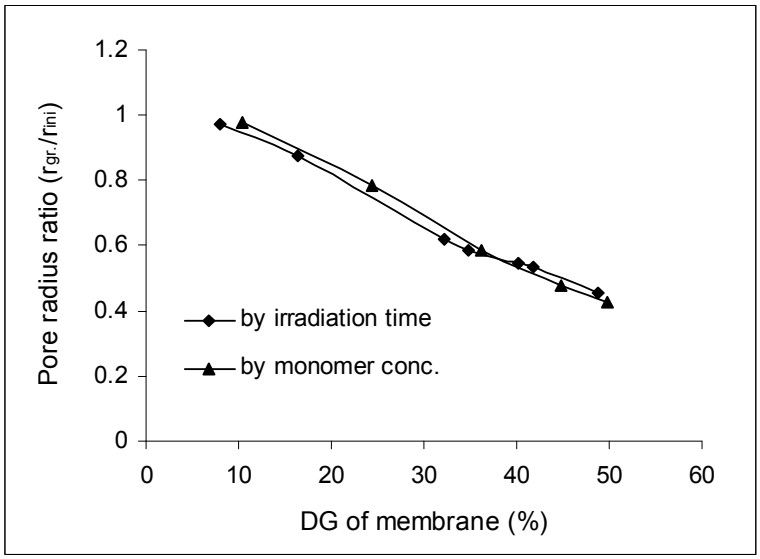

Figure 4.44: Dependence of pore radius ratio obtained from water permeability on DG values of membranes.

Grafted layers with various cross-linking degree have been prepared in acetonitrile solution containing AAm and EDMA with various ratios. Under the same graft polymerization conditions, the DG of membrane decreased with the rising EDMA content at the same total monomer concentration (Fig. 4.45). Then, similar DG value (here 14.8%) was obtained by modulating the total monomer concentration. Water permeability of these membranes has been measured (Fig. 4.46). The water permeability had a slight increase with the EDMA content at the low values (below 10%), and then a steep increase has been observed for 15% EDMA content, and the value for this membrane was close to that of iniferter-immobilized membrane. In addition, Fig. 4.47 shows the IR spectra of the selected membrane with similar DG grafted in the solution with different EDMA contents. For 100% EDMA, no amide I adsorption peak at 1675 cm^{-1} was observed, but the peak at 1728 cm^{-1}, corresponding to ester group, has been intensified compared with that for unmodified membrane. With the increase of AAm content, the signal at 1675 cm^{-1} gradually strengthened. Using these IR spectra, it is hard to determine the precise quantitative

cross-linking degree of actual grafted layers. The main reason is that the quantification of double bond in cross-linker is hardly achieved due to its weak absorption peak (covered by other absorption peak). However, compared with the IR spectrum of PAAm-grafted membrane with same DG (Fig. 4.40) and the water permeability data (cf. Fig. 4.46), the information could be acquired that the cross-linking degree in the grafted layer increased with the higher cross-linker content.

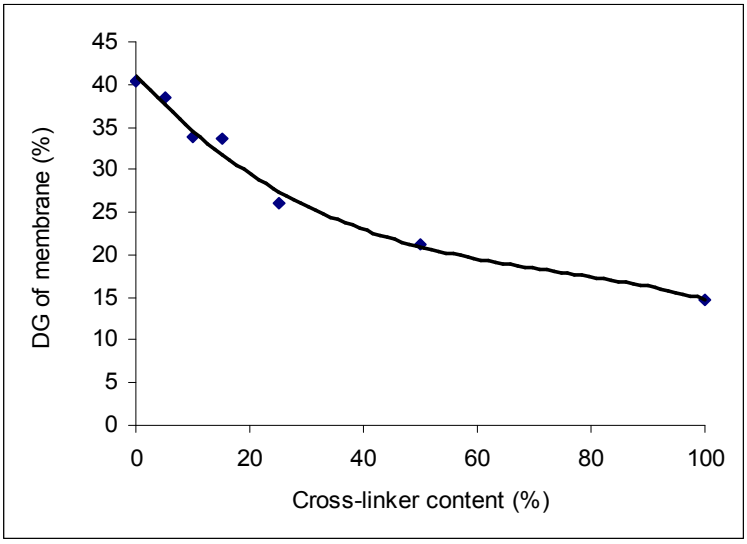

Figure 4.45: Dependence of DG value on cross-linker (EDMA) content in total monomer. Grafting conditions: 54 g/L total monomer in acetonitrile, 10 min UV irradiation.

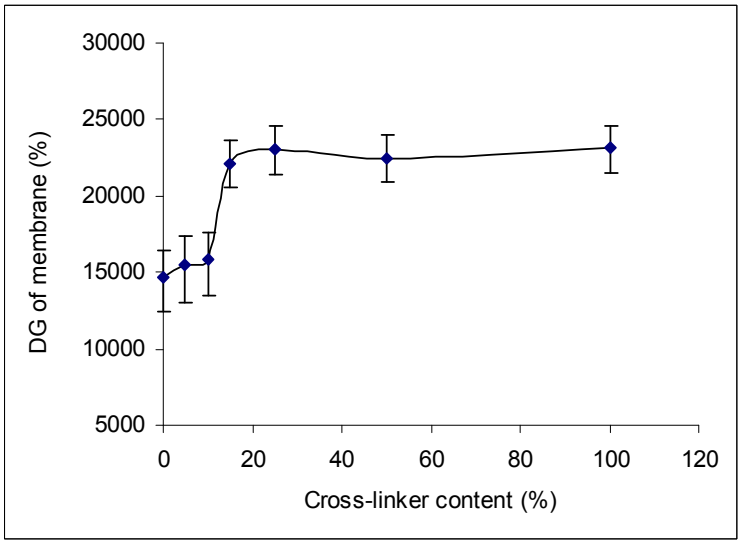

Figure 4.46: Dependence of water permeability on cross-linker (EDMA) content in total monomer concentration. All the membranes have similar DG (14.8%).

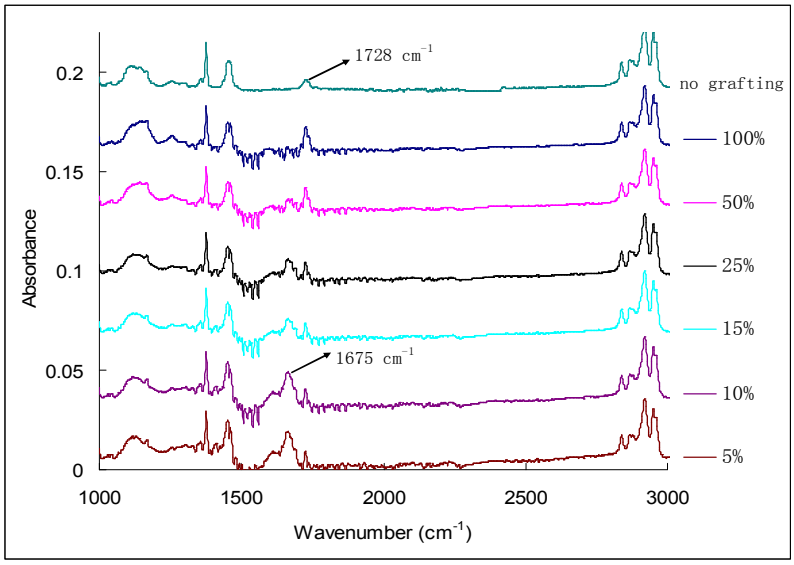

Figure 4.47: IR spectra of iniferter-immobilized and grafted membranes with various cross-linking degree (DG:14.8%); the percentages: EDMA contents in total monomer.

4.5.3 Livingness of graft polymerization

Theoretically, the grafted chains will remain "living" due to the photo-iniferter caps at the end of chains. The livingness of graft polymerization can be characterized generally by the linear relationship between molar mass of grafted chains and UV irradiation time. However, due to the inconvenience for molar mass measurement on the surface, growing polymer thickness and grafted polymer mass are very often used [184]; the synthesis of block copolymer gives indirectly information for living polymerization as well [181]. The obtained data above motivated the interest in studying the livingness of graft polymer. For this study, acetonitrile solution of 54 g/L AAm was applied to polymerize from iniferter-immobilized membranes by two methods: continuous (without interruption of UV irradiation) and intermittent UV irradiation (grafting of membrane was performed twice, each time with identical irradiation time). DG of membrane was used for characterization of livingness. Fig. 4.48 shows the effect of twice intermittent UV irradiation on DG of membrane. It is worth noting that the polymerization system was untouched during 1 min interval. It was found that only a little lower DG was observed via twice intermittent irradiation than via continuous method at short irradiation time. However, the reduction in DG became somewhat greater with the longer UV irradiation time. In addition, multi-time UV irradiation (each 1 min) has been carried out in the same grafting system (Fig. 4.49). The results demonstrate that with the repeating times of UV irradiation the amount of grafted PAAm increased based on the gravimetrical measurement and the increasing peak height or area at 1665 cm^{-1} in the IR spectra of grafted membranes, which are attributed to

amide I band (not shown). However, the grafting efficiency decreased rapidly with the repeating times compared with the data for continuous UV irradiation (Fig. 4.49).

To clarify the undesired phenomenon, more experiments have been done. One is to study the effect of interval between twice UV irradiation on membrane photo-grafting. It was found that the obtained DG value reduced gradually by about 10% when the interval was prolonged from 1 min to 20 min. On the other hand, with the constant interval 1 min, the location of membrane was changed in the same monomer solution during the interval or the membrane was shifted to a fresh monomer solution. Surprisingly, the transfer of membrane caused a clear decrease in DG vale, even the second grafting was undetectable gravimetrically in most of cases.

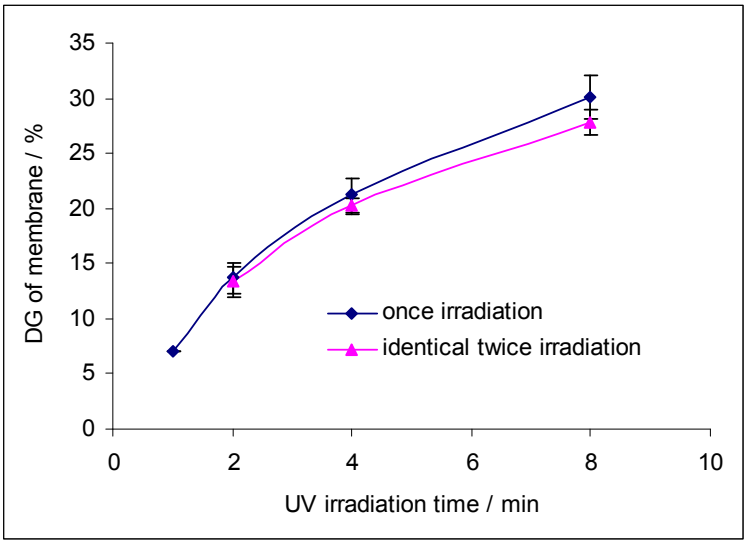

Figure 4.48: Effect of continuous and intermittent methods on DG of membrane. For intermittent irradiation, during 1 min interval, the polymerization system was untouched. 54 g/L AAm in acetonitrile was used.

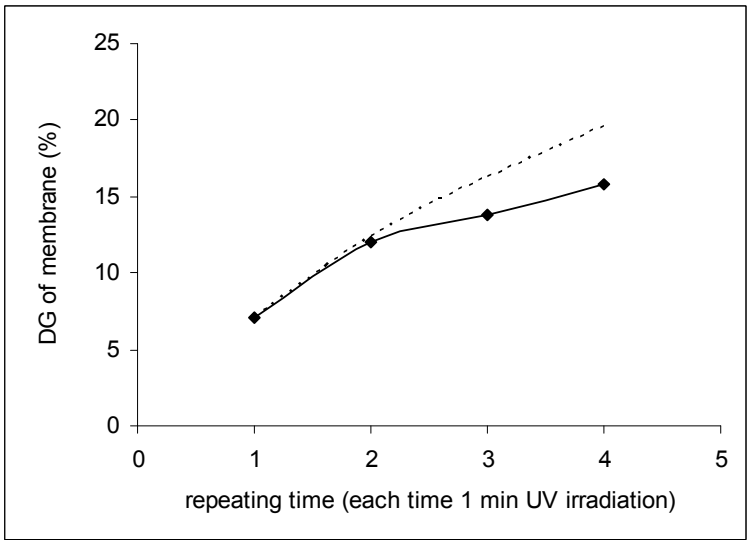

Figure 4.49: Effect of repeating times of UV irradiation on photo-grafting of membrane. Dotted line was obtained from the data for continuous grafting method. 54 g/L AAm in acetonitrile was used. During 1 min interval, the polymerization system was untouched.

4.6 Preparation and characterization of anion-exchange membrane adsorber

We have developed a novel highly surface-selective photo-grafting technique—synergist immobilization method—for functionalization of polymeric membranes (see section 4.4). Its high surface-selectivity and controllability of photo-grafting would make it feasible to prepare a well-defined grafted layer on the membrane surface. Therefore, this section focuses onto the direct preparation of anion-exchange membranes via this method using the functional monomer (2-(methacryloyloxy)ethyl)-trimethylammonium chloride (Fig. 4.50) and a hydrophilized PP MF membrane as porous support. The aim is 2-fold: one is to identify an efficient grafting technique for the preparation of membrane adsorbers with three-dimensional grafted layer; another aim is to investigate the dependence of protein binding capacity on architecture of grafted layer.

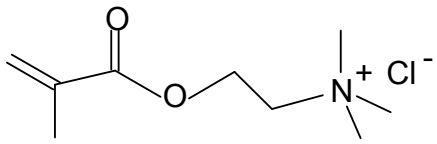

Figure 4.50: Chemical structure of (2-(methacryloyloxy)ethyl)-trimethylammonium chloride

4.6.1 Preparation of anion-exchange membranes

For the purposes above, anion-exchange membranes with various structures of grafted layer were prepared via two photo-grafting routes (cf. Fig. 5.8). For both synergist immobilization (see section 4.4) and photo-initiator adsorption methods [114], the length of grafted chains can be mainly adjusted by varied monomer concentration, while the grafting density remained essentially unchanged under constant other conditions. It should be noted that for synergist immobilization method, membranes with full coverage of the entire membrane surface with tertiary amino groups have been prepared for photo-grafting (cf. Fig. 4.12). As shown in Fig. 4.51, DG of membranes increased as a function of monomer concentration for all studied cases. However, evidently, the photo-grafting efficiency was significantly higher using synergist immobilization method, and a longer time delay for graft copolymerization was observed when using adsorption method. At the identical grafting conditions a higher monomer concentration was required to achieve the same DG value using only dissolved (0 mM in coating step) or dissolved and coated BP (10 to 100 mM). Furthermore, in the case of synergist immobilization method, a good linear correlation was observed between DG and monomer concentration in the studied

range. In contrast, for adsorption method, the DG increased as monomer concentration increased for all the cases at a given BP concentration. But as seen in Fig. 4.51, an irregular dependence of DG on monomer concentration was found. In addition, the DG value rose slightly at low monomer concentration with the increasing BP concentration employed for BP pre-adsorption. However, at high monomer concentration, overall, the coating of BP did not much enhance the DG value of membrane.

In the next stage, via synergist immobilization method an attempt was made to prepare anion-exchange membranes with a cross-linked functional layer. The DG of membrane slightly increased with the increasing fraction of cross-linker, MBAA, in monomer solution (Fig. 4.51). Similar to the preparations without cross-linker, the amount of grafted copolymer could be tuned readily according to the linear correlation of DG with monomer concentration.

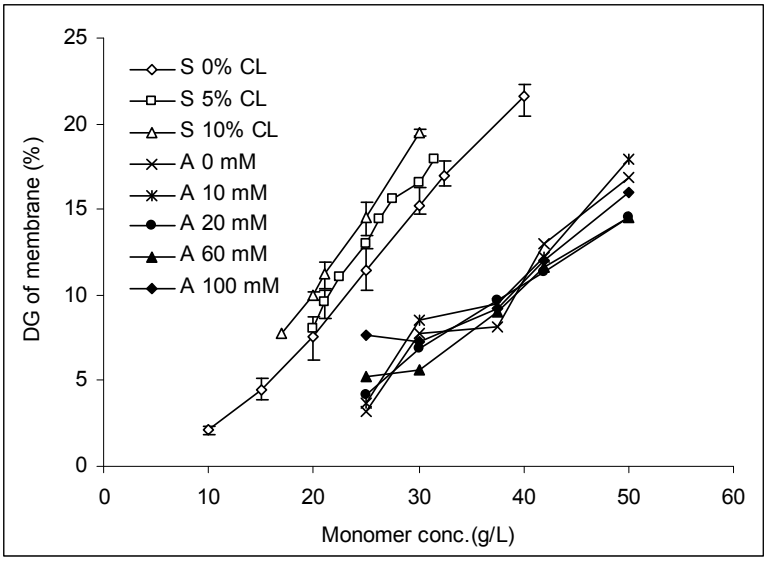

Figure 4.51: Dependence of DG of membranes on monomer concentration and photo-grafting route (BP concentration in the pre-coating step has been varied for the adsorption method; content of crosslinker in the reaction mixture has been varied for the synergist immobilization method).

4.6.2 Buffer permeability of anion-exchange membranes

One of the advantages of membrane chromatography over the conventional packed-bed column chromatography is its convective mass transfer, which can reduce both process time and recovery liquid volume. Therefore, the buffer permeability has been measured as one of the important parameters to evaluate the performances of anion-exchange membranes (Fig. 4.52).

Buffer flux reduced with increasing DG values, but strong influences of preparation conditions were seen. The influence of added salt concentration in the buffer was also

investigated in order to obtain information about the mobility of the grafted chains; selected results are shown in Fig. 4.53. Flux increased with increasing salt concentration until almost constant values were obtained for concentrations beyond 500 mM. Again, significant influences of the preparation conditions were also observed.

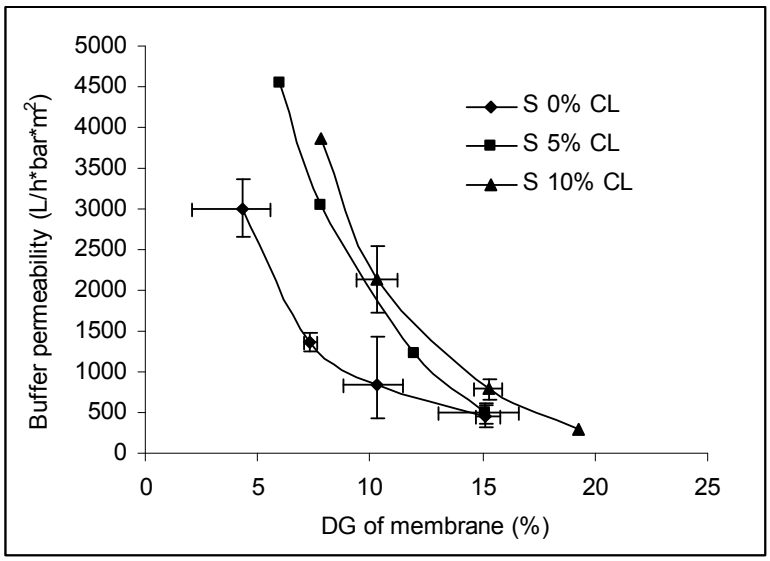

(a)

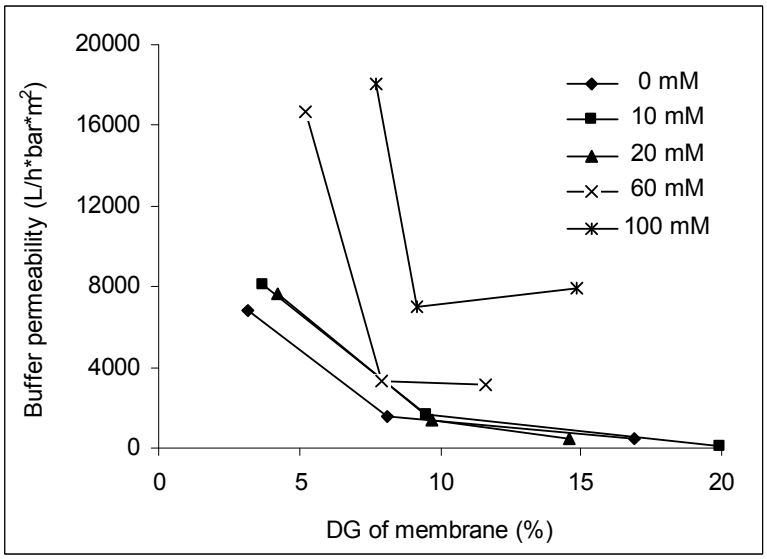

(b)

Figure 4.52: Effect of structure of grafted layer on buffer permeability of membranes, prepared (a) via synergist immobilization method, (b) via adsorption method. Buffer: 50 mM Tris-HCl, pH=7. 0.2-1.5 bar transmembrane pressure was used depending on the buffer flux.

For synergist immobilization method, as it was observed in Fig. 4.52a and Fig. 4.53a, membranes “S 0% CL” showed low buffer permeability, whereas, the buffer permeability of membranes enhanced with the increasing fraction of cross-linker. Furthermore, the collapse extent of the graft chains, which can be evaluated by the ratio of permeability

values of buffer with 1 M and without NaCl, was smaller for the membranes “S 5% CL” and “S 10% CL”. For instance, at the DG of about 16% the ratios were 7.4 and 3.2 for “S 0% CL” and “S 10% CL”, respectively (Fig. 4.53a). When using adsorption method, the configuration of grafted chains could change at varied BP concentration used in the BP-pre-coating step (cf. Fig. 5.8). Similar to membrane “S 0% CL”, low buffer permeability has been obtained for “A 0 mM” and “A 10 mM” membranes. In contrast, the buffer permeability of membranes “A 60 mM” and “A 100 mM” was significantly higher, as well as the collapse extent of their grafted chains in salt solutions was much less pronounced than those of membranes “A 0 mM”, “A 10 mM” and “A 20 mM” (Fig. 4.52b and 4.53b), all for similar DG values.

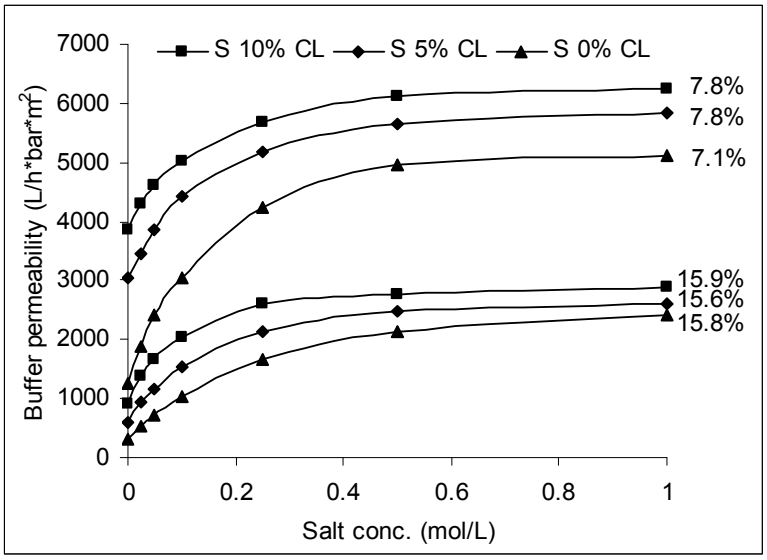

(a)

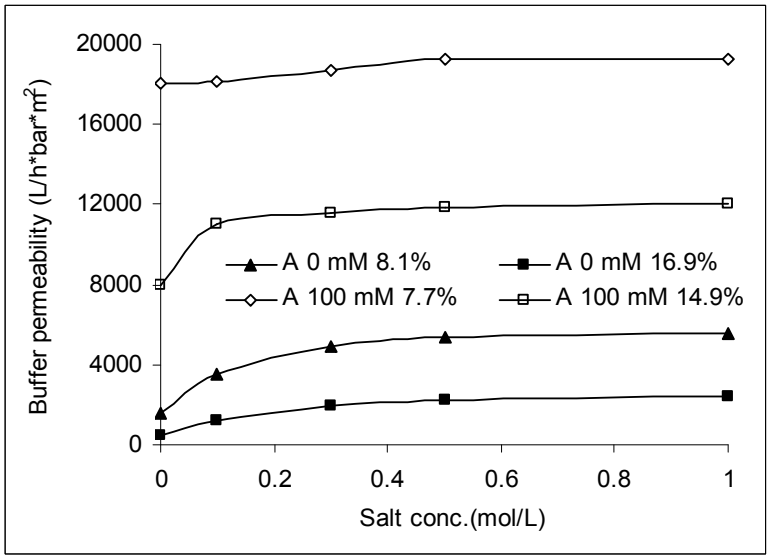

(b)

Figure 4.53: Effect of extra salt concentration in buffer solution (50 mM Tris-HCl, pH=7) on permeability of porous anion-exchange membranes. 0.2-1.5 bar transmembrane pressure was used depending on the buffer flux.

4.6.3 Static protein adsorption capacity

The static adsorption behavior of the resulting porous anion-exchange membranes was determined by batch experiments using two model proteins with different size but almost same isoelectric point (see Table 4.7).

Table 4.7: properties of BSA and Trp used for adsorption measurement of anion-exchange membrnaes.

Protein	Size (kDa)	pI
Bovin serum albumin (BSA)	67	4.9
Trypsin inhibitor (Trp)	20	4.5

Time-dependent experiments had revealed that 15 hr incubation was sufficient to reach maximum values (not shown). BSA binding capacity showed a rising tendency with the DG of membrane for all the cases (Fig. 4.54). However, considering the requirements of both high rate and high capacity in membrane chromatography, an appropriate range of DG value had to be selected for more detailed investigations in the subsequent work. A DG of 11.5 % has been chosen for all the different membrane types, and binding, elution and recovery data for both model proteins at same concentration are given in Fig. 4.55. The static binding capacity for trypsin inhibitor was much higher than that of BSA for all the cases. But similar ratios of binding capacities for trypsin inhibitor and BSA (about 1.6) had been observed except for membranes "A 100 mM", it had a slightly higher ratio (1.8).

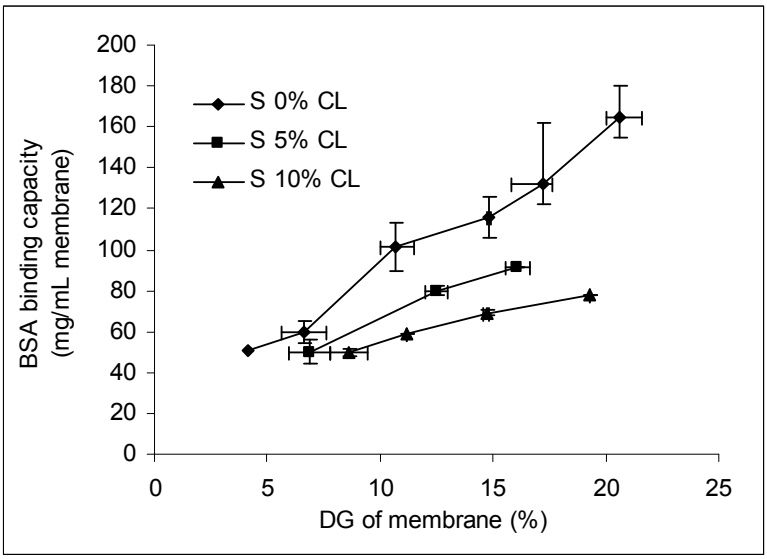

(a)

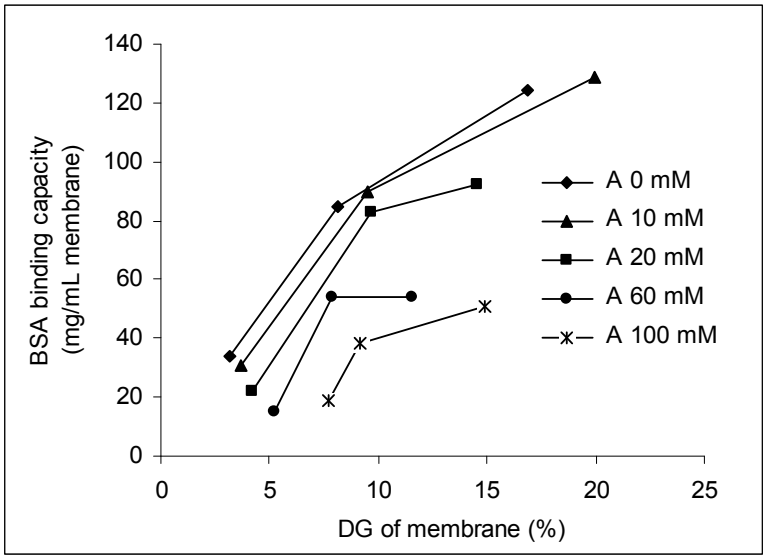

(b)

Figure 4.54: Dependence of BSA binding capacity on DG of membranes and structure of grafted layer. 3 mg/ml BSA solution was used. Membrane preparation: (a) via synergist immobilization method, (b) via adsorption method.

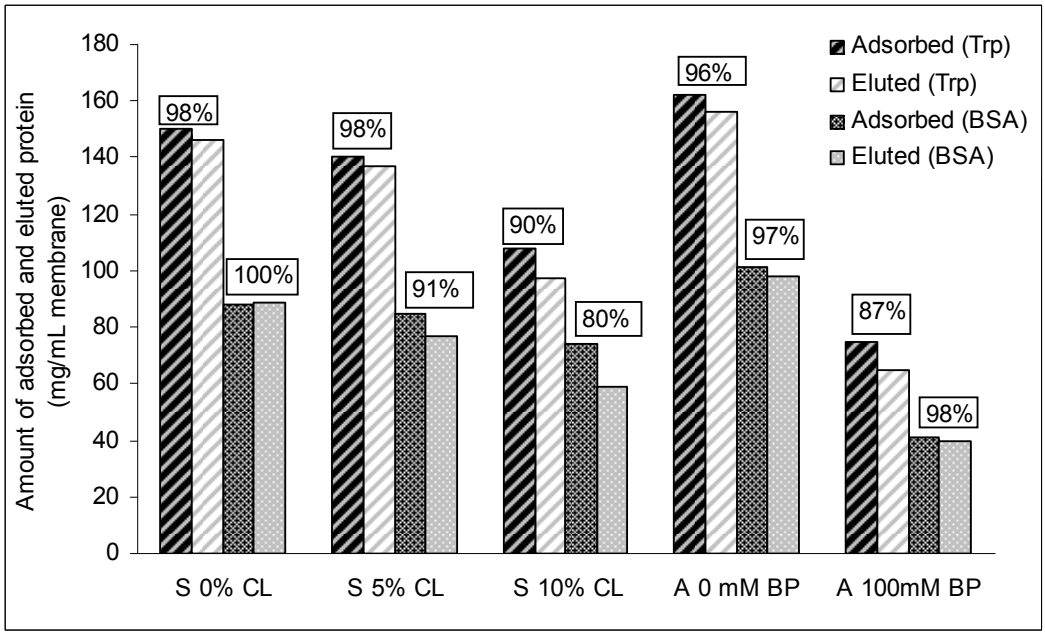

Figure 4.55: Effect of molecular size of proteins (BSA and trypsin inhibitor) on binding and recovery. DG was 11.5% for all the membranes. 3 mg/ml protein concentration was used. The percentage values in the figure are recovery estimated from data for adsorbed and eluted protein (cf. Experimental).

It can be observed from the Fig. 4.54 that at the same DG value, the BSA binding capacity was decreasing with the higher cross-linking. Nevertheless, rather high binding capacities have been achieved for "S 5% CL" and "S 10% CL" (~80 and 70 mg/ml membrane, respectively at 12% DG) compared with the previously reported values for BSA (20-50 mg/ml) [13, 174, 185]. In addition, with the increasing BP concentration for BP pre-coating the obtained membrane showed a reducing BSA binding capacity as well.

Similar to that of membrane "S 0% CL", the binding capacities of membranes "A 0 mM" and "A 10 mM" were about 100 mg/mL membrane at 12 % DG. In contrast, for membranes "A 60 mM" and "A 100 mM", quite low BSA binding capacities were obtained.

In the batch experiments, a lower recovery was observed for the membranes with cross-linked grafted layer than that of "S 0% CL". However, the effect of cross-linking on protein recovery was weaker for small size protein. Exceptionally, for membrane "A 100 mM", the recovery of trypsin inhibitor was lower than that of BSA (Fig. 4.55).

Fig. 4.56 shows the BSA adsorption isotherm curves for various anion-exchange membranes with similar DG value. These curves fit well the Langmuir adsorption isotherm model; from the fitted Langmuir adsorption equations, the binding constants and maximum normalized BSA adsorption capacities were obtained (Table 4.8). The difference in binding constant was not obvious (in the range of 1.9-6.7*10^6 M^{-1}) for all the membrane adsorbers, although the significant difference in binding capacity has been observed (cf. Table 4.8).

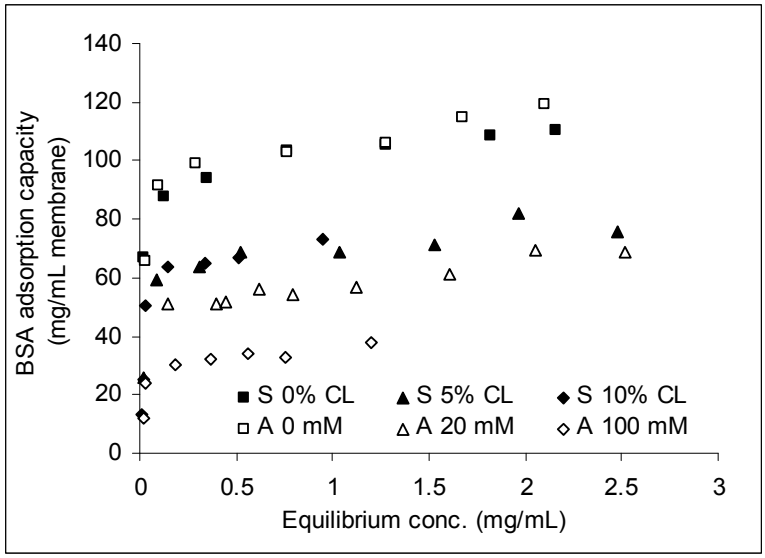

Figure 4.56: BSA adsorption isotherm curves (pH=7.0) of various membranes (all DG = 11.5%).

Table 4.8: Binding constant and BSA binding capacity for selected anion-exchange membrane adsorbers (obtained from the fitted Langmuir adsorption equations)

Membrane adsorber	S 0% CL	S 5% CL	S 10% CL	A 0 mM	A 20 mM	A 100 mM
R-squared value (%)	93	86	99.6	96	95	99.7
Binding constant K (mL/mg) /(*10^6 M^{-1})	100 / 6.7	48 / 3.2	28 / 1.9	45 / 3.0	56 / 3.8	28 / 1.9
Normalized BSA binding capacity ($mg_{BSA}/mg_{poly.}$)	3.54	2.84	2.50	3.58	2.28	1.22

4.6.4 Dynamic protein binding capacity

The dynamic adsorption behavior of membranes was evaluated by loading 3 g/L BSA solutions at a flow rate of 1 ml/min or 5 ml/min and monitoring the breakthrough curve. Irrespective of flow rate, identical breakthrough curves were obtained for all different anion-exchange membranes. The overview on all data from these experiments for the selected membranes is shown in Table 4.9. Except for two cases ("S 0% CL", "A 0 mM"), the normalized dynamic BSA binding capacity was identical or even slightly higher (by up to 10%) than the static binding capacity (cf. Table 4.8). For the two membranes without cross-linking ("S 0% CL") and the lowest grafting density ("A 0 mM"), each within the respective series, significantly lower values (in both cases by about 12%) have been observed.

Table 4.9: Overall data from BSA dynamic experiments for the selected porous anion-exchange membranes.

Membrane	Flow rate (ml/min)	Eluted BSA* (mg/ml)	Average eluted BSA (mg/mL)	Normalized capacity with DG* (mg_{BSA}/mg_{polym})	Recovery (%)	BTC slope** (ml^{-1})
"S 0% CL"	1	72	72	3.13	96	1.36
	5	72				
"S 5% CL"	1	59	59	2.98	96	1.92
	5	59				
"S 10% CL"	1	55	55	2.63	100	2.05
	5	55				
"A 0 mM"	1	87	87	3.15	91	0.97
	5	87				
"A 20 mM"	1	60	61	2.55	97	1.58
	5	61				
"A 100 mM"	1	31	31	1.33	100	3.85
	5	31				

* The sample diameter of 13 mm has been used for calculation of the membrane volume.
** Calculated from the breakthrough curves (BTC) in the range of 0-0.5 for the ratio "effluent conc./feed conc." (cf. Fig. 4.57).

Fig. 4.57 shows the breakthrough curves at a flow rate of 5 ml/min. In the case of membrane "A 100 mM", the breakthrough curve was very steep but the BSA binding capacity was relatively low, while "A 0 mM" and "A 20 mM" showed similar BSA adsorption behavior. However, for these membranes, the time delay for reaching the maximum capacity was very long. The dynamic capacities, i.e., the protein uptakes of the

membranes before the effluent concentration reached 10% of the loading concentration, were quite high and similar for all “S x% CL” cases, though the maximum capacity was slightly higher for “S 0% CL” than for “S 5% CL” and “S 10% CL”. However, like for the membranes “A 0 mM” and “A 20 mM”, the further BSA adsorption on the “S 0% CL” membrane to reach the maximum capacity occurred with a long time delay. This undesired effect was strongly reduced by cross-linking; both membranes prepared with cross-linker showed lower dispersion in the dynamic experiments as well as higher protein recovery. In addition, “S 0% CL” membrane exhibited the faster dynamic BSA binding than “A 0 mM” membrane from the breakthrough curves (Fig. 4.57a), although both membranes had similar maximum binding capacity.

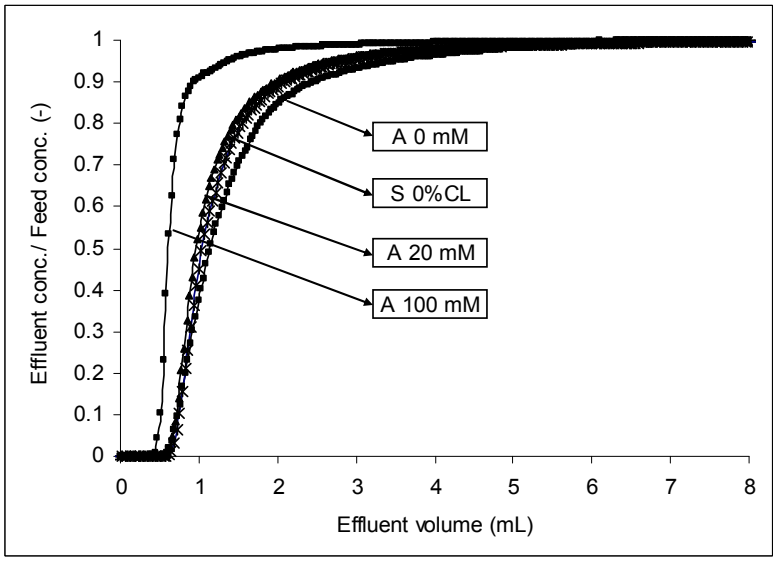

(a)

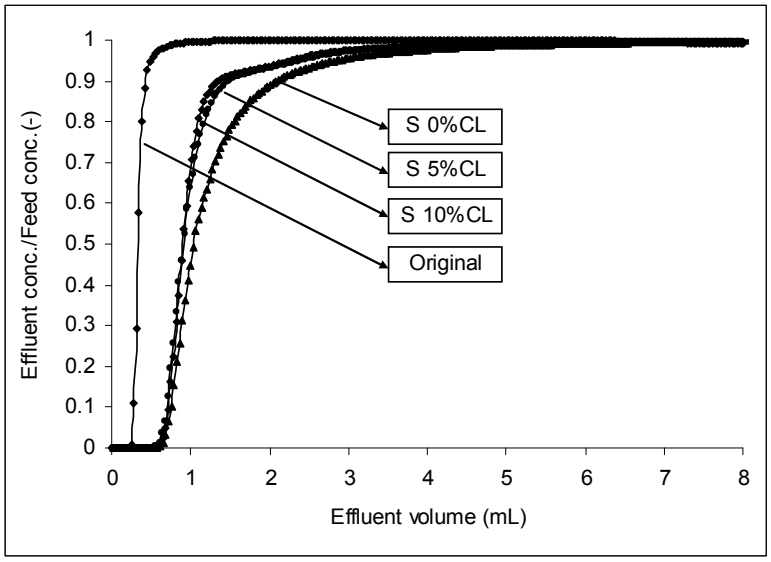

(b)

Figure 4.57: Breakthrough curves for various membranes, prepared via (a) synergist immobilization method, (b) adsorption method (BSA concentration: 3 g/l; Flow rate: 5 ml/min).

In addition, it can be observed from Fig. 4.58 that upon adsorbing protein, the backpressure went down quickly (in the first minute, i.e., the time it takes to reach saturation of binding sites). Especially for membrane "S 0% CL", the pressure declined strongly, from 0.95 MPa to 0.5 MPa. In comparison, the collapse of the polymer chains during the protein adsorption and elution phase was not that strong for "S 5% CL" and "S 10% CL". Moreover, these membranes showed a much lower backpressure before and during protein binding, and this is in line with buffer permeability data (cf. Fig. 4.52a).

The slope values calculated from the breakthrough curves in the range of 0-50% ratio of effluent conc./feed conc. (cf. Table 4.9) have been used as simple quantitative indicator because a detailed analysis within the frame of state-of-the-art models (cf., e.g., ref. [186]) is more complicated, especially because some membranes ("A 0 mM", "A 20 mM", "S 0% CL") revealed significant dispersion at higher degrees of saturation. This data could also be used to evaluate the potential selectivity of anion-exchange membranes in separations of proteins. The selected anion-exchange membranes could be classified into three groups: "S 0% CL" (1.36 ml^{-1}), "A 0 mM" (0.97 ml^{-1}) and "A 20 mM" (1.58 ml^{-1}) // "S 5% CL" (1.92 ml^{-1}) and "S 10% CL" (2.05 ml^{-1}) // "A 100 mM" (3.85 ml^{-1}).

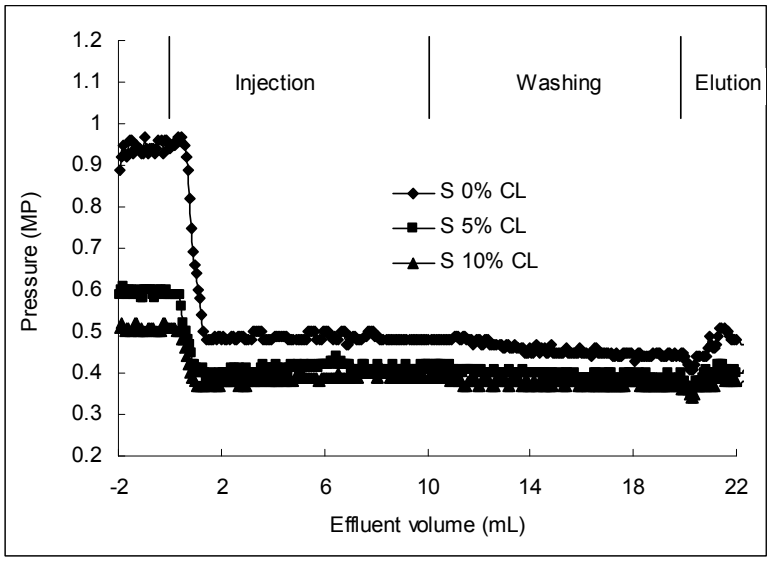

Figure 4.58: Chromatography system pressure during protein adsorption and elution for membranes prepared via synergist immobilization (BSA concentration: 3 g/l; Flow rate: 5 ml/min).

4.7 Preparation and Characterization of affinity membrane

This work was based on the previous work of the Schrader's group [187]. A functional copolymer of bisphosphonato-xylylene methacrylamide was synthesized in water (with bisphosphonate salt groups) and the high association constants were observed for several proteins due to the host-guest interactions between proteins and the functional copolymer. Interestingly, in aqueous solution of this copolymer, a significantly higher value was achieved for lysozyme than for cytochrome C. However, the difference in association constant between both proteins disappeared, when the same copolymer was coated on a planar surface. This was explained by the less flexibility of the copolymer chains on the planar surface.

In this study, affinity membranes were prepared using track-etched PET400 membrane as base membrane, on whose surface a similar bisphosphonato copolymer to that mentioned above was grafted via synergist immobilization method. Protein binding capacity has been measured and protein selectivity has been evaluated for the resulting affinity membranes.

4.7.1 Preparation of affinity membrane

In this study, the aminolysed PET400 membranes with constant tertiary amino group concentration and fixed UV irradiation time were applied, implying that a constant grafting density would be obtained for all the grafted membranes via synergist immobilization method. Therefore, the adjustment of DG value was attributed to the controllable grafted chain length, which has been realized by photo-graft polymerization of membranes in acetonitrile solutions with varied functional monomer concentration. As shown in Table 4.10, the DG value of the resulting membrane increased with M1 concentration until a plateau value (here 2.3 μg/cm^2) was reached at 0.8 mol/L. Therefore, the total concentration of 0.8 mol/L was also adopted for preparation of copolymer-grafted membranes (Table 4.10). Very similar DG value was obtained for poly(M1-co-M2)-grafted membrane. Moreover, the DG value was hardly varied by the subsequent ionization of poly(M1-co-M2)-grafted membrane with LiBr in dry acetonitrile.

Table 4.10: Preparation of various homo- and co-polymer grafted membranes

Membrane	M1 (mol/L)	M2 (mol/L)	Estimated DG (μg/cm^2)
PolyM1-grafted	0.5	-	0.9
	0.8	-	*2.3*
	1.0	-	2.3
Poly(M1-co-M2)-grafted	*0.64*	*0.16*	*2.2 ± 0.2*

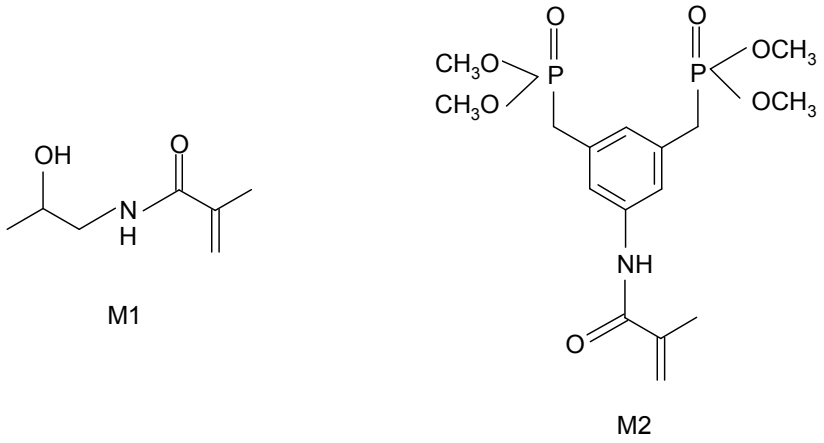

Figure 4.59: Chemical structures of monomers (M1 and M2) for preparation of affinity membranes.

In order to confirm the composition of the grafted layer, the polyM1- and copolymer-grafted membranes (including Li-salt of grafted membrane) have been analysed by ^{31}P solid state NMR. As shown in Fig. 4.60, compared with that of polyM1-grafted membrane, two additional resonance peaks (a strong and a weak peak at about 30 ppm and about 20 ppm, respectively) were observed in the spectrum of poly(M1-co-M2)-grafted membrane, most likely corresponding to phosphonate methyl ester and its partially phosphonate salt, respectively (typical ^{31}P NMR chemical shift in solution). After Li-ionization reaction, however, the peak became much weaker at 30 ppm but significantly stronger at 20 ppm.

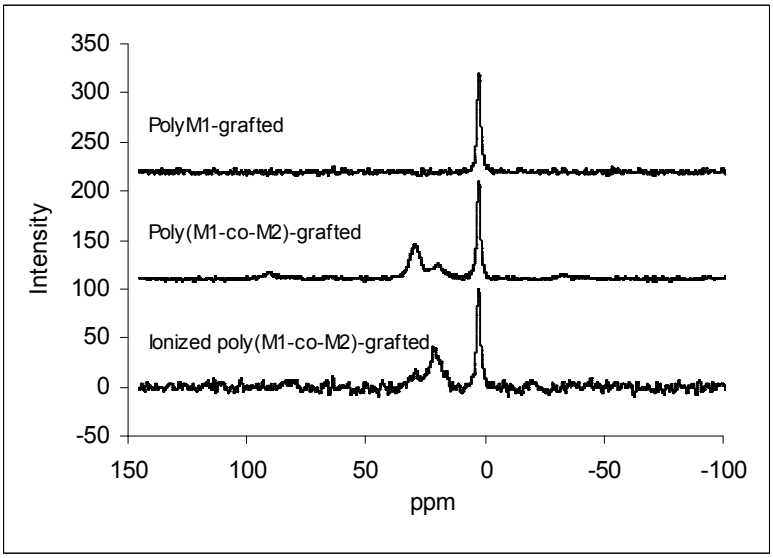

Figure 4.60: ^{31}P solid state NMR spectra of various grafted membranes.

In addition, contact angle and water permeability have been measured for various resulting membranes to determine the hydrophilic property of grafted layer (Table 4.11). Compared to the contact angle (approximately 48^0) of aminolysed PET membrane, three types of

functionalized membranes exhibited high hydrophilicity based on the significantly lower contact angle values. In comparison, a strong rise in hydrophilicity has been achieved for grafted copolymer, so that only a small difference in contact angle was observed after the subsequent Li-ionization reaction. As intended, the grafted polymer chains grew from the inner wall of membrane pores. Therefore, water permeability of membranes has measured to evaluate the stretching (swelling) degree of grafted polymer in water and to estimate membrane pore diameter (cf. section 5.2.3). As shown in Table 4.11, the water permeability values were significantly lower for all the functionalized membranes than for aminolysed membrane. Poly (M1-co-M2) exhibited a much greater swelling in water than polyM1, and the Li-ionization did not significantly improve its swelling much more, as judged from the obtained water permeability values. These results are in agreement with the contact angle measurements of various membranes.

Table 4.11: Contact angle and water permeability of various membranes

Membrane		Estimated DG ($\mu g/cm^2$)	Contact angle (^{0})	Water permeability (L/h bar m^2)
Aminolysed		-	48 ± 4	47500 61319*
PolyM1-grafted		2.3 3.5	36 ± 5	36700 52500*
Poly(M1-co-M2)-grafted (partially ionized as mentioned above)		2.3 3.5	29 ± 5	10570 25450*
Poly(M1-co-M2)-grafted	Before ionization	2.2		6579
	After ionization	2.2	23 ± 7	4586

*: 2nd batch of PET membranes with similar pore size to the 1st batch but higher porosity.

4.7.2 Static binding capacity of proteins

In order to evaluate the protein affinities of the above-described new membrane adsorbers, a series of proteins with different pI and size have been used to determine the binding capacity under the same conditions. As shown in Fig. 4.61, polyM1-grafted membranes, as blank samples, exhibited low binding capacity for all six selected proteins. Moreover, the non-specific binding reduced with the increase of protein size. However, a relatively higher binding capacity of poly(M1-co-M2)-grafted membrane has been observed to all the proteins. On the other hand, the specific binding correlated with pI values of proteins.

Interestingly, significantly higher binding capacity of lysozyme on this membrane has been observed than for the other proteins and for the blank membrane. Especially, cytochrome C, with the similar pI value and size to lysozyme, exhibited a comparatively lower binding as well.

In the case of Li-ionized poly(M1-co-M2)-grafted membrane, relatively high binding capacities have also been achieved for both lysozyme and cytochrome C, even a higher cytochrome C binding capacity was also observed than that of poly(M1-co-M2)-grafted membrane. However, no selective binding was observed between both proteins based on the similar binding capacities.

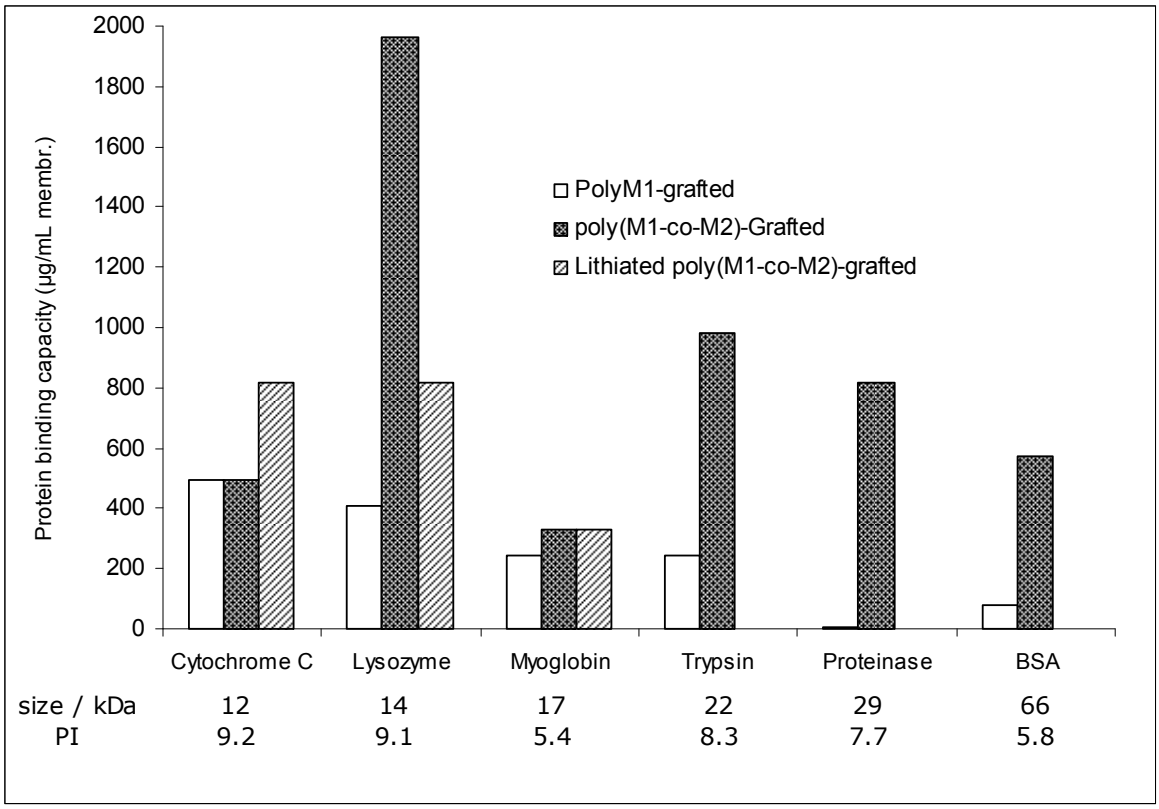

Figure 4.61: Static binding capacity of proteins for various grafted membranes.

Since poly(M1-co-M2)-grafted membrane had pronounced difference in binding capacity between lysozyme and cytochrome C, they were chosen to determine the isotherm adsorption curves for poly(M1-co-M2)-grafted membranes by batch experiments. Both adsorption curves fitted well the Langmuir adsorption isotherm model (see Fig. 4.62). Under the used conditions, the binding sites on the resulting affinity membranes have been saturated at the concentration of approximately 70 µg/mL for both proteins. According to the equations obtained from respective fitted Langmuir isotherm curve, the maximum binding capacities have been achieved to be about 2000 µg/mL per membrane volume and 800 µg/mL per membrane volue for lysozyme and cytochrome C, respectively (Fig. 4.62);

the corresponding binding constant was also much greater for lysozyme ($1.3*10^7$ M^{-1}) than for cytochrome C ($8.6*10^5$ M^{-1}).

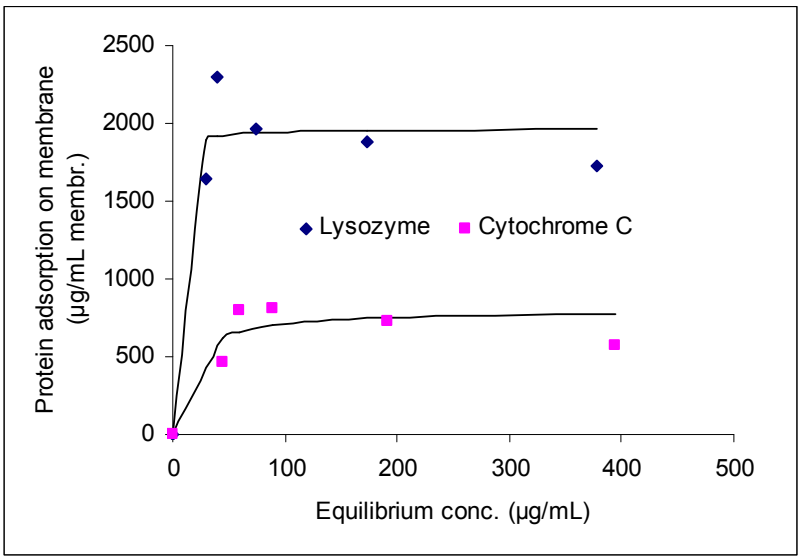

Figure 4.62: Lysozyme and cytochrome C isotherm adsorption curves of poly(M1-co-M2)-grafted membrane. The equations obtained from fitted Langmuir adsorption isotherm curves are A=1966*0.95*c/(1+0.95*c) (binding constant K=0.95 mL/µg (=$1.3*10^7$ M^{-1}) for lysozyme and A=805*0.072*c/(1+0.072*c) (K=0.072 mL/µg (=$8.6*10^5$ M^{-1}) for cytochrome C).

4.7.3 Separation of proteins

Based on the obtained static binding capacities and binding constant of various proteins on poly(M1-co-M2)-grafted membranes, the resulting affinity membrane showed strongly higher binding performance toward lysozyme. Taking advantage of this property, lysozyme was expected to be separated from protein mixtures. Therefore, in this work a 1:1 mixture solution of lysozyme and cytochrome C was used (Fig. 4.63), which are difficult to be separated by the conventional technique due to the high degree of similarity in physical and chemical properties. Same procedures were performed as for static binding capacity measurement. A total protein binding capacity of about 1500 µg/mL per membrane volume was obtained, which is comparable with pure lysozyme binding capacity but much higher than for pure cytochrome C (cf. Fig. 4.62). To identify the component of protein, the elution solution was analysed using UV-Vis spectrophotometer. For comparison, the UV spectra have been recorded for lysozyme and cytochrome C solutions with the same concentration like the eluted protein (18 µg/mL). As shown in Fig. 4.63, the only peak was found at 280 nm for lysozyme, where a very weak peak was also observed for cytochrome C. However, a strong representative peak appeared at around 410 nm for cytochrome C solution. In the spectrum of elution solution, an only apparent absorption peak was found

at around 280 nm, while no adsorption peak was observed at around 410 nm, indicating that no detectable cytochrome C was found in the elution solution.

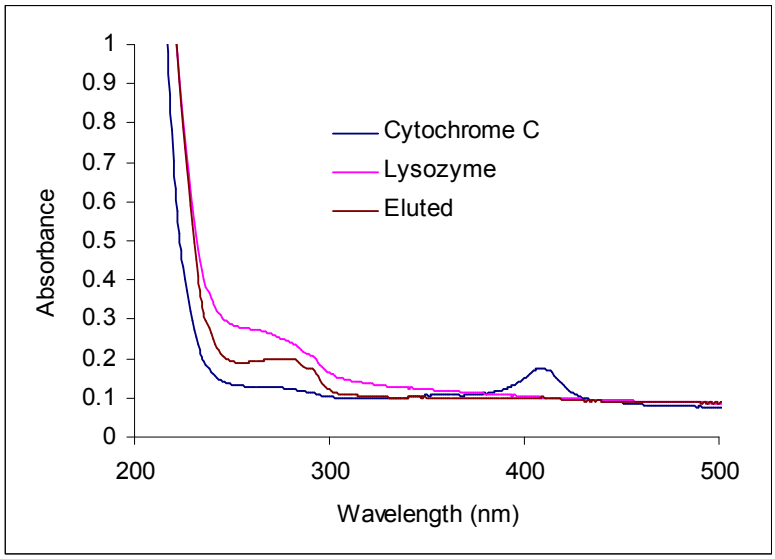

Figure 4.63: UV spectra of solutions of pure cytochrome C and pure lysozyme as well as solution eluted after binding from a 1:1 mixture of the two proteins to membrane grafted with poly(M1-co-M2), all at a concentration of 18 µg/mL in buffer.

4.8 Preparation and characterization of MIP composite membrane

Molecular imprinting, first reported by Wulff and Sarhan [188], is an appealing strategy to create specific enantioselective binding sites with well-defined shape and functionalities in prearranged fashion. And the application of molecularly imprinted polymers to membrane separation was first reported by Piletsky et al. [189]. However, in membrane separation, not only permselectivity, but also flux, is an important factor for the evaluation of membrane performance. For this purpose, surface functionalization of porous membranes as one of the effective solutions has attracted great attention to prepare thin-layer molecularly imprinted polymer (MIP) composite membranes with controlled specificity for individual compounds. Several routes have been developed for obtaining stable thin-layer MIPs [97, 105, 118]. However, to my best knowledge, the controllable surface-selective grafting from porous polymer membrane from organic solvents, which would enable to use more different templates and functional monomers for molecular imprinting, is not yet found to be reported. Therefore, in this study, it was attempted to prepare thin-layer MIP composite membrane for separation of Boc-D/L-PhA enantiomers (Fig. 4.64) using the proposed synergist immobilization and iniferter immobilization methods. Hydrophilized PP membrane was used as base membrane, Boc-L-PhA as template, AAm/MAA, EDMA and acetronitrile as functional monomer, cross-linker and solvent, respectively.

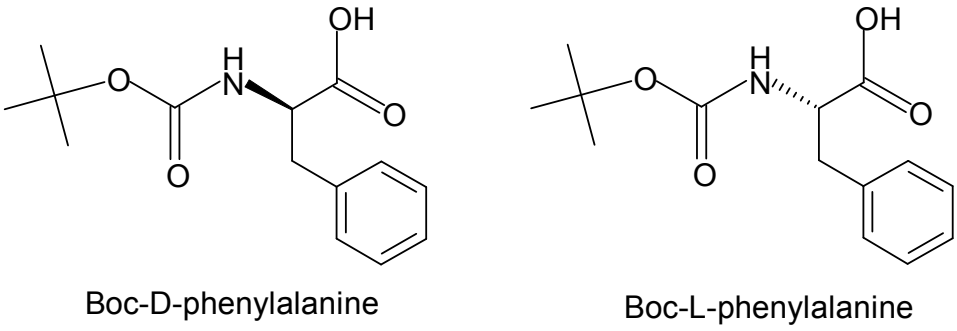

Figure 4.64: Chemical structures of enantiomers Boc-D/L-PhA.

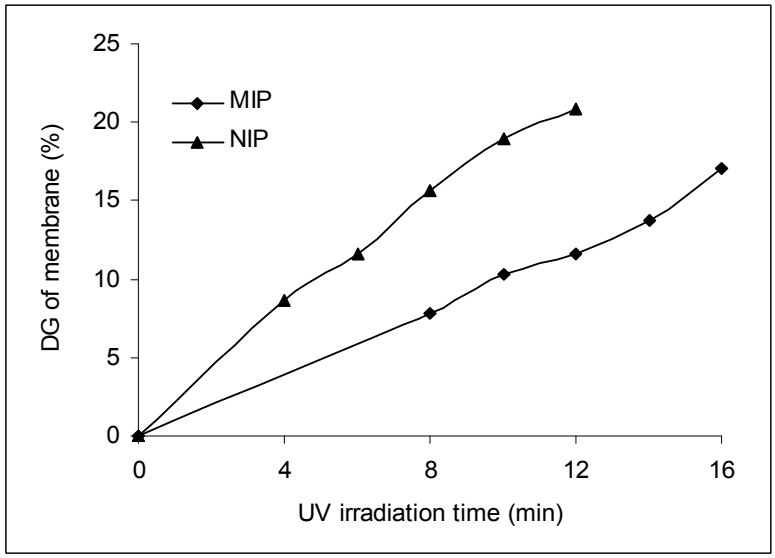

(a)

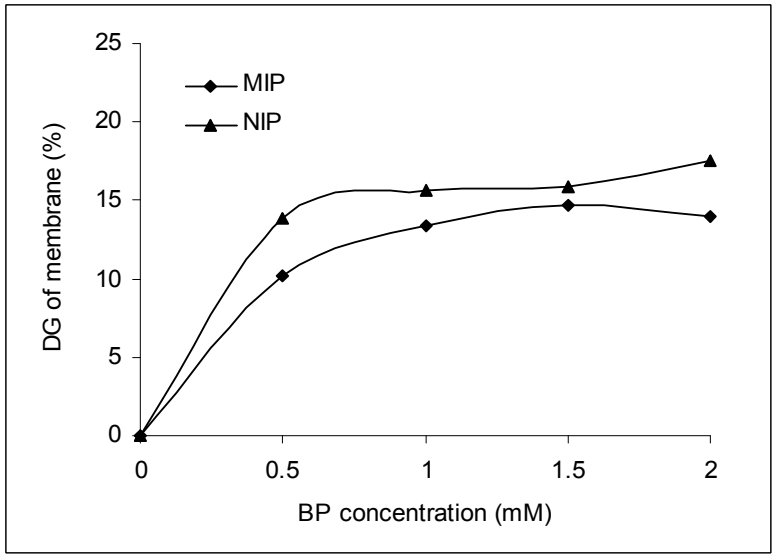

(b)

Figure 4.65: Effect of functionalization parameters on DG of MIP and NIP composite PP membranes grafted from acetonitrile solution of Boc-L-PhA / AAm / EDMA (10 / 40 / 200 mM) for MIP; 0 / 40 / 200 mM for NIP) via synergist immobilization method. (a) Effect of UV irradiation time; 1.0 mM BP concentration. (b) Effect of BP concentration. 8 min UV irradiation for NIP; 15 min for MIP.

4.8.1 Preparation of MIP composite membrane

First, synergist immobilization method was used to synthesize the Boc-L-PhA imprinted composite membrane. The DG value was adjusted by varied UV irradiation time and BP concentration (Fig. 4.65). The DG increased with UV irradiation time; with the increasing BP concentration, a plateau of DG value was reached at 1.0 mM BP concentration. Under the same grafting conditions, the significantly higher DG was obtained for NIP membranes than for MIP composite membrane (Fig. 4.65a). With similar DG value much longer grafting time was required for the synthesis of MIP layer (Fig. 4.65b).

In addition, using iniferter immobilization method, similar MIP/NIP composite PP membranes have been also prepared (Fig. 4.66). The DG was adjusted by UV irradiation time, and very similar DG was obtained for both MIP and NIP composite membranes under the same grafting conditions.

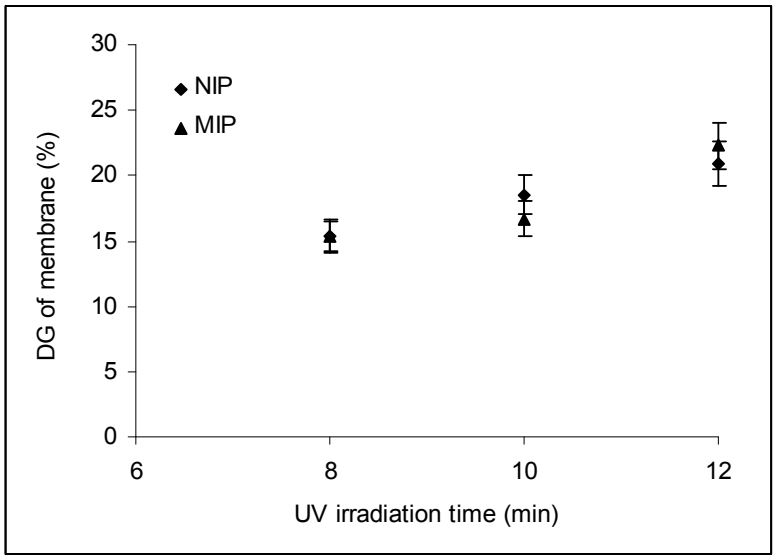

Figure 4.66: Syntheses of MIP/NIP composite membranes with different DG adjusted by varied UV irradiation time using iniferter immobilization method. Grafting proceeded in an acetronitrile solution of Boc-L-PhA / MAA / EDMA (10 / 50 / 250 mM) for MIP; 0 / 50 / 250 mM for NIP).

4.8.2 Characterization of MIP/NIP composite membranes

The amount of adsorbed and eluted Boc-L-PhA was determined spectrophotometrically at 217 nm for MIP membranes, together with NIP membranes as control samples. Fig. 4.67 shows the effect of DG on template (Boc-L-PhA) binding for the membranes, which was functionalized via synergist immobilization method. Compared with original hydrophilized PP membrane, all the MIP and NIP membranes exhibited significantly higher reversible Boc-L-PhA binding. In comparison, a pronounced higher Boc-L-PhA adsorption has been

observed for aminolysed membrane, but the eluted amount was even lower than that for MIP and NIP membranes. Viewing the data in Fig. 4.67 for all the MIP and NIP membranes, the very little influence of DG value was observed on the template binding capacity. Furthermore, imprinting effect was not achieved for MIP membranes since similar binding capacity was obtained for NIP membranes with the same DG value.

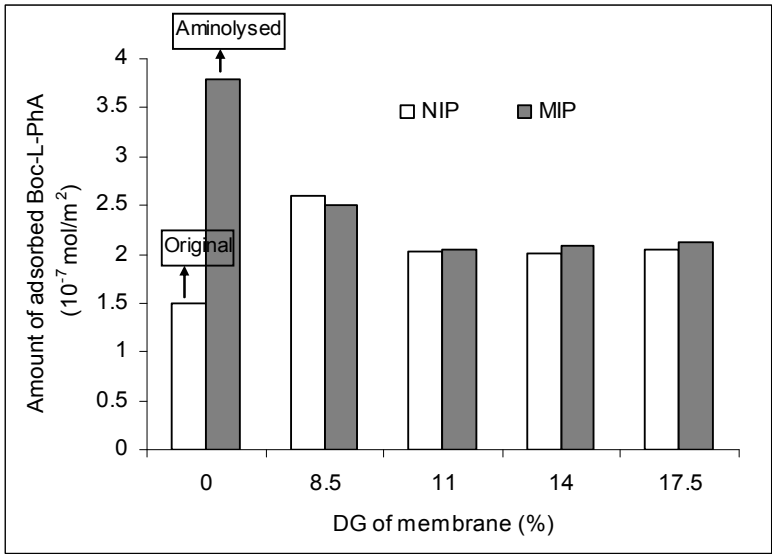

(a)

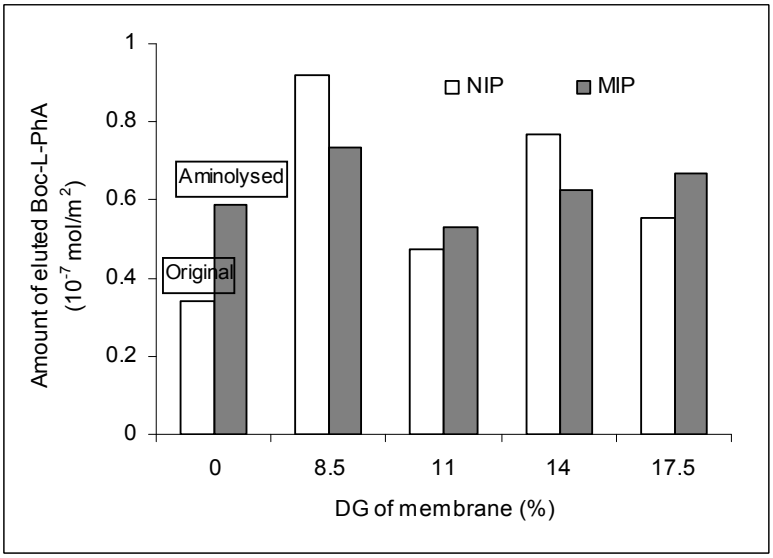

(b)

Figure 4.67: Effect of DG of MIP/NIP membranes grafted via synergist immobilization method on amount of adsorbed and eluted template (Boc-L-PhA). (DG=0% stands for aminolysed PP membrane). Membrane sample with a diameter of 25 mm was immersed in 2 mL 0.15 mM Boc-L-PhA solution in acetonitrile. After twice washing with acetonitrile, elution was carried out with 2 mL pure methanol.

Therefore, to optimize the composition of grafted MIP layer, various cross-linker concentration were used for the synthesis of MIP layer on membrnaes, and template binding capacities of the resulting MIP and NIP membranes have been measured (Fig.

4.68). However, the imprinting effect was not seen for any case.

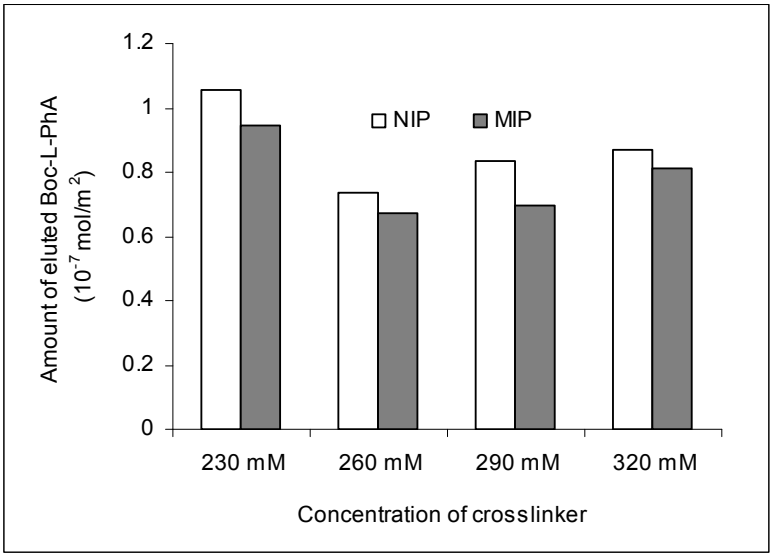

Figure 4.68: Effect of cross-linker concentration on amount of eluted template. All the membranes had similar DG value (about 16%). 0.15 mM Boc-L-PhA solution in acetonitrile was used as initial solution.

In the case of MIP/NIP composite membranes prepared via iniferter immobilization, the template binding measurements have been performed, but the obtained results were not highly reproducible (not shown). Therefore, further experiments and evaluation are required for more reliable data.

4.8.3 Preparation and characterization of MIP/NIP monoliths

In order to optimize the composition for preparation of grafted MIP thin-layer, MIP and NIP monoliths have been synthesized using different ratios among template, functional monomer and cross-linker via photo-induced radical polymerization (Table 4.12). The conversions of monomers were close to 100% for all the cases.

Table 4.12: Preparation of MIPs and NIPs with different compositions.

	Boc-L-PhA	MAA	EDMA	Acetonitrile	DMPAP
	Molar ratio				
MIP1	1	3	20	50 wt%	1 wt% of monomers
MIP2	1	5	20		
MIP3	1	8	20		
MIP4	1	10	20		
MIP5	1	12	20		
NIPs	All the conditions were same but without template				

Note: polymerization was performed under UV irradiation for 15 min. UV intensity: 3.5 mW/cm^2.

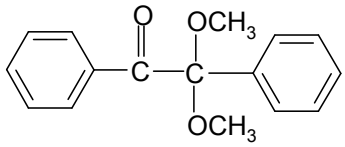

Figure 4.69: Chemical structure of DMPAP.

The enantioseparation of the synthesized MIPs and NIPs have been performed by incubating the polymers in racemic mixture solution of Boc-D/L-PhA, and the respective concentrations of initial and equilibrium solutions were measured by HPLC for determination of the separation factor (calculated though equation 3.10) and enatiomers binding capacity (Fig. 4.70). The samples M2 and M3 exhibited the highest Boc-D/L-PhA binding capacity and enantioselectivity, respectively.

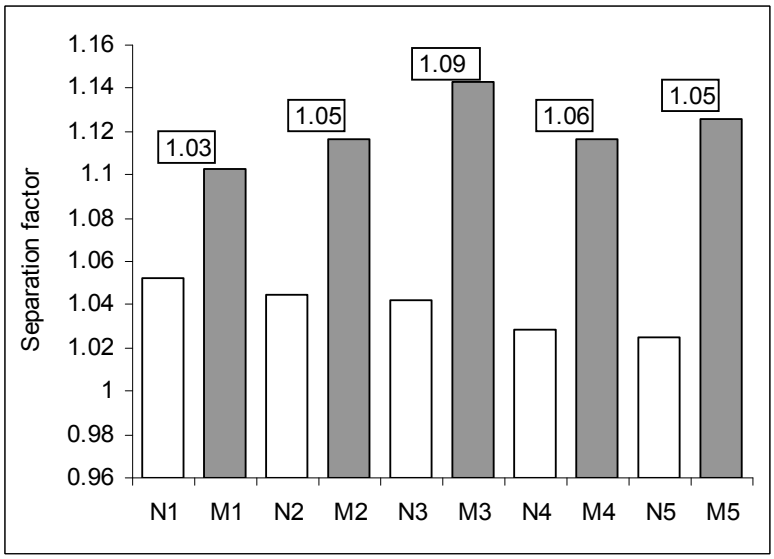

(a)

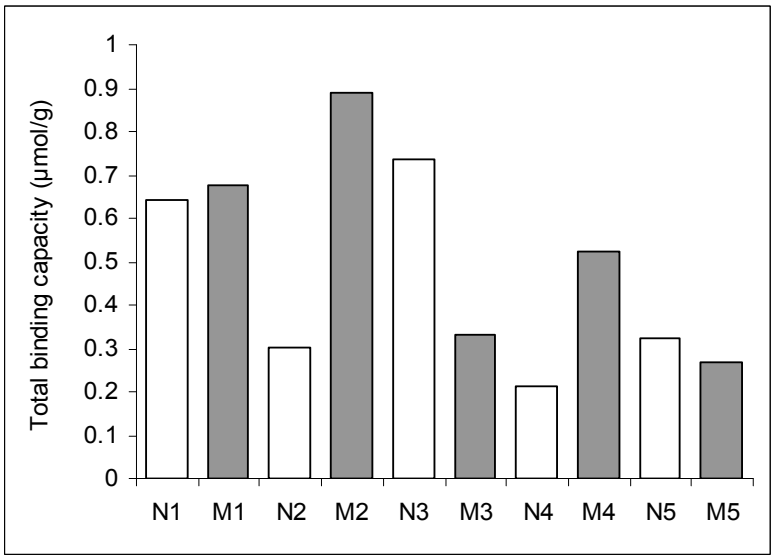

(b)

Figure 4.70: Separation factor (a) and total binding capacity of Boc-D/L-PhA (b) for MIPs and NIPs. The data above the bars in figure (a) are normalized separation factor (α_{MIP} / α_{NIP}). All the samples (N1-M5) were prepared according to Table 4.12. The racemic solution of Boc-D/L-PhA with a concentration of 0.1 mM, respectively, was used.

Chapter 5 Discussion

5.1 Characterizations of initial membranes

It is worth noting that the data from both liquid dewetting permporometry and liquid permeability measurements have been jointly used to determine some properties such as porosity. For liquid dewetting method, the pore diameter is determined by the effective barrier, which to large extent depends on the pore structure within the membrane. For instance, crossed pores, pore cavities and connected pores are often observed within the track-etched PET membrane and have much influence on the determination of pore diameter [190]. While water permeability values of membranes are more representative for the entire pore volume than the "barrier" permporometry data. Therefore, the combined evaluation by both methods would be more accurate for the pore-volume-related properties.

The pronounced discrepancy in pore diameter between data measured by liquid dewetting permporometry and supplied by manufacturers (Table 4.1 and 4.2) is probably due to the imprecise controllability in the preparation process, e.g., for PET membrane the "over etching" in the basic bath may lead to, on one hand, the over-increase of pore diameter; on the other hand, the part overlap of pores (but still isoporous structure), which is even more pronounced for the membranes with dense tracks (e.g., PET200 membrane). As a result, apparent pore diameter would be greater than that expected. At the same time, this also causes a significantly higher porosity. This explanation can be supported by the significant deviation between two batches of PET200 membranes as well (Table 4.2). As for conventional MF membrane, the nominal pore size diameter is determined by the efficiency of removal of size-known micron-particles (usually 95% or 98% retention). In addition, the high liquid permeability of MF membrane as another important property is taken into consideration. Therefore, for most of MF membranes, the characteristic pore sizes measured by permporometry are higher than the nominal one. The particle removal by MF membrane usually occurs by depth filtration and the effect of particle removal is similar to the specification [191].

From the comparisons of IR spectra and contact angle between both PP membranes (note that the high contact angle value of unmodified PP membrane can be explained by the porous PP surface, with air-filled pores contacting the test liquid water.), it can be deduced that the hydrophilic polymer coating on the hydrophilized PP membrane seems to contain ester and ether groups. This result is in agreement with the assumption that the

pre-modification of the PP membranes is performed via synthesis of a thin cross-linked hydrophilic polyacrylate, probably based on mono and bismethacrylates of ethyleneglycol derivatives (e.g., hydroxyethyl methacrylate and diethylene glycol bismethacrylate), covering the entire surface of the porous membrane [104]. According to the proposed polymer structure, the ester may be either part of the polymer chain (e.g., in an ethylene glycol-derived cross-linker) or the linker to a hydrophilic side group. The possible structures are shown in Table 4.2.

5.2 Photo-grafting technique for polymeric membranes

5.2.1 Photo-grafting methods

5.2.1.1 Photo-initiator entrapping method

Based on the occupied volume and mass loss values, a moderate swelling of bulk PP membrane has been achieved for chloroform, benzene and heptane due to their closer solubility parameters to that of PP membrane. Earlier, it had also been reported that the heptane sorption in PP films at room temperature had been estimated experimentally between 12 wt% [192] and 7.6 wt% [193], while the value for ethanol had been only 0.015 wt % [193]. But due to the short immersion time, the degree of swelling did not reach such a high value in this study. As expected, the BP uptake as function of soaking time and initial BP concentration demonstrates the successful initiator-entrapping in the membrane. Because there is a balance between swelling and dissolution of base polymer in heptane, a saturated swollen surface layer may be reached in a certain immersion time, leading to no further BP uptake with longer time (Fig. 4.3). However, more BP molecules could remain in the membrane surface volume at a high BP concentration. The slight increase of entrapped BP amount with BP concentration may be related to the drying and washing processes. In addition, the effective initiator-entrapping also has been supported by the subsequent photo-grafting of various membranes in aqueous solution (Fig. 4.4).

Surprisingly, more detailed investigations indicate that the entrapped photo-initiator in membrane can be extracted by the further washing with methanol, based on the detected data from multi-time-washed solutions (Table 4.4) and subsequent extraction solution with heptane (nearly no BP was detectable). This phenomenon is inconsistent with the previously reported results [13]. Earlier, it had been claimed that less than 10% could be removed with the polar methanol as compared with the non-polar heptane. Furthermore, as shown in Fig. 4.4, the reduction in DG value with the washing times provided another

proof. For this, the gradual reduction of the initiator concentration would be the only explanation. During the washing procedures, methanol, a good solvent of BP and a fine wetter for unmodified PP membrane, could also penetrate into the bulk polymer and extract the shallowly entrapped BP away from membrane surface, leading to a decreasing residual initiator concentration with washing times. Therefore, it is not surprising that the BP-entrapped membrane appeared to have a low photo-grafting efficiency when modified in acetonitrile solution of AAm, because the effective initiator concentration (in contact with membrane surface) went down by the extraction of BP into the bulk solution and more severely with the longer equilibrium and grafting time. On the other hand, the surface-selective graft polymerization could be still claimed compared to the very low DG values for control samples (Fig. 4.5), which would be attributed to the residue photo-initiator in/on membrane and the very small fraction of extracted initiator which dissolved in the bulk solution layer at the interface between membrane surface and bulk solution.

All the findings demonstrate that the immobilization of photo-initiator by 'entrapping' was clearly stronger than by simple physical adsorption. However, the reversible immobilization of initiator in polar organic solutions was unavoidable and caused a low photo-grafting efficiency.

5.2.1.2 Sequential photo-induced method

In the surface-initiator immobilization procedure, benzene was used as solvent due to its inert hydrogen atoms to the excited BP (the bond energy of $H\text{-}C_6H_5$ is about 110 kcal/mol [140]) and its low absorption of UV irradiation at >300 nm. In addition, the membrane dipped with BP solution was fixed between two pieces of glass during UV irradiation in order to reduce/avoid air and to prevent the reduction of UV intensity by BP solution layer.

The concentration of immobilized surface-initiator increased linearly as the function of UV irradiation time (Fig. 4.6), indicating that the initiator formation rate was nearly constant. This can be interpreted as follows: In terms of the equations of reaction (see Fig. 5.1) and the Lambert-Beer law, the kinetic equation of surface-initiator formation can be written as

$$d[BPS]/dt = k\, I_0\, (1- e^{-\varepsilon b[BP]}) \quad \text{.....(5.1)}$$

where BPS represents the surface-initiator formed in the hydrogen abstraction, k is the efficiency of surface-initiator formation, I_0 is the intensity of incident UV irradiation, ε is extinction coefficient, b is the thickness of the membrane where the hydrogen abstraction reaction occurs.

As shown in Fig. 4.6, BP concentration can be considered to be nearly constant due to the

very low BP conversion. As a result, a constant surface-initiator formation rate should be achieved under the ideal conditions, e.g., constant UV intensity, avoidance of undesired radical consumption.

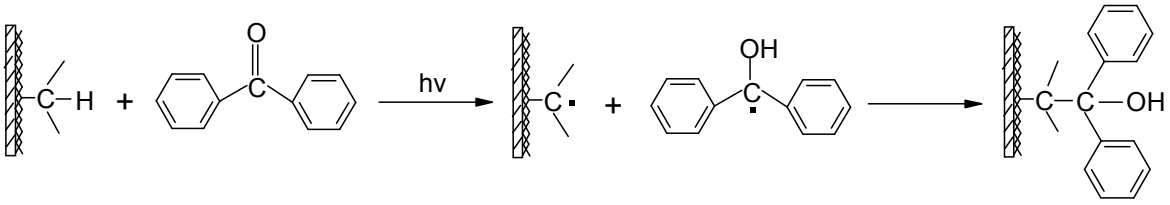

Figure 5.1: Schematic depiction of surface-initiator formation via sequential photo-induced method.

Based on the DG values in Fig. 4.7, the proposed mechanism turned out to be effective for photo-grafting of unmodified PP membrane. And the increase in DG was mainly attributed to the increasing grafting density. In addition, benzene can swell unmodified PP membrane (Table 4.3). Hence, initiator could be entrapped in the membrane volume during the immersion of membrane in the initiator solution in benzene, which was similar to that for photo-initiator entrapping method. Therefore, even though the system was not exposed under UV irradiation in the first step (the control sample without UV irradiation in the first step), a higher DG value was achieved than that of original membrane without any pre-treatment (Fig. 4.7).

However, when it comes to photo-grafting efficiency (DG value vs. initiator concentration), sequential photo-induced method would not be an efficient photo-grafting technique due to the requirement of high energy for the formation of initiating radicals (covalent bond dissociation). Moreover, the low photo-grafting efficiency appeared much more pronounced for membrane functionalization in polar organic solutions (Fig. 4.8).

5.2.1.3 Synergist immobilization method

Study on proposed mechanism

The synergist immobilization method was proposed, taking advantage of the characteristics of type II photo-initiator BP that a tertiary amine as co-initiator ("synergist") can accelerate its photo-reduction, and the amino-substituted alkyl radical formed is believed to be the main initiating radical. The detailed process for surface-selective functionalization of membrane is shown in Fig. 5.2. In the proposed process, the tertiary amino groups, acting as synergist of BP, are firstly introduced to the surface by aminolysis reaction between ester groups on the membrane surface and DEEDA. Subsequently, to evaluate

heterogeneous graft polymerization efficiency, the simultaneous method is adopted, i.e., monomer will be grafted to the membrane surface from organic solution containing BP under UV irradiation. Preferential hydrogen abstraction will be expected from tertiary amino groups on the membrane surface, and surface-selective and controllable photo-grafting should be realized using the surface-immobilized co-initiator (synergist; Fig. 5.2). In current work, both hydrophilized PP and track-etched PET membranes have been applied for investigation of this photo-grafting technique due to the presence of ester groups (see Table 4.2) on surface of both membranes (a pre-requisite of aminolysis reaction) and their excellent properties (for applications of functionalized membranes).

1st step : Aminolysis

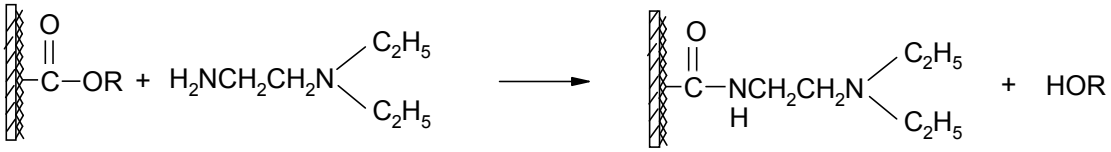

2nd step:

a) Formation of starter radical

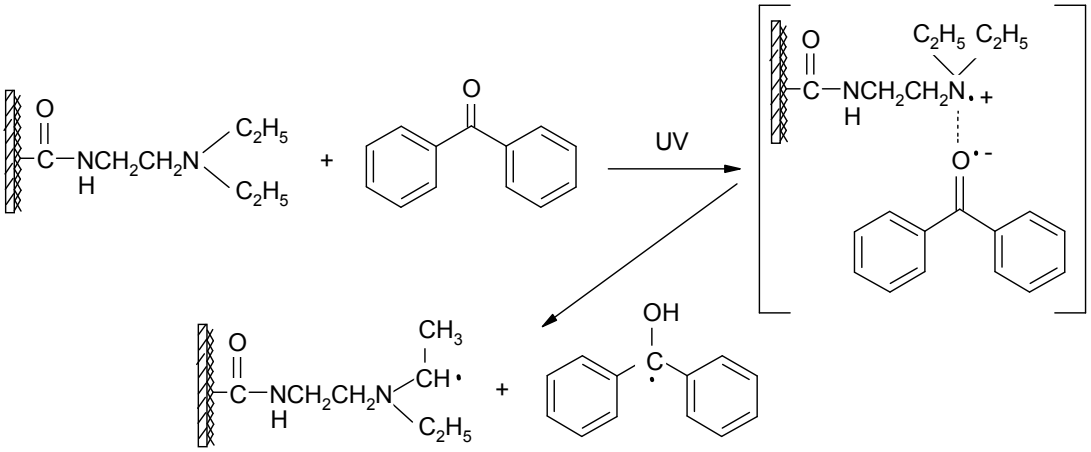

b) Graft copolymerization

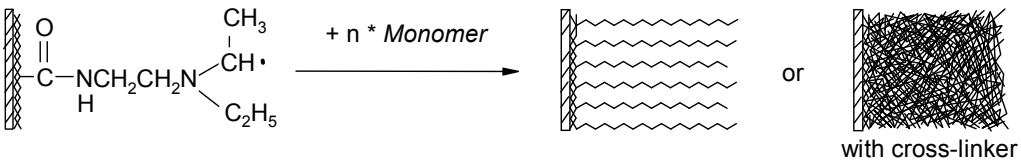

Figure 5.2: Schematic description of the synergist immobilization method for surface-selective photo-grafting.

Synergist immobilization. For aminolysis reaction of hydrophilized PP membrane, the qualitative determinations (the reduction of peak intensity ratio between at 1728 cm^{-1} and at 1375 cm^{-1} in IR spectrum (Fig. 4.10) and the appearance of wine red in characteristic color reaction) demonstrate that a small conversion of ester, presumably to amide, has taken

place, and the tertiary amino groups have been immobilized successfully onto the membrane surface under the selected conditions. Further evidence has been provided by the quantitative determination of cationic (tertiary amino) group amount. Its two-stage growth with the reaction time (Fig. 4.12b) could be explained by the following analysis. Assuming a two-dimensional interface structure and considering the specific surface area of the membrane (about 15 m^2/g), the tertiary amino group concentration of 350 $pmol/cm^2$ (after 2 hr) corresponds to an area of about 47.5 $Å^2$ per tertiary amino group. Estimated using Gaussian 98 software, DEEDA has an area of ~45 $Å^2$. Therefore, the first stage appeared probably because the whole specific surface of the membrane has been covered approximately with a monolayer of functional groups when the aminolysis proceeded up to 2 hr. A longer reaction time resulted in an even larger amount of amino groups due to further aminolysis deeper in the hydrophilic polymer layer, until reaching the significantly larger values of the second stage. This explanation was also supported by the DG data for heterogeneous graft copolymerization on the other membranes in Fig. 4.26b. By this means, 70^0C for 2 hr turned out to be the optimum conditions for the immobilization of a monolayer of tertiary amino groups on PET200 membrane, along with the analysis of membrane mass loss. During aminolysis reaction, PET chain scission led to the desired introduction of tertiary amino groups, on the other hand, to a fractional dissolution of the membrane polymer. Thus, the polymer layer on the membrane surface could be rearranged and surface roughness may significantly increase (larger specific surface area and average pore diameter (Fig. 4.27)). However, the membrane pore structure was still very well preserved, based on the similar SEM images and water permeability values for both membranes.

Photo-graft polymerization on membranes. According to the molecular structure of surface polymer layer, original hydrophilized PP and PET membranes have a weak hydrogen donor capacity. Therefore, only a small amount of starter radicals can be formed on the membrane surface by hydrogen abstraction of the excited BP, which leads to very low DG values. For instance, for hydrophilized PP membrane, a relatively high DG would be achieved only when the BP concentration in monomer solution was more than a certain value and graft polymerization proceeded under the optimum conditions (Fig. 4.16). While in most of cases, original PET membranes showed a very low surface selectivity of photo-grafting (nearly no grafting has been observed (Fig. 4.28a).

As shown in Fig. 5.3, however, the immobilized tertiary amino groups on the aminolysed membranes contain much more reactive hydrogen atoms to the exited BP, which accelerates

the formation of initiating sites for photo-graft polymerization. In consequence, markedly higher DG values have been obtained than for original membranes in all the cases (Fig. 4.18). This strongly supported the proposed mechanism based on a surface-immobilized synergist for the graft copolymerization, along with the increasing DG as a function of the surface concentration of tertiary amino groups (Fig. 4.12b). It must be noted that the accessibility to further increased number of functional groups obtained after the extended aminolysis for the photo-initiator and the monomer would be much lower than on the interface with the monomer solution. Therefore, no further increase in DG value was observed.

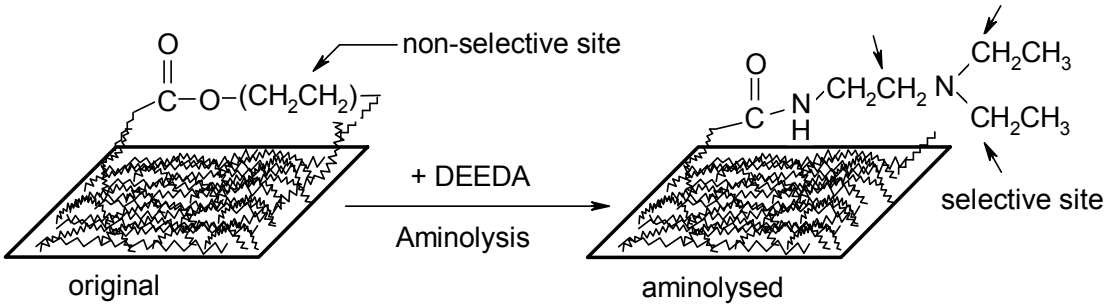

Figure 5.3: Schematic description of the surface structure of polymer materials containing ester groups: The reaction with N,N-diethylethylenediamine (DEEDA) leads to selective sites for photo-initiation of a graft copolymerization from the surface via hydrogen abstraction of the excited BP under UV irradiation.

In addition to the DG value, the additional peak in IR spectra corresponding to amide I group as well as the correlation of its height/area with DG values also (Fig. 4.13) verified the presence of newly grafted polymer, which can be directly seen from SEM images as well (Fig. 4.14). All these data imply the successful photo-grafting on the membrane.

On the other hand, the high DG ratio between aminolysed and original membranes demonstrates the high surface-selectivity of this method. Furthermore, the preparation of a cross-linked grafted thin-layer on the membrane surface provided another powerful evidence for this feature (see Fig. 4.23). Otherwise, cross-linked polymer formed in bulk solution will block the small membrane pores and can not be removed by washing.

Another important point for a successful photo-grafting technique is the uniformity of graft polymerization all over the whole membrane surface. This has been confirmed by the contact angle value (for outer surface; Fig. 4.30) and the streaming potential measurement of grafted PET400 membranes (for inner surface; Fig. 4.31) that nearly zero net charged inner pore walls have been achieved for PAAm-grafted membrane in 12 min UV irradiation. While after shorter grafting time the membranes exhibited positively charged pore surface because of the low grafting density as well as relatively short polymer chain length, making

the non-grafted (i.e., positive amino groups-covered) surface exposed in the measuring solution. In addition, the uniformity of grafting was also supported by the pore diameter measured by liquid dewetting method and calculated from ethanol permeability of grafted membranes. The pore diameters analyzed from both measurements were comparable with the results estimated from DG and specific surface area, on condition that membrane surfaces are uniformly covered by the grafted copolymer (cf. section 4.4.4 and 4.4.5).

Finally, from SEM images and liquid permeability values, it can be known that the membrane pore structure was well preserved after all the processes, which provided convincing evidences for the feasibility of the process conditions.

All the data and findings demonstrate that the proposed synergist immobilization method has succeeded in membrane photo-grafting from polar organic solution in terms of high photo-grafting efficiency, high surface-selectivity and uniform functionalization on the whole membrane surface as well as negligible impairment of base membranes.

However, to deeply understand the proposed strategy and to better control the membrane graft functionalization, more detailed investigations had been carried out and will be discussed below.

Factors affecting photo-graft polymerization

Immobilized synergist concentration. In the proposed mechanism (Fig. 5.2), tertiary amino groups immobilized on the membrane surface play key roles as co-initiator (synergist) of BP and subsequently initiating sites for graft polymerization, determining the photo-grafting efficiency and surface-selectivity. Therefore, a high synergist concentration promotes a more effective formation of initiating radicals because the reaction rate would be enhanced between excited BP and synergist. As a result, a high grafting density and DG value will be achieved (Fig. 4.12b). As already discussed before, the synergist concentration can be controlled by the varied aminolysis reaction conditions. Therefore, it is possible to adjust the grafting density and efficiency by controlling the synergist surface concentration. However, grafting density can also be modulated by other parameters such as grafting time and initiator concentration (below). In this work, therefore, considering photo-grafting efficiency and surface-selectivity, the aminolysed membranes with a monolayer of synergist had been prepared for more detailed investigations, i.e., aminolysis reaction proceeded at 60^0C for 2 hr and at 70^0C for 2 hr for hydrophilized PP membrane and PET membrane, respectively.

Solvent. Generally, there is an inhibition period during radical polymerization due to the

presence of oxygen in monomer solution. In current work, due to the relatively high hydrogen donor capacity of methanol, BP in its excited triplet state probably can react with methanol. Thus, a more effective consumption of oxygen in this photochemical reaction causes a more rapid depletion of oxygen in the solution, which shortens the inhibition period of graft polymerization in methanol solution (Fig. 4.15). However, for longer UV irradiation time, the photo-grafting rate of AAm appeared much higher from acetonitrile solution than from methanol solution. Although the polymerization reactivity of monomer in different solvents should be taken into account, it is believed that the reactivity of the solvents was mainly responsible for the pronounced difference. The hydrogen abstraction of the excited BP from methanol as a competing reation leads to a decrease in starter radical concentration on the membrane surface, and on the other hand, to the formation of initiating radicals in the bulk solution. Consequently, the graft copolymerization may slow down due to the fewer surface-initiating sites and the slower diffusion of monomer caused by the hindrance of homopolymer in the bulk solution. Similar results had been reported earlier by Tazuke and Kimura [194]. However, the difference is that in the early study, the addition of methanol inhibited the graft copolymerization from plain PP film surface, while in our work − due to the immobilization of synergist tertiary amino groups − the hydrogen donor capability of the membrane surface should be significantly larger than that of methanol and much higher than that of acetonitrile. This also explains the pronounced difference for original membrane grafted in methanol and acetonitrile solutions. Owing to the less reactive original surface, polymerization took place mainly in bulk methanol solution, leading to very low DG values in any case. While in acetonitrile solution, original membrane may exhibit its activity (but still weak) and relatively high DG could be obtained under the optimum conditions.

On the other hand, the low DG values obtained from methanol solutions suggest that the recombination of growing homopolymer chains with macroradicals at the surface should not play a significant role. Geuskens et al. [109] discussed this recombination as main mechanism for surface grafting initiated by “type II” photo-initiators, based on the fact that homopolymerization was always associated with surface grafting. In contrast, Tazuke et al. [195] claimed that such a termination reaction had been negligible under their experimental conditions. Consequently, the surface-selectivity of photo-grafting was much higher from acetonitrile solutions than from methanol solutions. This is even clearer when comparing the images and the water permeability of the membranes grafted in acetontile and methanol solutions containing a high amount of cross-linker, respectively (Fig. 4.23 and 4.24). Due to

the occurrence of polymerization in bulk methanol solution, a great number of polymer aggregates or globules have been formed on the grafted membrane surface probably by covalent or physical but loose combination of polymer formed in bulk solution with the grafted copolymer layer on the surface, leading to significantly reduced water permeability. While the high surface-selectivity of graft polymerization in acetonitrile solution induced an even and compact cross-linked grafted layer, preserving the high water flux, due to the suppression of swelling by polymer network.

Photo-initiator concentration. Since the surface layer functionalized with tertiary amino groups largely improved reactivity and selectivity for the graft copolymerization, only low photo-initiator concentration is required for the desired high DG value. Certainly, the formation rate for starter radicals would increase rapidly with the increase of BP concentration due to the accelerated reaction between BP and synergist. However, the formation of starter radicals on the surface is limited by the limited amount of synergist. Thus the further increase of BP concentration may not bring more benefit for the grafting of aminolysed membrane. On the other hand, when there exists a component with relatively high hydrogen donor capacity in bulk solution (e.g., in methanol solution), the increasing BP concentration will enhance the competing homopolymerization in the solution, which may inversely affect the photo-grafting from the membrane surface, e.g., by a reduction of monomer concentration or slowing down the monomer transport in the pores. Therefore, under the studied polymerization conditions, the highest DG value has been achieved at 0.625 mmol/L BP concentration in methanol solution. In contrast, a plateau of DG value was observed with the increasing BP concentration due to the inert character of acetonitrile to the excited BP, avoiding/largely suppressing the occurrence of homopolymerization in bulk solution; on the other hand, due to the limited synergist amount. In addition, it should be noted that with the increasing BP concentration, non-selective grafting of original membrane increased as well due to the greater possibility for generation of starter radicals, which would lead to a negative influence on the surface-selective of photo-grafting. For instance, the surface-selectivity is close to 1 at BP concentration of 5 mmol/L, when grafting proceeds in acetonitrile solution (Fig. 4.17).

In addition, at a given photo-grafting time, higher initiator concentration induces a greater amount of initiating radicals on the membrane surface, hence increases the grafting density. Therefore, with the same DG value, the water permeability would be higher than the membrane with low grafting density due to the shorter grafted chain length of the membrane with high grafting density (Fig. 4.22 and 5.5).

In conclusion, an appropriately low initiator concentration is required to reach a balance between high efficiency and high surface-selectivity of photo-grafting. Moreover, under a given UV irradiation time the adjustment of grafting density would be possible by the varied BP concentration.

UV irradiation time. The conversion of functional groups to starter radicals was enhanced with UV irradiation time, by which the grafting density could be adjusted. At the first few minutes of irradiation, formed starter radicals have been quenched by the dissolved oxygen (estimated concentration 1 to 10 mM) in the monomer solutions, so that the graft copolymerization efficiency was very low. However, the dependency of DG on UV irradiation time indicates that this inhibition effect could be overcome via consumption of oxygen by photo-chemically generated radicals. Afterwards, the continuous increase in DG may be due to the production of new initiation sites with time and longer period for polymer chain growth, which was supported by the reduction of water permeability with DG value adjusted by varied UV irradiation time (Fig. 4.22). In addition, the highest surface-selectivity has been found for shorter UV irradiation time (Fig. 4.18) due to the high photo-grafting efficiency for aminolysed membrane and the occurrence of non-selective grafting for original membrane at longer polymerization time.

Monomer concentration. Higher monomer concentration causes the greater chain propagation rate, leading to a longer polymer chain and keeping a constant grafting density under the identical conditions. Like for DG adjusted by UV irradiation time, the dependence of water permeability on DG value also reflected the increase in grafted chain length (Fig. 4.22). Combining the interplay of initiation efficiency (large differences between original and aminolysed membranes) and the chain propagation rate, the highest surface-selectivity would be achieved at an appropriately high monomer concentration (e.g., at 54 g/L AAm for methanol solution under current conditions (Fig. 4.18)). On the other hand, the large absolute DG differences obtained at the highest monomer concentrations offer a great potential for the application of the method with respect to an efficient change of surface properties. However, it should be noted that the DG may reach a plateau value at a certain high monomer concentration due to the slow diffusion of monomer to the initiating or propagating sites at a high DG.

UV irradiation intensity. It was confirmed that the higher UV intensity accelerated the reaction of BP with the substrate (including non-selective and selective surfaces) based on the significantly higher DG values obtained under high intensity UV irradiation (see Fig.

4.19). However, it has been discovered that a side graft polymerization would occur in the absence of BP, and it becomes more pronounced at the higher intensity UV irradiation. This implies that starter radicals could be formed by UV irradiation but a certain threshold concentration of these starter radicals is necessary in order to effectively compete with the inhibition by dissolved oxygen. Therefore, only detectable DG could be achieved under the UV irradiation beyond 20 mW/cm^2 for aminolysed PP membrane (Fig. 4.20). Comparing with zero DG for original membranes under the same conditions, the changed chemical structure of the polymer surface layer after aminolysis reaction would take responsibility for this side reaction. The explanation could be based on a mechanism according to the work of Coyle [196]: Aromatic amides with a 2-diethylaminoethyl substituent undergo a photo-induced Norrish type II cleavage reaction, and the quantum yields, although quite low, were 15 to 40 times higher than for amides without the amino substituent. Yang et al. [197] also believed that an effective grafting on a polymer film in the absence of a photo-sensitizer was initiated by the solvent DMF, which may generate starter radicals under UV irradiation mainly by means of hydrogen abstraction from the substrate. Consequently, it is believed that high-intensity UV irradiation will lead to the direct generation of starter radicals on the aminolysed membrane surface (Fig. 5.4). This new mechanism proposed above can help to explain the surprising effect for both aminolysed PP and PET membranes. While the difference in efficiency of direct cleavage (much higher for aminolysed PET membrane) can be interpreted by the aliphatic and aromatic character of the amide formed on the surface of hydrophilized PP and PET membranes, respectively.

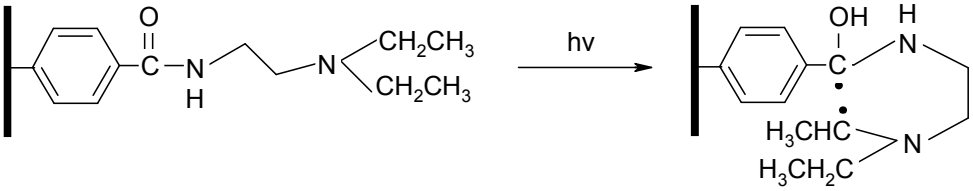

Figure 5.4: Schematic description of mechanism for direct generation of starter radicals on the aminolysed PET surface under high intensity UV irradiation.

Under high intensity UV irradiation two types of radicals are formed on the membrane surface, which can lead to a high grafting density. The addition of BP will reduce the generation of starter radicals via the intramolecular pathway (cf. above) because it absorbs UV light, at the same time the efficient bimolecular hydrogen abstraction by excited BP from the surface will also create starter radicals (cf. Fig. 5.2). Therefore, for example, in the case of PET200 membrane, under high intensity UV irradiation even higher DG was obtained for the cases without BP than for those with BP (Fig. 4.49). Furthermore, the

argument of high grafting density in the absence of BP can help to interpret the higher water permeability for the membrane with same DG value grafted without BP. In addition, the cross-linking might occur during the graft polymerization under high intensity UV irradiation by uncontrolled or by BP-initiated radical reactions, which led to the pronounced difference in water permeability between the membranes with same DG grafted under high and low intensity UV irradiation. Moreover, the water permeability data for those membranes with a slightly cross-linked grafted layer provided convincing evidence for this explanation (Fig. 4.33).

Consequently, control of the graft copolymerization from the surface with the immobilized synergist in the presence of BP becomes more complicated when high-intensity UV irradiation is adopted due to the possible co-existence of two photo-initiation mechanisms. Thus, selection of the lowest possible UV intensity is suggested in order to achieve maximum surface selectivity via one reaction mechanism (cf. Fig. 5.2).

Controllable grafted layer structure

As discussed above, well-defined grafted layer architecture could be realized by varying the main functionalization parameters under the optimum polymerization conditions via synergist immobilization method due to the possibility of independent adjustment for grafting density and grafted chain length. As shown in Fig. 5.5, with the same DG value, grafting density can be adjusted by the synergist concentration or UV irradiation time or initiator concentration (see Fig. 5.5a and b); keeping the grafted density constant, different grafted chain length can be achieved using varied monomer concentration (Fig. 5.5b and c).

Figure 5.5: Schematic depiction of linear grafted polymer layer with same DG value. (a) high grafting density; (b) low grafting density, long chain length; (c) low grafting density, short chain length.

In addition, due to the high surface-selectivity of photo-grafting the grafted layer with various cross-linking degree also can be realized by photo-grafting in monomer solution containing different cross-linker content (Fig. 5.6b). For instance, grafted layers with various cross-linking degree have been successfully grafted on the PET400 membrane surface via synergist immobilization method (Fig. 4.34). The DG dependence on

cross-linker content in monomer solution can be interpreted as follows: The reaction of the second double bond of EDMA in grafted chains with other growing polymer chains in the boundary layer leads to a grafted polymer network. By this means, macroradicals from chain transfer reactions (which would otherwise lead to polymer in solution), will also be incorporated in the grafted layer, leading to a higher DG than without cross-linker. But at high EDMA concentration, the highly cross-linked network would hinder the accessibility to the initiating sites for monomer, which affected the propagation rate, leading to lower DG values. In addition, the low polymerization reactivity of EDMA would be another reason, because EDMA was used as received, i.e., with a content of a small amount of stabilizer.

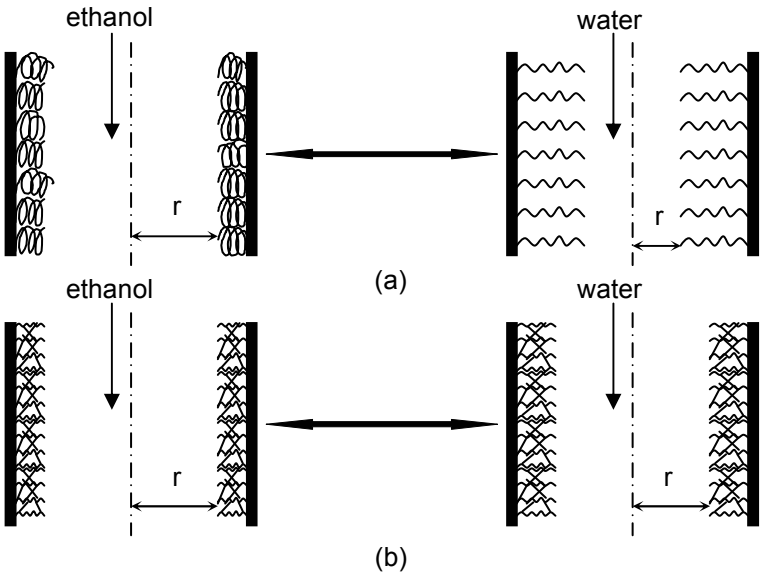

Figure 5.6: Schematic description of grafted layer structure in PET track-etched pores in ethanol and water. (a) linear polymer, (b) cross-linked polymer.

These structures can be characterized by ethanol and water permeability measurement due to the low solubility/swelling of PAAm in ethanol and its high swelling in water. Therefore, all grafted membranes exhibited high ethanol permeability irrespective of the grafted layer structure due to the very small grafted layer thickness relative to the large pore size, whereas, the water permeability would be much lower for the membrane with linear grafted polymer due to the stretching of polymer chains, leading to the reduced apparent pore diameter (Fig. 5.6a). Therefore, with the same DG value, the functionalized membranes with dense grafted chains show higher water permeability due to the shorter chain length. While with the same grafted chain length, the grafted membranes with varied grafting density could have similar water permeability. In this case, the surface coverage with grafted polymer (related to the grafting density) can be indirectly evaluated by contact angle and surface charge (streaming potential) measurements. As it is described in Fig. 5.7a, there is a critical grafting density,

where the contact angle (outer surface) and zeta potential (pore walls) reach a constant value with the increasing irradiation time, indicating the whole membrane surface is fully covered with grafted polymer. For example, with UV irradiation time, the contact angle and Zeta potential of PAAm-grafted PET400 membrane decreased until a lowest value (about 20^0) and nearly zero net charge, respectively, have been achieved for 12 min grafting (Fig. 4.31). Because the polymer chain stretching is suppressed by the polymer network, water permeability value could increase depending on the cross-linking degree (Fig. 4.35). Again, a critical cross-linking degree of grafted layer was observed, where the water permeability of the grafted membrane had an abrupt increase with the increasing content of cross-linker monomer due to the strong restriction of grafted chains by the formed polymer network, and this value was similar to that of aminolysed membrane (Fig. 5.7b). In addition, the lower water permeability value for the membrane with highly cross-linked grafted layer (Fig. 4.35) is related to the hydrophobicity of grafted layer.

(a) (b)

Figure 5.7: Schematic depiction of the critical grafting density (a) and critical cross-linking degree (b) of grafted layer reflected by the contact angle and streaming potential measurements (a) and water flux measurement (b).

As shown in Fig. 4.51, for membrane functionalization via synergist immobilization method, under the selected conditions, the grafting density of membrane may not reach the critical value in 15 min UV irradiation, so that functionalized membranes with a low grafting density have been obtained (see Fig. 5.8). In addition, the critical cross-linking degree was not observed up to 10% cross-linker content in the monomer solution, judged from the relatively low buffer permeability (Fig. 4.52). And the cross-linking degree could be adjusted by cross-linker content added in monomer solution. Therefore, for both cases, the further adjustment of grafted chain length was quite convenient based on the nearly linear correlation between DG value and monomer concentration (Fig. 4.51).

All data indicate that the membrane surface can be covered with a functional layer of adjustable structure, and –depending on the type of functional groups—such layers can be used, for example, for the reversible binding of protein with high capacity at high transmembrane pressure or for enantio-selective molecularly imprinted polymer with high cross-linking degree.

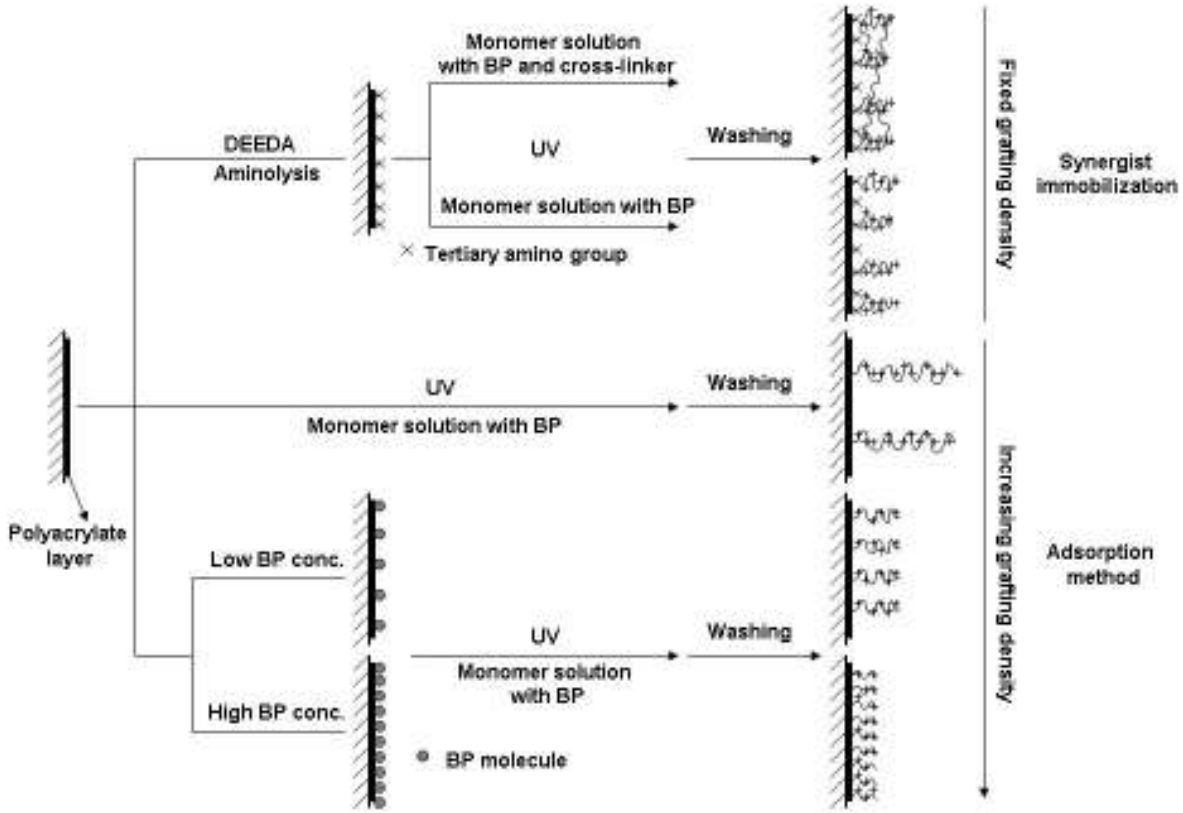

Figure 5.8: Schematic description of mechanisms and controlled photo-grafting of synergist immobilization and adsorption.

5.2.1.4 Iniferter immobilization method

Study on photo-grafting mechanism

As shown in Fig. 5.9, the covalent bond (C-S) between dithiocarbamate group and membrane surface is cleaved under UV irradiation and a pair of radicals are yielded. The radical on the membrane surface will initiate graft polymerization in the presence of monomer, while the dithiocarbamyl radical is less- or non-reactive but exclusively leads to termination reaction through recombination with a growing polymer chain on the membrane surface. The dithiocarbamyl end capped chain thus formed can be dissociated into a radical pair by further UV irradiation, and reinitiate polymerization.

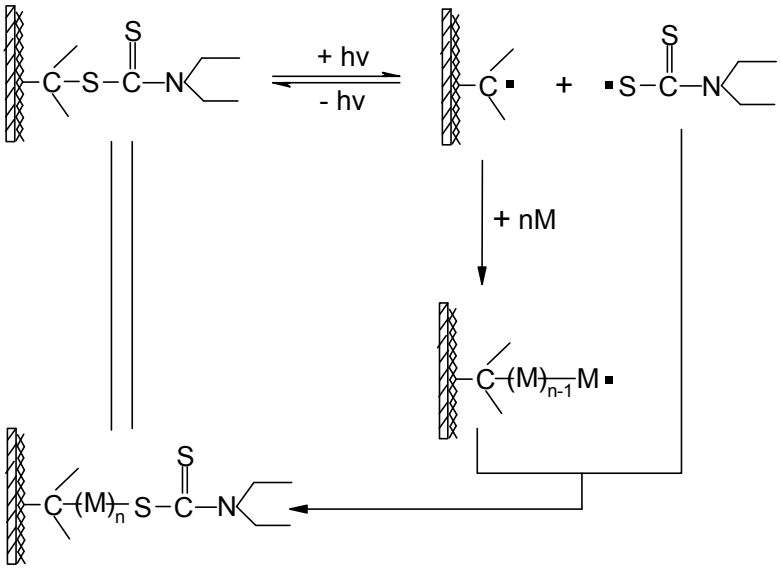

Figure 5.9: Mechanism of graft polymerization from immobilized iniferter on the membrane surface.

Therefore, two steps are involved for membrane photo-grafting using this method: immobilization of photo-iniferter, dithiocarbamate groups, on the membrane surface and graft polymerization in monomer solution under UV irradiation. The photo-iniferter was immobilized by three straightforward solid-phase reactions (see Fig. 4.36). Quantitative determination of amino groups (including immobilization in the first reaction (Fig. 4.37) and conversion in the second step (Table 4.6)) demonstrate that nearly a monolayer of bromoisobutylrate group was introduced on the membrane surface. The immobilized iniferter concentration was not analyzed but the high DG value for the resulting membrane (below) verified the success of iniferter immobilization, compared to the very low (nearly zero) DG for the bromoisobutylrated membrane. The SEM images and IR spectra (nearly no difference) for the membranes after each reaction indicate that the membrane pore structure was well preserved in the reactions for photo-iniferter immobilization.

High DG values and its good correlation with amino group concentration (hence, with iniferter concentration; Fig. 4.38) supported the proposed strategy and verified high surface-selectivity of this proposed method. The uniform functionalization all over the whole membrane could be seen directly from the SEM images of top surface and cross-sections (Fig. 4.41 and 4.42), which was also supported by the small DG difference between two stacked membranes grafted in the same solution. This difference was mainly caused by the reduction of effective UV intensity (from 7.0 mW/cm^2 to 1.0 mW/cm^2 through one layer of membrane). In addition, the correlation between pore diameter measured by permporometry and DG value as well as the comparability of the measured

value with the calculated dry grafted layer thickness provided another proof (see 4.5.2).

Controllability of photo-graft polymerization

As shown in Fig. 5.9, initiating sites are formed by the dissociation of photo-reactive covalent bond. Therefore, the photo-grafting efficiency, on one hand, depends on the bond dissociation energy. In this aspect, detailed investigations have been carried out by Ishizu et al [198]. It was concluded that steric factors are important in determining bond dissociation energy, hence the formation rate of initiating radical. Therefore, in this work, a relatively high C-S bond dissociation ability would be expected due to the influence of two methyl groups on the bond length of C-S. From this viewpoint, the structure of monomer used will also strongly affect its propagation rate, because dithiocarbamyl radical plays a role of terminator as well. Re-cleavage of formed monomer-S bond needs to be taken into account for re-initiation (in this case, the polymerization is undertaken by successive reactions rather than chain reactions). On the other hand, higher iniferter concentration would promote an effective graft polymerization. Higher grafting density can be achieved due to the more initiating sites created under UV irradiation. Therefore, the higher DG has been obtained for longer aminolysis reaction (finally leading to more immobilized dithiocarbamyl groups) (Fig. 4.38).

As presented in Fig. 4.39, DG of membrane can be adjusted by varied UV irradiation time and monomer concentration mainly by the growing grafted chains. Due to the uniform grafting, a good correlation has been observed between DG and characteristic IR adsorption peak intensity for newly grafted polymer (Fig. 4.40). However, for longer grafting time and high monomer concentration, the graft polymerization rate was affected by the quenching of initiating radicals and/or slower monomer transport at high DG, leading to a slower growth of DG value. Furthermore, according to the overlapped curves (i.e., water permeability vs. DG value adjusted by UV irradiation time and monomer concentration), similar grafting effect could be achieved, i.e., by the increase of grafting chain length. Moreover, the linear decline of apparent pore diameter with DG value implies that all the grafted chains seem to be growing simultaneously and the depletion of initiating radicals was negligible during the graft polymerization in the studied range. In addition, the grafted layers with various cross-linking degree have been prepared due to the high surface-selective photo-grafting (Fig. 4.45). The cross-linking degree in the actual grafted polymer could be adjusted by added cross-linker content (a precise measurement should be found for the detection of cross-linking degree). It should be noted that the quantitative determination by IR spectra was tried to detect the cross-linking degree, but failed because the adsorption peak of double

bond in the grafted polymer layer was weak and covered by other peaks. Anyway, a good correlation has been obtained between added cross-linker content and the height/area of characteristic IR adsorption peak (Fig. 4.47), which was also supported by the water permeability of various membranes (Fig. 4.46). Using this feature of high controllability, various membrane functions would be realized by grafting well-defined polymer layers, such as MIP composite membrane, high performance ion-exchange membrane.

However, all the data for the investigation of "living" character of polymerization indicate that the re-grafting of membrane has a low efficiency; in some cases even non-livingness can be detected. The undesired phenomena can be interpreted as follows: At the beginning of UV irradiation, there were a certain amount of radicals quenched by such as dissolved oxygen in monomer solution or by coupling of macroradicals. However, these side reactions were suppressed due to the depletion of oxygen and the higher dithiocarbamyl radical concentration in the system (when the growing radicals are terminated by side reactions, the excess dithiocarbamyl radicals still stay in the pores under UV irradiation), leading to smooth graft polymerization (the excess dithiocarbamyl radicals promote termination reaction). Even though UV irradiation was interrupted for a short time (here, 1 min), the grafting of membrane continued due to the re-dissociation of C-S at the end of grafted chains (Fig. 4.48). But with the prolonging interval between twice irradiation, the grafting efficiency fell down because the dithiocarbamate formed in bulk solution may diffuse out of the pores, which occurred more severely when the membrane was moved or shifted to a fresh solution. As a result, the balance between initiation and termination by dithiocarbamyl radicals has been destructed, leading to the sacrifice of more initiating sites.

5.2.2 Comparison of photo-grafting methods

As discussed above, this work covered four UV-induced approaches for polymeric membrane functionalization: photo-initiator entrapping method, sequential photo-induced method, synergist immobilization method and iniferter immobilization method. To some extent, all those methods are successful for membrane surface modification. However, each method also has its own disadvantages. In order to select a suitable method according to the functionalization system and the demands, a comprehensive understanding of each strategy is indispensable. An overall comparison will be given as follows (see Fig. 5.10).

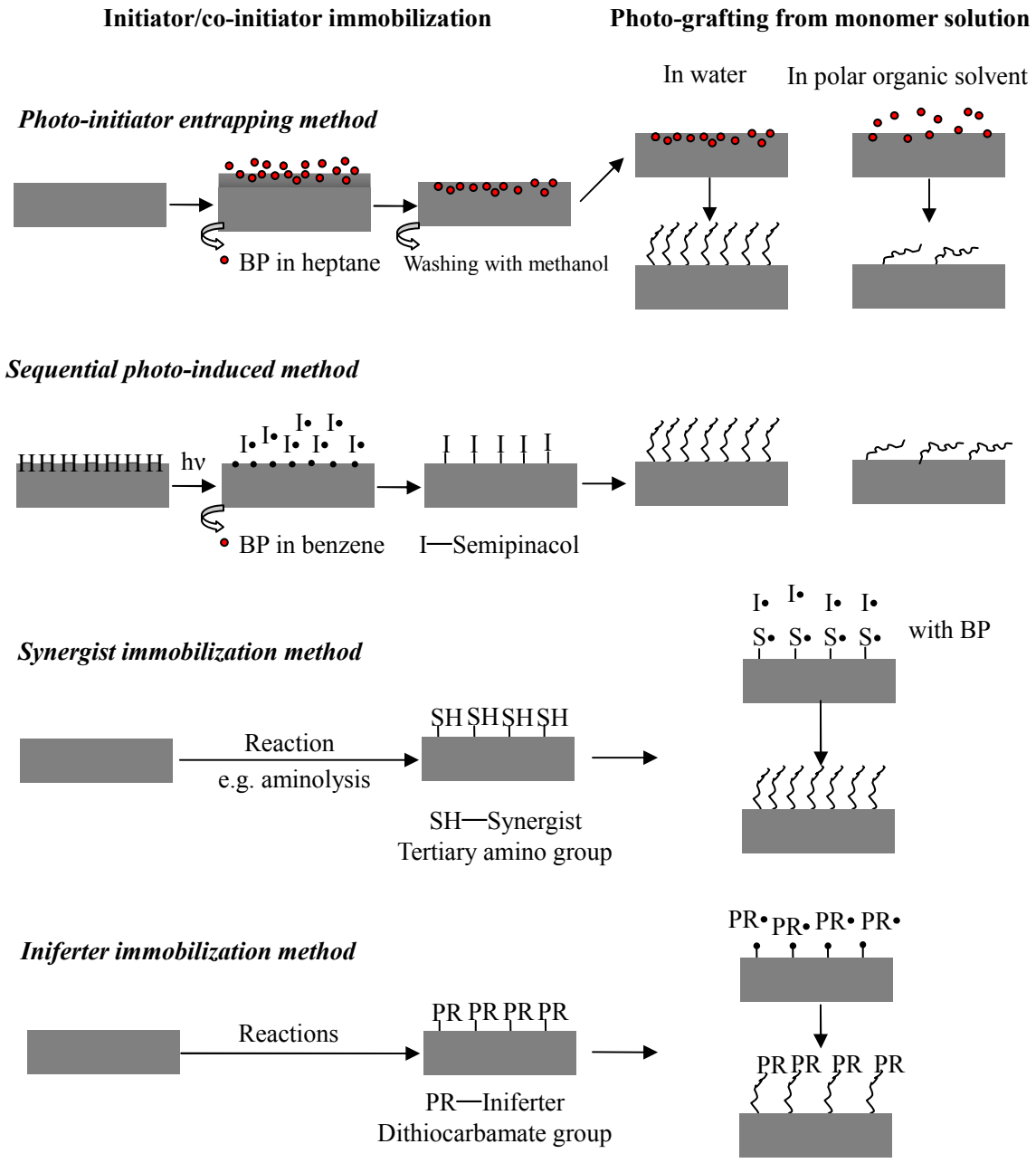

Figure 5.10: Schematic overall depiction of four photo-grafting methods.

Immobilization of photo-initiator/co-initiator: The strategy "photo-initiator entrapping" had been brought forward to improve/solve the disadvantage of reversible immobilization of initiator for conventional photo-initiator adsorption method. Due to the fixing action of base polymer chains towards entrapped initiator, the local concentration and distribution of photo-initiator would be more stable (Fig. 5.10). In this case, the swelling of base membrane polymer in initiator solution is the key factor to ensure entrapped initiator amount, along with the initiator concentration used. For sequential photo-induced method, the obtained surface-initiator binds covalently on the membrane surface by photo-reaction between BP

and base polymer (Fig. 5.10). Therefore, on one hand, the factors affecting the reaction rate for surface-initiator formation must be taken into account, for example, the hydrogen donor capacity of base polymer and solvent. On the other hand, side reactions would influence the recombination of two radicals formed under UV irradiation, for instance, the quenching of radicals by oxygen. Nevertheless, the initiators formed are strongly immobilized on the membrane surface. The surface-initiator concentration would be adjusted by UV irradiation time and initial initiator concentration. In synergist immobilization method, a new strategy had been proposed that co-initiator or synergist (tertiary amino groups) of BP instead of photo-initiator is introduced on the membrane surface by aminolysis reaction or other reactions depending on the base membrane and used reagent. Synergist concentration can be readily controlled by pre-functionalization conditions. In the case of iniferter immobilization method, like for sequential photo-induce method, dithiocarbamate groups as photo-iniferter was also covalently immobilized on the membrane surface by reactions. It should be noted that the reactions for synergist and photo-iniferter immobilization are limited with respect to base polymer.

Photo-grafting efficiency: For all four methods, the initiating sites are generated from membrane surface, which guarantees the surface-selectivity of graft copolymerization. For photo-initiator entrapping and synergist immobilization methods, the excited BP in the membrane surface and in bulk solution, respectively, abstracts hydrogen atom from membrane surface under UV irradiation. For the former, nearly all the immobilized initiator is in contact with base polymer in monomer aqueous solution, making the reaction relatively easy and effective. However, the hydrogen reactivity of base membrane should be considered, because generally, commercial membranes have quite low hydrogen donor capacity to the excited BP. Therefore, surface-grafting is prone to suffer from influence by the competition from grafting surroundings. As for synergist immobilization method, the photo-reduction of BP significantly is enhanced due to the introduction of highly reactive tertiary amino groups (Fig. 5.10), leading to more efficient formation of initiating sites on the surface. High surface-selectivity of photo-grafting would be expected. Because of the high grafting efficiency and surface-selectivity, membrane can be functionalized at the very low initiator concentration. For the other two methods, the initiating radicals are formed by dissociations of covalent bonds (Fig. 5.10). In comparison, higher energy is required to split the bond between membrane surface and semipinacol, which may cause a relatively low grafting efficiency. Furthermore, the degradation of base membrane should also be taken into account under the high-energy irradiation. In the case of iniferter immobilization

method, unlike conventional radical polymerization, the chain propagation proceeds by successive reactions rather than chain reactions due to the special photo-reactive moiety as initiator, transfer agent and terminator. As a result, the graft polymerization rate may be slower but more controllable. Moreover, the efficiency of scission is lower for re-initiation.

Sensitivity of photo-grafting to grafting system: As discussed above, the photo-grafting efficiency for entrapping method is much lower in polar organic solution than in aqueous solution due to the extraction of entrapped BP by solvent, leading to the reduction of effective initiator concentration and wide distribution on the surface. Therefore, this grafting method is more suitable to modify membrane with non- or poor-solvents of initiator as polymerization media, at the same time, the use of monomers which are insoluble in those solvents is also limited. In addition, as mentioned before, the base polymer with inert hydrogen atom to the excited BP would not be efficiently grafted via entrapping method. In sequential photo-induced method, due to the relatively low grafting efficiency caused by the requirement of high energy, the high polymerization reactivity of monomer in system may be required to achieve desired functionalization. For instance, in this work, this grafting method exhibited a quite low efficiency in acetonitrile solution of AAm. Via synergist immobilization method, so far, a high grafting efficiency and surface-selectivity has been achieved in whether polar organic or aqueous solution. However, it must be noted that the immobilized tertiary amino groups are weakly basic, thus its reactivity with excited BP could be influenced by the acid surroundings, i.e., the acidic monomer might show relatively lower graft polymerization reactivity. As for iniferter immobilization method, monomer structure has much influence on the photo-grafting efficiency due to the re-dissociation of monomer-S covalent bonds formed. For some monomers, the grafting time may be very long for a desired DG.

5.3 Membrane functionalities

5.3.1 Anion-exchange membrane

5.3.1.1 Preparation of anion-exchange membranes

Surface-graft functionalization has been proven to be efficient technique to enhance the protein binding capacity of membranes by “multilayer binding” of protein along the grafted polymer chains. On the other hand, it has been realized that a tradeoff between high protein binding capacity and low liquid permeability is still a challenging issue and must be overcome for full employment of the excellent mass transfer characteristics of

membrane adsorbers. For that, it is believed that the optimization of grafted layer structure would be an effective solution. However, to my best knowledge, relevant reports have rarely been found [9, 10, 185]. High cross-linking of grafted layer has been employed to enhance the stability and liquid permeability of membrane adsorbers; but this, however, led to a sacrifice of a great of binding capacity [9, 185].

In this work, therefore, various anion-exchange membrane adsorbers with respect to grafted layer architectures have been prepared via synergist immobilization method and conventional adsorption method. As it was discussed in section 4.4, 'low grafting density' and slightly cross-linked grafted layer can be readily realized via synergist immobilization method. Adsorption method was used, on one hand, as a control method; on the other hand, for the preparation of anion-exchange membranes with different grafting density, which can be adjusted by varying initiator concentration for initiator pre-coating [114] (Fig. 5.8). The grafted chain length was adjusted by varied monomer concentration for both photo-grafting methods. In comparison, the grafting efficiency was much higher for synergist immobilization under the same grafting conditions (Fig. 4.51), which is attributed to the immobilization of tertiary amino group as synergist on the membrane surface. For adsorption method, the grafting efficiency could be improved by increasing the initiator concentration applied for initiator pre-coating, which, at the same time, leads to the growing grafting density (Fig. 5.8). It seems that the control over the grafted chain length was relatively harder when using photo-initiator adsorption method, especially for the preparation of membranes with high grafting density. Nevertheless, three types of anion-exchange membrane adsorbers have been obtained via two photo-grafting methods: low grafting density ("A 0 mM", "A 10 mM" and "S 0% CL"), low grafting density but slightly cross-linked grafting ("S 5% CL" and "S 10% CL") and high grafting density ("A 60 mM" and "A 100 mM") (Fig. 5.11). These structures were verified by the buffer permeability of the resulting membranes (see below).

5.3.1.2 Evaluation of anion-exchange membranes

For all types of membranes, increasing DG led to growing protein binding capacity (Fig. 4.54) due to the "multilayer binding" of protein, e.g., estimated from the amount of BSA monolayer adsorption on a planar surface (~ 250 ng/cm^2) [74] and specific surface area of original membrane (15 m^2/g), an average of thirteen monolayers of BSA have been bound on the entire surface of membranes "S 0% CL" with 11.5 % DG. This strongly supported that the three-dimensional grafted layer have been prepared for all the resulting membranes. However, due to the mutual electrostatic repulsion for quaternary ammonium groups, the

grafted chains extended toward the interior of pores in the buffer solution, leading to the reduction of buffer permeability (Fig. 4.52). Moreover, this effect was more severe for higher DG. Therefore, from practical viewpoint, an appropriate range of DG values was selected for more detailed investigation (here about 12% DG).

In comparison to that of the low grafting density membranes, the relatively higher buffer permeability for “S 0% CL” and “S 10% CL” indicates that the grafted polymers were slightly cross-linked for both membranes. And the cross-linking of grafted layer restricted not only the extension of grafted polymer chains, but also the collapse extent in the elution solution (buffer solution with 1 mM NaCl). While the higher buffer permeability and low collapse extent for “A 60 mM” and “A 100 mM” confirmed the high grafting density structure, which, from another aspect, solved the problem of low liquid permeability for the membranes with the same ligand amount. Fig. 5.11 shows the grafted layer structures and the conformation of grafted layer in chromatographic processes for anion-exchange membrane adsorbers with same DG value as well as the protein binding behavior.

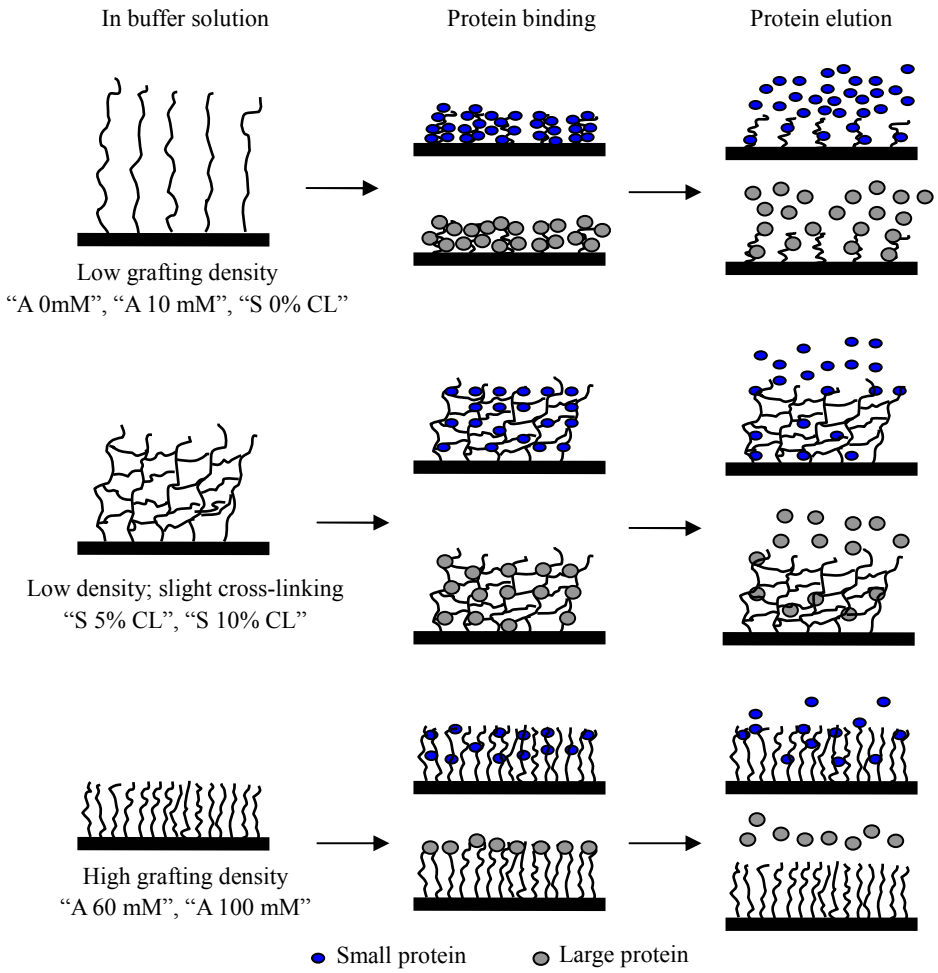

Figure 5.11: Schematic depiction of various grafted layer architectures for prepared anion-exchange membranes and protein adsorption and elution for those adsorbers.

For the low grafting density membranes the fully extended chains favored the protein binding. However, it was found that in the progress of protein binding, the grafted chains collapsed due to the charge screening by the bound proteins (Fig. 4.58). The same phenomenon had been reported by Saito et al. [199]. Therefore, with the longer incubation time, the protein was transported to ligands mainly by diffusion, leading to a further but slow increase in protein binding. A high static binding capacity could be achieved from batch experiments. Moreover, the influence of chain shrinkage on protein binding capacity and recovery was relatively weak because of the flexibility of linear polymer chains. However, from the breakthrough curves (Fig. 4.57), a long time delay was observed for this type of membrane to reach the maximum binding capacity, indicating a significant dispersion. In addition, the maximum dynamic binding capacity was significantly lower than the static one because the binding from the solution flowing through the pores may become less efficient with increasing thickness of the grafted layer.

Cross-linking to a certain extent hindered the accessibility of proteins to ligands, especially for large size protein (here, BSA), leading to a slightly lower protein binding capacity. Nevertheless, the binding capacity was still high enough (~80 and 70 mg/ml membrane for "S 5% CL" and "S 10% CL", respectively at 12% DG) compared with the data reported in literatures (20-50 mg/ml) [13, 174, 185]. Morover, a relatively lower protein recovery was obtained for large size protein because the bound proteins inside the grafted layer in the long incubation time may be not released due to probable further collapse of polymer networks in elution solution, whereas this effect was weaker for small proteins due to the slight cross-linking degree (Fig. 4.55). Although slightly lower binding capacity compared to that for low grafting density membranes, the dynamic performance of the membrane with slightly cross-linked grafted layer was strongly improved; both membranes exhibited low dispersion (Fig. 4.57). This was also supported by the slope values obtained from the breakthrough curves (in the range of 0~0.5 ratio of effluent conc./feed conc.). Furthermore, the protein recovery was high because the collapse of grafted chain was not that strong during the binding and elution of protein (Table 4.9).

In the case of high grafting density membranes, the accessible ligands inside the grafted layer were limited for large size protein (e.g., BSA) due to the clogging of the access to the inner ligands by previously adsorbed proteins. Therefore, the protein binding was limited to the surface of grafted layer, leading to a low binding capacity. While for the small proteins, the crowded structure significantly affected the protein mass transport but multilayer binding still could be achieved. Therefore, high grafting density membranes

showed molecular size exclusion. In contrast, other types of membrane adsorbers did not show this feature based on the lower and similar ratio between the static binding capacities for trypsin inhibitor and BSA (Fig. 4.55) due to the relatively small cross-linking degrees and the moderate grafting density. Different with other two types of membranes, the recovery of BSA for high grafting density membranes was higher than for small protein trypsin inhibitor due to the 'surface adsorption' of BSA on the grafted layer where it is readily eluted with buffer solution with extra salt. In addition, for this type of membrane adsorber, the breakthrough curve was very steep but the binding capacity was relatively low (Fig. 4.57 and Table 4.9).

Due to the fast BSA-ligand kinetic binding in comparison with convective transport through the pore space, the identical breakthrough curves were obtained for all different anion-exchange membranes irrespective of flow rate. Moreover, the normalized dynamic BSA binding capacities were comparable with the static binding capacities (cf. Table 4.8 and 4.9), implying that the anion-exchange groups in the grafted layers were well accessible under chromatography conditions.

In addition, it can be noticed that judged from protein binding capacities, membrane "A 0 mM" can compete with "S 0% CL" at same DG. However, the dynamic performance was much worse for membrane "A 0 mM" based on the breakthrough curves (Fig. 4.57). In addition, it should be noted that to obtain the identical DG value, 25 mg/ml and 42 mg/ml monomer solutions were employed for membranes "S 0% CL" and "A 0 mM", respectively (Fig. 4.51). This indicates that synergist immobilization method is a more efficient and suitable technique for the preparation of ion exchange membranes. Combining high protein binding capacity and recovery as well as steep breakthrough curves, the membranes prepared via the synergist method and using cross-linker monomer ("S 5% CL" and "S 10% CL") exhibited the best overall membrane adsorber performance.

5.3.2 Affinity membrane

As shown in Fig. 5.12, in free solution, the long polymer chain must wind around one or several protein targets, and undergoes an extensive induced-fit procedure on their surfaes to maximize favorable binding interaction. If the anionic polymer is bound to a cationic PEI layer, it does not only lose a substantial fraction of its binding sites for the immobilization, but also becomes confined to a two-dimensional flat arrangement, which reduces the accessibility of globular proteins from all sides [187]. Therefore, the strategy of this study is to graft a similar functional copolymer on the track-etched PET400 membrane surface. This

"vertical architecture" of grafted layer would improve the flexibility of functional copolymer (relative to the "horizontal architecture" on the planar surface). Protein binding behavior was expected to be similar to that in free solution. In addition, the isoporous structure and larger surface area of track-etched PET membrane facilitate the characterization of affinity adsorber performance and the stability of grafted copolymer on the membrane surface would be greatly enhanced by covalent bonding.

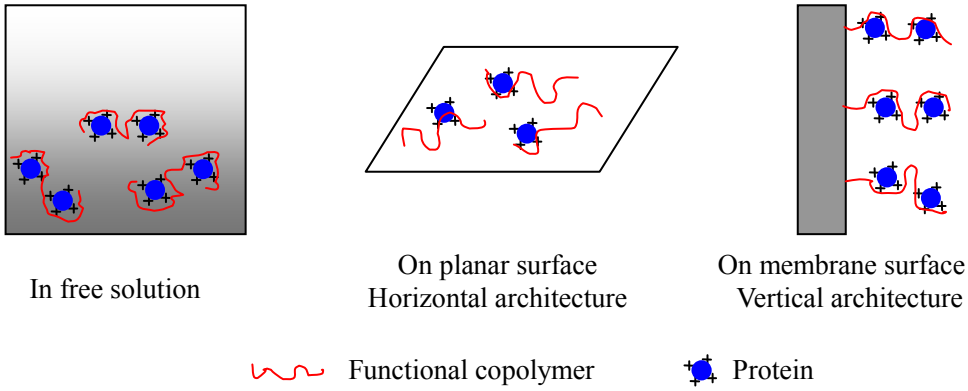

Figure 5.12: Schematic depiction of protein binding of functional copolymer in various architectures.

5.3.2.1 Preparation of affinity membranes

Based on the analysis of ^{31}P solid state NMR (Fig. 4.60), three types of grafted membranes have been successfully synthesized. The unwanted small fraction of bisphosphonate salt group was present in the poly(M1-co-M2)-grafted membrane, which can be tentatively explained by nucleophilic attack of the tertiary amino groups on the phosphonate esters at elevated temperature, leading to quarternary ammonium phosphonate salts. Furthermore, the composition of grafted copolymer seemed to be similar to the ratio between two monomers added based on the similar DG value obtained for polyM1-grafted and poly(M1-co-M2)-grafted membranes and due to the similar polymerization reactivity [187]. The chemical structures of grafted layers are shown in Fig. 5.13.

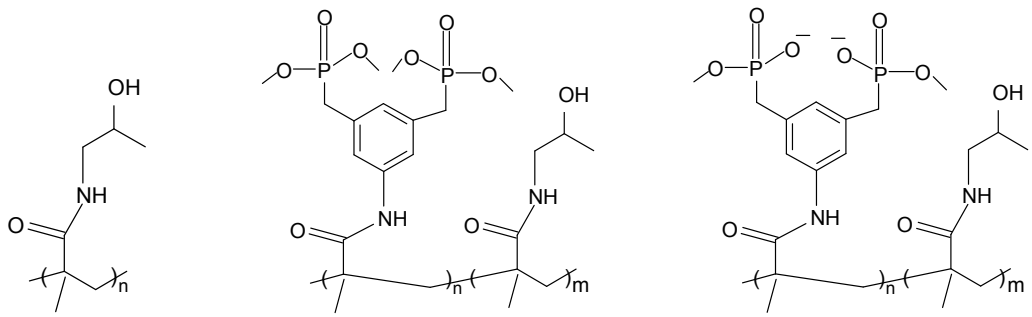

(a) PolyM1-grafted (b) Poly(M1-co-M2)-grafted (c) Ionized poly(M1-co-M2)-grafted

Figure 5.13: Chemical structures of grafted layer for synthesized affinity membranes.

5.3.2.2 Characterization of affinity membranes

It seems that the 20% of highly polar M2 comonomers in the grafted copolymer dominated the surface and volume properties of the resulting membranes, leading to the low contact angle and high swelling in water (Table 4.11), and the stretching of the grafted chains would contribute to protein binding.

Due to the relatively high grafting density, large size proteins could suffer from steric hindrance for diffusion into the grafted layer. For the blank membrane, size exclusion effect was observed (Fig. 4.61) due to the small binding entropy, which resulted from the weak hydrogen binding between the proteins and methacrylamide backbone/hydroxyls in the grafted layer. While this effect was overcome by the higher binding entropy for the cases of poly(M1-co-M2)-grafted and ionized copolymer-grafted membranes due to the stronger specific interactions between proteins and functional groups on both membrane surfaces. Both membranes exhibited higher binding capacity for all the selected proteins than for blank membrane. However, the difference in binding capacity for different proteins would be mainly attributed to the pI value or/and surface structure.

For poly(M1-co-M2)-grafted membrane, the significant difference in binding capacity between lysozyme and cytochrome C could be interpreted by the different arginine content. Lysozyme is an arginine-rich protein (61%), whereas cytochrome C is lysine-rich (89%). Therefore, the binding between cytochrome C and bisphosphanate ester group was mainly by π-cation interation between lysine and the coplanar electron-rich m-xylylene host surface, while generally, the π-cation interation is stronger for arginine compared with for lysine; besides, the additional hydrogen bonding further reinforced the formation of complex between arginine-rich lysozyme and bisphosphanate ester (Fig. 5.14). The stronger interaction between lysozyme and grafted neutral copolymer was also verified by significant higher binding constant for lysozyme (Fig. 4.62), which was even higher than the binding constant for the ionic interaction between BSA and quarternary ammonium group (Table 4.8). As a result, lysozyme has been already separated from a lysozyme/cytochrome C (1/1) mixture solution with a high selectivity with this type of affinity membrane (Fig. 4.63).

After Li-ionization, however, the electrostatic interaction between lysine or arginine and bisphosphanate salt, which are stronger than π-cation ineraction alone, dominated over the formation of complexes, leading to similar binding capacity for both proteins and higher cytochrome C binding capacity than for the neutral poly(M1-co-M2)-grafted membrane. However, for the phenomenon that a higher lysozyme binding capacity was observed for the neutral copolymer-grafted membrane than for the ionized copolymer-grafted membrane, the

explaination is still unclear. Further investigation may be necessary to be carried out, e.g., the determination of lysozyme and cytochrome C adsorption isotherm curves for ionized poly(M1-co-M2)-grafted membrane.

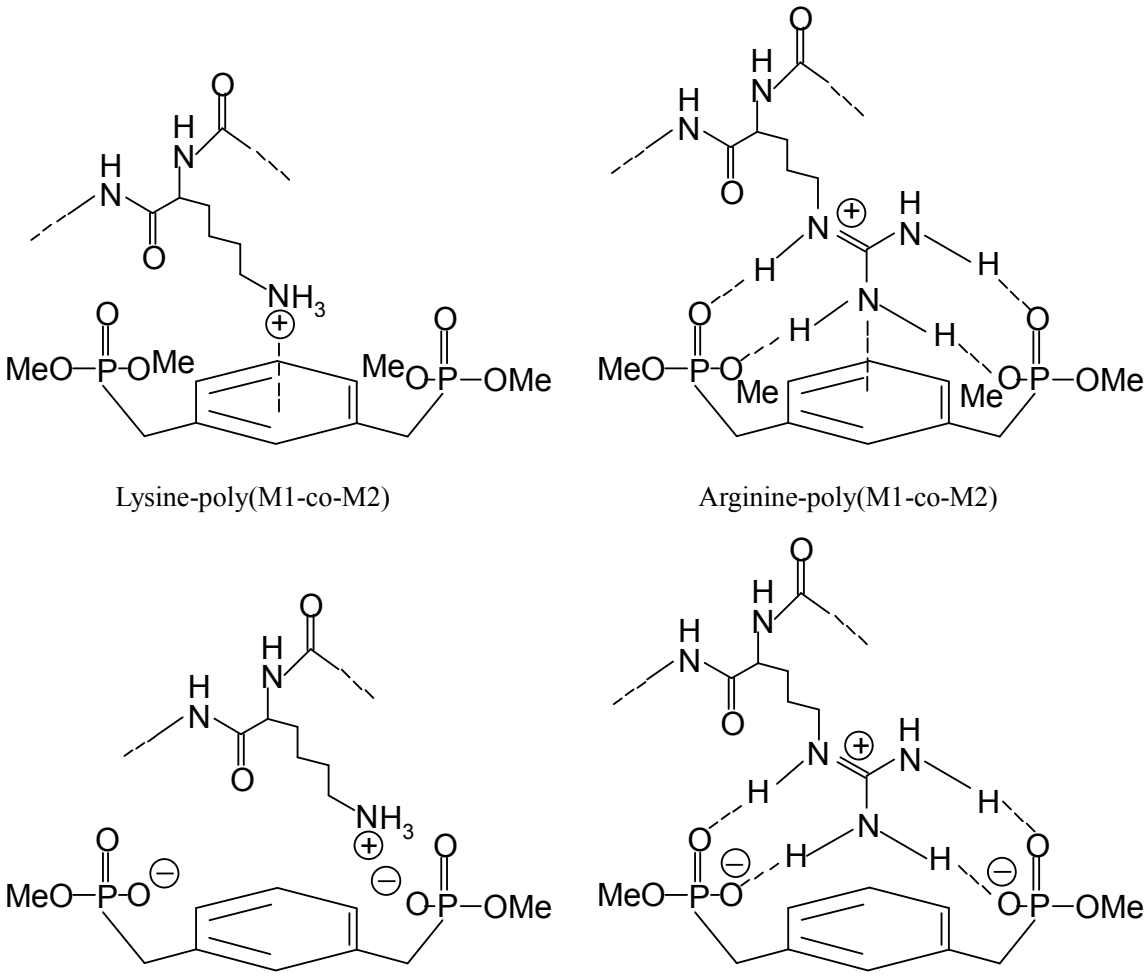

Lysine-poly(M1-co-M2) Arginine-poly(M1-co-M2)

Lysine-ionized poly(M1-co-M2) Arginine-ionized poly(M1-co-M2)

Figure 5.14: Specific interactions between lysine (arginine) and poly(M1-co-M2) (ionized poly(M1-co-M2).

5.3.3 MIP composite membrane

As shown in Fig. 5.2, for synergist immobilization method, tertiary amino groups on the membrane surface as co-initiator accelerate the photo-reduction of BP, and formed amino-substituted alkyl radicals are main initiating radicals. However, in the presence of template Boc-L-PhA for synthesis of MIP thin-layer, the carbonyl group of template interacted with the tertiary amino group on aminolysed PP membrane by electrostatic interaction (Fig. 5.15b), which influenced the capacity of electron transfer, reducing the photo-grafting efficiency. Therefore, much lower DG was obtained for MIP composite

membrane that for NIP composite membrane (Fig. 4.64). This explanation was also supported by the high template adsorption for aminolysed membrane and the lower reversibility in methanol due to the stronger electrostatic interaction. This strong interaction resulted in, on one hand, the decomposition of the formed complex between functional monomer and template (Fig. 5.15a), on the other hand, significant low template concentration in the bulk solution. Therefore, the imprinting effect of the resulting MIP composite membranes was strongly influenced (Fig. 4.67 and 4.68).

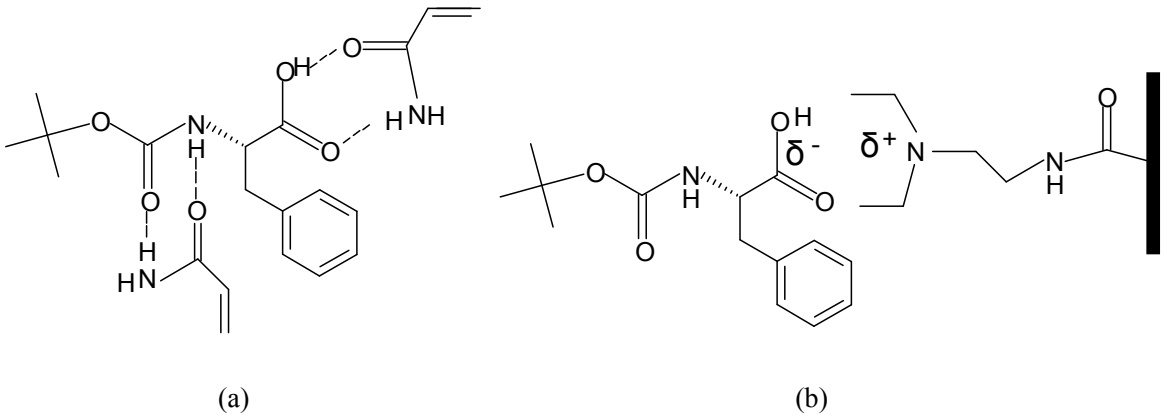

(a) (b)

Figure 5.15: Chemical structures of formed complexes between template (Boc-L-PhA) and functional monomer by hydrogen bonds (a) and between template and tertiary amino group on the membrane surface by electrostatic interaction (b).

Iniferter immobilization method would be a promising alternative. The MIP composite membrane has been prepared. The controlled DG would be possible by adjusting UV irradiation time (Fig. 4.66). The evaluation of such MIP composite membranes is still under way.

Evaluation on monolith

For effective performance imprinted polymers should be highly cross-linked thus enabling the selective cavities to retain their shape after removal of the template. However, a compromise should be found between the degree of cross-linking needed for polymer stability and a certain degree of polymer chain's flexibility which provides rapid equilibration with the template to be bound. Therefore, the highest separation factor has been achieved for the MIP with moderate functional monomer content and cross-linking (Fig. 4.70). The template binding capacity was related to functional groups and pore structure.

Chapter 6 Conclusions

Already known photo-initiator entrapping method and sequential photo-induced method have been evaluated with respect to the photo-grafting efficiency from polar organic solutions. Low photo-grafting efficiency has been obtained for both grafting methods in selected grafting system based on the much lower DG value compared with that for grafting in aqueous solution. For photo-initiator entrapping method, the entrapped initiator BP was extracted by organic solvent and local effective initiator concentration was much reduced during graft polymerization, which led to the low grafting efficiency. While in the case of sequential photo-induced method, the low grafting efficiency should be attributed to the requirement of high energy for initiating radical formation.

Two novel surface-selective photo-grafting methods have been developed: synergist immobilization and iniferter immobilization methods. Synergist immobilization method, based on the immobilization of tertiary amino groups as synergist for the photo-initiator BP, has been evaluated for commercial hydrophilized PP MF membrane. The introduction of tertiary amino groups via aminolysis reaction has been optimized. Compared with original membrane, aminolysed membrane demonstrated high surface-selectivity for photo-grafting of PAAm from methanol or acetonitrile solution based on the significantly higher DG values. Various factors affecting photo-grafting efficiency, surface-selectivity and grafting controllability such as solvent, UV irradiation time and intensity, concentration of monomer and photo-initiator have been investigated in detail. The obtained results showed that the competition of solvent with membrane surface towards the generation of starter radicals can lead to a decrease of DG and surface-selectivity of photo-grafting. High UV intensity accelerated the graft polymerization, but it significantly reduced the surface-selectivity of grafting. Furthermore, under such conditions, radical sites were probably generated on the propagating polymer chains or already formed polymer that led to cross-linking in the grafted layer. In addition, at high UV intensity and in the absence of BP, another functionalization mechanism was discovered that is based on the direct generation of a new type of starter radical from the synergist group on the membrane surface. An appropriately low photo-initiator concentration was also required to assure maximum surface-selectivity. Under the optimized conditions (inert solvent, appropriately low UV intensity and BP concentration), the grafted layer could be well controlled by synergist concentration, UV irradiation time, monomer and initiator concentration. Furthermore, synthesis of cross-linked grafted layer structure has also been realized due to

the high surface-selectivity of grafting. Based on the measurements for surface properties (contact angle and zeta potential) and water permeability measurement, two critical values have been observed: critical grafting density for full surface coverage with grafted polymer and critical cross-linking degree where the water permeability value showed an abrupt increase, i.e., swelling of prepared layer was minimized by cross-linking. In addition, this photo-grafting method was successfully applied to track-etched PET membrane. Therefore, selective photo-grafting on other polymer materials with a similar chemical structure will be possible by this method, and hence more applications for the surface design of polymeric materials are expected (such as various membrane adsorbers).

Iniferter immobilization method has been developed based on the immobilization of dithiocarbamate group as photo-iniferter. The reaction conditions for iniferter immobilization have been optimized. The photo-grafting efficiency, uniformity and controllability have been confirmed base on DG, SEM images, permeability and pore size distribution measurements. In addition, the livingness of graft polymerization was investigated by continuous and intermittent UV irradiation methods. Results demonstrated that the re-initiation efficiency was quite low under the selected conditions. Nevertheless, it is an efficient photo-grafting technique for membrane surface modification; various grafted layer structures have been obtained via this method.

Various anion-exchange membrane adsorbers have been prepared from aqueous solution via synergist immobilization and photo-initiator adsorption methods such as low grafting density and high grafting density membranes as well as the membrane adsorbers with slightly cross-linked grafted layer. Based on the permeability, static and dynamic binding capacity measurements for the resulting membrane adsorbers, it could be concluded that low grafting density membrane exhibited high protein binding capacity, but low buffer permeability and a significant dispersion (a long time delay to reach the maximum binding capacity). Both cross-linking structure and high grafting density improved the liquid permeability. Moreover, high grafting density membrane exhibited a steep breakthrough curve, however, the protein binding capacity was relatively low and molecular size exclusion has been observed. In comparison, the membranes with slightly cross-linked grafted layer showed an improved overall performance (relatively high protein binding capacity and low dispersion). In addition, compared with photo-initiator adsorption method, synergist immobilization method exhibited significantly higher grafting efficiency. Moreover, for same type of membrane adsorber (low grafting density), the dynamic performance was much better for the membrane adsorber prepared via synergist

immobilization method based on the breakthrough curve. This indicates that synergist immobilization method is a more efficient and suitable grafting technique for synthesis of anion-exchange membranes with “tailored” three-dimensional grafted functional layer.

Synergist immobilization method is an efficient grafting technique for synthesis of membrane adsorbers with “vertical architecture” grafted affinity copolymer. Even a 20% 5-(methacryloylamino)-m-xylylene bisphosphonic acid tetramethylester (M2) comonomer content in the grafted copolymer dominated the volume and surface properties of the resulting affinity membranes. Therefore, a good swelling of grafted copolymer in water was observed, which may contribute to the protein binding. Due to the specific interactions between proteins and functional groups (bisphosphonate ester groups and its salt) along the grafted copolymer, higher protein binding capacities have been obtained for both copolymer-grafted affinity membranes compared with for blank membrane. Especially, poly(M1-co-M2)-grafted membrane demonstrated the significantly high binding capacity and affinity for lysozyme compared with those for cytochrome C, although both proteins have similar pI values and protein sizes. The separation of lysozyme from a 1:1 mixture solution of lysozyme and cytochrome C has been realized with a very high selectivity with poly(M1-co-M2)-grafted affinity membrane.

MIP composite membranes have been synthesized via synergist immobilization method. However, due to the interaction between template (Boc-L-PhA) and synergist (tertiary amino groups) on the membrane surface, the formed complex between functional monomer and template may be decomposed and the template concentration in bulk solution was significantly reduced. Therefore, imprinting effect was not observed for the resulting MIP membrane.

Using the optimized composition for MIPs, MIP composite membranes have also been prepared via iniferter immobilization method. This method would be a promising alternative. The evaluation of MIP membranes and further investigation is in progress.

Outlook

The further work will emphasize on the synthesis of MIP thin-layer composite membranes via iniferter immobilization method and evaluation of the resulting MIP membranes. Before that, the selection of functional monomer and optimization of the composition for preparation of MIP thin-layer will be performed in more detail.

References

[1] Afeyan NB, Fulton SP, Gordon NF, Mazsaroff I, Varady L and Regnier FE. Perfusion chromatography—an approach to purifying biomolecules. Bio/technol. 1990; 8: 203-206.

[2] Brandt S, Goffe RA, Kessler SB, O'Connor JL and Zale SE. Membrane-based affinity technology for commercial scale purifications. Bio/Technol. 1988; 6: 779-782.

[3] Muller W. New ion-exchangers for the chromatography of biopolymers. J. Chromatogr. 1990; 510: 133-140.

[4] Tsuneda S, Saito K, Furusaki S and Sugo T. High-throughput processing of proteins using a porous and tentacle anion-exchange membrane. J. Chromatogr. A. 1995; 689: 211-218.

[5] Sun L, Dai J, Baker GL and Bruening ML. High-capacity, protein-binding membranes based on polymer brushes grown in porous substrates. Chem. Mater. 2006; 18: 4033-4039.

[6] Roper DK and Lightfoot EN. Separation of biomolecules using adsorptive membranes. J. Chromatogr. A 1995; 702: 3-26.

[7] Klein E. Affinity membranes: a 10-year review. J. Membr. Sci. 2000; 179: 1-27.

[8] Ghosh R. Protein separation using membrane chromatography: opportunities and challenges. J. Chromatogr. A. 2002; 952: 13-27.

[9] Sunaga K, Kim M, Saito K and Sugita K. Characterization of porous anion-exchange membranes prepared by cografting of glycidyl methacrylate with divinylbenzene. Chem. Mater. 1999; 11: 1986-1989.

[10] Yusof AHM and Ulbricht M. Polypropylene-based membrane adsorbers via photo-initiated graft copolymerization: Optimizing separation performance by preparation conditions. J. Membr. Sci. 2008; 311: 294-305.

[11] Singh N, Wang J, Ulbricht M, Wickramasinghe SR and Husson SM. Surface-initiated atom transfer radical polymerization: A new method for preparation of polymeric membrane adsorbers. J. Membr. Sci. 2008; 309: 64-72.

[12] Borcherding H, Hicke HG, Jorcke D and Ulbricht M. Surface functionalized microfiltration membranes for affinity separation. Desalination 2002; 149: 297-302.

[13] Ulbricht M and Yang H. Porous polypropylene membranes with different carboxyl polymer brush layers for reversible protein binding via surface-initiated graft copolymerization. Chem. Mater. 2005; 17: 2622-2631.

[14] Geismann C, Ulbricht M. Photoreactive functionalization of poly(ethylene terephthalate) track-etched pore surfaces with "smart" polymer systems. Macromol. Chem. Phys. 2005; 206: 268-281.

[15] Ma H, Davis RH and Bowman CN. A novel sequential photoinduced living graft polymerization. Macromolecules. 2000; 33: 331-335.

[16] Bhattacharya A, Misra BM. Grafting: a versatile means to modify polymers techniques, factors and applications. Prog. Polym. Sci. 2004; 29: 767-814.

[17] Kang YS, Lee SW, Kim UY and Shim JS. Pervaporation of water-ethanol mixtures through crosslinked and surface-modified poly (vinyl alcohol) membrane. J. Membr. Sci. 1990; 51: 215-226.

[18] Lee YM, Shin EM. Pervaporation separation of water-ethanol through modified chitosan membranes. IV. Phosphorylated chitosan membranes. J. Membr. Sci. 1991; 64: 145-152.

[19] Zhang W, Li G, Fang Y and Wang X. Maleic anhydride surface-modification of crosslinked chitosan membrane and its pervaporation performance. J. Membr. Sci. 2007; 295: 130-138.

[20] Obendorf SK, Tan K. Surface modification of microporous polyurethane membrane with poly(ethylene glycol) to develop a novel membrane. J. Membr. Sci. 2006; 274: 150-158.

[21] Papra A, Hicke HG and Paul D. Synthesis of peptides onto the surface of poly(ethylene terephthalate) particle track membranes. J. Appl. Polym. Sci. 1999; 74: 1669-1674.

[22] Yuan XY, Sheng J, He F, Tang Y and Shen NX. Surface modification of acrylonitrile copolymer membranes by grafting acrylamide. II. Initiation by Fe^{2+}/H_2O_2. J. Appl. Polym. Sci. 1998; 69: 1907-1915.

[23] Belfer S, Purinson Y, Fainshtein R, Radchenko Y and Kedem O. Surface modification of commercial composite polyamide reverse osmosis membranes. J. Membr. Sci. 1998; 139: 175-181.

[24] Yuan XY, Sheng J, He F, Lu XL and Shen NX. Surface modification of acrylonitrile copolymer membranes by grafting acrylamide. I. Initiation by ceric ions. J. Appl. Polym. Sci. 1997; 66: 1521-1529.

[25] Garg DH, Lenk W, Berwald S, Lunkwitz K, Simon F and Eichhorn KJ. Hydrophilization of microporous polypropylene Celgard® membranes by the chemical modification technique. J. Appl. Polym. Sci. 1996; 60: 2087-2104.

[26] Pathak TS, Chung KY. Surface modification and permeation characteristics of PVDF membrane after graft polymerization using polar monomer. J. Ind. Eng. Chem. 2006; 12: 539-545.

[27] Wang YW, Liu Z, Han B, Dong Z, Wang J, Sun D, Huang Y and Chen G. pH Sensitive polypropylene porous membrane prepared by grafting acrylic acid in supercritical carbon dioxide. Polymer 2004; 45: 855-860.
[28] Qiu GM, Zhu BK, Wang XQ and Xu YY. Surface modification of PVDF porous membrane in supercritical carbon dioxide fluids. ACTA Polym. SINICA 2005; 5: 783-787.
[29] Singh N, Husson SM, Zdyrko B and Luzinov I. Surface modification of microporous PVDF membranes by ATRP. J. Membr. Sci. 2005; 262: 81-90.
[30] Yang Q, Tian J, Hu MX and Xu ZK. Construction of a comb-like glycosylated membrane surface by a combination of UV-induced graft polymerization and surface-initiated ATRP. Langmuir 2007; 23: 6684-6690.
[31] Friebe A, Ulbricht M. Controlled pore functionalization of poly(ethylene terephthalate) track-etched membranes via surface-initiated atom transfer radical polymerization. Langmuir 2007; 23: 10316-10322.
[32] Alem H, Duwez AS, Lussis P, Lipnik P, Jonas AM and Demounstier-Champagne S. Microstructure and thermo-responsive behavior of poly(N-isopropylacrylamide) brushes grafted in nanopores of track-etched membranes. J. Membr. Sci. 2008; 308: 75-86.
[33] Nasef MM, Hegazy ESA. Preparation and applications of ion exchange membranes by radiation-induced graft copolymerization of polar monomers onto non-polar films. Prog. Polym. Sci. 2004; 29: 499-561.
[34] Saito K, Kaga T, Yamagishi H, Furusaki S, Sugo T and Okamoto J. Phosphorylated hollow fibers synthesized by radiation grafting and cross-linking. J. Membr. Sci. 1989; 43: 131-141.
[35] Tsuneda S, Saito K, Furusaki S, Sugo T and Okamoto J. Metal collection using chelating hollow fiber membrane. J. Membr. Sci. 1991; 58: 221-234.
[36] Shinano H, Tsuneda S, Saito K, Yamagishi H, Furusaki S and Sugo T. Preparation of microfiltration membranes containing anion-exchange groups. Biotechnol. Prog. 1993; 9: 193-198.
[37] Koguma I, Sugita K, Sugita K, Saito K and Sugo T. Multilayer binding of proteins to polymer chains grafted onto porous hollow-fiber membranes containing different anion-exchange groups. Biotechnol. Prog. 2000; 16: 456-461.
[38] Liu F, Zhu BK and Xu YY. Improving the hydrophilicity of poly(vinylidene fluoride) porous membranes by electron beam initiated surface grafting of AA/SSS binary monomers. Appl. Surf. Sci. 2006; 253: 2096-2101.
[39] Reddy PRS, Agathian G and Kumar A. Preparation of strong acid cation-exchange

membrane using radiation-induced graft polymerization. Radiat. Phys. Chem. 2005; 73: 169-174.

[40] Liu Q, Zhe ZY, Yang XM, Chen XL and Song YF. Temperature-sensitive porous membrane production through radiation co-grafting of NIPAAm on/in PVDF porous membrane. Radiat. Phys. Chem. 2006; 76: 707-713.

[41] Fang YE, Ma CX, Chen Q and Lu XB. Radiation-induced graft copolymerization of 2-hydroxyethyl methacrylate onto chloroprene rubber membrane. II. Characterization of grafting copolymer. J. Appl. Polym. Sci. 1998; 68: 1745-1750.

[42] Denes FS, Manolache S. Macromolecular plasma-chemistry: an emerging field of polymer science. Prog. Polym. Sci. 2004; 29: 815-885.

[43] Chen H, Belfort G. Surface modification of poly(ether sulfone) ultrafiltration membranes by low-temperature plasma-induced graft polymerization. J. Appl. Polym. Sci. 1999; 72: 1699-1711.

[44] Wavhal DS, Fisher ER. Modification of porous poly(ether sulfone) membranes by low-temperature CO_2-plasma treatment. J. Polym. Sci. 2002; 40: 2473-2488.

[45] Gancarz I, Pozniak G and Bryjak M. Modification of polysulfone membranes. 3. Effect of nitrogen plasma. Eur. Polym. J. 2000; 36: 1563-1569.

[46] Kim KS, Lee KH, Cho K and Park CE. Surface modification of polysulfone ultrafiltration membrane by oxygen plasma treatment. J. Membr. Sci. 2002; 199: 135-145.

[47] Steen ML, Butoi CI and Fisher ER. Identification of gas-phase reactive species and chemical mechanisms occurring at plasma-polymer surface interfaces. Langmuir 2001; 17: 8156-8166.

[48] Bhat NV, Wavhal DS. Preparation of cellulose triacetate pervaporation membrane by ammonia plasma treatment. J. Appl. Polym. Sci. 2000; 76: 258-265.

[49] Bryjak M, Gancarz I, Pozniak G and Tylus W. Modification of polysulfone membranes. 4. Ammonia plasma treatment. Eur. Polym. J. 2002; 38: 717-726.

[50] Ulbricht M, Belfort G. Surface modification of ultrafiltration membranes by low temperature plasma. I. Treatment of polyacrylonitrile. J. Appl. Polym. Sci. 1995; 56: 325-343.

[51] Ulbricht M, Belfort G. Surface modification of ultrafiltration membranes by low temperature plasma. II. Graft polymerization onto polyacrylonitrile and polysulfone. J. Membr. Sci. 1996; 111: 193-215.

[52] Lee YM, Shim JK. Preparation of pH/temperature responsive polymer membrane by plasma polymerization and its riboflavin permeation. Polymer. 1997; 38: 1227-1232.

[53] Liang L, Shi M, Viswanathan VV, Peurrung LM and Young JS. Temperature-sensitive polypropylene membranes prepared by plasma polymerization. J. Membr. Sci. 2000; 177: 97-108.

[54] Wavhal DS, Fisher ER. Membrane surface modification by plasma-induced polymerization of acrylamide for improved surface properties and reduced protein fouling. Langmuir 2003; 19: 79-85.

[55] Zhao ZP, Li J, Chen J and Chen CX. Nanofiltration membrane prepared from polyacrylonitrile ultrafiltration membrane by low-temperature plasma. 2. Grafting of styrene in vapor phase. J. Membr. Sci. 2005; 251: 239-245.

[56] Kang MS, Chun B and Kim SS. Surface modification of polypropylene membrane by low-temperature plasma treatment. J. Appl. Polym. Sci. 2001; 81: 1555-1566.

[57] Gancarz I, Pozniak G, Bryjak M and Tylus W. Modification of polysulfone membranes. 5. Effect of n-butylamine and allylamine plasma. Eur. Polym. J. 2002;38:1937~1946.

[58] Candan S, Beck AJ, O'Toole L and Short RD. Effects of "processing parameters" in plasma deposition: acrylic acid revisited. J. Vac. Sci. Technol. A 1998; 16: 1702 ~1705.

[59] Ulbricht M. Advanced functional polymer membranes. Polymer. 2006; 47: 2217-2262.

[60] Kotzyba-Hibert F, Kapfer I and Goeldner M. Recent trends in photoaffinity labeling. Angew. Chem. Int. Ed. Engl. 1995; 34: 1296-1312.

[61] Darkow R, Yoshikawa M, Kitao T and Tomaschewski G. Photomodification of a poly(acrylonitrile-co-butadiene-co-styrene) containing diaryltetrazolyl groups. J. Polym. Sci. A: Polym. Chem. 1994; 32: 1657-1664.

[62] Trushinski BJ, Dickson JM, Childs RF and McCarry BE. Photochemically modified thin-film composite membranes. I. Acid and ester membranes. J. Appl. Polym. Sci. 1993; 48: 187-198.

[63] Trushinski BJ, Dickson JM, Childs RF, McCarry BE and Gagnon DR. Photochemically modified thin-film composite membranes. II. Bromoethyl ester, dioxolan, and hydroxyethyl ester membranes. J. Appl. Polym. Sci. 1994; 54: 1233-1242.

[64] Bora U, Sharma P, Kannan K and Nahar P. Photoreactive cellulose membrane─A novel matrix for covalent immobilization of biomolecules. J. Biotechnol. 2006; 126: 220-229.

[65] Kumar S, Nahar P. Sunlight-induced covalent immobilization of proteins. Talanta 2007; 71: 1438-1440.

[66] Rajam S, Ho C. Graft coupling of PEO to mixed cellulose esters microfiltration membranes by UV irradiation. J. Membr. Sci. 2006; 281: 211-218.

[67] Ulbricht M, Hicke HG. Photomodification of ultrafiltration membranes. 1. Photochemical modification of polyacrylonitrile ultrafiltration membranes with aryl azides. Angew. Makromol. Chem. 1993; 210: 69-95.

[68] Ulbricht M, Hicke HG. Photomodification of ultrafiltration membranes. 2. Ultrafiltration properties of polyacrylonitrile membranes photochemically modified with aryl azides. Angew. Makromol. Chem. 1993; 210: 97-117.

[69] Thom V, Jankova K, Ulbricht M, Kops J and Jonsson G. Synthesis of photoreactive α-4-azidobenzoyl-ω-methoxy-poly(ethylene glycol)s and their end-on photo-grafting onto polysulfone ultrafiltration membranes. Macromol. Chem. Phys. 1998; 199: 2723-2729.

[70] Thom VH, Jonsson G. Photochemical grafting of poly(ethyleneglycol)s yielding low-protein-adsorbing UF membranes, Acta Polytech. Scand. Chem. Technol. Ser. 1997; 247: 35-50.

[71] Tian M, Zhong R, Sun SD, Zhao CS, Huang XH and Yue YL. Comparison of two approaches to grafting hydrophilic polymer chains onto polysulfone films. J. Appl. Polym. Sci. 2007; 103: 3818-3826.

[72] Thom VH, Altankov G, Groth T, Jankova K, Jonsson G and Ulbricht M. Optimizing cell – surface interactions by photo-grafting of poly(ethylene glycol). Langmuir 2000; 16: 2756-2765.

[73] Altankov G, Thom VH, Groth T, Jankova K, Jonsson G and Ulbricht M. Modulating the biocompatibility of polymer surface with poly(ethylene glycol): Effect of fibronectin. J. Biomed. Mater. Res. 2000; 52: 219-230.

[74] Lazos D, Franzka S and Ulbricht M. Size-selective protein adsorption to polystyrene surfaces by self-assembled grafted polyethylene glycols with varied chain lengths. Langmuir 2005; 21: 8774-8784.

[75] Park YS, Ito Y and Imanishi Y. Permeation control through porous membranes immobilized with thermosensitive polymer. Langmuir 1998; 14: 910-914.

[76] Lequieu W, Shtanko NI and Du Prez FE. Track etched membranes with thermo-adjustable porosity and separation properties by surface immobilization of poly(N-vinylcaprolactam). J. Membr. Sci. 2005; 256: 64-71.

[77] Yang B, Yang W. Photografting modification of PET nucleopore membranes. J. Macromol. Sci. A: Pure Appl. Chem. 2003; A40: 309-320.

[78] Park YS, Won J and Kang YS. Preparation of poly(ethylene glycol) brushes on polysulfone membranes for olefin/paraffin separation. Langmuir 2000; 16: 9662-9665.

[79] Crivello JV, Belfort G and Yamagishi H. Low fouling ultrafiltration and microfiltration aryl polysulfone. US Patent 5,468,390, 1995.

[80] Yamagishi H, Crivello JV and Belfort G. Development of a novel photochemical technique for modifying poly(arylsulfone) ultrafiltration membranes. J. Membr. Sci. 1995; 105: 237-247.

[81] Kilduff JE, Mattaraj S, Zhou M and Belfort G. Kinetics of membrane flux decline: the role of natural colloids and mitigation via membrane surface modification. J. Nanopart. Res. 2005; 7: 525-544.

[82] Ulbricht M, Riedel M and Marx U. Novel photochemical surface functionalization of polysulfone ultrafiltration membranes for covalent immobilization of biomolecules. J. Membr. Sci. 1996; 120: 239-259.

[83] Yamagishi H, Crivello JV and Belfort G. Evaluation of photochemically modified poly(arylsulfone) ultrafiltration membranes. J. Membr. Sci. 1995; 105: 249-259.

[84] Kaeselev B, Pieracci J and Belfort G. Photoinduced grafting of ultrafiltration membranes: comparison of poly(ether sulfone) and poly(sulfone). J. Membr. Sci. 2001; 194: 245-261.

[85] Taniguchi M, Belfort G. Low protein fouling synthetic membrane by UV-assisted surface grafting modification: varying monomer type. J. Membr. Sci. 2004; 231: 147-157.

[86] Pieracci J, Crivello JV and Belfort G. UV-assisted graft polymerization of N-vinyl-2-pyrrolidinone onto poly(ether sulfone) ultrafiltration membranes using selective UV wavelengths. Chem. Mater. 2002; 14: 256-265.

[87] Taniguchi M, Pieracci J, Samsonoff WA and Belfort G. UV-assisted graft polymerization of synthetic membranes: Mechanistic studies. Chem. Mater. 2003; 15: 3805-3812.

[88] Pieracci J, Wood, D, Crivello J and Belfort G. UV-assisted graft polymerization of *N*-vinyl-2-pyrrolidinone onto poly-(ether sulfone) ultrafiltration membranes: comparison of dip versus immersion modification techniques. Chem. Mater. 2000; 12: 2123-2133.

[89] Pieracci J, Crivello JV and Belfort G. Increasing membrane permeability of UV-modified poly(ether sulfone) ultrafitration membranes. J. Membr. Sci. 2002; 202: 1-16.

[90] Susanto H, Ulbricht M. Photografted thin polymer hydrogel layers on PES ultrafiltration membranes: characterization, stability, and influence on separation performance. Langmuir 2007; 23: 7818-7830.

[91] Susanto H, Balakrishnan M and Ulbricht M. Via surface functionalization by photograft copolymerization to low-fouling polyethersulfone-based ultrafiltration membranes. J. Membr. Sci. 2007; 288: 157-167.

[92] Nayak A, Liu H and Belfort G. An optically reversible switching membrane surface. Angew. Chem. Int. Ed. 2006; 45: 4094-4098.

[93] Bequet S, Remigy JC, Rouch JC, Espenan JM, Clifton M and Aptel M. From ultrafiltration to nanofiltration hollow fiber membranes: a continuous UV-photografting process, Desalination 2002; 144: 9-14.

[94] Yanagishita H, Kitamoto D, Ikegami T, Negishi H, Endo A, Haraya K, Nakane T, Hanai N, Arai J, Matsuda H, Idemoto Y and Koura N. Preparation of photo-induced graft filling polymerized membranes for pervaporation using polyimide with benzophenone structure. J. Membr. Sci. 2002; 203: 191-199.

[95] Qiu C, Xu F, Nguyen QT and Ping Z. Nanofiltration membrane prepared from cardo polyetherketone ultrafiltration membrane by UV-induced grafting method. J. Membr. Sci. 2005; 255: 107-115.

[96] Qiu C, Nguyen QT and Ping Z. Surface modification of cardo polyetherketone ultrafiltration membrane by photo-grafted copolymers to obtain nanofiltration membranes. J. Membr. Sci. 2007; 295: 88-94.

[97] Wang HY, Kobayashi T and Fujii N. Surface molecular imprinting on photosensitive dithiocarbamoyl polyacrylonitrile membranes using photograft polymerization. J. Chem. Technol. Biotechnol. 1997; 70: 355-362.

[98] Hattori K, Hiwatari M, Iiyama C, Yoshimi Y, Kohori F, Sakai K and Piletsky SA. Gate effect of theophylline-imprinted polymers grafted to the cellulose by living radical polymerization. J. Membr. Sci. 2004; 233: 169-173.

[99] Guan J, Gao C, Feng L and Shen J. Functionalizing of polyurethane surface by photografting with hydrophilic monomers. J. Appl. Polym. Sci. 2000; 77: 2505-2512.

[100] Guan J, Gao C, Feng L and Shen J. Surface photo-grafting of polyurethane with 2-hydroxyethyl acrylate for promotion of human endothelial cell adhesion and growth. J. Biomater. Sci. Polym. Ed. 2000; 11: 523-536.

[101] Guan J, Gao C, Feng L and Shen J. Preparation of functional poly(ether-urethane) for immobilization of human living cells. 1. Surface graft polymerization of

poly(ether-urethane) with 2-(dimethylamino)ethyl methacrylate and quaternization of grafted membrane. Eur. Polym. J. 2000; 36: 2707-2713.

[102] Gao C, Guan J, Zhu Y and Shen J. Surface immobilization of bioactive molecules on polyurethane for promotion of cytocompatibility to human endothelial cells. Macromol. Biosci. 2003; 3: 157-162.

[103] Steuck M J. US Patent 4618533, 1986.

[104] Hu H, Cai Z. US Patent 5209849, 1993.

[105] Kochkodan V, Weigel W and Ulbricht M. Thin layer molecularly imprinted microfiltration membranes by photofunctionalization using a coated alpha-cleavage photoinitiator. Analyst 2001; 126: 803-809.

[106] Hilal N, Kochkodan V. Surface modified microfiltration membranes with molecularly recognizing properties. J. Membr. Sci. 2003; 213: 97-113.

[107] Tazuke S, Kimura H. Surface photografting modification of polypropylene film surface by graft polymerization of acrylamide. Makromol. Chem. 1978; 179: 2603-2612.

[108] Yang W, Ranby B. Radical living graft polymerization on the surface of polymeric materials. Macromolecules 1996; 29: 3308-3310.

[109] Ruckert D, Geuskens G. Surface modification of polymers. IV. Grafting of acrylamide via an unexpected mechanism using a water soluble photo-initiator. Eur. Polym. J. 1996; 32: 201-208.

[110] Yang B, Yang W. Thermo-sensitive switching membranes regulated by pore-covering polymer brushes. J. Membr. Sci. 2003; 218: 247-255.

[111] Yang B, Yang W. Novel pore-covering membrane as a full open/close valve. J. Membr. Sci. 2005; 258: 133-139.

[112] Wu G, Li Y, Han M and Liu X. Novel thermo-sensitive membranes prepared by rapid bulk photo-grafting polymerization of N,N-diethylacrylamide onto the microfiltration membranes nylon. J. Membr. Sci. 2006; 283: 13-20.

[113] Kim J H, Ha S Y, Nam SY, Rhim JW, Baek KH and Lee YM. Selective permeation of CO_2 through pore-filled polyacrylonitrile membrane with poly(ethylene glycol). J. Membr. Sci. 2001; 186: 97-107.

[114] Ulbricht M, Oechel A, Lehmann C, Tomaschewski G and Hicke HG. Gas-phase photoinduced graft polymerization of acrylic acid onto polyacrylonitrile ultrafiltration membranes. J. Appl. Polym. Sci. 1995; 55: 1707-1723.

[115] Ulbricht M. Photograft-polymer-modified microporous membranes with environment-sensitive permeabilities. React. Funct. Polym. 1996; 31: 165-177.

[116] Ulbricht M, Richau K and Kamusewitz H. Chemically and morphologically defined ultrafiltration membrane surfaces prepared by heterogeneous photo-initiated graft polymerization. Colloids Surf. A: Physicochem. Eng. Asp. 1998; 138: 353-366.
[117] Borcherding H, Hicke HG, Jorcke D and Ulbricht M. Affinity Membranes as a tool for life science applications. Ann. NY Acad. Sci. 2003; 984: 470-479.
[118] Piletsky SA, Matuschewski H, Schedler U, Wilpert A, Piletska E, Thiele TA and Ulbricht M. Surface functionalization of porous polypropylene membranes with molecularly imprinted polymers by photograft copolymerization in water. Macromolecules 2000; 33: 3092-3098.
[119] Ulbricht M, Riedel M. Ultrafiltration membrane surfaces with grafted polymer 'tentacles': preparation, characterization and application for covalent protein binding. Biomaterials 1998; 19: 1229-1237.
[120] Hicke HG, Ulbricht M, Becker M, Radosta S and Heyer AG. Novel enzyme-membrane reactor for polysaccharide synthesis. J. Membr. Sci. 1999; 161: 239-245.
[121] Sergeyeva TA, Matuschewski H, Piletsky SA, Bendig J, Schedler U and Ulbricht M. Molecularly imprinted polymer membranes for substance-selective solid-phase extraction from water by surface photo-grafting polymerization. J. Chromatogr. A 2001; 907: 89-99.
[122] Ulbricht M, Schwarz HH. Novel high performance photo-graft composite membranes for separation of organic liquids by pervaporation. J. Membr. Sci. 1997; 136: 25-33.
[123] Frahn J, Malsch G and Schwarz HH. Generation of a selective layer on polyacrylonitrile membrane supports for separation of aromatic/non-aromatic hydrocarbon mixtures by pervaporation. Macromol. Symp. 2001; 164: 269-276.
[124] Wenzel A, Yanagishita H, Kitamoto D, Endo A, Haraya K, Nakane T, Hanai N, Matsuda H, Koura N, Kamusewitz H and Paul D. Effects of preparation condition of photoinduced graft filling-polymerized membranes on pervaporation performance. J. Membr. Sci. 2000; 179: 69-77.
[125] Frahn J, Malsch G and Schwarz HH. Photo-initiated generation of a selective layer on polyacrylonitrile (PAN) composite membranes. J. Mater. Proc. Technol. 2003; 143-144: 277-280.
[126] Frahn J, Malsch G, Matuschewski H, Schedler U and Schwarz HH. Separation of aromatic/aliphatic hydrocarbons by photo-modified poly(acrylonitrile) membranes. J. Membr. Sci. 2004; 234: 55-65.

[127] Ulbricht M, Matuschewski H, Oechel A and Hicke HG. Photo-induced graft polymerization surface modifications for the preparation of hydrophilic and low-protein-adsorbing ultrafiltration membranes. J. Membr. Sci. 1996; 115: 31-47.

[128] Ulbricht M. Membrane separations using molecularly imprinted polymers. J. Chromatogr. B 2004; 804: 113-125.

[129] Schneider F, Piletsky S, Piletsky E, Guerreiro A and Ulbricht M. Comparison of thin-layer and bulk MIPs synthesized by photo-initiated in situ crosslinking polymerization from the same reaction mixture. J. Appl. Polym. Sci. 2005; 98: 362-372.

[130] Conesa A, Palet C. Molecularly imprinted membranes (MIM) for the enantioseparation of selenoaminoacid compounds. Desalination 2006; 200: 110-111.

[131] Donato L, Figoli A and Drioli E. Novel composite poly(4-vinylpyridine)/polypropylene membranes with recognition properties for (s)-naproxen. J. Pharm. Biomed. Anal. 2005; 37: 1003-1008.

[132] Salam A, Ulbricht M. Effect of surface modification on synthesis of pore-filling polymeric monoliths in microfiltration membranes made from polypropylene and poly(ethylene terephthalate). Macromol. Mater. Eng. 2007; 292: 310-318.

[133] Becker M, Provart N, Lehmann I, Ulbricht M and Hicke HG. Polymerization of glucans by enzymatically active membranes. Biotechnol. Prog. 2002; 18: 964-968.

[134] Geismann C, Yaroshchuk A and Ulbricht M. Permeability and electrokinetic characterization of poly(ethylene terephthalate) capillary pore membranes with grafted temperature-responsive polymers. Langmuir 2007; 23: 76-83.

[135] Yang Q, Xu ZK, Dai ZW, Wang JL and Ulbricht M. Surface modification of polypropylene microporous membranes with a novel glycopolymer. Chem. Mater. 2005; 17: 3050-3058.

[136] Yang Q, Hu MX, Dai ZW, Tian J and Xu ZK. Fabrication of glycosylated surface on polymer membrane by UV-induced graft polymerization for lectin recognition. Langmuir 2006; 22: 9345-9349.

[137] Yang Q, Xu ZK, Hu MX, Li JJ and Wu J. Novel sequence for generating glycopolymer tethered on a membrane surface. Langmuir 2005; 21: 10717-10723.

[138] Yu HY, Xu ZK, Lei H, Hu MX and Yang Q. Photoinduced graft polymerization of acrylamide on polypropylene microporous membranes for the improvement of antifouling characteristics in a submerged membrane-bioreactor. Sep. Purif. Technol. 2007; 53: 119-125.

[139] Hu MX, Yang Q and Xu ZK. Enhancing the hydrophilicity of polypropylene microporous membranes by the grafting of 2-hydroxyethyl methacrylate via a synergistic effect of photoinitiators. J. Membr. Sci. 2006; 285: 196-205.
[140] Ma H, Davis RH and Bowman CN. Principle factors affecting sequential photoinduced graft polymerization. Polymer 2001; 42: 8333-8338.
[141] Ma H, Bowman CN and Davis RH. Membrane fouling reduction by backpulsing and surface modification. J. Membr. Sci. 2000; 173: 191-200.
[142] Yu HY, Xu ZK, Yang Q, Hu MX and Wang SY. Improvement of the antifouling characteristics for polypropylene microporous membranes by the sequential photoindueced graft polymerization of acrylic acid. J. Membr. Sci. 2006; 281: 658-665.
[143] Xu ZK, Dai QW, Wu J, Huang XJ and Yang Q. Covalent attachment of phospholipid analogous polymers to modify a polymeric membrane surface: a novel approach. Langmuir 2004; 20: 1481-1488.
[144] Sun L, Baker GL and Bruening ML. Polymer brush membranes for pervaporation of organic solvents from water. Macromolecules 2005; 38: 2307-2314.
[145] Hicke HG, Becker M, Paulke BR and Ulbricht M. Covalently coupled nanoparticles in capillary pores as enzyme carrier and as turbulence promoter to facilitate enzymatic polymerization in flow-through enzyme-membrane reactors. J. Membr. Sci. 2006; 282: 413-422.
[146] Yang H, Viera C, Fischer J and Etzel MR. Purification of a large protein using ion-exchange membranes. Ind. Eng. Chem. Res. 2002; 41: 1597-1602.
[147] Charcosset C. Purification of proteins by membrane chromatography. J. Chem. Technol. Biotechnol. 1998; 71: 95-110.
[148] Nachman M, Azad ARM and Bailon P. Efficient recovery of recombinant proteins using membrane-based immunoaffinity chromatography (MIC). Biotechnol. Bioeng. 1992; 40: 564-571.
[149] Adachi T, Mogi M, Harada M and Kojima K. Selective removal of immunoglobulin-E from rat-blood by membrane-immobilized antibody. J. Chromatogr. B 1995; 668: 327-332.
[150] Ahmed SR, Lutes AT and Barbari TA. Specific capture of target proteins by oriented antibodies bound to tyrosinase-immobilized protein A on a polyallylamine affinity membrane surface. J. Membr. Sci. 2006; 282: 311-321.

[151] Dancette OP, Taboureau JL, Tournier E, Charcosset C and Blond P. Purification of immunoglobulins G by protein A/G affinity membrane chromatography. J. Chromatogr. B 1999; 723: 61-68.

[152] Wolman FJ, Grasselli M and Cascone O. Rapid neutral protease purigication by dye-affinity membrane chromatography. Proc. Biochem. 2006; 41: 356-361.

[153] Grasselli M, Camperi SA, del Canizo AAN and Cascone O. Direct lysozyme separation from egg white by dye membrane affinity chromatography. J. Sci. Food Agric. 1999; 79: 333-339.

[154] de Aquino LCL, de Sousa HRT, Miranda EA, Vilela L and Bueno SMA. Evaluation of IDA-PEVA hollow fiber membrane metal ion affinity chromatography for purification of a histidine-tagged human proinsulin. J. Chromatogr. B. 2006; 834: 68-76.

[155] Serafica GC, Pimbley J and Belfort R. Protein fractionation using fast-flow immobilized metal chelate affinity membranes. Biotechnol. Bioeng. 1994; 43: 21-36.

[156] Platonova GA, Pankova GA, II'ina IY, Viasov GP and Tennikova TB. Quantitative fast fractionation of a pool of polyclonal antibodies by immunoaffinity membrane chromatography. J. Chromatogr. A. 1999; 852: 129-140.

[157] Tuneda S, Shinano H, Saito K, Furusaki S and Sugo T. Binding of lysozyme onto a cation-exchange microporous membrane containing tentacle-type grafted polymer branches. Biotechnol. Prog. 1994; 10: 76-81.

[158] Piletsky SA, Dubei IY, Fedroyak DM and Kukhar VP. Substrate-selective polymeric membranes. Selective transfer of nucleic acid components. Biopolym. Kletka 1990; 6: 55-58.

[159] Briefs KG, Kula MR. Fast protein chromatography on analytical and preparative scale using modified microporous membranes. Chem. Eng. Sci. 1992; 47: 141-149.

[160] Suen SY, Etzel MR. A mathematical analysis of affinity membrane bioseparations. Chem. Eng. Sci. 1992; 47: 1355-1364.

[161] Suen SY, Caracotsios M and Etzel MR. Sorption kinetics and axial diffusion in binary-solution affinity-membrane bioseparations. Chem. Eng. Sci. 1993; 48: 1801-1812.

[162] Sarfert FT, Etzel MR. Mass transfer limitations in protein separations using ion-exchange membranes. J. Chromatogr. A 1997; 764: 3-20.

[163] Yang H, Bitzer M and Etzel MR. Analysis of protein purification using ion-exchange membranes. Ind. Eng. Chem. Res. 1999; 38: 4044-4050.

[164] Tennikova TB, Svec F. High-performance membrane chromatography: highly efficient separation method for proteins in ion-exchange, hydrophobic interaction and reversed-phase modes. J. Chromatogr. 1993; 646: 279-288.
[165] Tejeda A, Ortega J, Magana I and Guzman R. Optimal design of affinity membrane chromatographic columns. J. Chromatogr. A 1999; 830: 293-300.
[166] Boi C, Dimartino S and Sarti GC. Modelling and simulation of affinity membrane adsorption. J. Chromatogr. A 2007; 1162: 24-33.
[167] Shi W, Zhang F and Zhang G. Mathematical analysis of affinity membrane chromatography. J. Chromatogr. A 2005; 1081: 156-162.
[168] Ge D, Shi W, Ren L, Zhang F, Zhang G, Zhang X and Zhang Q. Variation analysis of affinity-membrane model based on Freundlich adsorption. J. Chromatogr. A 2006; 1114: 40-44.
[169] Ghosh R, Wong T. Effect of module design on the efficiency of membrane chromatographic separation process. J. Membr. Sci. 2006; 281: 532-540.
[170] Reichert U, Linden T, Belfort G, Kula MR and Thömmes J. Visualising protein adsorption to ion-exchange membranes by confocal microscopy. J. Membr. Sci. 2002; 199: 161-166.
[171] Wickramasinghe SR, Carlson JO, Teske C, Hubbuch J and Ulbricht M. Characterizing solute binding to macroporous ion exchange membrane adsorbers using confocal laser scanning microscopy. J. Membr. Sci. 2006; 281: 609-618.
[172] Zeng X, Ruckenstein E. Membrane chromatography: preparation and applications to protein separation. Biotechno. Prog. 1999; 15: 1003-1019.
[173] Kubota N, Kounosu M, Saito K, Sugita K, Watanabe K and Sugo T. Protein adsorption and elution performances of porous hollow-fiber membranes containing various hydrophobic ligands. Biotechnol. Prog. 1997; 13: 89-95.
[174] Avramescu M, Girones M, Borneman Z and Wessling M. Preparation of mixed matrix adsorber membranes for protein recovery, J. Membr. Sci. 2003; 218: 219-233.
[175] Avramescu M, Borneman Z and Wessling M. Dynamic behavior of adsorber membranes for protein recovery, Biotechnol. Bioeng. 2003; 84: 564-572.
[176] Li J, Li T, Zhang Q and Zhang G. Determination of content of tertiary amino organosilicon by spectrophotometric method. Silicone Mater. 2004; 18: 20-22.
[177] Yang WT, Ranby B. Bulk surface photografting process and its application. I. Reactions and kinetics. J. Appl. Polym. Sci. 1996; 62: 533-543.
[178] Avny Y, Rebenfeld L. Chemical modification of polyester fiber surfaces by

amination reactions with multifunctional amines. J. Appl. Polym. Sci. 1986; 32: 4009-4025.

[179] Zhu Y, Gao C, Liu X and Shen J. Surface modification of polycaprolactone membrane via aminolysis and biomacromolecule immobilization for promoting cytocompatibility of human endothelial cells. Biomacromolecules 2002; 3: 1312-1319.

[180] Rückert B, Hall AJ and Sellergren B. Molecularly imprinted composite materials via iniferter-modified supports. J. Mater. Chem. 2002; 12: 2275-2280.

[181] Nakayama Y, Matsuda T. Surface macromolecular microarchitecture design: Biocompatible surface via photo-block-graft-copolymerization using N,N-diethyldithiocarbamate. Langmuir 1999; 15: 5560-5566.

[182] Nakayama Y, Matsuda T. Surface macromolecular architecture design using photo-graft copolymerization based on photochemistry of benzyl N,N-diethyldithiocarbamate. Macromolecules 1996; 29: 8622-8630.

[183] Hattori K, Hiwatari M, Iiyama C, Yoshimi Y, Kohori F, Sakai K and Piletsky SA. Gate effect of theophylline-imprinted polymers grafted to the cellulose by living radical polymerization. J. Membr. Sci. 2004; 233: 169-173.

[184] De Boer B, Simon HK, Werts MPL, Van der Vegte EW and Hadziioannou G. "Living" free radical photopolymerization initiated from surface-grafted iniferter monolayers. Macromolecules 2000; 33: 349-356.

[185] Gebauer KH, Thömmes J and Kula MR. Breakthrough performance of high-capacity membrane adsorbers in protein chromatography. Chem. Eng. Sci. 1997; 52: 405-419.

[186] Yang H, Etzel MR. Evaluation of three kinetic equations in models of protein purification using ion-exchange membranes. Ind. Eng. Chem. Res. 2003; 42: 890-896.

[187] Renner C, Piehler J and Schrader T. Arginine- and lysine-specific polymers for protein recognition and immobilization. J. Am. Chem. Soc. 2006; 128: 620-628.

[188] Wulff G, Sarhan A. The use of polymers with enzyme-analogous structures for the resolution of racemates. Angew. Chem. Int. Ed. Engl. 1972; 11: 341.

[189] Piletsky SA, Dubei IY, Fedroyak DM and Kukhar VP. Substrate-selective polymeric membranes. Selective transfer of nucleic acid components. Biopolym. Kletka 1990; 6: 55-58.

[190] Geismann C. Schaltbar Kapillarporenmembranen durch Oberflächenfunktionalisierung mit stimuli-responsiven Polymersystemen. Dissertation. Essen, 2007.

[191] Ulbricht M, Schuster O, Ansorge W, Ruetering M and Steiger P. Influence of the

strongly anisotropic cross-section morphology of a novel polyethersulfone microfiltration membrane on filtration performance. Separ. Purif. Technol. 2007; 57: 63-73.
[192] Michaels AS, Vieth WR and Alcalay HH. The solubility parameter of polypropylene. J. Appl. Polym. Sci. 1968; 12: 1621-1624.
[193] Mar'in AP, Bonora M and Greci L. Washing out oligomeric triazinic-hindered amine from polypropylene. J. Appl. Polym. Sci. 2000; 78: 2158-2165.
[194] Tazuke S, Kimura H. Surface photografting. 2. Modification of polypropylene film surface by graft polymerization of acrylamide. Makromol. Chem. 1978; 179: 2603-2612.
[195] Tazuke S. Thin-layer photografting as a method of polymer surface modification. Polym. Plast. Technol. Eng. 1980; 14: 107-134.
[196] Coyle JD. Electron-transfer photochemistry of organic amides and imides. Pure & Appl. Chem. 1998; 60: 941-946.
[197] Yang P, Deng W and Yang WT. Surface photografting polymerization of methyl methacrylate in N,N-demethylformamide on low density polyethylene film. Macromol. Chem. Phys. 2004; 205: 1096-1102.
[198] Ishizu K, Khan RA, Ohya Y and Furo M. Controlled radical polymerization of 2-hydroxyethyl methacrylate initiated by photofunctional 2-(N,N-diethyldithiocarbamyl)isobutyric acid. J. Polym. Sci. A. Polym. Chem. 2004; 42: 76-82.
[199] Kawai T, Sugita K, Saito K and Sugo T. Extension and shrinkage of polymer brush grafted onto porous membrane induced by protein binding. Macromolecules 2000; 33: 1306-1309.

Appendix-1

List of abbreviations

AA	acrylic acid
AAm	acrylamide
AO	acid orange II
ATRP	atom transfer radical polymerization
ABMPEG	α-4-azidobenzoyl-ω-methoxy-PEG
Boc-D/L-PhA	Boc-D/L-phenylalanine
BP	benzophenone
BSA	bovine serum albumin
CL	cross-linker
DEEDA	N,N-diethylethylene diamine
DG	degree of grafting
DMAP	4-(dimethylamino)pyridine
DMPAP	2,2-dimethoxy-2-phenylacetophenone
EDMA	ethylene glycol dimethacrylate
GMA	glycidyl methacrylate
HEMA	2-hydroxyethyl methacrylate
M1	methacryloyamino-2-hydroxy-propane
M2	5-(methacryloyamino)-m-xylylene bisphosphonic acid tetramethylester
MAA	methylacylic acid
MAETMAC	(2-(methacryloxy)ethyl) trimethylammonium chloride
MBAA	methylene bisacrylamide
MF	microfiltration
MIP	molecularly imprinted polymer
NF	nanofiltration

NIP	non-imprinted polymer
NIPAAm	N-isopropyl acrylamide
PAA	poly(acrylic acid)
PAAm	polyacrylamide
PAN	polyacrylonitrile
PC	polycarbonate
PE	polyethylene
PEG	poly(ethylene glycol)
PEGMA	poly(ethylene glycol methacrylate)
PEO	poly(ethylene oxide)
PES	poly(ether sulfone)
PET	Poly(ethylene terephthalate)
PI	polyimide
PMA	polymethacrylate
PP	polypropylene
PPO	poly(propylene oxide)
PSf	polysulfone
PSt	polystyrene
PTFE	polytetrafluoroethylene
PU	polyurethane
PV	pervaporation
PVA	poly(vinyl alcohol)
PVC	poly(vinyl chloride)
PVDF	poly(vinylidene fluoride)
TEPA	tetraethylenepentamine
TIPS	thermally induced phase separation

THO	theophylline
Tris	tris-(hydroxymethyl)-aminomethane
Trp	trypsin inhibitor
UF	ultrafiltration

Appendix-2

List of publications and conferences

Papers in Journals (Peer-reviewed)

1. D.M. He and M. Ulbricht. Surface-selective photo-grafting on porous polymer membranes via synergist immobilization method. *J. Mater. Chem.* 2006, 16, 1860.

2. D.M. He and M. Ulbricht. Synergist immobilization method for photo-grafting: Factors affecting surface selectivity. *Macromol. Chem. Phys.* 2007, 208, 1582.

3. D.M. He and M. Ulbricht. Preparation and characterization of porous anion-exchange membrane adsorbers with high protein-binding capacity. *J. Membr. Sci.* 2008, 315, 155.

4. D.M He, H. Susanto and M. Ulbricht. Photo-irradiation for preparation, modification and stimulation of polymeric membranes. *Prog. Polym. Sci.* Submitted.

5. D.M. He, W. Sun, T. Schrader and M. Ulbricht. Protein-selective affinity membrane adsorber based on grafted copolymers containing bisphosphonato-xylylene recognition moieties. In preparation.

Conferences

2007 **North American Membrane Society (NAMS) Annual Meeting 2007, Orlando, United States.**

"Surface-selective photo-grafting for preparation of macroporous membrane adsorbers" ***(oral paper).***

PERMEA 2007, Siofok, Hungary.

"Surface-selective photo-grafting via synergist immobilization method for preparation of thin-layer MIP composite membranes" ***(oral paper).***

2006 **3rd Graduate Student Symposium on Molecular Imprinting Technology, University of Dortmund, Dortmund, Germany.**

"Surface-selective photo-grafting for MIP membrane preparation via synergist immobilization method" ***(oral presentation).***

20th Bratislava International Congress on Macromolecule, Advanced Polymeric Material (APM-2006), Bratislava, Slovakia.

"Surface-selective photo-grafting for MIP membrane preparation via synergist immobilization method" ***(poster paper).***

Polymers & Coating 2006, Universität Mainz, Mainz, Germany.

"A controllable surface-selective functionalization of polymer membranes" ***(poster paper).***

Appendix-3

Curriculum Vitae

Name: Dongming He

Place/Date of Birth: Jiangxi, China / 25, Aug. 1976.

Educational Background

2005-2008 (Ph.D): Technical Chemistry, University of Duisburg-Essen, Germany.

Advisor: Prof. Dr. Mathias Ulbricht

1998-2001 (M.E.): Material Science, Wuhan University of Technology, China.

Advisor: Prof. Dr. Chaocan Zhang

1994-1998 (B.E.): Polymer Science and Engineering, Wuhan University of Technology, China.

Work Experience

2001-2004: Assistant (2001-2003) and Lecturer (2003-2004)
Wuhan University of Technology, China.